MEASUREMENT OF ELECTROMAGNETIC SIGNAL VELOCITIES IN SATURATED FINE-GRAINED SOILS

By

ANDREW MARK THOMAS

A thesis submitted to
The University of Birmingham
For the degree of
DOCTOR OF PHILOSOPHY

UNIVERSITY OF BIRMINGHAM

University of Birmingham Research Archive

e-theses repository

ABSTRACT

Electromagnetic signal velocity measurements are common in soil disciplines, often involving Time-Domain Reflectometry. However, Time-Domain Reflectometry measurements are of limited use where velocity is frequency dependent, such as in fine-grained soils. Therefore, Quarter-Wavelength Analysis was developed for measurements of velocities in fine-grained soils. The developed measurement cell was used to undertake velocity measurements in parallel with geotechnical index tests, in order to develop cross-disciplinary relationships. It was found that relationships exist between velocities and geotechnical properties, both for a wide range of soils at their Liquid Limits and for two fine-grained soils over their full saturated water content ranges. Also, it was found that Atterberg Limits can be used to define water content ranges over which different mixing models are required to relate velocity and water content. This led to initial development of mixing models specifically for the saturated state to allow more accurate use of laboratory velocity measurements in determining fine-grained soil water contents. Furthermore, it was found that variations in velocities between low and high frequencies relate to linear shrinkage. These relationships have wide-ranging uses in engineering, including rapid index testing, geo-hazard monitoring, improved electromagnetic field surveys, and researching the properties of soil pore-water.

DEDICATION

This thesis is dedicated to all researchers, past, present and future, who contribute to our understanding of the electromagnetic properties of soils and their potential to aid humanity.

Most of all, however, it is dedicated to my family.

"Every individual ... has to retain his way of thinking if he does not want to get lost in the maze of possibilities. However, nobody is sure of having taken the right road, me the least." - Albert Einstein (in a letter to John Moffat, 25th May, 1953).

ACKNOWLEDGEMENTS

CONTENTS

LIST OF FIGURES

LIST OF TABLES

GLOSSARY

Absorption - The conversion of electromagnetic energy to heat energy due to the inefficiency of charge storage, during reorientation of particles with respect to an electromagnetic field. Elevated phases of absorption accompany **dispersion** during **relaxation**.

Adsorbed Water - Water attached to the surface of a solid fraction of a soil that is considered to have reduced potential to rotate in response to an electromagnetic field, due to surface charges on a solid. Such water is generally considered to be within the **Diffuse Double Layer** and in engineering terms to have elastic, rather than viscous, properties. Also known as bound water, to contrast with **free water**, adsorbed water is considered to have a very low **permittivity** compared to other forms of liquid water.

Attenuation - Reduction in amplitude of an electromagnetic wave, as a function of distance propagated through a material.

Attenuation Coefficient (α) - Reduction in electromagnetic wave energy, per unit distance, used to determine **attenuation**.

Conductivity (σ) - The ability of charges (e.g. ionic and electronic) to move through a material. Conductivity is the inverse of **resistivity**.

Dielectric - An insulating material, such as used between capacitor plates to control the build-up of charge on them. Lossy dielectrics are those where the insulating properties are not ideal, causing loss of charge.

Dielectric Constant - The **relative permittivity** of a material (generally referring to the value at low frequencies). The dielectric constant is often not a constant at all, and so the term **relative permittivity** is preferable.

Diffuse Double Layer - A theory that the water phase around charged mineral particles will comprise a thin bound layer of ion-rich water (the Gouy layer) adjacent to mineral particles, which are themselves surrounded by a diffuse layer (the Chapman layer) that is influenced by the surface charge of the minerals in a manner that reduces with distance.

Dipolar Molecules - Dipolar molecules can be considered to be those which have net charges separated by a small distance, such that the molecule will attempt to reorient itself to an applied electromagnetic field. In soils, water forms the dominant source of dipolar molecules.

Dispersion - In the context of soil electromagnetics is a **relaxation** in the permittivity of a material with frequency, named due to the dispersion of light that has passed through a prism. However, electromagnetic dispersion should not be confused with the same term used in geotechnical engineering.

Free Space - A complete vacuum with no properties that may influence the propagation of an electromagnetic wave. Therefore, free space is a theoretical construct that differs only slightly from the concept of a vacuum.

Free Water - In the context of soil pores, free water is considered to be water which has little dependence on solid surface charges and boundaries for its properties and may act as a viscous liquid.

Impedance - The equivalent of **resistivity** for alternating signals, impedance defines the degree to which a material impedes the propagation of electromagnetic signals through it. It is defined by the **permittivity** and **magnetic permeability** of the material, as well as its means of containment. In simple terms it is the ratio of the electric to magnetic field strength in a material, akin to the resistance expressed in Ohms Law.

Impedance of Free Space - The ratio of the electric to magnetic field strength of an electromagnetic signal in **Free Space**. The impedance of free space is $120\pi \; \Omega$.

Magnetic Permeability - The ability of a material to store energy due to the lining up of atomic and electronic spins in response to an electromagnetic wave. Magnetically permeable materials may exhibit **dispersion** and **absorption** responses with frequency in a similar manner to **permittivity**.

Permittivity (ε) - The ability of a material to store energy due to the separation of charged particles (e.g. ions, atoms, electrons) in response to an electromagnetic wave.

Phase Constant (β) - A measure of the phase change, generally measured in radians, occurring for an electromagnetic wave over unit distance.

Polarization - The term polarization is used in two different ways. As used in this study, it is the degree to which energy has been stored through separation of charges. It can also be used to mean the orientation of an electromagnetic wave.

Reflection Coefficient - The amount of electromagnetic energy that is reflected from an interface between materials of differing **impedance**, expressed as a proportion of the incident energy.

Relative Permittivity (ε_r) - The ratio of the **permittivity** of a material to that of **free space** ($\varepsilon_0 = 8.854 \times 10^{-12}$ Fm^{-1}).

Relative Magnetic Permeability (μ_r) - The ratio of the **magnetic permeability** of a material to that of **free space** ($\mu_0 = 4\pi \times 10^{-7}$ Hm^{-1}).

Relaxation - A reduction in the **permittivity** of a material, over a **dispersion** spectrum, centred on a relaxation frequency, with an accompanying phase of elevated **absorption**. The probability of relaxation occurring at a particular frequency is described by the **dispersion** model for the material in question.

Resistivity (ρ) - The degree to which the ability of charges to move through a material is impeded. Resistivity is the inverse of **conductivity**.

Signal - For the purposes of this thesis a signal can be considered an electromagnetic wave purposely created to propagate through a material for determination of its velocity. Noise is therefore not a signal, but impacts on the detection of signals, the degree of impact generally being expressed as the signal-to-noise ratio,

Transmission Coefficient - The amount of electromagnetic energy that is able to pass through an interface between materials of differing **impedance**, expressed as a proportion of the incident energy.

Velocity of light (c) - The velocity of an electromagnetic wave in **free space** ($2.9979 \times 10^8 ms^{-1}$) and so also the maximum velocity that can be achieved by an electromagnetic **signal**.

Wavenumber - See **phase constant**

Wavelength (λ) - The scalar distance through which an electromagnetic wave travels during a phase change of two PI radians.

SYMBOLS AND UNITS

Symbol	Unit	Description
α	nepers.m^{-1}	Attenuation coefficient
β	rad.m^{-1}	Phase constant
γ		Propagation constant ($\alpha + j\beta$)
λ	m	Wavelength
μ	H.m^{-1}	Magnetic permeability
ω	rad.s^{-1}	Radian frequency ($2\pi f$)
ε	F.m^{-1}	Permittivity
μ_0	H.m^{-1}	Magnetic permeability of free space ($4\pi \times 10^{-7}$) [A]
ε_0	F.m^{-1}	Permittivity of free space (8.854×10^{-12}) [A]
σ_{dc}	S.m^{-1}	Static (DC) conductivity
μ_r		Relative magnetic permeability (μ/μ_0)
ε_r		Relative Permittivity ($\varepsilon/\varepsilon_0$)
ε_r^*		Apparent (relative) permittivity
c	m.s^{-1}	Velocity of light in free space (2.9979×10^8) [A]
f_{rel}	Hz	Relaxation frequency of a water molecule (c. 17 GHz @ 25˚C) [B]
I_P	%	Plasticity Index of a soil
W_L	%	Liquid Limit of a soil
W_P	%	Plastic Limit of a soil
Z	Ω	Impedance
Z_0	Ω	Impedance of free space (120π) [A]

[A] *Values taken from Calvert and Farrar, 1999.*
[B] *Values taken from Heimovaara, 1994.*

CHAPTER 1 - INTRODUCTION

1.1 OVERVIEW

As should become apparent during the progression of this thesis, a central philosophy of the research described herein is that measurement of electromagnetic signal velocities in soils is of significant use for geotechnical engineering and research. Therefore, this chapter first seeks to provide a brief background to that philosophy. Following from this, the aims and objectives of the research will be detailed, in order that readers may understand the elements considered most important for inclusion in the research. A brief description of, and introduction to, the subsequent chapters is then provided.

1.2 BACKGROUND

Near-surface engineering involves undertaking work within a complex environment (e.g. pipes, cables, soil, aggregates, concrete, voids) the properties of which are often not known in advance with certainty. Geophysical methods are becoming commonly used in an attempt to 'see' through the ground, with much interest in their potential applications (Pitchford, 1996). They are considered a useful and cost effective means by which to improve geotechnical investigations (Anderson et al., 2008) and location of buried utilities (Gamba and Belotti, 2003). They also allow for progression of non-intrusive underground construction methods that may otherwise be difficult or impossible to achieve. For instance, given the congested nature of many

urban underground spaces, there is significant potential for collision with underground features such as utilities when carrying out directional drilling, a problem which has been recognised through development of look-ahead ground penetrating radar (ORFEUS, 2009). Therefore, much recent research has focussed on improved methods and equipment (Metje et al., 2008), as well as combining them to improve performance (Metje et al., 2007).

All of these activities can be considered largely dependent on a knowledge of the geophysical properties of the near subsurface, such as soils (e.g. Topp et al., 1980; Wensink, 1993; Arcone et al., 2008), asphalts (Al-Qadi et al., 2001; Dashevsky et al., 2004) and concrete (Jaselskis et al., 2003; Lorenzo et al., 2001; Robert, 1998), and the application of those data to geophysical non-destructive testing (Bandara and Briggs, 2004; Buettner et al., 1996; Dérobert et al., 2001; Saarenketo and Scullion, 2000). Extension of previous materials characterisation work to further our ability to 'see' into the underground can, therefore, be considered important to mitigate the estimated £7billion spent annually in the UK on direct and social costs associated with street works (McMahon et al., 2005). Knowledge of the effects of these materials on geophysical signals is of significant benefit in terms of interpreting remotely located buried utility surveys (Thomas et al., 2007), which often require location within very tight tolerances (Thomas et al., 2008a). Also, there are many other engineering scenarios where an improved knowledge of soil geophysical properties would be of benefit: for example in the development of improved soil water content measurement systems (Evitt and Parkin, 2005), and in monitoring natural hazards (Kariuki et al., 2003; Chabrillat et al., 2002) such as those associated with swelling clays. In short, a greater understanding of soil geophysical properties allows for more informed planning

of geophysical survey methods, improved data interpretation, and a greater understanding of how those properties are geospatially distributed.

However, soil samples often may not be available for measurement of geophysical properties, including electromagnetic properties that are widely used for ground penetrating radar (e.g. Huisman et al., 2003a) and soil water content measurement (e.g. Robinson et al., 2003a). This is because many urban areas are primarily hard surfaced, and excavation through those surfaces to gain access to soil would cause highway disruption that would add to the costs identified by McMahon et al. (2005). Even if soil samples were readily available, the cost of undertaking sufficient electromagnetic tests to allow soil suitability mapping (extending on that of the United States - see Doolittle et al., 2006) would be very high. However, geotechnical testing is commonly undertaken as part of civil engineering projects, and large amounts of data have been gained over time from boreholes, soils reports and student projects, all of which could be available to inform electromagnetic methods if desired. Such data could also be used in conjunction with electromagnetic techniques that attempt to non-invasively reconstruct soil electromagnetic data (e.g. Lambot et al., 2004; Sugak, 2003), where such techniques can be made use of in congested urban environments.

Therefore, it could be argued that two improvements could significantly benefit our understanding of soil electromagnetic properties on a wide geographical basis. Firstly, development of simple electromagnetic measurement systems suitable for use in routine geotechnical testing could allow increased collection of soil electromagnetic data. In this thesis, the term 'simple' is used in this context to describe tests which are quick and require limited knowledge of electromagnetics, as this could be important to acceptance in many geotechnical laboratories. Secondly, through linking basic

geotechnical index tests (i.e. the most commonly employed) to soil electromagnetic properties, it could be possible to supplement direct testing with estimated electromagnetic properties. In terms of electromagnetic measurement, a simple, robust and often acceptably accurate system is available in the form of time-domain reflectometry (TDR), which measures the two-way travel time for an electrical pulse propagating along a probe, but it will be shown in this thesis that TDR in its common form does not provide sufficient detail in relation to geotechnical index tests.

In terms of interlinking geotechnical data with geophysical data, the United Kingdom can be taken as an example. Rogers et al. (2009) illustrate that the British Geological Survey (BGS) hold data covering all major population centres in the United Kingdom, including a wealth of index testing data. Those data include approximately 24500 Plastic Limits, 25500 Liquid Limits, 24500 plasticity indexes, and 11000 assessments of the proportion of fine-grained soils (i.e. $\leq 425\mu m$) (based on Rogers et al., 2009). BGS also hold soil hazard datasets that include information on soil shrinkage/swelling for the UK. Therefore, it is apparent that enabling estimation of electromagnetic properties from such geotechnical index tests as the Plastic and Liquid Limits would potentially allow exploitation of a very large amount of data, including for informing the planning of geophysical surveys.

This study therefore has two aims: to develop a simple electromagnetic signal velocity testing methodology of potential use in a geotechnical testing environment, and to further knowledge on the fine-grained soil aspect of the underground, as the dominant material found in the shallow UK urban subsurface (Rogers et al., 2009). In particular the latter aspect attempts to focus on determining potential links between simple water

content related geotechnical indicator tests and soil electromagnetic properties, as widespread data are available for such tests (Rogers et al., 2009).

1.3 AIMS AND OBJECTIVES

The central aim of this research is to extend, and improve on, TDR to include frequency-domain data, within the commonly employed frequency range of 100MHz to 1GHz, that allow consideration of potential electromagnetic dispersion in fine-grained soils. In terms of this research, electromagnetic dispersion can be defined as a variation in electromagnetic signal velocities as a function of their frequency. Therefore, the primary objectives of this research are:

1) To investigate current knowledge of electromagnetic signal velocity measurement in soils through a comprehensive literature search and review, including consideration of geotechnical factors that may be relevant to soil electromagnetic properties.

2) To obtain a range of soils suitable for use in both geotechnical and electromagnetic testing, including characterisation of their geotechnical and electromagnetic properties.

3) To devise, test and model a coaxial measurement cell, and methodology for its use, suitable for extending TDR to include data on electromagnetic dispersion directly measured in the frequency domain and with similar simplicity to use of TDR. As part of this, to discuss the potential accuracies achievable with the developed methodology, together with brief consideration of the use of TDR-style probes in place of the cell.

4) To undertake initial development of the cell and measurement methodology in a geotechnical testing environment, with similar levels of quality safeguards to those appropriate to simple geotechnical index testing, including consideration of whether relationships exist between geotechnical and electromagnetic data for saturated soils under such geotechnical laboratory conditions.

1.4 STRUCTURE OF THE THESIS

An outline of this thesis is provided in Figure 1.1. This is followed by a brief description of how the outline corresponds to subsequent thesis chapters in Table 1.1.
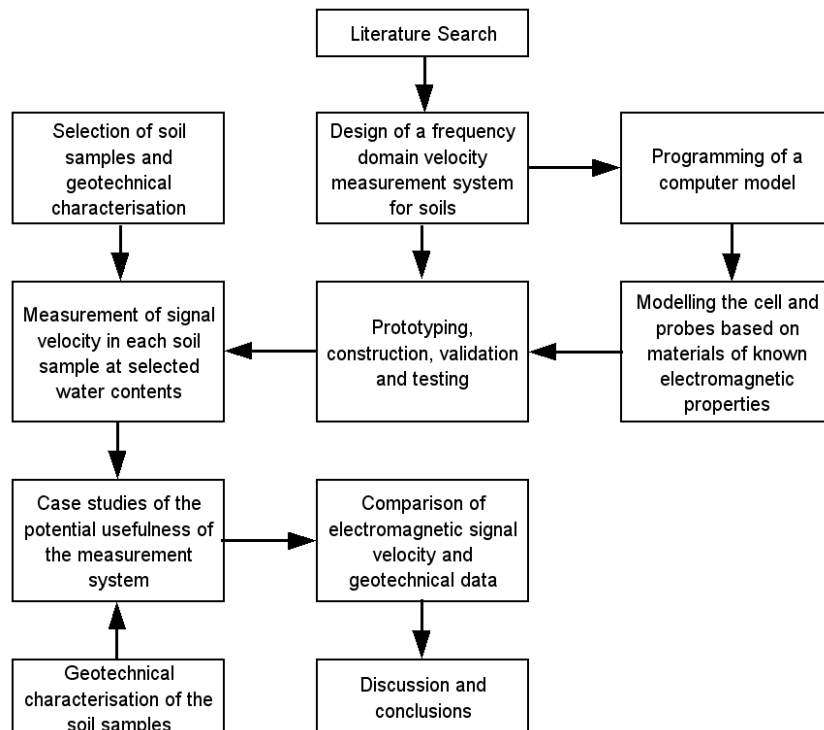
Figure 1.1. Outline structure of the research and thesis.

Table 1.1. Brief description of subsequent chapters.

Chapter	Brief description
2	Comprises the literature review, and considers the state of current knowledge available in the literature on soil electromagnetic properties and available signal velocity measurement methods for use with soils in a geotechnical testing environment.
3	Details the soils selected for use in electromagnetic signal velocity testing, providing relevant geotechnical characterisation data for each soil sample used in subsequent chapters.
4	Details the prototyping, construction, modelling and validation of the electromagnetic signal velocity testing apparatus, and its operational methodology, using a coaxial measurement cell.
5	Describes four sets of measurements designed to illustrate the potential uses for electromagnetic signal velocity data in geotechnical engineering, including relationships between those data and simple geotechnical index tests. Included in this chapter are the potential use of probes instead of cells, and the potential effects of magnetically susceptible soils on signal velocities.
6	Extends and discusses the outcomes of Chapters 3 through 5, particularly in terms of discussing the developed electromagnetic testing methodology, its potential accuracy in comparison to TDR, the links between electromagnetic and geotechnical data, the potential role that pore water plays in this, and the possibility of providing improved water content determination in fine-grained soils.
7	Provides conclusions on the outcomes of the research and suggests possible directions for continuation of this research into the future.

CHAPTER 2 – LITERATURE REVIEW

2.1 OVERVIEW

Electromagnetic waves are an integral part of daily life, bringing heat and light from the Sun, as well as allowing communications across great distances (Wilson, 1993). In their classical representation, electromagnetic waves are considered to have amplitudes that vary in a sinusoidal relationship as a function of time, frequencies that represent the number of sinusoidal cycles occurring each second, and wavelengths that are a function of frequency and velocity. The range of their frequencies and wavelengths can be described by the Electromagnetic Spectrum shown in Figure 2.1.
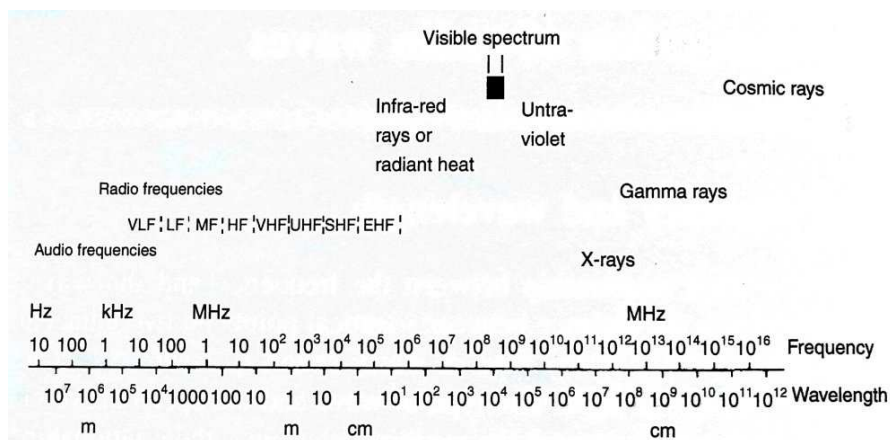
Figure 2.1. The Electromagnetic Spectrum (Winder and Carr, 2002).

For the purposes of this thesis, where frequencies are not significantly greater than a billion cycles per second (1GHz), we may limit our consideration of electromagnetic waves to radio waves and microwaves. We may also note that electromagnetic waves

may occur naturally or, as in the case of this thesis, may be artificially introduced into the material to be studied. We can represent the latter case using the term 'signals' in order to differentiate them from natural sources that may also be present in experimental data as noise.

Electromagnetic signal velocities and wavelengths vary depending on the material through which they propagate, such as soils. Therefore, there is significant complexity in the study of soil electromagnetic properties. For that reason, this literature review is intended to follow the sequence detailed below:

2.2. A brief history of electromagnetics prior to 1980: As Isaac Newton would say, to see further one must stand on the shoulders of giants, and so it is necessary to consider the long line of giants on whose work this thesis is based. This section is therefore intended to set the historical scene for an understanding of electromagnetics and its application to soils.

2.3. Fundamental electromagnetic parameters: The fundamental propagation parameters of electromagnetic signals in soils are elaborated on in order to provide an understanding of why they are important and how they relate to soil electromagnetic properties. Associated loss mechanisms are also introduced in this section.

2.4. Propagation of electromagnetic signals: Having developed an understanding of the propagation parameters, and loss mechanisms, their role in determining the velocity and attenuation of electromagnetic signals in soils will be developed in this section.

2.5. Soil as an electromagnetic propagation medium: In this section, the effect of soil properties on the electromagnetic parameters and propagation velocity, such as water content, will be considered. Variations in electromagnetic parameters due to frequency, known as electromagnetic dispersion, are also considered.

2.6. Composite soil electromagnetic properties: As electromagnetic signal velocity measurements are often used to determine soil water content, this section provides a brief introduction to the various mixing models and methods currently available for such use.

2.7. Geotechnical characterization parameters: Soil water contents, densities and mineral surface areas are important factors in the effects of soils on electromagnetic signals. Therefore, consideration will be given here to potential geotechnical parameters that provide insight into soil electromagnetic properties.

2.8. Measurement of soil electromagnetic velocity spectra: Time-domain reflectometry (TDR) will be explained and consideration will be given to potential methods of extending its use to provide data on electromagnetic dispersion in fine-grained soils.

2.9. Identified Knowledge Gaps: Knowledge gaps in the literature of relevance to this research will be identified, providing a basis for research undertaken in subsequent chapters which will attempt to fill those gaps. Significant knowledge gaps of relevance to future research, intended to build on the work contained in this research, will also be identified.

2.2 A BRIEF HISTORY OF ELECTROMAGNETICS PRIOR TO 1980

Given the common use of electricity and electromagnetic waves in our modern society, it is perhaps difficult to imagine that knowledge of them in ancient times was limited. In ancient Greece it was known that rubbing amber would allow it to attract straw (Kirby et al., 1990). This observation is credited to Thales of Miletus (640-546BC), who also knew that lodestone (i.e. magnetite) could attract iron (Cajori, 1935). The attraction of straw to amber may appear simple, but it is from the term amber (known as electron in ancient Greece) that the word electricity originates. Although there is some evidence that small earthenware pots were used as batteries in Iraq as early as 2000 years ago (Staubach, 2005), Shadowitz (1998) describes the intervening time between the work of ancient Greece, and the birth of modern scientific investigation, as "Twenty-two centuries of standing still!". However, Shadowitz may have been a little unfair in this comment, as the related branch of optics was studied by Al Hasen (c.965-1038) who extended Greek knowledge of reflection angles (an early form of Snells Law) and studied **reflections** from mirrors. The ending point for Shadowitz's period of standing still may be ascribed to William Gilbert who, in 1600 AD, published his findings that amber was not the only material that could be used to attract other materials, and that it was also possible to cause a repulsive force (Shadowitz, 1988). However, in terms of our ability to utilise electricity for the generation of electromagnetic signals, potentially the most important milestone is the invention of the electric battery, then termed a pile, by Alessandro Volta and announced in 1800 (Kirby et al., 1990). This provided a power source for many ensuing experiments, including those of Humphrey Davy (Cajori, 1935) and subsequently of his apprentice Michael Faraday (Faraday, 1861).

In the early 19th century electricity and magnetism became an important part of natural philosophy. In 1819 Hans Christian Oersted carried out his famous experiment to deflect a magnetic needle using a current carrying wire, and the field of **electromagnetics** was born (Cajori, 1935). Experiments were later carried out in an attempt to show rotation of current carrying wires around a permanent magnet (Morus, 2004) and the great experimental scientist Michael Faraday is credited as the first scientist to demonstrate this (Kirby et al., 1990), a significant milestone that, in fact, almost ended his career (Morus, 2004). This led to the development of the electric motor, but Faraday also realised that the reverse was true: a moving magnetic field could be used to generate electricity and that it was the relative motion of the two that produced this effect (Kirby et al., 1990). This was the birth of the alternating, or oscillatory, electrical potential and so it could be argued that Faraday's 1820 experiments (Figure 2.2), in taking us beyond direct current electricity, provided the concept of the **sinusoidal signal** and its **frequency**.
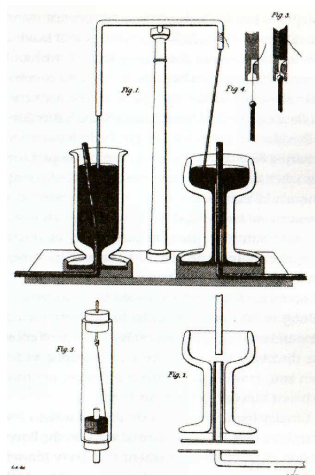
Figure 2.2. Faraday's 1820 rotating wire experiments (Morus, 2004).

Soon afterwards, a further fundamental propagation parameter can be argued to have come from the work of Georg Simon Ohm who, in 1826, published experimental proof of Ohms law (Cajori, 1935). Ohms law states that the resistance of a material to electricity causes proportionality between the applied voltage and the resulting current flow, giving rise to the principle of **conductivity** which will, in subsequent sections, be seen to be an important concept in electromagnetic signal propagation.

Although Ohms law relates to the direct current electricity relevant to Volta's batteries, it paved the way for the concept of **impedance** in alternating current flow, which is important in determining the strength of electromagnetic reflections at boundaries. This was obviously an exciting time in the development of electromagnetics as, within a decade, Faraday had realised that electric charges were not unaffected in the propagation of their force by intervening matter, and so he coined the term 'dielectrics' to describe this phenomenon (Cajori, 1935). Using a version of a Leyden Jar, Faraday showed that the attractive or repulsive forces were scaled by the properties of a material used in place of air within the jar. In using air as a reference for this scaling effect, Faraday essentially conceived of the **dielectric constant**, or **relative permittivity**, that is also now a fundamental parameter for electromagnetic signal propagation.

Through the above achievements, Faraday developed the concept of lines of force, and speculated that light, electricity and magnetism are related (Cajori, 1935), providing a significant foundation for later scientific investigations in electromagnetics. One of the most important scientists involved in that later work was James Clerk Maxwell who, in contrast to the great experimental skills of Faraday, was a great theorist. His theoretical skills allowed him to translate the experimental work of Gauss and Faraday

into mathematical terms (Cajori, 1935), from which he was able to significantly expand on them. The famous Maxwell Equations describing the **propagation** of electromagnetic energy still provide the basis for our classical understanding, which is significant when one considers that Maxwell worked at a time when the nature of electromagnetic waves was unknown and that he considered propagation to be within an 'all pervading ether'. As described by Everitt (1975), Maxwell's ether (Figure 2.3) was made up of minute vortices and "Each vortex is separated from its neighbours by a layer of minute particles, identified with electricity, counter-rotating like the idle wheels of a gear train." Science has since largely dismissed the ether, but Maxwell provided a theory that fitted with real world observations and so is still of great use to this day.
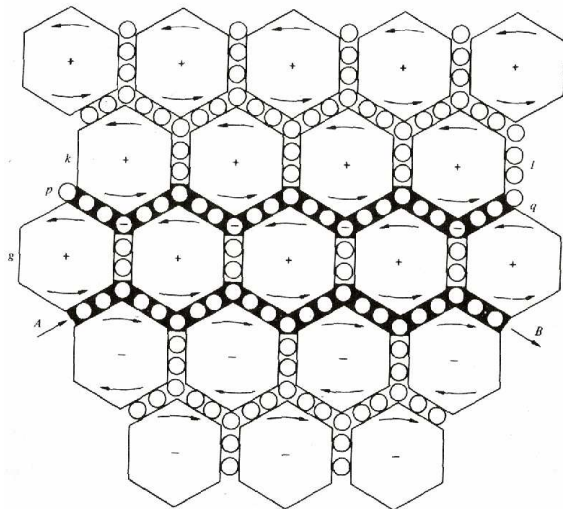
Figure 2.3. Maxwell's 1861 concept of the ether (Everitt, 1975).

While Maxwell's work provided a significant advancement in knowledge of electromagnetic propagation, it was considered unwieldy for general use. His equations

were therefore simplified, and adapted to describe electric and magnetic field vectors, by Oliver Heaviside at the end of the 19th Century (Crease, 2009). It should be noted that Heaviside was also responsible for incorporating **imaginary numbers** into electrical analysis (Crease, 2009).

Maxwell's Equations are described by Equations 2.1 to 2.4 (Fleisch, 2008). As well as describing the motion of an electromagnetic signal, Maxwell's Equations were also used to show that even a vacuum has an **impedance** (377Ω - Hayt and Buck, 2006) and from this can be determined the **velocity of light** *in-vacuo*. Of particular significance, however, is that Maxwell's Equations provided an insight into the connected nature of electric and magnetic fields: i.e. that a magnetic field can give rise to an electric field, and *vice versa* (Fleisch, 2008).

$$\nabla \bullet \mathbf{E} = \frac{\rho}{\varepsilon_0} \qquad\qquad\qquad \text{[Eq. 2.1]}$$

$$\nabla \times \mathbf{E} = -\frac{\delta \mathbf{B}}{\delta t} \qquad\qquad\qquad \text{[Eq. 2.2]}$$

$$\nabla \bullet \mathbf{B} = 0 \qquad\qquad\qquad \text{[Eq. 2.3]}$$

$$\nabla \times \mathbf{B} = \mu_0 \left(\mathbf{J} + \varepsilon_0 \frac{\delta \mathbf{E}}{\delta \mathbf{t}} \right) \qquad\qquad\qquad \text{[Eq. 2.4]}$$

where $\mathbf{E}$ is the electric field (v.m^{-1}), $\mathbf{B}$ is the magnetic field (webers.m^{-2}), ρ is the charge density (C.m^{-3}), t is time (s), $\mathbf{J}$ is the current density (A.m^{-2}), and μ_0 and ε_0 are respectively the **magnetic permeability** and **permittivity** of **free space** (e.g. a vacuum or, in Maxwell's time, the ether).

However, despite the brilliance of his work, Maxwell's Equations were always purely theoretical during his life. Although a number of scientists came close to discovering electromagnetic waves, this proof came from Heinrich Rudolf Hertz who, in 1888, developed a means of detecting electromagnetic waves caused by sparks in Leyden jars (Cajori, 1935). Hertz was thus able to show that electromagnetic waves exist, that they may be reflected and transmitted, and that they can interfere constructively, and destructively, to create maxima and minima in **interference patterns**. The ability to detect electromagnetic waves sparked a whole new area of study, that of using them to transmit information: in 1901 Marconi made the first trans-Atlantic radio transmission, making him famous and marking a turning point in our ability to control and utilise electromagnetic waves.

It was also around this time that advances were made in other aspects of electromagnetic propagation that are important to soils research. Newton had already undertaken experiments on **dispersion** of light through prisms and it was known that materials have a refractive index, i.e. light may travel through them at different velocities to those in a vacuum. Fox Talbot, in the 19th century, knew of **anomalous dispersion** where the dispersion of light is different to that of a prism, and that some wavelengths may be absorbed more than others (Cajori, 1935). Drude (1902) made advances in this area and helped define our modern understanding of anomalous dispersion, which he says would occur only where the investigation covered natural periods (i.e. of oscillation) of ions. Further work culminated in the theories of Debye (1929) who defined the frequency dependence of water from which the associated variations in electromagnetic wave **velocity** and **attenuation** may be determined. Debye's theories also considered the effects of ions in solution on the permittivity of

water and this is significant given the work between c.1879 and c.1924 on diffuse double layer theory, which can be attributed to the work of Helmholtz, Nernst, Gouy, Chapman and Stern, amongst others. Their work provided a theoretical description of the distribution of mineral surface charges and ions within soil pores, which can be considered an important aspect of **anomalous dispersion** in soil pore water. It is this **anomalous dispersion** that we now term simply **electromagnetic dispersion** when referring to differing electromagnetic properties in soils at different frequencies. Further refinements were made to the theories of Debye in subsequent years, including the work of Cole and Cole (1941), but the basic principle that water has a **relaxation frequency**, around which the **velocity** and **attenuation** of electromagnetic waves vary, was by then well established.

Given the widespread adoption of electromagnetic waves for communications using radio, it is not surprising that researchers started to consider the electromagnetic properties of soils. Of particular note is the work of Smith-Rose (1935) who found **electromagnetic dispersion** in soils, and Cownie and Palmer (1951) who advanced the theory that more than one form of water may exist in a soil: **bound water** and **free water**. This hypothesis was based on the fact that the **permittivity** of some soils, at low water contents, does not increase in proportion to the amount of water added, but at higher water contents significant increases occur. However, it also brings forward another aspect of soil electromagnetics: that the different types of water may have different **relaxation frequencies**, causing a great deal of complexity in determining the frequency dependence of electromagnetic properties in electromagnetically **dispersive soils**. Over the subsequent decades research into soil electromagnetic properties steadily progressed. Of note during those times is the work of Hoekstra and Delaney (1974) who

used a **time-domain reflectometry** (**TDR**) technique (with inversion to the frequency domain) to measure the electromagnetic properties of both sand and clay. Their data showed that the soils exhibited **dispersion** of a Debye (1929) type as well as illustrating low water content variations due to **bound water** and **free water**. However, their system was limited to **gravimetric water contents** up to 15%, thus limiting our interpretation of their data.

Of particular significance was that, during this time, other researchers were also using **TDR** for determination of soil water content and their equipment was based on commercial cable testers. That fact, small as it may seem, allowed the widespread testing of soil electromagnetic properties, and their application to soil state monitoring. This work culminated in the seminal paper of Topp et al. (1980) and the work they described has become the basis for the highly popular field of soil **TDR**. Although this work faced initial strong opposition (Topp et al., 2003), it also provided a model for relating an **apparent permittivity** (essentially a representation of signal velocity) to **volumetric water content**, thus helping ensure its subsequent success. The work of Hoekstra and Delaney (1974) and Topp et al. (1980) also demonstrates significant difficulty associated with soil electromagnetic measurements: different researchers often use different measures of water content.

In concluding this introduction we must understand that the equations of Maxwell, and others, associated with the propagation of electromagnetic waves, are a classical representation of what is, in effect, a quantum system. Feynman (1985) quite clearly states that electromagnetic energy does not exist in the form of waves, but rather as packets (or quanta) of energy known as **photons,** which have rotational properties

giving rise to apparently sinusoidal variations in intensity with time and distance. Through his work on Quantum Electro-Dynamics, he also showed that our classical concepts of the constant velocity of light in a vacuum, and even the laws of reflection and refraction, are actually only based on the fact that photons not following those rules cancel each other out, due to their incompatible phases (Feynman, 1985). Furthermore, Einstein's theory of relativity showed that even the **magnetic field** is illusory, it being a representation of the transformation of an **electric field** for a moving observer, and that the apparent discrepancy this holds for permanent magnets can be explained by the relativistic effects caused by electrons having spin (Shadowitz, 1988). While an understanding of these quantum effects is not necessary in order to understand the classical rules for electromagnetic wave propagation, it is important to understand that it is just that: a representation that allows us to dispense with much of the overwhelming complexity we would otherwise have to work within.

2.3 FUNDAMENTAL ELECTROMAGNETIC PARAMETERS

2.3.1 Introduction

The propagation of electromagnetic waves is governed by four basic parameters:

Frequency (f): A measure of the variation in amplitude occurring in an electromagnetic signal as a function of time. This variation can be considered sinusoidal for single-frequency signals, or a convolution of a number of sine-waves where an electrical pulse is used.

Conductivity (σ): A measure of the degree to which a soil allows the passage of

electrical charge through it. In most soils the conductivity is ionic and so dependent on the prevalence and mobility of ions in the pore water.

Permittivity (ε): A measure of the signal energy that can be stored in a material, through separation of charges (e.g. ions, protons, electrons) in a material. Permittivity is divided between a real part representing the storage of energy (ε') and an imaginary part representing loss mechanisms that degrade energy storage (ε''). The permittivity of a material is generally expressed in terms of its ratio to the permittivity of a vacuum, and then is known as the relative permittivity or dielectric constant (ε_r).

Magnetic permeability (μ): A measure of signal energy stored in a material due to the lining up of atomic and sub-atomic particle spin directions. As with permittivity, magnetic permeability can be divided into real (μ') and imaginary (μ'') aspects, although in practice most soils are considered to have simple magnetic properties and so loss mechanisms are often ignored. It is also commonly referred to as a relative property based on its ratio to the magnetic permeability of a vacuum (μ_r).

These factors, in combination, determine the velocities of electromagnetic signals (Reppert et al., 2000; Reynolds, 1997), their attenuation, or loss of energy, over distance (Milsom, 1996) and even the degree to which they will be reflected by sub-surface objects and interfaces (Leckerbusch and Peikert, 2001). In soils these parameters will vary due to the proportions of mineral particles, water and air within the soil matrix (Saarenketo, 1998), with water potentially the most significant of these constituents.

These factors create significant complexity in modelling the propagation of electromagnetic waves in the sub-surface, often causing assumptions to be made in the

interpretation of geophysical survey data. Therefore, in order to consider the electromagnetic properties of soils, it is important first to consider in detail the four basic propagation parameters, prior to developing an understanding of how they relate to velocity and attenuation.

2.3.2 Frequency

Single-frequency electromagnetic signals can be described using the sinusoidal relationship shown in Figure 2.4, where the amplitude, or signal strength, varies as a sine function of a change in phase angle. Such sinusoidal signals have a wavelength representing a phase change range of 2π radians (i.e. 360°), and an amplitude that varies with the phase angle. In Figure 2.4, the maxima are used by convention to represent the wavelength, but any other identifiable repetitive points may also be used.

In mathematical terms, this relationship can be described using Equation 2.5. In electromagnetics research, the amplitude can be considered both in terms of the voltage of a sinusoidal signal in an electrical conductor and as the voltage potential that an electromagnetic signal can induce in a conductor per unit of length (i.e. measured in $V.m^{-1}$).

$$A_1 = A_0 \sin(\omega t + \theta) \hspace{4cm} \text{[Eq. 2.5]}$$

where A_1 is the amplitude at time t (s) along the signal propagation path, A_0 is the maximum signal amplitude, and ω is the phase change per unit time ($rad.s^{-1}$). The parameter θ (radians) is used to adjust the phase to compensate for phase angles not equal to zero at time zero. $\omega t + \theta$ is therefore the angle of phase change at time t.

Based on Equation 2.5, it can be seen that the wavelength can also be represented as a period of oscillation, i.e. the time taken for the wave to complete one wavelength. The number of such oscillation cycles completed each second thereby defines the frequency (f), which is measured in Hertz (Hz). There are, therefore, two representations of frequency used in electromagnetic measurements, one based on cycles per second (f), and one based on phase angle change per second (ω). These are simply related, as described in Equation 2.6.
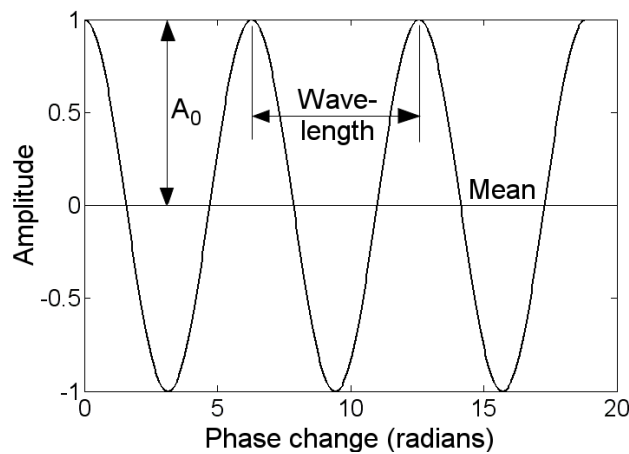
Figure 2.4. A sinusoidal signal.

$$\omega = 2\pi f \qquad\qquad\qquad\qquad \text{[Eq. 2.6]}$$

where f is the frequency (Hz).

On entering a physical medium, such as soil, the frequency of an electromagnetic wave is unaffected by the physical and electrical properties of that medium. However, it is apparent from Equation 2.5 that changes in velocity will result in different phase changes, due to the corresponding change in propagation time. Therefore, the velocity (v) and wavelength will alter while the frequency (and so the oscillation period) remains

constant (Tareev, 1975). This illustrates that the frequency of an electromagnetic signal is related not just to wavelength but also to velocity, as illustrated in Equation 2.7.

$$\lambda = \frac{v}{f}$$ [Eq. 2.7]

where v is the velocity (m.s^{-1}) and λ is the wavelength (m).

2.3.3 Conductivity

The conductivity of a material can be considered to be the extent to which it allows, or impedes, the movement of an electric charge through it. This is particularly important in geophysical investigations because highly conductive materials rapidly dissipate electromagnetic energy and so restrict the depth to which surveys can penetrate (Doolittle and Collins, 1995). In fact, it has been said that many soils, because of their high electrical conductivity, are essentially opaque to electromagnetic signals (Holden et al., 2002). There are three ways in which a current may flow in a soil, each of which contributes to the materials conductivity. These can be summarized as (after Reynolds, 1997):

Electrolytic –involves the relatively slow motion of ions in an electrolyte towards an opposite charge (i.e. cations toward a positive charge and anions toward a negative charge).

Electronic –involves the more rapid motion of electrons towards a positive charge, as in metals. Electronic conduction is also known as 'ohmic' conduction.

Dielectric –involves the separation of charges at atomic level (generally in weakly conducting, or insulating, materials) in response to electromagnetic radiation. The

separation of charges then causes an induced electric field that opposes the incident signal (Fleisch, 2008).

Perhaps the most important equation governing the relationship between applied electromagnetic field intensity and current density is Ohms Law (Nabighian, 1987). This states that the current (I) flowing in a given material is proportional to the electrical potential (V) across that material (Duncan, 1997). This proportionality is governed by the resistance (R), a measure of the degree to which current flow is impeded, and can be summarised in Equation 2.8.

$$V = IR \hspace{4cm} \text{[Eq. 2.8]}$$

where V is voltage (V), I is current (A) and R is resistance (Ω).

However, it should be noted that the resistivity of a material is only a part of the overall extent to which the motion of a charge can be impeded. In an alternating potential, such as in the case of an electromagnetic signal, further resistance to current flow will result from the reactance of the material. The total opposition to current flow in a material is based on both the resistance and reactance and is termed the impedance. In situations of alternating potential, the impedance (Z Ω) replaces the resistance in Ohms Law (Duncan, 1997).

For soils the resistance is generally referred to independently of the physical dimensions of the electrical flow path. Two interrelated properties of a material are commonly used to characterise this property, these being the resistivity and the conductivity, which are inversely proportional (Nabighian, 1997): see Equation 2.9.

$$\rho_R = \frac{1}{\sigma}$$
[Eq. 2.9]

where ρ_R is the resistivity ($\Omega.m$) and σ is the conductivity ($S.m^{-1}$).

For a theoretical unit block of material, the resistance is proportional to the length of the current path, and inversely proportional to the cross sectional area. Therefore, the relationship between resistance and resistivity of a material can be summarized in Equation 2.10 (Tareev, 1975).

$$R = \rho_R \frac{L}{A}$$
[Eq. 2.10]

where R is the resistance (Ω), ρ_R is the resistivity ($\Omega.m$), A is the cross sectional area (m^2) and L is the length (m), which, using Ohms Law, rearranges to Equation 2.11 (Reynolds, 1997).

$$\rho_R = \frac{VA}{IL}$$
[Eq. 2.11]

where V is the voltage (V) and I is the current (A).

In most soils, conduction occurs by way of pore fluids acting as an electrolyte, with the actual grains, except in rare cases where they are themselves good electrical conductors, contributing very little to the overall conductivity of the material (Reynolds 1997). The flow of a current through such materials would, therefore, depend on such factors as the type of ion in the pore water solution, the ionic concentration and the mobility of ions. For clays, resistivity is usually considered to be within the range 1 to 100 $\Omega.m$ (Giao et al., 2003). However, in their study of clays Giao et al. (2003) reported

a much smaller range (1 to 12 Ω.m) indicating that variation in clay resistivity is likely to be location, mineralogy and pore water chemistry specific.

Many factors affect the conductivity of soils, making their values a dynamic quantity based on diverse environmental factors. For instance, it has been identified that the interconnectedness of conducting minerals in a soil will have a significant effect on the extent to which they interact with electromagnetic signals (Van Blaricom, 1980). It should also be noted that, due to the electrolytic nature of conductivity in soils, the dielectric properties of pore water influence ionic concentration, due to a direct relationship to the mutual attraction of ions in solution. For example, the attraction between two oppositely charged ions dissolved in water is approximately 1/81 as strong as it would be in air. This, together with the fact that water molecules tend to attach themselves to ions, results in water having a high capacity to dissolve ionic substances (Brownlow, 1996). Also, the conductivity of a mineral is not necessarily constant and may vary with time, temperature, pressure and other factors (Nabighian, 1987).

2.3.4 Permittivity

In simple terms, permittivity is a measure of the amount of electric field energy stored in a medium, as demonstrated by Faraday's experiments in a Leyden Jar. This can be described as the polarization of atoms and molecules: the separation of charges in a material when an electric field is applied (Saarenketo, 1998), from equilibrium to non-neutral positions until the force between them balances the applied force of the electric field (Nabighian, 1987). Four polarization mechanisms are relevant to the permittivity of soils (Nabighian, 1987, Saarenketo, 1998 and Tareev, 1975):

Electronic polarization – A separation of sub-atomic charges (i.e. protons and electrons) within an atom, thus causing a deformation in the shape of the electron cloud surrounding the atomic nucleus and so of the atom or molecule as a whole, in response to an electromagnetic wave.

Atomic polarization – A separation of the positively and negatively charged component ions of a molecule in response to an electromagnetic wave.

Dipolar polarization – A separation of charges between dipolar molecules due to the rotation of the molecule away from a position of equilibrium, in response to an electromagnetic wave. In saturated earth materials, such as clays, this is considered the most significant form of polarization (Carreón-Freyre et al., 2003).

Space charge polarization – A separation of charges due to the drifting of dissociated ions away from equilibrium positions in response to an electromagnetic wave, and possibly toward opposite charges from which they are generally repelled.

The polarization of individual atoms and molecules, for all polarization mechanisms, can be summarized as the product of the distance vector involved in the charge separation and the atomic charge involved (therefore measured in coulomb-metres), and is termed the induced electric moment (Equation 2.12, Shadowitz, 1988).

$$\mathbf{P} = Np \hspace{4cm} \text{[Eq. 2.12]}$$

where the vector P is the Polarization (Coulomb.m), N is the number of atoms or molecules and p is the induced dipole moment vector per atom or molecule (Coulomb.m). Dipole moments for pure unconfined water are approximately 6.2×10^{-30} Coulomb.m (Good, 1999).

As described in Equation 2.12, the overall polarization of a homogenous medium containing atoms or molecules, each with an induced dipole moment, is a function of the number of atoms or molecules present. It should also be noted that it is a vector property and so, in the presence of more than one electromagnetic signal, the polarization may be increased or decreased dependent upon the relative direction of each vector.

However, for low field strengths, as is the case for geophysical survey techniques, **P**/N may be significantly less than p due to the thermal agitation of molecules occurring in water (Good, 1999), which acts against the applied electromagnetic field. An important aspect of Equation 2.12, known since the early days of soil electromagnetic testing (Millard, 1953), can be seen in Figure 2.5: an increase in soil bulk density can cause an increase in permittivity.

As increased bulk density will increase the number of atoms and molecules present (N) and available for polarization, it can be expected that variations in soil electromagnetic properties will occur due to density, and so also water content, variations.

In order to account for the effects of temperature on the ability of an applied field to polarize a material, Equation 2.12 may be replaced by the Langevin Formula shown in Equation 2.13 (Good, 1999). Also, from the perspective of measuring electromagnetic properties, it highlights the need to ensure that temperature variations are small, although under normal geotechnical testing conditions this may be difficult.

$$\frac{\mathbf{P}}{N} = p\frac{pE}{3kT} \qquad\qquad\qquad \text{[Eq. 2.13]}$$

where k is the Boltzman Constant (1.381×10^{-23} J/K), E is the electric field strength
($V.m^{-1}$) and T is the absolute temperature.
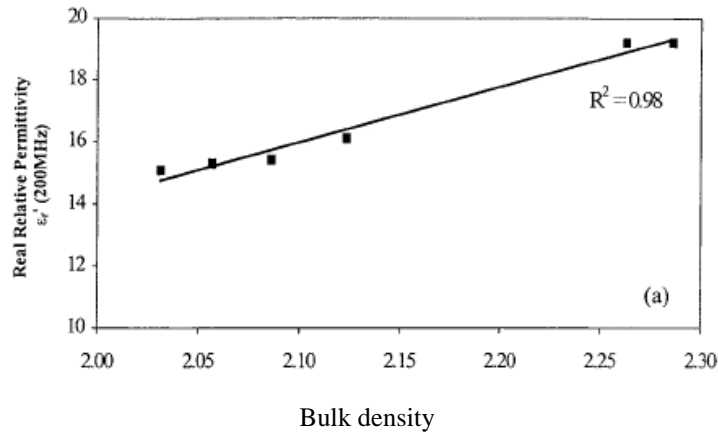
Figure 2.5. The effects of bulk density on soil permittivity (Scholte et al., 2002).

Equation 2.13 also illustrates that the electromagnetic properties of a material may
be dependent on the electrical field strength that it is subjected to. It is therefore
important to note that electromagnetic measurements are generally undertaken at low
signal strengths as dielectrics are generally then insensitive to voltage variations below
a threshold at which breakdown of the dielectric properties of the material occur
(Tareev, 1975).

The permittivity of a material is often referred to as its ratio to the permittivity of
a vacuum. This value is known as the relative permittivity, which can be calculated
using Equation 2.14 (Tareev, 1975). The relative permittivity is also often referred to as
the dielectric constant.

$$\varepsilon_r = \frac{\varepsilon_d}{\varepsilon_0}$$ [Eq. 2.14]

where ε_r is the relative permittivity, ε_d is the permittivity of the dielectric and ε_0 is the permittivity of free space (8.85×10^{-12} F.m^{-1} – Reynolds, 1997, Nabighian, 1987).

However, its value varies with such factors as temperature and pressure (Tareev, 1975), as well as with water content and density (Saarenketo, 1998). Also, it can only be treated as a constant in low-frequency, low-loss situations (Dobbs, 1984). Therefore, the term dielectric 'constant' should be used with care, in order to minimize ambiguity.

The value of relative permittivity for air, as with many other gases, is generally quoted as unity, even though the actual value is approximately 1.00058 (Tareev, 1975) this small difference generally being considered insignificant. Similarly, for water the relative permittivity is often taken as approximately 80 or 81 even though small variations may occur due to temperature and ion content.

In order for any understanding of the permittivity of a material containing water to be complete it is necessary to consider the frequency dependence of the water phase. All polarization mechanisms are subject to relaxation phenomena, where the permittivity reduces around a particular 'relaxation frequency'. This is accompanied by increased absorption of energy, and associated loss of that energy as heat. The change in permittivity around the relaxation frequency gives rise to frequency dependence that is termed electromagnetic dispersion as illustrated, for pure unconfined water, in Figure 2.6 (Logsdon, 2005a).

The frequency at which relaxation occurs is a result of the time required by the

water dipole to reorient itself to an equilibrium state once the induced field returns to

zero, as reduction of the oscillation period with increasing frequency will affect the time

available for the reorientation to occur.
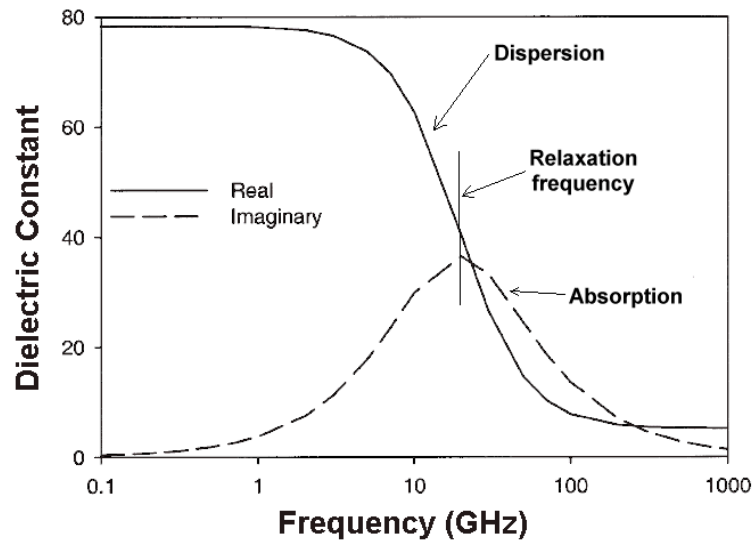
Figure 2.6. Dispersion and absorption in water (after Logsdon, 2005a).

Wu (1964) showed that this frequency relates to water content in fine-grained

soils, with significantly increased relaxation times when the water content comprises

two to three molecular layers. This reorientation is illustrated in Figure 2.7, which

shows the dipole moment of a water molecule (Figure 2.7(a)), effectively describing the

separation of an atomic charge over a small distance, together with the effect of an

electromagnetic signal on the preferred orientation of water molecules. In the absence of

a signal, the water molecules take up random orientations determined by the hydrogen-

bonding between them and fluctuations due to temperature (Figure 2.7(b)). When a

signal is introduced, there is a tendency for water molecules to align themselves to the

signal propagation direction (Figure 2.7(c)). The time period is referred to as the

relaxation time and, in the Debye (1929) model, is calculated using Equation 2.15.

$$\tau_D = \frac{\zeta}{2kT}$$ [Eq. 2.15]

where τ_D is the relaxation time (s), k is the Boltzman Constant, T is the absolute temperature and ζ is a constant referring to the friction controlling the rotation of a water molecule.
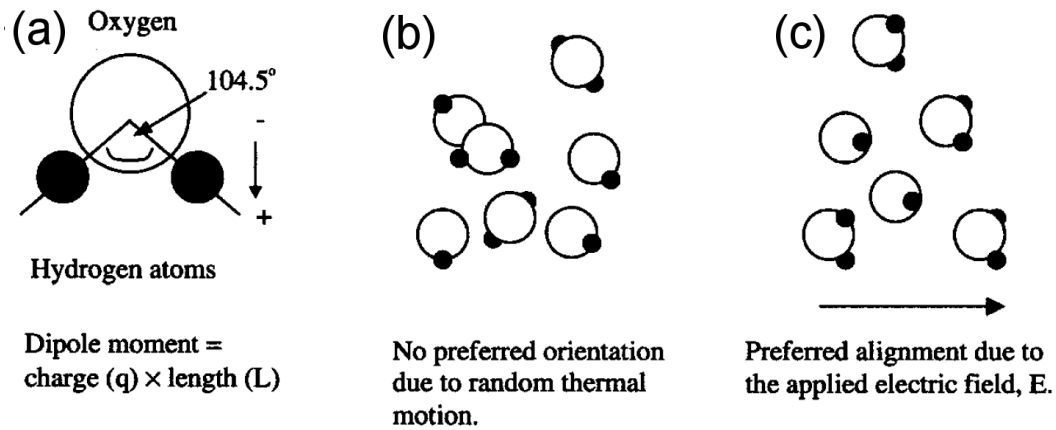
Figure 2.7. Dipolar relaxation (a) the dipole moment of water, and water molecules (b) without and (c) with an external field applied (after Robinson et al., 2003a).

The friction constant given by Debye (1929) relates to the macroscopic friction encountered by a sphere rotating within a liquid, and is therefore based on Stokes' Law as shown in Equation 2.16.

$$\zeta = 8\pi\eta a^3$$ [Eq. 2.16]

where η is the dynamic, or shear, viscosity and a is the radius of the spherically

represented water molecule. For ordinary room temperatures (c. 17 to 22ºC), $\eta = 0.01$ and $a = 2 \times 10^{-8}$ m (Debye, 1929).

Debye gave the relaxation time of a water molecule as approximately 0.25×10^{-10} seconds (Debye, 1929). As the relaxation frequency is inversely proportional to the relaxation time, it can be calculated using Equation 2.17. The relaxation frequency, for pure unconfined water, has thus been estimated as 17.113 GHz at 25˚C (Heimovaara, 1994).

$$f_{rel} = \frac{1}{\tau_D}$$
[Eq. 2.17]

where f_{rel} is the relaxation frequency (Hz).

As well as allowing calculation of the relaxation time of water, the work of Debye resulted in a model for the frequency dependence of the real and imaginary permittivities, as shown in Equation 2.18.

$$\varepsilon_r = \varepsilon_{r\infty} + \frac{\varepsilon_{rs} - \varepsilon_{r\infty}}{1 + j\omega\tau_D}$$
[Eq. 2.18]

where ε_r is the frequency dependent relative permittivity, $\varepsilon_{r\infty}$ is the high frequency relative permittivity (i.e. at frequencies above relaxation) and ε_{rs} is the low frequency relative permittivity (i.e. significantly below relaxation).

While the results of the Debye model are considered to be generally in agreement with observation (e.g. Kaatze, 1989), minor criticisms can be made. One such criticism is that the model only relates to a single relaxation frequency which does not entirely agree with observation (Cole and Cole, 1941). Also, the symmetry of dispersion and

absorption, around the relaxation frequency, exhibited by the Debye model, has not always been fully evident for materials other than water and this has resulted in a number of alternative forms of the Debye relationships, such as the Cole and Cole, Davidson and Cole, and Havriliak and Negami equations (Kao, 2004). These alternative equations are based closely on those of Debye, with additional parameters added to allow modification of the shape of the Debye data. However, the most widely used alternative to the Debye (1929) model, in soils literature, is that of Cole and Cole (1941) shown in Equation 2.19.

$$\varepsilon_r = \varepsilon_{r\infty} + \frac{\varepsilon_{rs} - \varepsilon_{r\infty}}{1 + (j\omega\tau)^a} \qquad \text{[Eq. 2.19]}$$

where a is a fitting parameter appropriate to the material.

However, as these models only represent dielectric mechanisms, they require adaptation to include the effects of conductive losses, as can be achieved through Equation 2.20 (Kao, 2004, Hasted, 1973). From this formula, it can be expected that the effects of conductivity, as a loss mechanism, will diminish with frequency. In testing over a wide range of soil types, including clays, Wensink (1993) found that the permittivity was only weakly dependent on pore water salinity at frequencies around 1GHz, but the dependence increased as the frequency reduced.

$$\varepsilon_r^* = \varepsilon_{r\infty} + \frac{\varepsilon_{rs} - \varepsilon_{r\infty}}{1 + (j\omega\tau)^a} - j\frac{\sigma_S}{\omega\varepsilon_0} \qquad \text{[Eq. 2.20]}$$

where σ_S is the static, direct current, conductivity (S.m^{-1}).

It should also be noted that the Debye model was formulated from a macroscopic

phenomenon (i.e. viscosity) that cannot easily be applied to the microscopic realm of the water molecule and preceded any conclusive evidence for the molecular structure of the hydrogen-oxygen-hydrogen atom configuration. The availability of associated hydrogen bonds has since been proposed as the controlling mechanism for the relaxation frequency of unconfined water (Buchner et al., 1999) and the reduction in permittivity of water close to interfaces (Despa et al., 2004). Research on water structure (Eisenberg and Kauzmann, 1969; Zahn, 2004), and the relaxation of water molecules (e.g. Agmon, 1996; Buchner et al., 1999; Kropman and Bakker, 2004; Logsdon and Laird, 2004) has largely concentrated on the energy required to allow a water molecule to rotate through an energy barrier to a new hydrogen bonded configuration, rather than having to relax to its original equilibrium state. The relaxation time for such a model can be represented through the Arhenius Equation described in Equation 2.21 (Jansson and Swenson, 2003, Kao, 2004).

$$\tau_D = \tau_0 \exp\left(\frac{H}{kT}\right) \qquad\qquad \text{[Eq. 2.21]}$$

where τ_D is the relaxation time (s), τ_0 is an empirical factor, H is the activation energy (i.e. the energy barrier that must be overcome in order to break hydrogen bonds), k is the Boltzman Constant and T is the absolute temperature.

A final aspect of the work of Debye that should be considered here is that the dissolved ions associated with ionic conduction in soil pore water are not just of importance in the measurement of conductivity, but also affect the permittivity. Debye theorised that electrical saturation may occur around ions in water, in that the field strength of the ion (see Equation 2.22) may be much larger than that of the externally

applied field, causing a spherical 'cavity' within which water molecules are rendered

inactive (Debye, 1929). As shown in Figure 2.8, this effect may cause a slight reduction

in permittivity as the salinity of the pore water increases.

$$E_{ion} = \frac{e_{ion}}{\varepsilon_{water} r^2}$$ [Eq. 2.22]

where E_{ion} is the effective charge, ε_{water} is the permittivity of the surrounding water, e_{ion}

is the ionic charge and r is the distance from the centre of the ion. Debye proposed that

the water permittivity, at small concentrations, could be expressed through a function of

the form shown in Equation 2.23.

$$\varepsilon_{water} = \varepsilon_{noion} (1 - a.c)$$ [Eq. 2.23]

where ε_{water} is the permittivity of the water phase, ε_{noion} is the permittivity of the water

phase in the absence of dissolved ions, a is a constant characteristic of the salt and c is

the concentration (mol.l^{-1}).
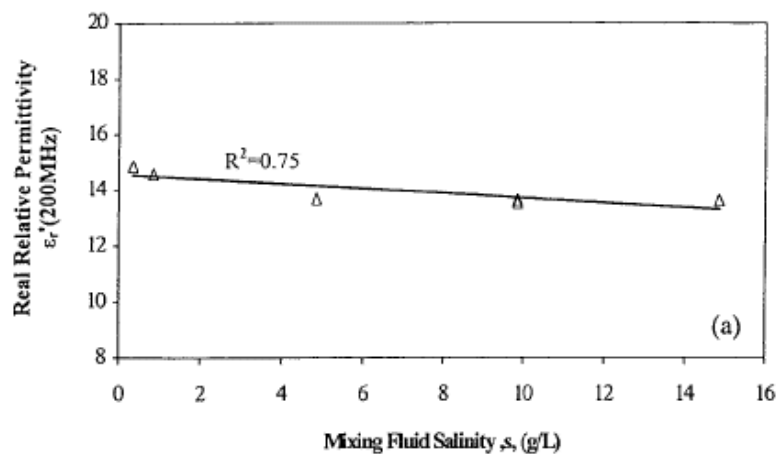
Figure 2.8. The effects of water salinity on its permittivity (Scholte et al., 2002).

2.3.5 Magnetic Permeability

The magnetic permeability of soils is generally considered negligible in electromagnetic signal velocity measurements (Robinson et al., 2003a) due to low iron contents. However, as there may be occasions where soils are tested that do exhibit magnetic effects, and as even small amounts of magnetic materials such as magnetite may cause significant variations in propagation properties (Cassidy, 2007), a brief discussion of it is included here. At an atomic level, the motion of electrons around atoms and molecules cause electromagnetic fields to be generated, and the fact that atoms and molecules may also have spin adds to this field generation. In most materials these spins are not aligned and so the fields act against each other and cancel. However, under an external magnetic field the orientation of atoms and molecules is changed such that their spins line up (Telford et al., 1990), due to the field acting on the electrons of individual atoms causing orbitals to exist with slightly different energy levels and with different spatial locations (Brownlow, 1996). The lining up of spin creates a corresponding lining up of internal dipoles, also known as magnetic polarization (Telford et al., 1990), allowing the field of each atom to be complementary.

The degree to which the magnetic field produced by a material is uniform throughout its volume determines the degree to which the material can be considered magnetized. The degree to which a material can be magnetized is termed its magnetic susceptibility and bodies having a uniform field are termed uniformly magnetized (Telford et al., 1990). However, it should also be noted that magnetic permeability in geophysics is, more often than not, considered anisotropic (Nabighian, 1987). The magnetic susceptibility determines a factor by which the permeability of free space may

be multiplied to provide the magnetic permeability of a particular material, through the relationship described in Equation 2.24 (Nabighian, 1987). The strength of the magnetic field will determine the overall reorientation of atoms and molecules and hence, in contrast to other electromagnetic properties, the magnetic permeability of a material can have a complicated dependence on field strength (Nabighian, 1997, BSI, 1999).

$$\mu = \mu_0 (1 + \chi_m)$$ [Eq. 2.24]

where μ is the magnetic permeability of the material, μ_0 is the magnetic permeability of a vacuum (see below) and χ_m is the magnetic susceptibility.

As with permittivity, magnetic permeability also has a value in a vacuum (μ_0, $4\pi \times 10^{-7}$ Henry.m^{-1}, Telford et al., 1990). Also, the magnetic permeability of a material may be referred to as the relative magnetic permeability (μ_r), which is the ratio of the magnetic permeability of a material to that of a vacuum. Based on Equation 2.24, it can be seen that the relative permeability can be defined by Equation 2.25.

$$\mu_r = \left(1 + \chi_m\right) = \frac{\mu}{\mu_0}$$ [Eq. 2.25]

In terms of the parameters affecting electromagnetic wave propagation in the sub-surface, the relative magnetic permeability has the most limited range of values, a normal maximum for geophysical work is 3, but generally taken as being close to unity (Telford et al., 1990). It has also been suggested that magnetic permeability generally only affects geophysical surveys when large quantities of Fe_2O_3 are present (Reppert et al., 2000) and that the presence of iron and iron oxides can enhance magnetic permeability (Van Dam and Schlager, 2000). Therefore, while there are many types of

magnetization, soils with relative magnetic permeability greater than unity are generally considered to exhibit ferromagnetism (Olhoeft, 1998).

As the magnetic permeability of a soil determines the extent to which it can be magnetized under an external field, it can be determined through measuring its attraction to a magnetic field (BSI, 1999). This provides a useful means of determining whether a soil has any significant magnetic permeability in the field or laboratory by attempting to attract it to a strong permanent magnet, even if the determination of the actual relative magnetic permeability is more complicated. However, for geophysical testing it is important to realise that the magnetic permeability under an applied electromagnetic signal will not necessarily be the same as that in a static magnetic field. This is because relaxation mechanisms may change the properties as a function of frequency. Such relaxations may be considered similar to the Debye (1929) relaxations in permittivity and have been expressed using the Cole and Cole (1941) model as described in Equation 2.26 (Olhoeft, 1998).

$$\mu' - j\mu'' = \mu_\infty + \frac{\mu_S - \mu_\infty}{1 + (j\omega\tau)^\alpha} \qquad\qquad \text{[Eq. 2.26]}$$

where μ' is the real magnetic permeability, μ'' is the imaginary magnetic permeability, μ_S is the low frequency magnetic permeability, μ_∞ is the high frequency magnetic permeability, τ is the relaxation time and α is the Cole and Cole parameter which, according to Olhoeft (1999) is dependent upon the magnetic grain size distribution and, for a single relaxation, equals unity. The relaxation frequency can be determined from the relaxation time in the same manner as for permittivity (see Section 2.3.4).

This illustrates that magnetic permeability need not be a real number, instead

potentially exhibiting energy storage and loss mechanisms associated with real and imaginary parts. Therefore, it is important to understand that published soil magnetic permeability data may not be representative of all frequencies, particularly as it has been said that most such soils have not been tested at high frequencies (Olhoeft, 1998).

2.3.6 Loss Mechanisms

When an electromagnetic signal propagates in matter a certain amount of the energy is dissipated as heat. This is analogous to the way in which microwave ovens use electromagnetic waves to produce heat in materials with a water content (Reynolds, 1997) and why relative permittivity properties have been described as 'a measure of its ability to convert microwave energy into heat' (Knott, 2005). The dissipation of energy in this manner is known as the dielectric loss (Tareev, 1975) and is not instantaneous, thereby causing losses during polarization and subsequent relaxation. Therefore, complex permittivity can be defined in terms of a real part (ε') and an imaginary part (ε''), with the real part representing the ability of the material to store electromagnetic energy in polarization, and the imaginary part representing the loss of electromagnetic field energy (Shang et al., 1999). The ratio between the real and imaginary parts is described by the loss tangent (tan δ - Tareev, 1975), as defined by Equation 2.27. Basically, the higher the value of tan δ (also known as the dielectric loss index), the greater the loss of energy will be for an electromagnetic signal, with a lossless dielectric having a value of 0. In soils, both real and imaginary permittivities are considered largely a function of water content. This is illustrated in Figure 2.9, which shows both aspects of the permittivity increasing with water content and illustrates that they vary also between soil types.
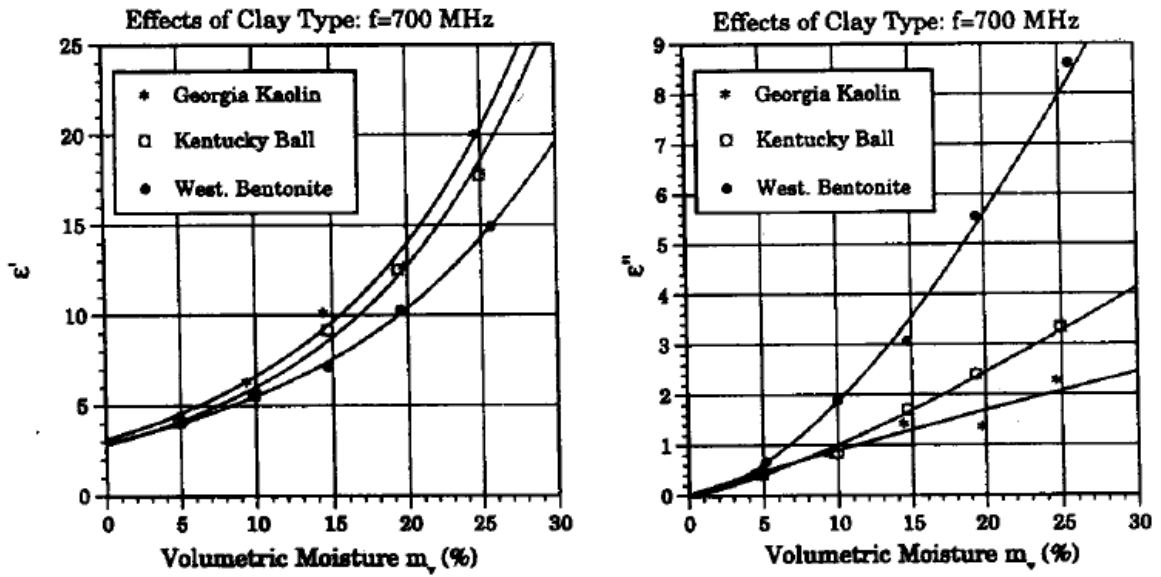
Figure 2.9. Real and imaginary permittivities in soils (Peplinski, 1995).

$$\tan \delta = \frac{\varepsilon''}{\varepsilon'}$$ [Eq. 2.27]

In terms of geophysical surveys, the loss tangent is often simplified to include only conductive losses, as shown in Equation 2.28 (Reynolds, 1997; Milsom, 1996). This is an important factor for conductive soils because, as illustrated in Figure 2.10, the changes in permittivity of pore water with an increase in salinity (Figure 2.8) are also accompanied by increases in the imaginary permittivity and hence increased attenuation.

$$\tan \delta = \frac{\sigma}{\omega \varepsilon}$$ [Eq. 2.28]

The relationship between complex, real and imaginary permittivity is shown in Equation 2.29 (Shang et al., 1999).

$$\varepsilon = \varepsilon' - j\varepsilon'' \qquad\qquad\qquad [Eq. 2.29]$$

where ε is the complex permittivity ($F.m^{-1}$) and j is the square root of -1.
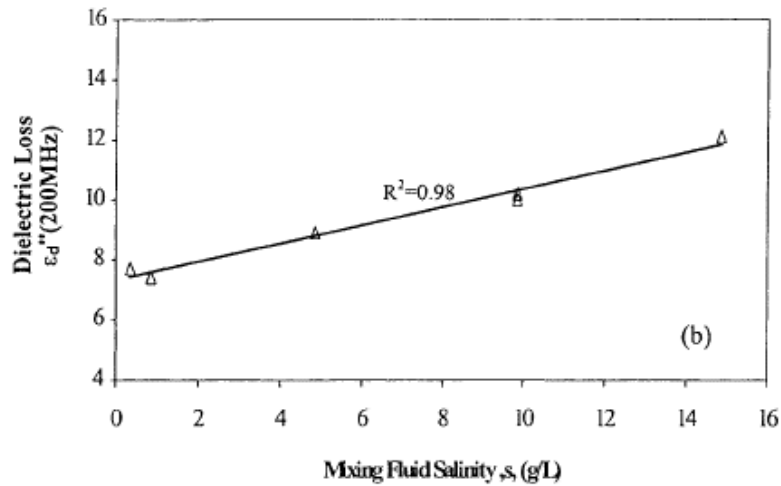
Figure 2.10. Water salinity versus its dielectric loss (Scholte et al., 2002).

As with relative permittivity, complex permittivity can be expressed in terms of its ratio to the permittivity of free space, through Equation 2.30 (Shang et al., 1999).

$$\varepsilon_r = \frac{\varepsilon}{\varepsilon_0} = \frac{\varepsilon'}{\varepsilon_0} - j\frac{\varepsilon''}{\varepsilon_0} = \varepsilon'_r - j\varepsilon''_r \qquad\qquad [Eq. 2.30]$$

However, for materials that also have a conductivity greater than zero (as is generally the case in geophysical investigations), the complex permittivity will also be related to that conductivity and can be calculated using Equation 2.31 (Reynolds, 1997).

$$\varepsilon_r = \varepsilon'_r + j\left(\varepsilon''_r + \frac{\sigma_s}{\omega\varepsilon_0} \right) \qquad\qquad [Eq. 2.31]$$

where σ_S is the static (also known as DC) conductivity.

2.4 PROPAGATION OF ELECTROMAGNETIC SIGNALS

The basic parameter for describing the propagation of electromagnetic waves is the complex propagation constant (γ), as described in Equation 2.32 (after IEEE, 1990).

$$\gamma = jk = \alpha + j\beta \qquad\qquad\qquad \text{[Eq. 2.32]}$$

where k is the complex wave number, α is the attenuation constant (nepers.m^{-1}), describing the loss in amplitude of the wave, and ß is the phase constant (radians.m^{-1}), describing the motion of the wave and hence determining the wave velocity.

Whereas in free space the amplitude of an electromagnetic wave will be unaffected by the medium, in lossy (attenuative) media, such as is the case with wet soils, the amplitude of the signal decays exponentially as a function of frequency, permeability, permittivity and conductivity. This decay in amplitude is illustrated in Figure 2.11 (Ovchinkin and Sugak, 2002) where wave 2 ignores attenuation and wave 1 includes for its effects.
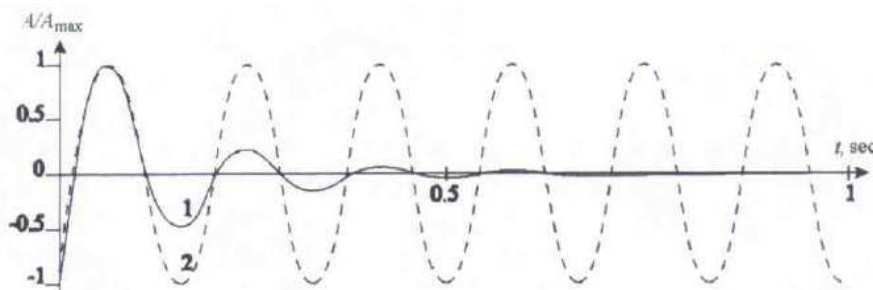
Figure 2.11. The decay in amplitude of a signal (Ovchinkin and Sugak, 2002).

43

As the attenuation coefficient describes the loss of energy embodied in a wave, its depth of penetration can be determined through an exponential relationship to α. A simple visualization of this relationship is known as the skin depth, which can be calculated using Equation 2.33 and describes the depth to which an electromagnetic wave will have penetrated at the point where the amplitude has reduced to 1/e (approximately 37%) of its original value (Ovchinkin and Sugak, 2002, e is the base of natural logarithms).

$$\delta = \frac{1}{\alpha} \qquad\qquad \text{[Eq. 2.33]}$$

where δ is the skin depth (m).

The exponential decay in amplitude with depth through a homogeneous medium is shown in Equation 2.34 (Lal and Shukla, 2004). A significant aspect is that the attenuation factor is frequency dependent, reducing the penetration distance of electromagnetic waves with increasing frequency.

$$A_2 = A_1 e^{-\alpha(r_2 - r_1)} \qquad\qquad \text{[Eq. 2.34]}$$

where A_1 is the amplitude at distance r_1, A_2 is the amplitude at greater distance r_2 and e=2.71828 (Calvert and Farrar, 1999).

Similarly, the velocity (v m.s^{-1}) of propagation of an electromagnetic wave can be calculated through the relationship between velocity, frequency and ß, as described in Equation 2.35 (Hayt and Buck, 2006).

$$v = \frac{\omega}{\beta} = \frac{2\pi f}{\beta} \qquad\qquad \text{[Eq. 2.35]}$$

Calculations of α and ß can be divided into those for lossless, or low loss, materials (i.e. materials with low α values) and those for lossy materials (i.e. materials where the conductive and dielectric properties cause significant α values). As described in Section 2.3.6, the degree of loss in a material can be described using the loss tangent. Attempts to simplify the propagation of electromagnetic waves in soils have included the consideration of the soil as a lossless material, with a loss tangent of unity resulting in an attenuation factor of zero (i.e. infinite penetration) and the velocity described in Equation 2.36 (Hayt and Buck, 2006).

$$v = \frac{1}{\sqrt{\mu\varepsilon}} \qquad\qquad \text{[Eq. 2.36]}$$

From this equation, it can be seen that the phase constant is considered only to include the permittivity and magnetic permeability, as shown in Equation 2.37.

$$\beta = \omega\sqrt{\mu\varepsilon} \qquad\qquad \text{[Eq. 2.37]}$$

As the relative magnetic permeability of soil is often considered to be close to unity, Equation 2.36 is often also further reduced to that shown in Equation 2.38 (Lin, 2003).

$$v = \frac{c}{\sqrt{\varepsilon_r}} \qquad\qquad \text{[Eq. 2.38]}$$

where c is the velocity of light *in-vacuo* (2.9979×10^8 m.s^{-1} - Calvert and Farrar, 1999).

Equations 2.36 to 2.38 may be perfectly adequate for use in low loss soils, such as when they are dry. However, in wet soils, losses are associated with the dipolar

45

polarization of water molecules and the increase in conductivity as water contents increase. This problem, together with difficulty in predicting the complex permittivity of soils of unknown composition, leads to a common consideration of the soil as a perfect conductor, where dipolar polarization losses are ignored. This results in the propagation coefficients shown in Equations 2.39 and 2.40 (Hayt and Buck, 2006).

$$\alpha = \omega \sqrt{\frac{\mu\varepsilon'}{2}\left(\sqrt{1+\frac{\sigma^2}{\omega^2\varepsilon'^2}}-1\right)^{\frac{1}{2}}}$$ [Eq. 2.39]

$$\beta = \omega \sqrt{\frac{\mu\varepsilon'}{2}\left(\sqrt{1+\frac{\sigma^2}{\omega^2\varepsilon'^2}}+1\right)^{\frac{1}{2}}}$$ [Eq. 2.40]

While conductive losses may be significant (that significance decreasing with frequency) the effects of dipolar relaxation may also occur, and so conductive losses cannot be considered the only loss mechanism under all circumstances. For this reason, the propagation parameters described in Equations 2.41 and 2.42 (Hayt and Buck, 2006) are required for calculation of propagation where the dipolar relaxation mechanism is significant. It should also be noted that the reduction in real permittivity involved in relaxation causes frequency dependency in these parameters.

$$\alpha = \omega \sqrt{\frac{\mu\varepsilon'}{2}\left(\sqrt{1+\left(\frac{\varepsilon''}{\varepsilon'}\right)^2}-1\right)^{\frac{1}{2}}}$$ [Eq. 2.41]

$$\beta = \omega \sqrt{\frac{\mu\varepsilon'}{2}\left(\sqrt{1+\left(\frac{\varepsilon''}{\varepsilon'}\right)^2}+1\right)^{\frac{1}{2}}}$$ [Eq. 2.42]

where ε'' is the sum of the frequency dependent conductivity and dielectric losses, as

described in Equation 2.43.

$$\varepsilon'' = \varepsilon_{dp} + \frac{\sigma_S}{\omega} \qquad\qquad \text{[Eq. 2.43]}$$

where ε_{dp} is the imaginary permittivity associated with dipolar relaxation losses.

2.5 SOIL AS AN ELECTROMAGNETIC PROPAGATION MEDIUM

It has been known for many decades that soils are not simple materials in terms of their electromagnetic properties. Cownie and Palmer, as early as 1951, collected available data relating to measurements of the dielectric constant of soils and their review, illustrated in Figure 2.12, showed that variations in the dielectric constant of soils, with water content, were already well known, if not so well understood. They therefore undertook their own study of a soil, described by them as a boulder clay, over a wide range of water contents, at a frequency of 430MHz, their results being shown as Curve J in Figure 2.12. It can also be seen from Figure 2.12 that it was already apparent at this time that soils may have different properties at different frequencies.

Based on their data, Cownie and Palmer (1951) advanced the theory that the low dielectric constant at low water contents was due to two forms of water being present: 'bound' water with a dielectric constant close to that of ice (c. 3), and 'free' water (c. 80) "...with its normal value of dielectric constant". It should be noted, however, that this description is a little inexact as the low-frequency static permittivity of ice may actually be greater than that of unconfined water, so such an analogy is only likely to be accurate at frequencies above 1MHz (Klein and Wang, 2005).
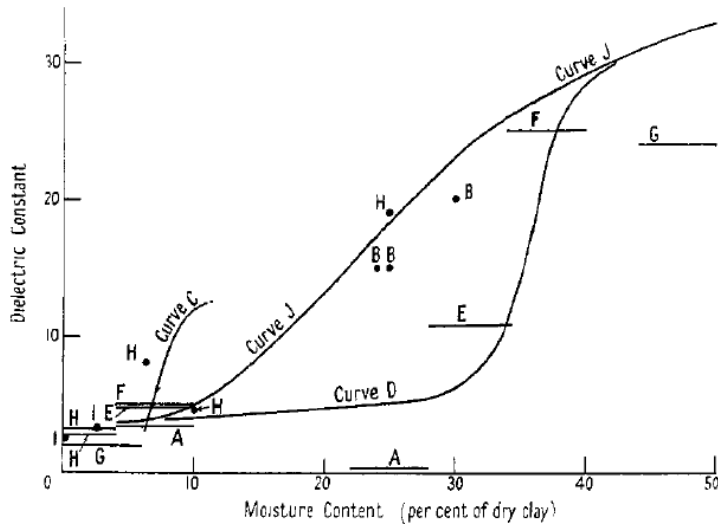
Fig. 1. Comparison of results (for key to lettering see below).

Reference	Author	Year	Mc/s
A	McPetrie	1934	200 (dry) 650 (wet)
B	Smith-Rose	1935	100
C	Banerjee and Joshi	1938	70 9
D	Chakravarty and Khastgir	1938	82
E	Palmer and Forrester	1941	407
F	McPetrie and Saxton	1945	60
G	Ford and Oliver	1946	3330
H	Straiton and Tolbert	1948	9375
I	Chatterjee	1950	450
J	Cownie and Palmer	1951	430

Figure 2.12. 1951 review of soil electromagnetic properties (Cownie and Palmer, 1951).

Unfortunately, Cownie and Palmer (1951) did not comment on the reduction in slope of their graph as it approached water contents of 40% by mass and above, but bound and free water have remained the favoured theory to explain the nature of soil electromagnetic property variations with water content (e.g. Ishida et al., 2000). A significant reason for this is that continued research into the properties of soils has shown that soil type has a significant impact on the water content over which the bound water effect occurs, as shown in Figure 2.13. This indicates that sands, which have larger grain sizes and hence lower surface areas, tend to exhibit much less retardation in

the growth of apparent permittivity with water content than clays. According to Klein and Wang (2005) the proportion of free water can be expected to decrease with increasing specific surface area.

However, it should be noted that Serbin et al. (2001) utilised TDR (see Section 2.8) and so it is not known whether the relationships of Figure 2.13 hold at all frequencies (the TDR frequency being indeterminate). Also, the water content range for the Serbin et al. (2001) graph is limited to much lower values than that of Cownie and Palmer (1951) and so it is not evident whether a reduction in slope would occur above 35% water content by volume.
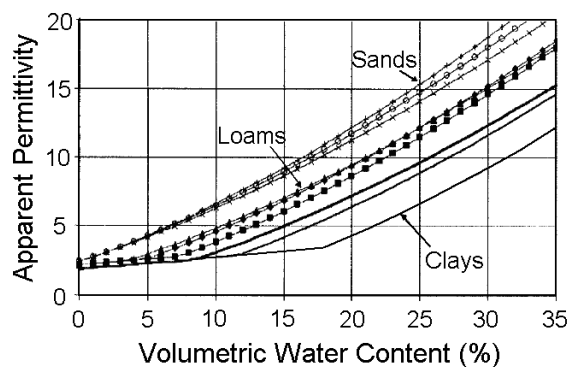
Figure 2.13. The effects of soil texture on the retardation of permittivity at low water contents (Serbin et al., 2001).

However, some data are available in the literature that cover wider water content ranges, such as those of Curtis (2001) shown in Figure 2.14, which significantly provides data on both the permittivity and conductivity. However, these data are also limited by two factors. Firstly, data above volumetric water contents of 50% are much sparser than for lower water contents. Secondly, the data provide an indication of the variability of permittivity values, but they do not allow consideration of any

relationships between permittivity and water content, although importantly they show

potential upper and lower bounds. This work by Curtis (2001), however, is also useful

in indicating that the apparent permittivity to volumetric water content relationship in

soils may break down above water contents close to 40%. Also, as for the Serbin et al.

(2001) graph, the exact measurement frequency is unknown and so relationships

between permittivity, frequency and water content cannot be derived from Figure 2.14.
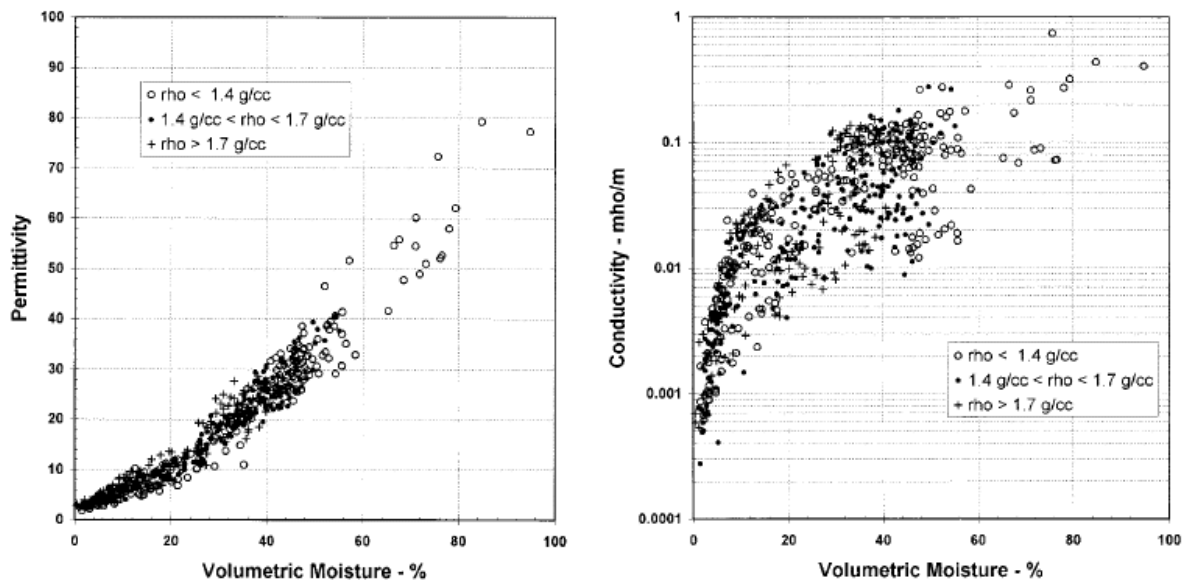
Figure 2.14. The permittivity and conductivity of soils over a wide range of water contents (Curtis, 2001).

In respect of the relationship between water content and electromagnetic

properties, the work of Saarenketo (1998), illustrated in Figure 2.15, is therefore

significant as it provides close spacing of data points for a soil illustrating the gradual

build up of both permittivity and conductivity with increasing water content. In this

study, Saarenketo (1998) even went as far as to speculate that a new form of water,

which he termed 'capillary' water, could be used to explain steps in the graphs of Figure 2.15. However, in attempting to compare these data to those of Cownie and Palmer (1951), Serbin et al. (2001) and Curtis (2001), a significant limitation of the literature is evident: as well as covering different water content ranges, the use of gravimetric and volumetric water contents between different authors causes significant difficulties in relating their data, as the dry density is often not provided to allow conversion. Therefore, while the work of Cownie and Palmer (1951) faced difficulties because the different "...natures of the soils used by different experimenters introduce another variable, the effect of which cannot be taken into consideration when comparing the measurements on soils from different localities." it is apparent that modern researchers face similar difficulties due to use of different methods of measuring water content.
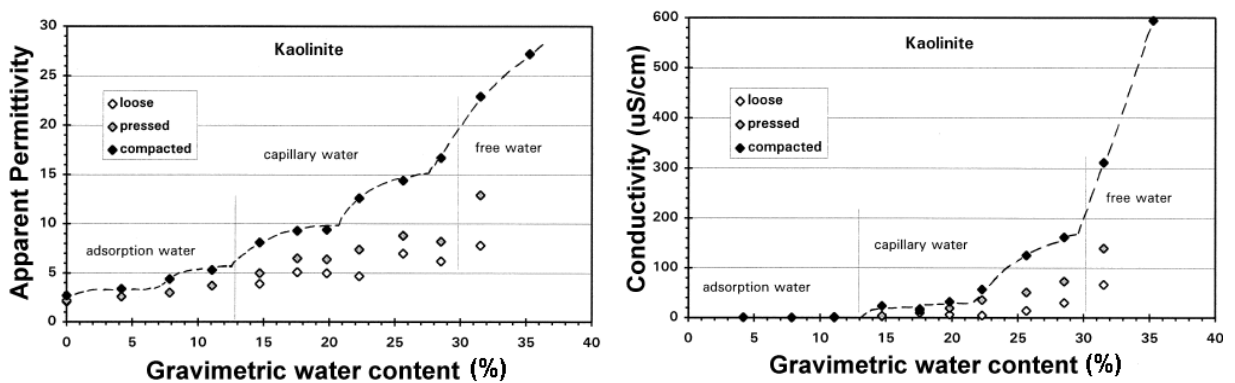
Figure 2.15. The permittivity and conductivity of Kaolinite versus water content (Saarenketo, 1998).

As well as changes in electromagnetic properties with water content, soils are considered to exhibit relaxations due to the properties of the water within their pores, and so are considered electromagnetically dispersive. That the permittivity of a soil can

vary with frequency has been known for many decades, Smith-Rose (1935) providing

an early indication of the phenomenon for frequencies between 1 and 100 MHz. A good

illustration of these relaxations is provided by Wensink (1993), as shown for a clay soil

from Birmingham in the UK in Figure 2.16. Wensink found that the relaxations in the

soils tested were of a Debye (1929) type and that they were centred around relaxation

frequencies between 1MHz and 7MHz. The imaginary permittivity in the work of

Wensink (1993) includes that due to both the electrical conductivity and dipolar

polarization, but gives little information on the relative importance of each. However,

Topp et al. (2000) estimate that the ratio of dipolar to conductivity losses, in soils they

studied, were approximately 1.5 and that it depended on the amounts of salts, clay and

water present.
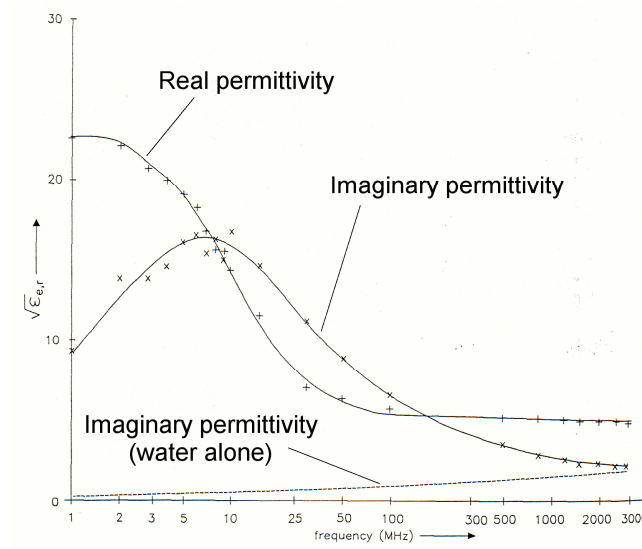
**Figure 2.16. Relaxations in a clay soil at a volumetric water content of 44.5%
(after Wensink, 1993).**

Another example of relaxation in a soil is that of Matzler (1998) who found that

relaxations also occurred even when the soil was close to dry, as illustrated in Figure

2.17 for a Sahara sand. It can be seen from the figure that the relaxation is much smaller

than for the clay soil of Figure 2.16, which is to be expected due to the low water

content as indicated by the low real permittivities (0.3% by volume). Also of note is that

this relaxation occurs around a frequency of approximately 400MHz, which is much

higher than that found by Wensink (1993). It is, therefore, possible that relaxation

frequencies in sands and clays may be different, due to different types of water being

present in non-cohesive and cohesive soils.
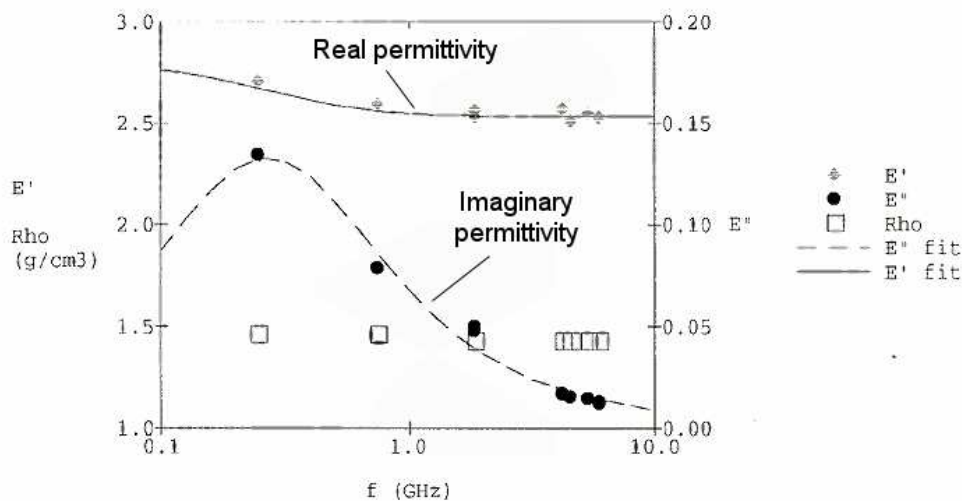
Figure 2.17. Relaxation in a sand at a volumetric water content of 0.3% (after Matzler, 1998).

From the above discussion it can be seen that soil cannot be considered a simple

entity in terms of the interaction between it and electromagnetic signals, due to the

varying properties of the individual components of which it is composed. Therefore it is

considered a complex system in geophysical terms (Ben-Dor, 2002). These individual

components are termed phases and soil forms a multi-phase material comprising

mineral particles, water and air, with additional phases being introduced to account for experimental observations, including bound and free water. As the grain size and porosity, and hence the overall structure, of a soil are based on the depositional history, a relationship also exists between sedimentary structures and dielectric properties, from which can be inferred that sequence boundaries can cause a reflection of electromagnetic energy (Van Dam and Schlager, 2000). Furthermore, these factors also apply to the conductivity of a soil, with porosity, degree of saturation, salts in solution and presence of clay having been cited as the main factors (Doolittle and Collins, 1995). It has also been identified that compaction can significantly affect relative permittivity, largely due to the induced change in volumetric water content (Saarenketo, 1998) and dry density, which highlights the view that the properties of soils will vary over time where consolidation processes occur. As both the electromagnetic and geotechnical properties of soils are largely dependent on the nature of the soil fabric and pore water, it has been suggested that these two classes of properties are closely related, at least for clayey sediments (Carreón-Freyre et al., 2003).

A major aspect of the propagation of electromagnetic signals in soils relates to the impact of water content on permittivity and conductivity. It is known that the ability of a sediment to hold water is important and that high porosities, coupled with high water levels, cause higher relative permittivities but, above the water table, this is controlled by the ability of the sediment to retain water (Van Dam and Schlager, 2000). Also, it has been known for many decades that the dielectric properties of water in soil pores cannot be explained by a single water phase, with early research suggesting that 15% to 20% of soil water is 'bound' tightly to mineral particle surfaces, with a relative permittivity close to that of ice (Cownie and Palmer, 1951). It should also be noted that

some researchers consider that 'bound' water may only be bound at lower water contents, the whole water layer achieving a permittivity equivalent to 'free' water once a certain water content is reached (Boyarskii et al., 2002).

However, the properties of water confined in a soil pore are not the same as those for unconfined water (e.g. Low, 1979). Under an applied voltage, unconfined water molecules do not normally fully orient themselves with the current flow path until the field strength exceeds 10^9 Vm^{-1} (Choi et al., 2005). However, research indicates that, for confined water dipoles, the required field strength may be reduced by as much as a factor of 1000 and that there is a reduced energy barrier for translation of water molecules (Choi et al., 2005).

This is particularly significant for fine soils, where pore sizes can be smaller than 10nm and have been reported as being centred around plate separations as small as 3nm (Sills et al., 2006). Also, in rarer cases where zeolitic clays are present in the soil structure, pores may be as small as 1nm, with associated disruption of the hydrogen bonding potential of water to the degree that the water may be unable to freeze even within a super-cooled temperature region of 150 to 235 ºK (Jansson and Swenson, 2003). Furthermore, Hoekstra and Delaney (1974) considered that unfrozen water may exist in soils at temperatures below -30ºC and detailed results indicate that, in montmorillonite clays, some water may even be unfrozen at -80ºC. Even at only -4°C, Wu (1964) found that up to 22% of water may be unfrozen in clays and that the amount may increase with the Liquid Limit of a soil.

Also, Hoekstra and Doyle (1970), working with sodium montmorillonite at 9.8GHz, showed that below 0°C the relative permittivity drops rapidly to much lower

values than would be expected for temperatures above the freezing point of water. All of these factors lead to a need to consider the composite electromagnetic properties of soils.

2.6 COMPOSITE SOIL ELECTROMAGNETIC PROPERTIES

Predicting the overall electromagnetic parameters of a soil from those of its individual constituents is important to a full understanding of the mechanisms responsible for the measurement of soil water content from electromagnetic measurement data. However, this causes a great deal of complexity due to the wide range of mixing models available, with at least twenty two different models to choose between (van Dam et al., 2005). That so many models exist indicates that no one model can be expected to provide theoretical predictions of soil electromagnetic properties under all circumstances (Boyarskii et al., 2002), and potentially variation in relevance between complex and non-complex valued data (Sihvola, 1991). Also, for acceptable accuracy soil-specific calibration curves are often considered necessary (e.g. Logsdon, 2005b), despite the wide range of models available. However, these models can, in simple terms, be loosely categorized as simple volumetric models, empirical models and phenomenological models.

An example of the first category is volumetric mixing, which is based simply on a pro-rata proportioning of the permittivity of each phase according to the volume each occupies. As described earlier, the polarization of individual atoms and molecules can be summarized as the product of the distance vector involved in the charge separation

and the atomic charge involved, with the polarization of a specific mass of uniform material being simply the product of this value and the number of polarizations involved (Dobbs, 1984). This, therefore, introduces the simple model for the permittivity of a composite material shown in Equation 2.44 (Tareev, 1975):

$$\varepsilon = \sum_{i=1}^{i=m} y_i \varepsilon_i \qquad\qquad [Eq.\ 2.44]$$

where ε is the effective permittivity, ε_i is the permittivity of the fraction and y_i is the fractional volume.

The concept of a mixing model can therefore be introduced, with Equation 2.44 providing the simplest means by which composite properties can be determined. It should also be noted that this equation is not limited to theory as it has been used practically within geophysics, such as in a recent study of thermal microwave emission depth and soil moisture remote sensing (Nedeltchev, 1999). However, the permittivity of most composite dielectrics could be considered that of a chaotic, or stochastic, mixture of several components (Tareev, 1975), leading to potential for the bulk electromagnetic properties of an inhomogeneous material to act as a random distribution of individual properties. Therefore, in his work on the physics of dielectrics, Tareev (1975) introduces the Wiener equalities, which give theoretical upper and lower limits for the likely permittivity of static mixtures (see Equation 2.45).

$$\frac{1}{\sum_{i=1}^{i=m} \dfrac{y_i}{\varepsilon_i}} \leq \varepsilon \leq \sum_{i=1}^{i=m} y_i \varepsilon_i \qquad\qquad [Eq.\ 2.45]$$

Other such theoretical bounds are also available, which are claimed to decrease

the potential range between possible upper and lower values (Sihvola, 2002), however they provide no exact value for composite electromagnetic properties. A further problem with simple volumetric models, and theoretical bounds, is that they require advance knowledge of the properties of each phase both in terms of water content and frequency variations, and potentially the proportions of bound and free water. They can also suffer additional complexity where the mixing is based on calculations for inclusions in a background medium, as it can be unclear as to which phases should be considered inclusions and which background: an important consideration for soils where water contents can potentially range from very low to very high. The Hashin-Shrikman upper and lower bounds, for instance, are composed of the same model but with the phases representing inclusions and background interchanged (Sihvola, 2002).

Therefore, for inhomogeneous multi-phase soil mixtures (i.e. those consisting of various proportions of air, water and soil particles) there was a need for a more sophisticated mixing method, but the properties of an inhomogeneous dielectric were considered too complex to model as a simple summation of fractional permittivity. There is also difficulty inherent in modelling bulk behaviour at an atomic level, as permittivity in geophysical terms is a macroscopic parameter rather than a property of each individual atom and molecule in the substance (Tareev, 1975). A more sophisticated model for use on composite dielectrics is the Lichtenecker-Rother formula, also known as the 'logarithmic law of mixing', which adapts Equation 2.44 by utilising the base 10 logarithm of the permittivity values (Tareev, 1975).

Similarly, mixing models also exist that rely on adding an exponent to Equation 2.44 and so are referred to as the exponential formulas (Sihvola, 1991). While some

mixing models are two-phase in calculating composite permittivity of inclusions in a background permittivity, exponential formulae, including the implicit exponent of 1 in Equation 2.44, have the advantage of being symmetrical: i.e. there is no confusion as to what phases can be considered inclusions or background (Sihvola, 1991). One of these, the Complex Refractive Index Model (CRIM), takes an exponent of 0.5, so transforming the mixing of permittivity values to the equivalent refractive indices. CRIM (Equation 2.46: after Cassidy, 2008) has become popular for near surface applications because it is generally considered simple, robust and generally of acceptable accuracy, and because it has the advantage of requiring knowledge only of the permittivity of a materials constituents (Cassidy, 2008). In TDR testing, for volumetric water contents below 40%, using the square root of permittivity has been shown to give acceptably accurate linear relationships to apparent permittivity (Siddiqui et al., 2000).

$$\sqrt{\varepsilon} = \sum_{i=1}^{i=m} y_i \sqrt{\varepsilon_i} \qquad\qquad \text{[Eq. 2.46]}$$

where ε is the effective permittivity, ε_i is the permittivity of the fraction, and y_i is the fractional volume.

While simple volumetric mixing is adequate for simple mixtures, it could be considered inadequate for complex, often largely inhomogenous, soils and so has not been widely used for predicting soil electromagnetic properties. The rise in popularity of time-domain reflectometry (TDR) since the early 1980s, however, has illustrated that a different approach to soil electromagnetic prediction is possible that can provide accurate relationships between an apparent permittivity and volumetric water content

based upon empirical relationships. An important example of such empirical work is that of Topp et al. (1980) who studied the effects of water content on a number of soils, and some examples of their data are illustrated in Figure 2.18. Their work resulted in the Topp model (Topp et al., 1980), shown in Equation 2.47.
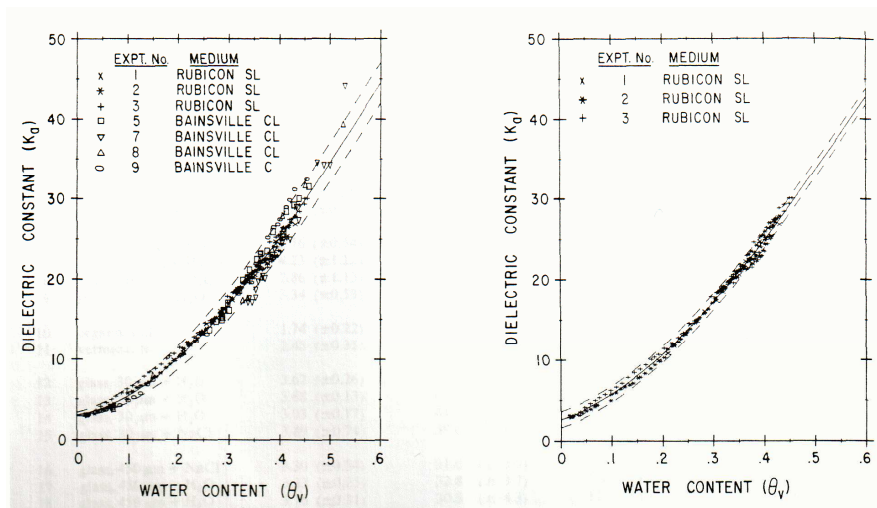
Figure 2.18. Some of the soil data that culminated in the Topp Model (Topp et al., 1980).

$$\varepsilon_r^* = 3.03 + 9.3\theta + 146.0\theta^2 - 76.7\theta^3 \hspace{3cm} \text{[Eq. 2.47]}$$

where θ is the volumetric water content (%).

However, the Topp model is based entirely on TDR data, which measures signal velocities over a wide frequency range, and from them provides a single frequency-indeterminate permittivity value. Therefore, its applicability is not universal, as it does not provide any data on variations in measured electromagnetic properties with changes in frequency. While the Topp et al. (1980) model has been shown to provide accurate data for many soils, it has also been said to be embedded in the literature with unintended consequences, and to have held back the field of water content monitoring

through misapprehension that all sensors, whether time- or frequency-domain, measure comparable apparent permittivity data (Evitt and Parkin, 2005). However, models do exist that can be considered to represent variations due to both frequency and water content. An example of such a model is that of Wensink (1993) which was based on measurement of the complex permittivity in soils at frequencies between 1MHz and 3GHz. From these tests Wensink determined two mixing models, one for 50MHz and one for 1GHz, as shown in Figure 2.19 and Equations 2.48 and 2.49.
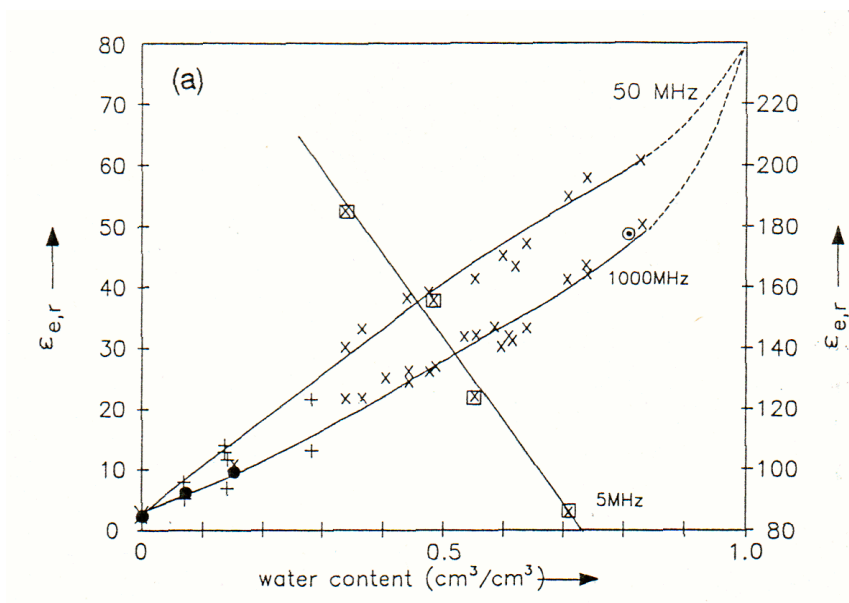
Figure 2.19. Data used in the Wensink 50MHz and 1GHz models (Wensink, 1993).

$$\varepsilon_r(50\text{MHz}) = 1.4 + 87.6\theta - 18.7\theta^2 \qquad \text{[Eq. 2.48]}$$

$$\varepsilon_r(1\text{GHz}) = 3.2 + 41.4\theta + 16.0\theta^2 \qquad \text{[Eq. 2.49]}$$

The 1GHz model is of particular significance as these data showed that the effects of relaxation in the soils tested were minimal at that frequency. This accords with the

findings of other researchers that methods such as TDR are generally insensitive to operating frequency above approximately 500MHz (Kelleners et al., 2005a; Evitt and Parkin, 2005). Therefore, the 1GHz model could be used as a measure of the electromagnetic properties of a soil largely free from the effects of dispersion, whereas the 50MHz model could provide an indication of the magnitude of any dispersion that may occur at lower frequencies. In comparison to other models, the Wensink model is particularly significant due to it providing multi-frequency data, and because it shows that there are some common features between soil electromagnetic properties and water content at both of those frequencies.

Despite their obvious importance in relating soil electromagnetic properties and water content, neither the Topp et al. (1980) nor Wensink (1993) models include geotechnical parameters other than water content. This could be considered a limitation given that it has been shown that such factors as dry density may also play a role in the propagation of electromagnetic waves in soils. Therefore, it is also important to acknowledge the existence of semi-empirical models based on a wider range of physical properties. An important example of this sort of model is that of Peplinski et al. (1995). However, while more detailed geotechnically than those of Topp et al. (1980) and Wensink (1993), the model of Peplinski et al. (1995) has some limitations of note in this study. For instance, the frequency range covered was 300MHz to 1.3GHz, thus giving limited low-frequency information on the effects of dispersion. Also, it requires advance knowledge of soil texture (i.e. sand, silt and clay proportions) which limits its potential application in non-contact water content determination.

The Topp et al. (1980) model has often proven acceptable for all but dispersive

soils, and has found extensive use in the monitoring of soil water content using TDR. Also, the Wensink model has shown itself to provide useful correlations to real permittivity data close to 1GHz (Thomas et al., 2008b) and the work of Peplinski et al. (1995) provides a geotechnically more advanced model, albeit limited in terms of water content measurement. However, each, while of significant value in allowing interpretation of electromagnetic data, are entirely empirical models and so do not illuminate the underlying mechanisms responsible for the composite electromagnetic properties. This limitation of empirical models is partly addressed by phenomenological models based on theoretical electromagnetic properties of, and interactions between, microscopic particles. Generally, these are based around considering bound and free pore water to act differently in terms of their electromagnetic properties. A popular example is the De-Loor model (Dirksen, 1999), which is based on the theoretical interactions between disc-shaped particles in soils. For a four phase soil system, this model has been reduced to Equation 2.50 (Dobson et al., 1985).

$$\varepsilon_r^* = \frac{3\varepsilon_s + 2(\theta - \theta_{bw})(\varepsilon_{fw} - \varepsilon_s) + 2\theta_{bw}(\varepsilon_{bw} - \varepsilon_s) + 2(\phi - \theta)(\varepsilon_a - \varepsilon_s)}{3 + (\theta - \theta_{bw})\left(\dfrac{\varepsilon_s}{\varepsilon_{fw}} - 1\right) + \theta_{bw}\left(\dfrac{\varepsilon_s}{\varepsilon_{bw}} - 1\right) + (\phi - \theta)\left(\dfrac{\varepsilon_s}{\varepsilon_a} - 1\right)} \qquad \text{[Eq. 2.50]}$$

where Φ is the porosity, θ is the volumetric water content and ε is the relative permittivity of each phase. The subscripts a, s, bw and fw correspond to air, soil minerals, bound water and free water, respectively.

However, while very sophisticated, the De-Loor model has been criticized for not being capable of describing the complex permittivity at lower frequencies (Heimovaara, 1994). Also, it is apparent that this model requires advance knowledge of the amounts of bound and free water present, which would most likely be unknown. It has been

widely reported that bound and free water, in soils, have different properties in terms of their interaction with electromagnetic signals, with large increases in relative permittivity when the transition point between the two is reached (Alex and Behari, 1998). It has therefore been suggested that soils act as a four phase material in terms of permittivity, with values of relative permittivity quoted as 4.5-7 for mineral particles, 1 for air, 3.5-3.8 for bound water and 81 for free water (Huang et al., 2005). However, other sources put the range of relative permittivity of bound water as 6-30 for the first and second water layers (Serbin and Or, 2005) and potentially higher in the work of Saarenketo (1998). The significance of bound water is that, due to dielectric losses being based on the intermolecular bond types and strengths (Saarenketo, 1998), it is rotationally hindered (Debye, 1929) by its orderly attachment to mineral particles. This is why tightly bound water nearer the mineral surface is considered to have a relative permittivity close to that of ice (Saarenketo, 1998), because in ice the tight binding of the water molecules also hinders their rotation. It is, therefore, interesting to note that the texture of a soil is considered by some as closely related to the bound and free water content (Alex and Behari, 1998).

Research in recent years has indicated that soils may reach relative permittivities in excess of that which could be calculated using a simple summation of the fractional permittivities, with values significantly in excess of 81 having been reported in some samples (Saarenketo, 1998). This is illustrated in Figure 2.20 for a number of clay samples. The results of this research led Saarenketo (1998) to conclude that '… the relation between dielectric value and moisture content is more likely to be a series of logarithmic functions than the exponential relationship that is usually used with dielectric mixture models' (Saarenketo, 1998). This perspective challenges the generally

applied mixing models and indicates that further research is required if a mixing model

is to be formulated that is considered to work acceptably under all geophysical

circumstances. However, it must be noted that the work of Saarenketo (1998) was

confined to gravimetric water contents below 40% (and often below 30%).
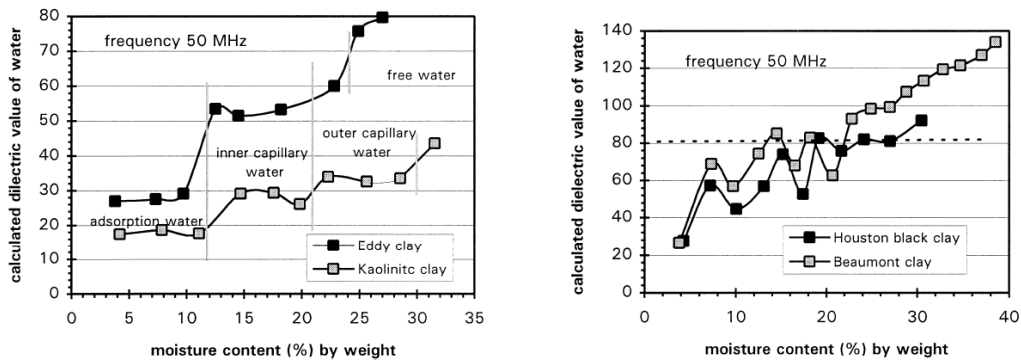
**Figure 2.20. Calculated permittivity of the water phase in a number of soils
(Saarenketo, 1998).**

Fine-grained soils, such as clays, are likely in the field to have water contents

between their Plastic and Liquid Limits (Craig, 1997), which could have impacts on the

usefulness of lower water content data. Furthermore, the water phase permittivity data

of Saarenketo (1998) are only valid for low frequencies around 50MHz, so do not

provide a full picture for a dispersive soil. Also of interest in this regard is the study of

Topp et al. (2000), who concluded that the presence of salts and clay causes a reduction

in the real part of the apparent permittivity of the water phase in soils, in comparison to

free water. Furthermore, it has been suggested that the shape of soil particles, and the

associated shape anisotropy, may cause variations in apparent permittivity

measurements depending on the orientation of the measurement (Arulanandan and

Smith, 1973; Beroual et al., 2000; Hillhorst et al., 2000; Jones and Or, 2002; Jones and

Friedman, 2000; Kärkkäinen et al., 2001; Muhunthan et al., 2000; Whites and Wu, 2002), which also relates to magnetic properties (Negi and Saraf, 1989).

While it could be concluded that knowledge of the fractional proportions of each soil phase may provide an approximation of the composite permittivity, it should be noted that these properties may themselves be dynamic. Topp et al. (1980) studied the effects of temperature on soil, as shown in Figure 2.21. They concluded that temperature may not be a significant factor in the apparent permittivity of a soil under normal circumstances. However, it should be noted that their data did not include low temperatures below 10ºC which could feasibly occur under field conditions, nor the sub 0°C temperatures that Hoekstra and Doyle (1970) showed would result in significantly reduced relative permittivity.
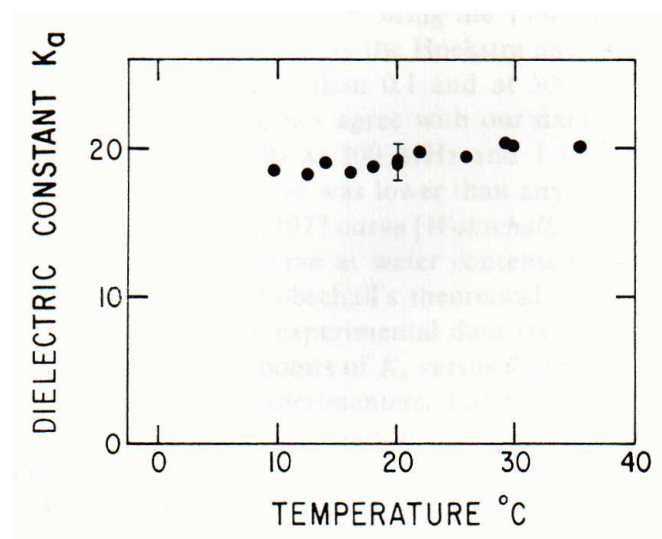
Figure 2.21. Variations in the apparent permittivity of a soil due to temperature (Topp et al., 1980).

Under normal circumstances, the permittivity of water in a material is expected to decrease with increasing temperature (as this would be the case for pure water - Hasted, 1973), but research has indicated that, for some soils, the reverse may occur (Jones and Or, 2002). It has been speculated that this may be due to the amount of water adsorbed on a mineral particle at a particular temperature, with variation in temperature affecting the proportion of total water in each of the bound and free pore water phases (Wraith et al., 2001; Or and Wraith, 1999; Klein and Wang, 2005). The degree to which permittivity may increase with temperature may, therefore, be dependent on the specific surface area and would be expected to have a soil-specific limiting temperature (above which permittivity would not increase) due to depletion of adsorbed water molecules. There is some evidence in the literature to support this view, including the study by Drnevich et al. (2001a) illustrated by Figure 2.22. That study indicated that sand permittivity may have a tendency to either remain constant, or decrease, with increasing temperature, but that cohesive soils may have a tendency to rise.
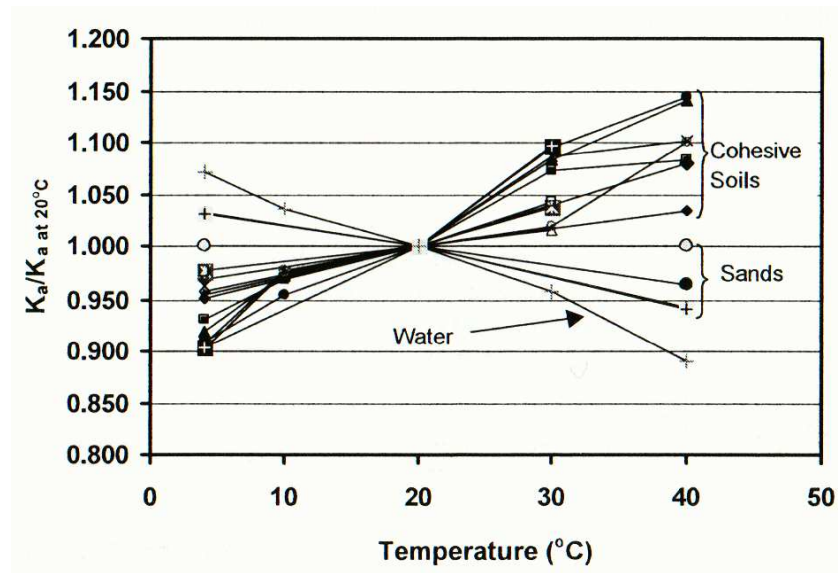
Figure 2.22. Temperature dependence of apparent permittivity in cohesive soils and sands (Drnevich et al., 2001a).

However, it should be noted that their data show that the apparent permittivity may change at a rate of approximately 10% per 10ºC of temperature change, compared with measurements at a temperature of 20ºC. It is also possible that such variations are associated more with high water contents than low ones (Evitt et al., 2005). Therefore, for laboratory measurements it can be seen that it is important to ensure that room temperature variations are not large, but not to the extent that it should be a significant problem when testing is carried out in a geotechnical testing laboratory. But, for field measurements, it is apparent that temperature corrections will be necessary to account for the much wider temperature variations. Also of interest in the work of Drnevich et al. (2001a) is that they attempted to relate their data to the Plastic Limit, as shown in Figure 2.23.
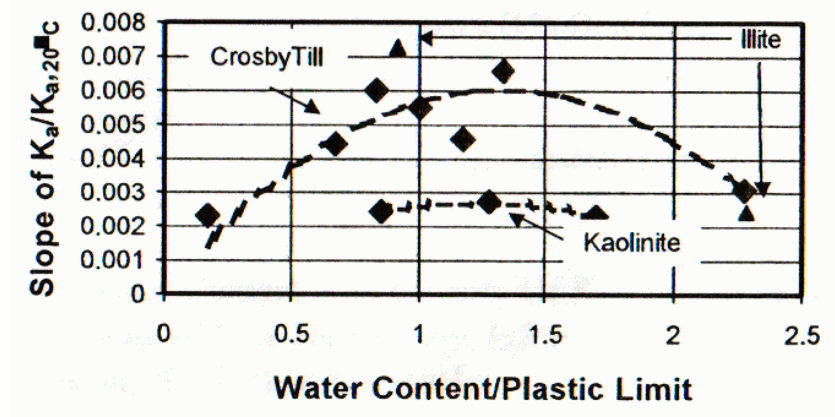
Figure 2.23. Slope of the apparent permittivity temperature variation of clay soils versus the ratio of water content to Plastic Limit (Drnevich et al., 2001a).

They found that the tendency of the cohesive (i.e. fine-grained) soils to vary with temperature was not necessarily a function just of the water content, but potentially has

a maximum at a water content above the Plastic Limit. However, it should be noted that the work of Drnevich et al. (2001a) is limited in terms of full consideration of temperature effects at all frequencies, as their measurements are based on TDR data. This is significant as the changes in apparent permittivity may therefore be due to changes in permittivity, conductivity, measurement frequency, or all three. As ionic conductivity can be expected to increase with temperature, the mechanism behind these temperature variations is therefore unknown. However, work by Hoekstra and Delaney (1974) suggests that the relative permittivity may indeed increase with temperature up to 30ºC, although close to 0ºC and below it will drop quickly as the water freezes such that the relative permittivity is in the region of three to four.

2.7 GEOTECHNICAL CHARACTERISATION PARAMETERS

An important aspect of fine-grained soils is that their mineral surfaces can be considered to have similar surface charges per unit of surface area (Mitchell and Soga, 2005). On this basis it can be expected that the amounts of ions present, and their effects on the properties of the pore water, will be largely dependent upon the specific surface area of the soil and its dry density, the two together providing the available surface area per unit of soil volume. Also, the quantity of water present can be expected to be very significant: firstly because it will displace air (Lin, 2003) so changing the spacing between soil particles and, secondly, because this will change the dry density in saturated soils (Thomas et al., 2008b). Similarly, it could be expected that the pore size will be dictated largely by the quantity of water present and the surface area, so the thickness of water layers would also be determined by them. Therefore, it could be

argued that geotechnical properties associated with surface area, including any potentially associated with bound and free water, could be significant in terms of electromagnetic properties. It is, therefore, interesting to note the work of Wraith et al. (2001) who suggest that there is a fundamental relationship between the effects of bound water on signal velocity measurements, and the mineral surface area. Similarly, it has been suggested that the Liquid Limit of a soil, in practice a measurement of its shear strength, is linearly related to its specific surface area, including through the formula of Farrar and Coleman (1967) given in Equation 2.51.

$$W_L = 19 + 0.56A_S \hspace{3cm} \text{[Eq. 2.51]}$$

where W_L is the Liquid Limit (% by mass) and A_S is specific surface area ($m^2.g^{-1}$).

This has been taken further as a concept by other researchers and the work of Dolinar and Trauner (2005) is a useful example. In their work they related the specific surface area and inter-grain water content at the Liquid Limit in a range of soils of different mineralogy. They concluded that this relationship was also linear, as demonstrated by Figure 2.24 and Equation 2.52. However, it should be noted that the linear relationships are not the same in Equations 2.51 and 2.52, the former representing total water content and the latter measuring inter-grain water only. This causes some difficulty as it is not necessarily possible to determine the amount of inter-sheet water that will be lost through oven drying at 105ºC when the Liquid Limit is determined. However, it can be implied by these linear relationships that the Liquid Limit is a useful indicator of the specific surface area of a soil. This is significant as other geotechnical parameters could also be considered related to surface area.

Dolinar and Trauner (2005) also concluded that the undrained shear strength of fine soils, which is effectively what the Liquid Limit test measures, is proportional to the free pore water, but does not depend on the amount of water firmly bound to clay mineral particles between individual sheets. This is significant, as this could imply that a duality of electromagnetic properties may be caused by free pore water related to the Liquid Limit, and bound, inter-sheet, water related to the clay mineralogy: that is, it could be speculated that the bound water of electromagnetic research is actually inter-sheet water, and free water may then be inter-grain water.
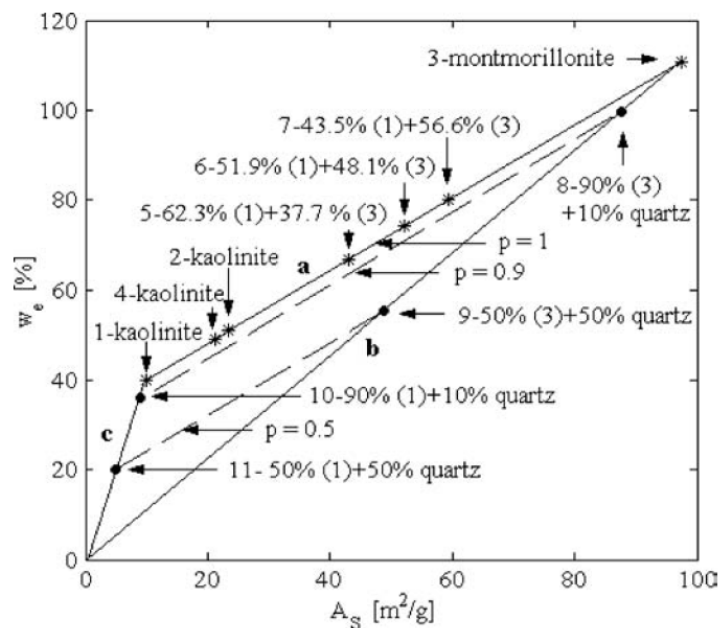
Figure 2.24. The inter-grain gravimetric water content as a function of the specific surface area of clays (Dolinar and Trauner, 2005).

$$w_e = 31.9 + 0.81A_S \qquad \text{[Eq. 2.52]}$$

where w_e is the inter-grain water content (% by mass).

The influence of mineralogy on the diffuse double layer, said to exist around mineral particles, is also an important aspect of the links between electromagnetic and geotechnical properties. For instance, Prakash and Sridharan (2004) investigated the relationship between mineralogy and free-swelling properties by comparing the volume of soils in water and carbon tetrachloride, the latter being non-polar and so suppressing the effects of the diffuse layer, thereby encouraging flocculation. They found that not only could the free-swell properties be used to predict mineralogy, but also that this could similarly be achieved using the Liquid Limit. This is interesting in relation to the two separate linear relationships between the Liquid Limit and specific surface area discussed above. As one was based on total measured water content, and the other only on inter-grain water, it could be considered that the divergence of these water contents with increasing Liquid Limit could be based on changes in specific surface areas brought about by mineralogical differences.

Also, the degree of change of shear strength in the Liquid Limit cone-penetrometer test, with changes in water content, known as the flow index, could be expected to be steeper for soils with higher specific surface areas. This is because the displacement of mineral particles in a saturated soil due to addition of water, while being similar in mass between soils, will cause proportionally higher changes in surface area per unit volume as specific surface area increases, as has been demonstrated by the work of Sridharan et al. (1999). Further research of interest is that of Sridharan and Nagaraj (1999) who investigated the absorption of water into twenty seven different soil samples when placed over saturated sand. These data they then related to the measured water content at the Liquid Limit (Figure 2.25).
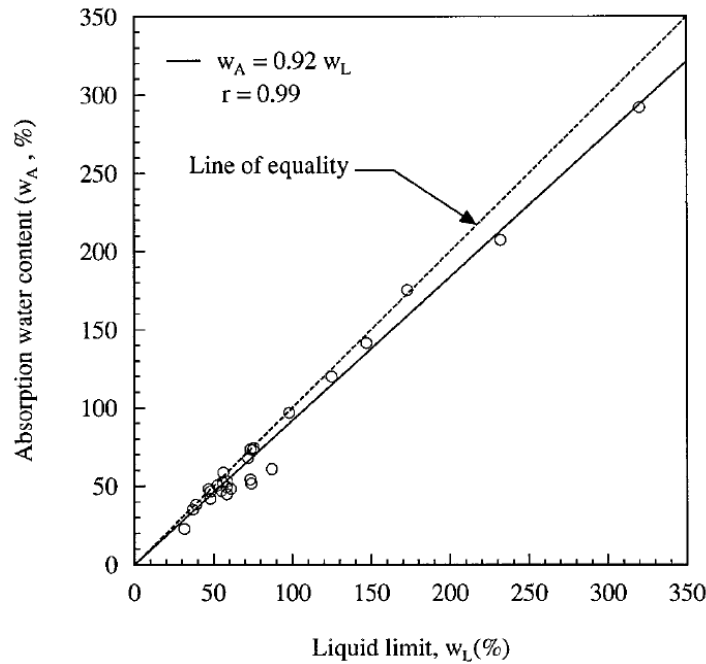
Figure 2.25. Absorption water content versus Liquid Limit (Prakash and Sridharan, 2004).

Their results showed that fine-grained soils are capable of absorbing significant quantities of water under unconfined conditions and that the resulting water contents were close to the Liquid Limit. The linearity of their relationship also implies that there is some commonality of properties between soils, as is also shown by the Liquid Limit to specific surface area relationship. It should also be noted that the work of Prakash and Sridharan (2004) raises the possibility that there may be relationships between electromagnetic properties and shrink/swell behaviour in fine soils. Furthermore, as shrinkage could be loosely considered related to mineralogy by that study, and as Dolinar and Trauner (2005) indicate a relationship between mineralogy and inter-grain water content at the Liquid Limit, it is possible that shrinkage properties can provide some indication of electromagnetic properties. However, as shown through investigating the shrinkage and Liquid Limits of soil mixtures, at varying proportions,

Sridharan and Prakash (2000a) found that the relationship between the two parameters is not entirely clear. Examples of their data are shown in Figure 2.26 and it can be seen that it cannot be concluded that shrinkage proportions will show the same relationships to specific surface area that are apparent for the Liquid Limit, at least in mixtures of soils of different origins.
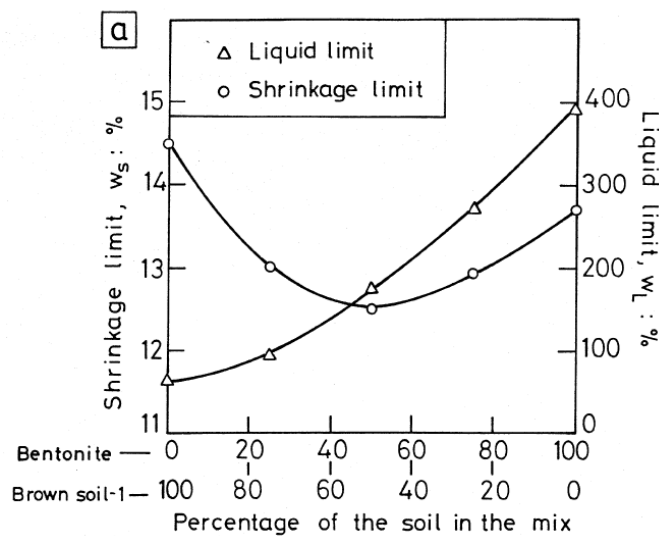
Figure 2.26. Liquid and shrinkage limits in soil mixtures (Sridharan and Prakash, 2000a).

As it is the clay fraction of fine-grained soils that is associated with the highest specific surface areas, the percentage clay fraction could be considered to be a useful means of gauging the amounts of different types of pore water present. However, as indicated by Dolinar and Trauner (2005), it is possible that the amount of inter-grain water is of greatest importance and that total water at the Liquid Limit may be less relevant, although this could be disputed by the work of Farrar and Coleman (1967).

Therefore, it cannot be conclusively determined whether there should be a good relationship between clay content and specific surface area for the purposes of this study. However, work by Sridharan and Prakash (2000a), illustrated by Figure 2.27, indicates that there may not be such a relationship if other factors, such as mineralogy, are ignored. However, for the work of Peplinski et al. (1995), whose complex permittivity studies of five clays showed correlation to clay content, it is possible that for the small number of soils tested some relationship may however exist. As their study utilised soils with clay contents between 5% and 20%, it is also possible that there may be relationships between clay content and complex permittivity when variations in specific surface area are averaged over small clay contents. However, for fine grained soils, where particles may potentially be anywhere up to 425μm in size, Figure 2.27 indicates that caution needs to be exercised in considering clay proportions to be a useful indicator of specific surface area.
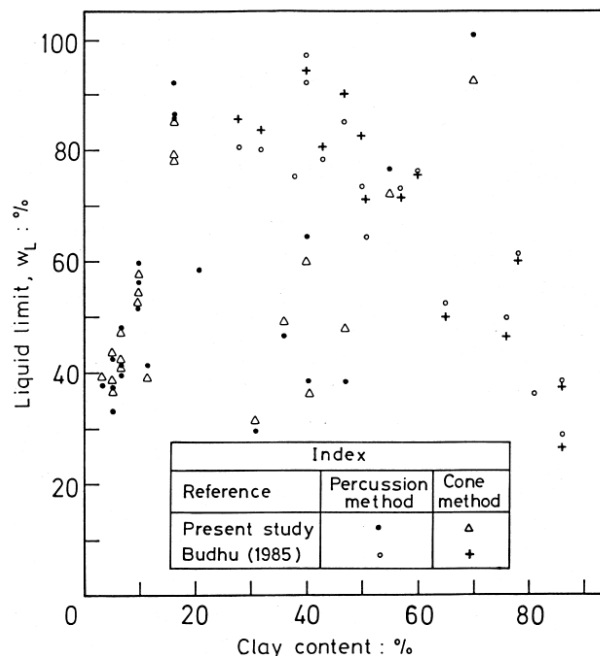
Figure 2.27. Liquid Limit versus clay content (Sridharan and Prakash, 2000a).

However, regardless of the potential lack of correlation between the proportion of clay present in a soil and the Liquid Limit or specific surface area, it is to be expected that the specific surface area of the smallest size fractions will be greater than the largest. Therefore, the effects of any bound water could also be greatest for the smaller sized particles and so they may also be more dispersive (Raythatha and Sen, 1986). This is illustrated by the work of Arcone et al. (2008) which measured the complex permittivity of different size fractions of a soil over a very wide frequency range, as illustrated in Figure 2.28.
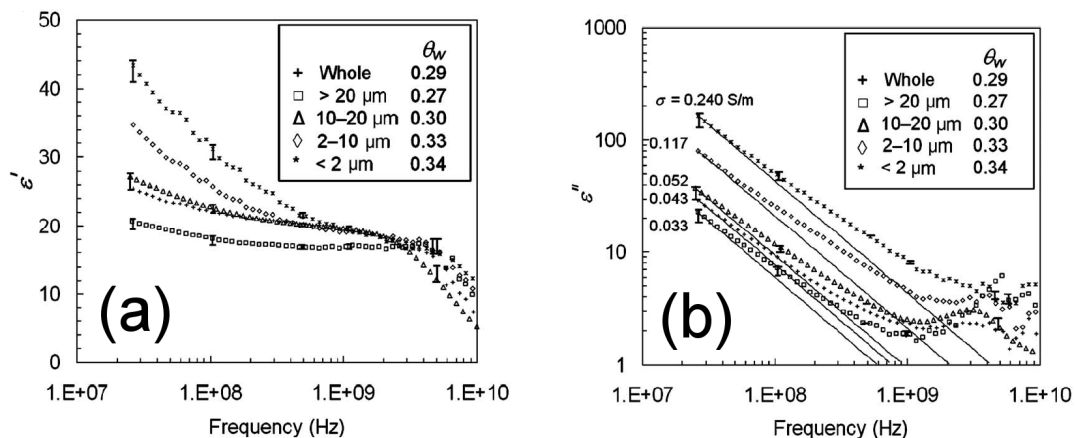
Figure 2.28. The permittivity of different particle size components of a soil: (a) real and (b) imaginary parts (Arcone et al., 2008).

It can be seen from Figure 2.28 that there is significantly greater dispersion, and associated losses in the imaginary part, for the smallest particle sizes, as would be expected from the work of Raythatha and Sen (1986). For the soil studied, the fraction greater than 20μm exhibited lower permittivity than the soil as a whole, and that below approximately 1GHz the smaller particles less than 10μm had much greater permittivity

than the whole and exhibited significantly greater dispersion. Therefore, as the specific surface area of each particle size would be dependent upon mineralogy, it could be argued that the specific surface area and size distribution of particles are both important in terms of electromagnetic signal velocities. It is also significant to note that the smaller size fractions, all of which have similar water contents, converge at frequencies close to 1 GHz in the data of Arcone et al. (2008). This is interesting in relation to the 1GHz relationship found by Wensink (1993).

In considering geotechnical data it should also not be forgotten that an objective of this study is to allow use of simple geotechnical indicator tests to estimate the electromagnetic properties of soils. Sources of such indicator data can be found, for instance, in widespread soil survey reports, student projects and theses. Taking the UK as an example, such data are widespread, as indicated by Rogers et al. (2009), and illustrated in Figure 2.29 which shows the extent of geotechnical data held by the British Geological Survey (BGS). As Figure 2.29(a) shows, the majority of geotechnical samples studied by the BGS have been dominated by the size fraction of 425µm or less, which means that a study of fine-grained soils would be fully relevant to the dominant fraction.

Also, from Figure 2.29(b) it can be seen that those data are relevant to near surface applications and, from Figure 2.29(c) it can be seen that the data well represent low-lying UK areas where most major population centres are to be found. Furthermore, Rogers et al. (2009) show that the geotechnical A-Line provides a good correlation between the Liquid Limit and index of plasticity, as shown in Figure 2.29(d). Given that the BGS database includes more than twenty thousand data locations for geotechnical

indicator tests, as shown in Figure 2.29, it is apparent that an approach tailored to estimating electromagnetic properties from those simple laboratory tests may yield a widely relevant cross-disciplinary methodology.
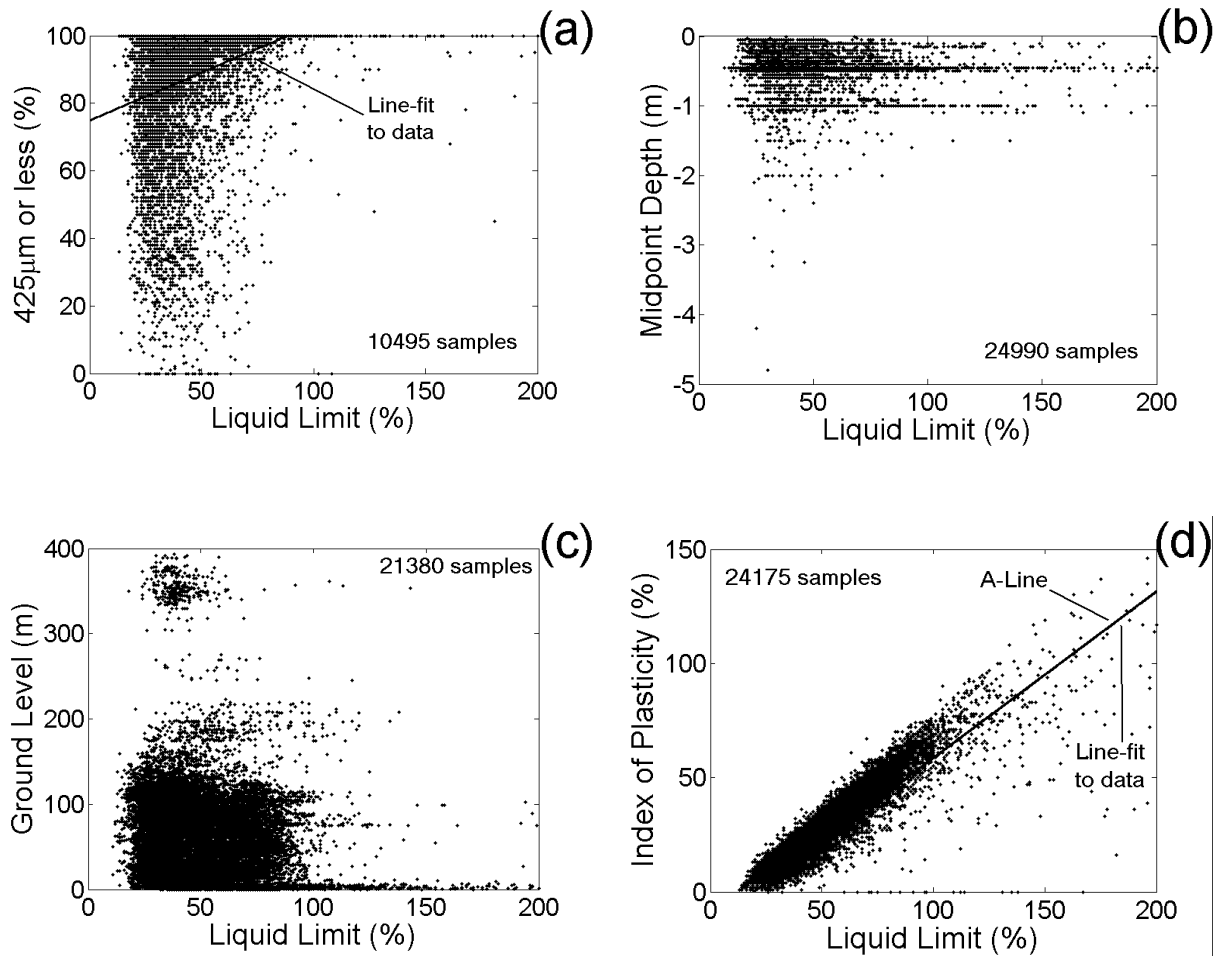
Figure 2.29. Examples of UK geotechnical data held in the British Geological Survey's National Geotechnical Properties Database (Rogers et al., 2009): (a) proportion of fine-grained soils, (b) depths represented, (c) ground levels covered and (d) relationship to A-Line.

2.8 MEASUREMENT OF SOIL ELECTROMAGNETIC VELOCITY SPECTRA

2.8.1 Time-Domain Reflectometry (TDR)

The popularity of TDR, as a means of measuring soil electromagnetic signal velocities, grew from work in the mid 1970s (Robinson et al., 2003a) and culminated in the work of Topp et al. (1980). It was developed largely as a means of measuring volumetric water contents in soils through their relationship to signal velocity. Prior to the work of Topp et al., TDR had been used for soils research, as demonstrated by the seminal work of Hoekstra and Delaney (1974) covering a wide frequency range (through inversion of time-domain data) and gravimetric water contents between zero and 15%. However, the work of Topp et al. (1980) did not require the complex sampling oscilloscopes and measurement diodes of Hoekstra and Delaney (1974) and, although the data provided by the system of Topp et al. (1980) were orders of magnitude less detailed than that of Hoekstra and Delaney, it showed correlations to soil water content without complex data inversion. Although at first there was opposition to this new method (Topp et al., 2003), and despite there being other methods for electromagnetic measurement and in-situ water content determination (Gray et al, 1982; Dorsey et al., 2005; Venkatesh and Raghavan, 2005), it is now a widely used, well-characterized, soil physics measurement tool. Therefore, it is apparent that the main advantages of the work of Topp et al. (1980), from which the popularity of TDR grew, was the simplicity it offered in terms of equipment and data processing, in comparison to otherwise similar TDR systems. It has also found a wide range of applications including agricultural water content determination (e.g. Nadler et al., 2006), correlation of soil electromagnetic properties to ground penetrating radar data where good

correlation has been found (Pettinelli et al., 2007), and even determination of ground shear locations using buried cables (Dowding et al., 2002).

The time-domain reflectometry (TDR) measurement system can be explained through the illustration of Figure 2.30. In simple terms, an electrical pulse is injected into a coaxial cable and a proportion of the pulse is reflected from any impedance mismatches encountered, and potentially some may radiate from an open end (Bakhtiari et al., 1994). This reflected energy is then sampled at high speed inside the TDR equipment, to provide a graph of reflected signal energy versus time. If the distance between two reflections is known, as is the case for the start and end of a probe, the time axis can then be converted to one of distance. If the velocity changes, as when a probe is placed in soil or water, so too will the time measured between the reflections. This, therefore, results in a change in measured distance, which can be used to calculate the velocity at which the pulse propagates.
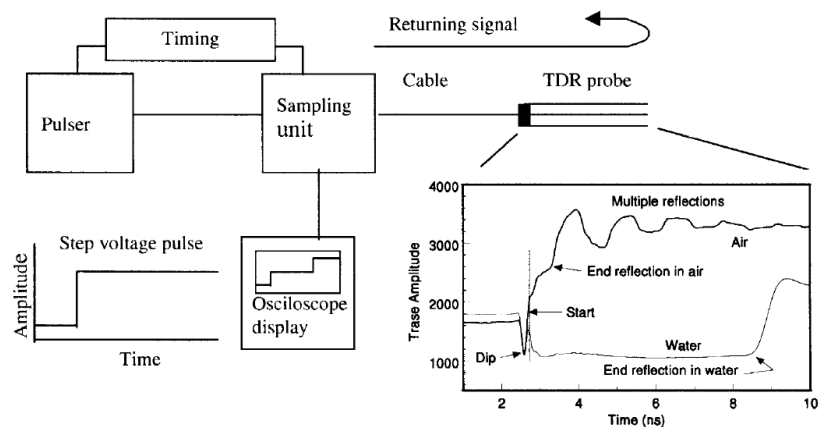
Figure 2.30. The TDR measurement system (Robinson et al., 2003a).

On this basis, if the time is considered to be that for two-way travel in the probe (i.e. inward and reflected from the end) as shown in Equation 2.53, and the propagation velocity is treated as lossless (Equation 2.54, repeated for convenience from Equation 2.38), then the time can be determined from Equation 2.55 (after Kelleners et al., 2005b). However, as will be recalled from the discussion of loss mechanisms and propagation, the velocity in soils is generally not that of a lossless case. Therefore, the apparent permittivity is neither the real nor imaginary part of the permittivity, but instead a representation of signal velocity (Lin et al., 2003). In low loss cases, the apparent and real permittivities can be expected to be close in value and, as losses increase so also will their divergence.

$$t = \frac{2L}{V} \qquad\qquad\qquad \text{[Eq. 2.53]}$$

$$V = \frac{c}{\sqrt{\varepsilon_r^*}} \qquad\qquad\qquad \text{[Eq. 2.54]}$$

$$t = \frac{2L\sqrt{\varepsilon_r^*}}{c} \qquad\qquad\qquad \text{[Eq. 2.55]}$$

where t is the travel time of the pulse (s), L is the physical length over which the pulse propagates (m), V is the signal velocity (m.s^{-1}), c is the velocity of light *in-vacuo* (m.s^{-1}), and ε_r^* is the apparent permittivity.

Equation 2.55 can be re-arranged to provide the apparent permittivity from the measured time between reflections. However, one of the reasons why TDR became so popular after the work of Topp et al. (1980) was their use of commercial TDR equipment that reduced the cost to a level suitable for common use in soils research.

The equipment used, designed to determine the distance to faults in cables, therefore provided distance data rather than time data. This was achieved by setting the cable propagation velocity on the equipment. Therefore, it is traditional in TDR measurements to undertake calculations based on a distance scale determined by an assumed constant velocity, the velocity of light *in-vacuo* often being chosen. In this case it can be seen from Equation 2.55 that the distance to a reflection will increase in proportion to the apparent permittivity of the material being tested, leading to the relationship of Equation 2.56 between measured and physical length that is scaled as a function of the equipment propagation velocity setting (Jones et al., 2002). In reality the physical probe length is adjusted through measurements in materials of known apparent permittivity (generally air and water) to account for any deviation of the measurement system from an ideal configuration. For simplicity, the propagation velocity factor can be set to unity, resulting in Equation 2.57, where it should be noted that the cable tester automatically corrects two-way travel times to give the one-way distance.

$$\varepsilon_r^* = \left(\frac{x_2 - x_1}{V_P L} \right)^2 \qquad\qquad \text{[Eq. 2.56]}$$

$$\varepsilon_r^* = \left(\frac{L_{TDR}}{L_{PROBE}} \right)^2 \qquad\qquad \text{[Eq. 2.57]}$$

where x_2 and x_1 are distances to the probe end and start reflections respectively (m), L_{TDR} is the probe length measured using TDR (m) and L_{PROBE} is the physical probe length (m).

However, one aspect that is not clear in these measurements is the frequency at which the TDR data are valid. For a lossless material, it could be expected that the

apparent permittivity would be frequency-independent due to a lack of water, but in dispersive materials the wide frequency range inherent in the TDR pulse could be expected to cause electromagnetic dispersion. However, while TDR measurements are commonly associated with frequencies close to 1GHz (Evitt and Parkin, 2005), research has indicated that the power level of the frequency band generated by the electrical pulse in TDR equipment may be significantly biased to frequencies below 500MHz in wet soils (Friel and Or, 1999). Therefore, higher frequencies may be attenuated in conductive soils to the extent that they have little influence on time-domain measurements. The total bandwidth (i.e. frequency range) of the TDR pulse is equipment dependent and proportional to the pulse rise-time employed. Robinson et al. (2005) consider the effective maximum frequency in the pulse to be as shown in Equation 2.58.

$$f_{eff} = \frac{0.35}{t_r} \qquad\qquad \text{[Eq. 2.58]}$$

where f_{eff} is the effective maximum frequency (Hz) and t_r is the pulse rise time between 10% and 90% amplitude (s).

It is apparent that short pulse rise times will be associated with higher frequencies than long rise times. It has been suggested that the measurement frequency of TDR corresponds to the highest frequency provided by the pulse (Lin et al., 2003), although this frequency may reduce in comparison to that of Equation 2.58 due to the attenuation of higher frequency components in soils as observed by Friel and Or (1999).

As can be seen in the above discussion, TDR benefits from a very simple measurement methodology, combined with relatively inexpensive and commercially

available equipment that is easily transferred to soil geophysics. While this adds to the popularity of TDR, the probes used with it are also an important factor. The most common types of TDR probes are illustrated in Figure 2.31 and essentially each consists of a cable connector mounted on the probe head (generally metal or plastic) and a number of metal pins or plates. One of the pins, or plates, is connected to the inner conductor of the cable, and the others to the cable electrical earth. According to Zegelin et al. (1989), the two-pin configuration was the first to be used with TDR, by the team of Topp et al. (1980), but this form of probe caused significant impedance mismatch at the cable/probe interface.
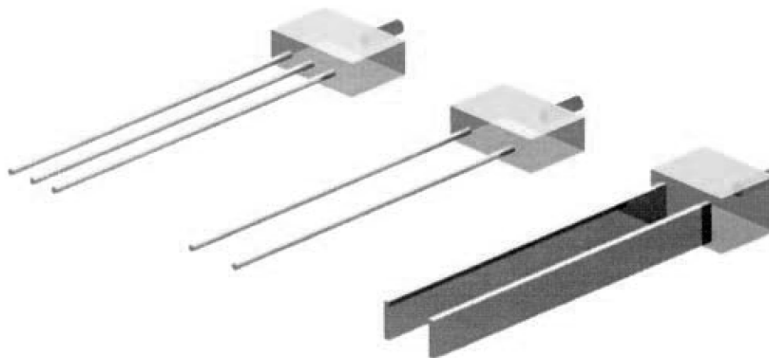
Figure 2.31. Common TDR probe types (Robinson et al., 2003a).

They therefore developed the three-pin configuration in order to remove "considerable signal and information loss" and found this, and a similar four-pin probe, to have electrical properties close to those of coaxial transmission lines (Zegelin et al., 1989). The three-pin probes are essentially a refinement of the two-pin versions, with both outer pins connected to an electrical earth. The construction of these probes is,

therefore, quite simple and robust and they may be simply constructed by the user, although commercial versions are also available. It should be noted however that Jones et al. (2002) caution against repeated insertion and removal of probes, as this may result in air gaps that can degrade the accuracy of TDR data. It has been noted by Whalley (1993) that the wide variety of probes and cells developed for use with TDR also has a negative aspect in that it can be difficult to "contrast these designs to enable the experimenter to select an appropriate system."

The ease of construction of the probes has led also to more complex TDR probe designs, although still compatible with the TDR methodology described in this section. For instance, TDR probes are generally too large for use in standard geotechnical experiments and this led Persson et al. (2006) to develop a small probe suitable for such uses as measurements of water content in small soil columns (Figure 2.32(a)). Essentially, the physical length of the probe measured by TDR is increased, in relation to the total probe length, by winding the central conductor into a spiral. This has the advantage that the short probe length does not cause a reduction in apparent permittivity resolution, which would be associated with the travel time measurement resolution of the TDR equipment (i.e. the travel time remains large in relation to the minimum measured time increment). Also of note is the variable-volume TDR probe of Souza et al. (2004), which eliminates the restrictions of the probe head by replacing it with separate cables for each pin/rod (Figure 2.32(b)). While the lack of a probe head does cause the additional work of separately inserting and removing each pin, this is mitigated by greater flexibility in the choice of probe geometry and the potential to measure water content over variable soil volumes.

Further proof of the versatility of TDR in geotechnical research has also been provided by Lin and Tang (2005) who used it for the construction of an extensometer, a moveable impedance mismatch connected to the displacement to be measured, allowing determination of the displacement from TDR distance measurements. If required, TDR may also be used to provide an estimate of electrical conductivity (Jones et al., 2002, Robinson et al., 2003a), although great care is required as instrument errors and cable resistance may cause significant inaccuracies (Lin et al., 2007).
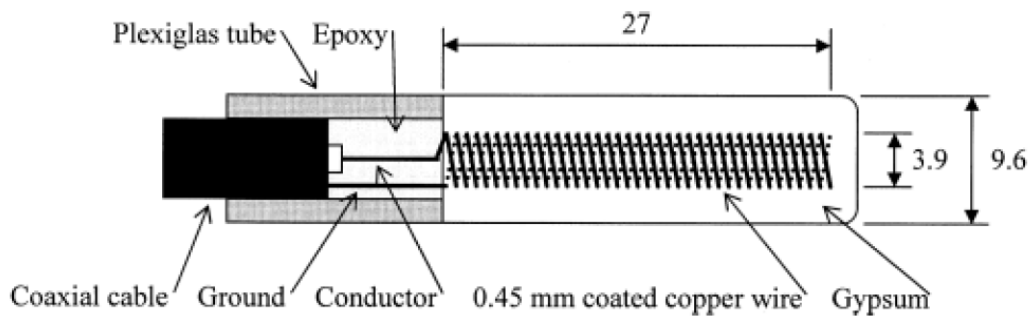
(a)
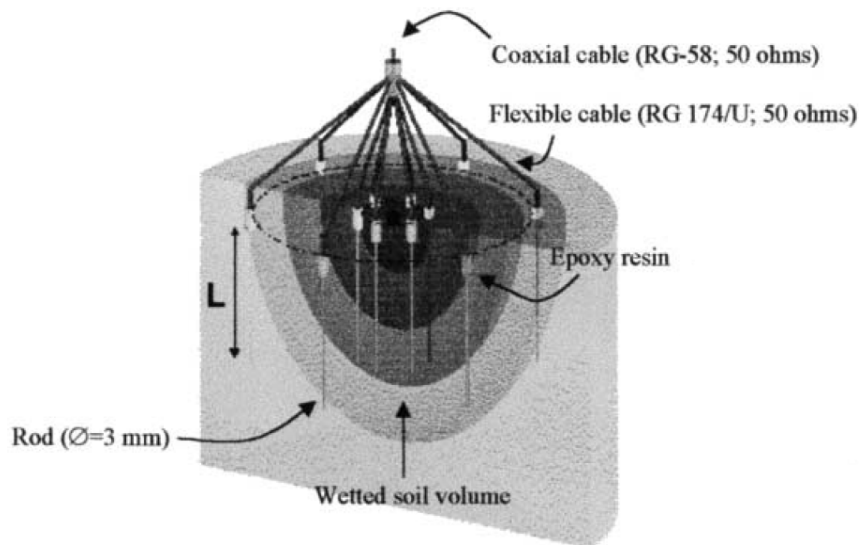
(b)

Figure 2.32. Two alternative TDR probe designs: (a) small probe for laboratory testing (Persson et al., 2006), and (b) variable-volume probe for field use (Souza et al., 2004).

From the discussions on signal propagation in Section 2.4, it is evident that reflections within soil will diminish as the loss mechanisms increase (Yanuka et al., 1988), and this can be a significant problem in high surface area soils (Logsdon, 2005b). Also, from Equation 2.34, it is further evident that this loss of reflection strength will increase with the length of probe used. Therefore, TDR probes must be carefully selected for the soil they are to be used in. As shorter probes will have travel times closer to the resolution of the TDR equipment, it can be expected that longer probes may be more accurate. As probe length must reduce with soil losses, there is therefore a trade-off between the ability to detect reflections and the accuracy of the resulting apparent permittivity data. The difficulty in determining the end-of-probe reflection distance in lossy (attenuative) materials is illustrated in Figure 2.33: the end reflection becomes significantly less pronounced as the probe length increases.
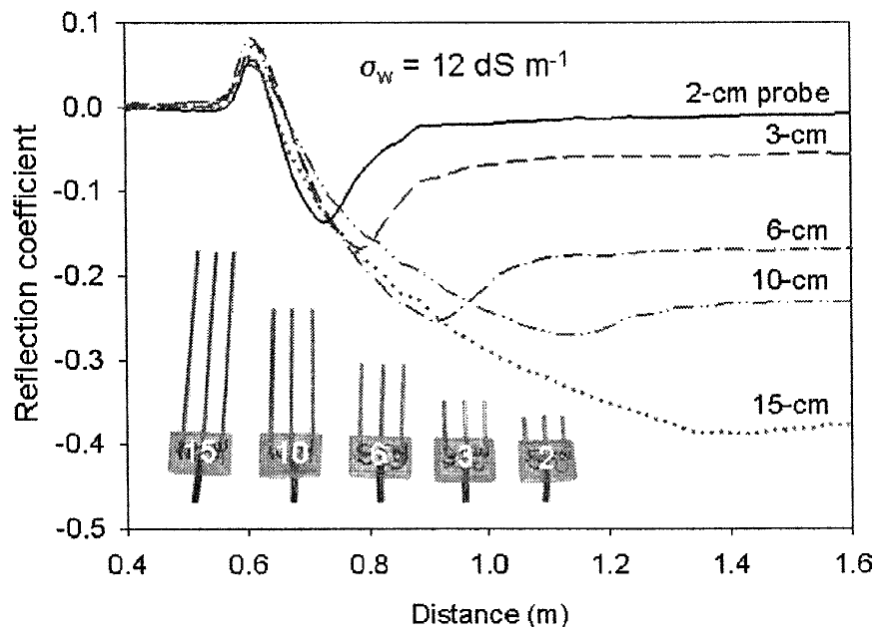
Figure 2.33. Variations in TDR reflections due to probe length (Jones and Or, 2004).

As the conductivity of the material in Jones and Or's (2004) study was not abnormal for a clay soil, it can be seen that the maximum probe length useful under many circumstances may be of the order of 100mm. However, for low-loss soils, longer probe lengths may be appropriate and would increase the depth over which the TDR measurement is valid. However, longer probes may lead to greater potential for the velocity measurement to span more than one layer of soil, in which case greater care may have to be taken if the TDR data are to be accurately interpreted (Schaap, et al., 2003).

Another important aspect of TDR probes is the distribution of the electromagnetic field around them, as this will affect the sampling area and volume. As illustrated in the simulations of Figure 2.34, there is significant variation in field distribution between the common probe types. For each, however, it is apparent that the majority of the electromagnetic field strength is concentrated close to the conductors and in the space between them. However, as some of the field also extends away from the probe conductors, it is possible that any reflections associated with the outer field will be different to that of the main field, if the total field is not enclosed in a uniform soil mass. Therefore, changes in material properties within the area occupied by the electromagnetic field could cause degradation of the time-domain data. It can be seen that two-pin probes can have larger sampling volumes than three-pin probes (Jones et al., 2002) and so may be more susceptible to changes in nearby soil conditions. Also, where two probes are installed at close enough proximity to allow their fields to interfere, it has been demonstrated that this may affect TDR data. For instance, Castiglione et al. (2006) found differences between TDR time-domain data with and without a second, interfering, probe close by, which they considered could cause

significant inaccuracy in conductivity estimates. However, they found that the interference did not affect calculation of the travel time from reflections, nor associated apparent permittivity and water content determination.
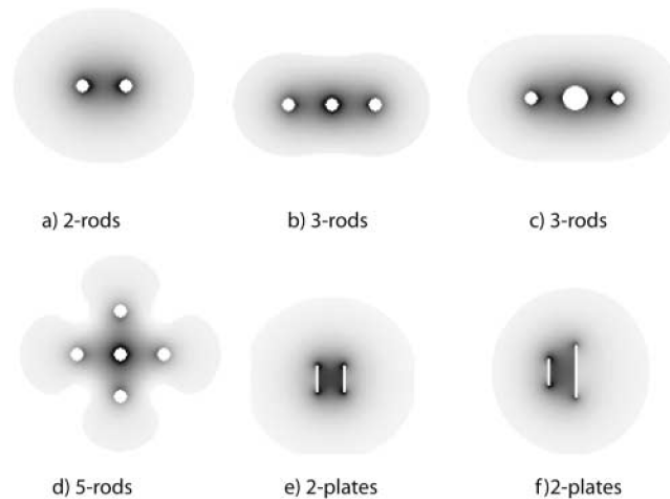
Figure 2.34. Simulated electromagnetic field densities around TDR probes (Robinson et al., 2003a).

The importance of the way in which the field is concentrated around a probe was investigated by Knight (1992), who concluded that it is largely a function of the diameter and spacing of the electrodes. It was concluded that, for greatest accuracy, the electrode diameter should be as large as possible, as small diameters would cause a high energy density around the conductors, causing any non-uniformity at the soil interface to affect measurements. However, Zegelin et al. (1989) also recognized that larger probe diameters cause greater disturbance of soil structure and water flow than small diameters, and hence concluded that, as a compromise for practical purposes, "the ratio of electrode spacing to wire diameter should not be greater than about 10." It should

also be noted that the measurements of apparent permittivity by TDR methods will provide different data depending not just on the length of the probe/cell, but also due to the rod spacing (Whalley, 1993). Therefore, changes in the geometry of the probe/cell could require separate calibrations.

2.8.2 Coaxial Measurement Cells

While TDR probes are adequate for many uses, for accurate results it could be argued that they are not true coaxial cells, although they can closely approximate them (Zegelin et al., 1989). This could cause problems where the highest accuracy is required in measurement and modelling, where the more defined geometry of a coaxial cell could be considered more appropriate. Cownie and Palmer (1951) describe two early methods of measuring the dielectric constant of soils. One of these involved anchoring one end of an antenna into soil and injecting a signal into the other end. This, they say, involved large amounts of soil that made measurements with accurate water content adjustment impractical. Therefore, they undertook their measurements using a coaxial cell, short circuited at one end and with the signal injected at the other end. This they found a satisfactory method and coaxial cell use has remained common in electromagnetic testing of soils. Also, even the seminal work of Topp et al. (1980) was developed using a large cell of coaxial geometry. Therefore, a short discussion is provided here pertaining to coaxial measurement cells.

As can be seen in the example of Figure 2.35, a coaxial cell simply comprises a metal inner conductor of circular cross-section, surrounded by a metal tube similarly of circular cross-section. Electromagnetic propagation within such coaxial geometries has been well characterized in the literature, and so the annulus between the two conductors

can be filled with soils in order to determine their electromagnetic properties. As with TDR probes, coaxial cells are not considered to have electromagnetic fields that are consistent over the full cross section of the annulus, the field being stronger near the centre conductor. It is necessary therefore to ensure that the contents are in close contact with the centre conductor (Janezic and Jargon, 1999).
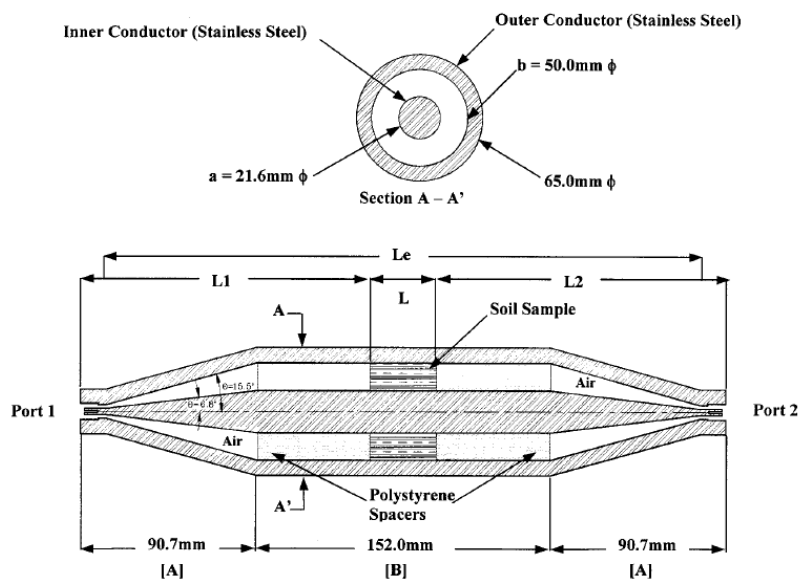
Figure 2.35. An example of a coaxial measurement cell (Shang et al., 1999).

Measurements using coaxial cells, often termed transmission lines, depend on injecting a signal into the cell and measuring the voltage reflected as a proportion of the injected voltage. The part of the voltage not reflected is then transmitted into the cell, where it may either exit through the end, or be reflected back to the signal injection point, depending on the design of the cell. The reflection of electromagnetic signals is governed by the impedance (Z) of materials at an interface (put simply, the opposition provided by the material to time varying signals), which itself is governed by

permittivity, magnetic permeability and conductivity. The impedance can be represented by Equation 2.59 (Hayt and Buck, 2006), and it should be noted that this parameter may be a complex value for lossy (attenuative) materials. It should also be noted that this is not necessarily the complex permittivity of the soil, but rather that of the soil and cell in combination.

$$Z = \sqrt{\frac{\mu}{\varepsilon}}$$
[Eq. 2.59]

A difference in the impedance, often termed impedance mismatch, at an interface between contrasting electromagnetic properties (e.g. at the cell ends) causes a proportion of the signal energy to be reflected away from the interface and the remainder to be transmitted onward. The energy involved is governed by the reflection (Γ) and transmission (τ) coefficients, as defined in Equations 2.60 and 2.61 (Hayt and Buck, 2006), which when applied as a factor to the incident amplitude provide the amplitude of the reflected and transmitted signal.

$$\Gamma = \frac{Z_1 - Z_0}{Z_1 + Z_0}$$
[Eq. 2.60]

$$\tau = \frac{2Z_1}{Z_0 + Z_1}$$
[Eq. 2.61]

where Z_0 is the impedance of the material through which the signal passes toward the interface and Z_1 is the material towards which the signal travel is occurring.

It should be noted, due to the large variation of soil permittivity and conductivity with water content, that reflections often vary significantly due to the amount of water present (Milsom, 1996). Equations 2.60 and 2.61 relate to reflections due to signals normal to the reflecting boundary, and so are suitable for use with a coaxial cell.

Where the propagation parameters are themselves complex values, the values of the reflection and transmission coefficients will also be complex, in which case the magnitude of the coefficient provides the scale factor for incident amplitude and the associated phase angle represents the change in phase of the reflected and transmitted signals relative to that of the incident signal. For lossless materials, the coefficients will be real values. Therefore, it can be seen that measurement of the reflected and transmitted signal voltages can, if the reflection due to the cell impedance can be removed, be used to determine soil electromagnetic properties. Fortunately, the impedance of coaxial cells has been widely studied and can be represented by Equation 2.62 (Wadell, 1991).

$$Z_{cell} = \frac{138}{\sqrt{\varepsilon_r}} \log_{10}\left(\frac{r_{outer}}{r_{inner}}\right) \qquad \text{[Eq. 2.62]}$$

where Z_{cell} is the characteristic impedance of the cell (Ω), r_{outer} is the inner radius of the outer conductor (m) and r_{inner} is the outer radius of the inner conductor (m).

However, the characteristic impedance is a measure of reflections for a transmission line of infinite length (or signals within it are fully attenuated), so fluctuations in reflected signal strength would be expected to occur due to reflections within the coaxial cell.

The variations in reflected signal strength, due to multiple reflections, can be considered an impedance variation. These impedance variations (termed the input impedance) are predictable and can be determined through use of Equation 2.63 (Wadell, 1991).

$$Z_{in} = Z_{cell} \left(\frac{Z_{term} \cosh \gamma L + Z_{cell} \sinh \gamma L}{Z_{cell} \cosh \gamma L + Z_{term} \sinh \gamma L} \right)$$ [Eq. 2.63]

where Z_{in} is the input impedance, Z_{term} is the impedance at the far end of the cell, γ is the complex wave number, and L is the cell length (m).

However, it should be noted that the cable used with TDR probes also forms a coaxial transmission line (Lin, 2001). Therefore, where cables are not detachable from probes, measurement equipment would not be able to remove their effects. So, Equation 2.63 would have to be applied firstly to the probe/cell, and then to the cable assuming the probe/cell input impedance to be the termination impedance of the cable. This highlights the usefulness of being able to cancel cable effects during measurement system calibrations.

2.8.3 Techniques Available For Extending TDR Data

In order to determine the best manner in which TDR measurements can be improved upon, it is necessary to consider other available methods. Therefore, a wide range of electromagnetic measurement systems described in the literature are detailed in Table 2.1.

A very significant factor in deciding upon a suitable measurement system is whether any non-probe systems are one-port or two-port. The cell illustrated in Figure 2.35 shows that Shang et al. (1999) used a method requiring connection of an analyzer to two ports, one at either end of the cell. Therefore, their methods rely on measurement of reflections from Port 1 and transmitted signal voltages at Port 2.

Table 2.1. Summary of relevant permittivity measurement systems.

Reference	Sensor Type	Measured Domain	Frequency (c. MHz)	Ports
Topp et al. (1980)	Cell/Probe	Time	Unknown	One
Hoekstra and Delaney (1974)	Cell	Time	100-26000	One
Wensink (1993)	Cell	Frequency	1-3000	Two
Gorritti and Slob (2005)	Cell	Frequency	0-3000	Two
Shang et al. (1999)	Cell	Frequency	0.3-1300	Two
Scholte at al. (2002)	Cell	Frequency	0-1400	Two
Logsdon (2005a)	Cell	Frequency	0.3-3000	One
Thomas (1966)	Probe	Frequency	30	One
Weir (1974)	Cell	Frequency	100-18000	Two
Cownie and Palmer (1951)	Cell	Frequency	430	One
Xu et al. (2007)	Cell	Frequency	0-1500	One/Two
Zheng and Smith (1991)	Surface probe	Frequency	0-5000	One
Campbell (1990)	Probe	Frequency	1-50	One
Huang (2001)	Cell	Frequency	50-1000	One
Birchak et al. (1974)	Probe	Frequency	4000-6000	Two
Chazelas et al. (2007)	Cell	Frequency	100-1300	One
Jones et al. (2005)	Cell	Time	Unknown	One
Nussberger et al. (2005)	Probe	Time	Unknown	One
Klein and Santamarina (1997)	Surface probe	Frequency	20-1300	One
Logsdon and Hornbuckle (2006)	Probe	Frequency	0-100	One
Heimovaara (1994) and Heimovaara et al. (1996)	Probe	Frequency	0-2000	One

In practice, however, the measurements can be made in the reverse direction, but the essential element of importance is that measurements must be made at both ends of the cell. In a one-port system, reflection measurements are only made at Port 1, Port 2 being left either open- or short- circuited. Therefore, in terms of one aim of this thesis, i.e. the potential use of probes, it can be seen that two-port systems would cause significant problems due to both ends of the probe requiring connection to the analyzer, even though one end is buried within the soil. Therefore, for any measurement system requiring use of cells and probes, one-port measurement methods have obvious practical advantages.

Two of the methods in Table 2.1 are TDR based and, as such, cannot be considered to potentially extend their own functionality. The work of Hoekstra and Delaney (1974) did provide frequency domain data but only through inversion from the time-domain, so as with other such inversion methods (e.g. Lin, 2001, Lin, 2003, Heimovaara, 2001) it requires understanding of a complex mathematical model for adequate inversion. Of the other available methods, a large proportion can be considered inappropriate because they employ two-port measurements and so the data processing is also not suitable for use with standard probes. Of interest is the work of Xu et al. (2007) which extends on the previous work of Shang et al. (1999) and Scholte et al. (2002) that allows their two port cell to be used as a one-port system, by removing one port and replacing it with a steel plate to short-circuit the end of the cell. This allows much greater flexibility, but their system has not been used with probes. Of the measurement systems considered, two employ surface probes, which do not provide data on properties within the bulk soil mass, and therefore could be considered susceptible to boundary effects. Also of interest is the work of Huang (2001) who used

a one-port cell similar in construction to that of Xu et al. (2007) and Chazelas et al. (2007). However, as is noted by the authors, the interpretation of data from a one-port system is "one of the major problems with this method." and it should be noted that they required measurements using different lengths in order to obtain full complex propagation data. Their method, and the majority of other frequency-domain methods, also provides data on complex propagation parameters, rather than the directly measured signal velocity or apparent pemittivity provided by TDR. While this is not a major problem, it does however add complexity that may distract from a simple and robust extension to TDR.

Of the systems considered, it should be noted that some initially appear eminently suitable for use in geotechnical research. For instance, an early probe for measurement of soil electromagnetic properties, and water content, was a capacitance probe developed by Thomas (1966) due to difficulties he expressed in using commercial capacitance probes in moist soils. The probe (Figure 2.36) worked by measuring the capacitance changes around two stainless steel conductors attached as a point on a perspex rod, giving the advantage that it could be driven into the ground to a depth close to one metre. This therefore allowed determination of water content at a number of depths, albeit with some disturbance of the soil. However, a limitation of the system was that it was single-frequency and, at 30MHz, would not provide extensive signal velocity and dispersion data. Similarly, the method of Cownie and Palmer (1951) may also be discounted as it is single-frequency, although it should be noted that Cownie and Palmer (1951) employed a short-circuited coaxial cell which could be used over a wider frequency range. The work of Birchak (1974), which used a specially designed microwave soil probe, also poses difficulties for extending TDR, as it was designed for

a frequency range much too high for consideration of electromagnetic dispersion in soils.
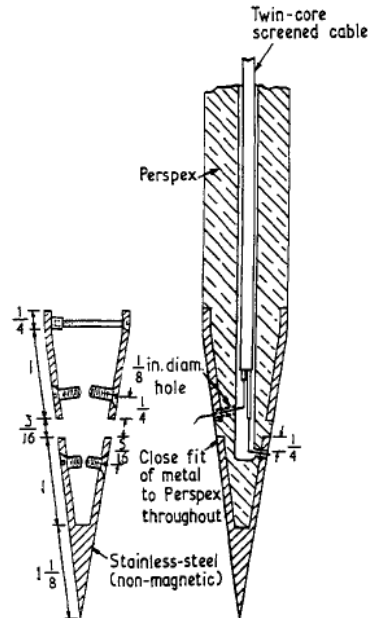
Figure 2.36. An early soil capacitance probe (Thomas, 1966).

Another method of interest is that of Nussberger et al. (2005) who utilised a single-rod probe for TDR, with a metal earth plate at surface level. However, this has some disadvantages for measurement of electromagnetic dispersion, where homogeneity would be desired, as it was found to be more sensitive to nearby scattering than multiple-rod probes, and so has a correspondingly larger sampling area (Nussberger et al., 2005). Also, Jones et al. (2005) describe an interesting TDR cell designed to allow manipulation of water content, but it is not clear that the design would be appropriate to this study, for expansive soils at volumetric water contents above their maximum of 45%, as it may be difficult to ensure that the soil water content distribution is homogenous.

Of particular interest, however, is the technique described by Heimovaara (1994) and Heimovaara et al. (1996) for characterization of a seven-conductor TDR probe in air and water (based on the low-frequency impedance probe design of Campbell, 1990). This described a simple method for calculating apparent permittivity at discrete frequencies in the voltage reflection spectrum from a TDR type probe connected to a vector network analyzer (VNA). Network analyzers measure the reflected and transmitted signals, such as for coaxial cells, as well as determining their phase (Hook et al., 2004) relative to the injected signal. These discrete frequencies are those which are associated with quarter-wavelengths that are equal to the length of the probe.

An important aspect of TDR is that the effects of any variations in the cable properties can be removed by considering only the probe/cell start and end reflection distances. Similarly, the Quarter-wavelength analysis (QWA) technique described by Heimovaara (1994) and Heimovaara et al. (1996), measures reflected voltage maxima and minima relating to the interaction of injected and reflected signals within a probe, and so could be expected to be less sensitive to changes in cable and connection properties. This factor is of particular importance should an extended TDR system be used in the field, as it has been demonstrated that the effects of large temperature variations on cable end reflections can be significant and may increase with cable length (Robinson et al., 2003b). Also, the calculation of apparent permittivity is relatively simple and straightforward, as shown in Equation 2.64 (Heimovaara et al., 1996).

$$ f_{qw} = \frac{(2n-1)c}{4\sqrt{\varepsilon_r^*(f_{qw})}L} \qquad\qquad \text{[Eq. 2.64]} $$

where f_{qw} is the quarter wavelength frequency (Hz), n is an index (n=1,2,3,4,...), $\varepsilon_r^*(f_{qw})$ is the apparent permittivity at the measured quarter-wavelength frequency, and L is the cell/probe length (m).

Due to these factors, it could be argued that QWA provides a relatively simple and robust method for determining apparent permittivity in the frequency-domain. A limitation, however, is that the apparent permittivity values are only measured at discrete intervals controlled by the wavelength, but these values are directly determined values rather than requiring calculation from the basic propagation parameters. The QWA technique (together with related non-TDR frequency-domain probe techniques) has been also used successfully by researchers such as Logsdon (2005a), in conjunction with a short coaxial cell. However, that cell utilised an inner conductor 17mm long (Logsdon, 2006a) and so did not provide permittivity data suitable for detailed consideration of electromagnetic dispersion.

Logsdon (2006a) describes the first quarter-wavelength frequencies as being between 0.4 to 1.1GHz, with usable data usually having a range up to 100MHz. Logsdon and Hornbuckle (2006) also describe the use of a short twelve-conductor coaxial probe for field soil measurements, although this does not appear to have been based on quarter-wavelength data and provided low frequency values to approximately 100MHz. Some researchers have also made limited use of the technique to validate methods for the inversion of TDR probe data to the frequency domain, including Cataldo et al. (2007) using a coaxial liquid testing probe and Jones and Or (2004) with a three-conductor TDR soil probe. However, both identified quarter-wavelengths from inverted data, rather than by directly measuring them in the frequency domain.

In their 1974 paper, Hoekstra and Delaney also mention using the positions of minima in reflection data, but do not give full details of this. Apart from these examples, the use of QWA appears limited in the literature and not fully developed as a soil electromagnetic measurement methodology. Regardless of this, QWA appears to have the potential to provide TDR with additional data on frequency-domain electromagnetic variations in soils, directly measured in the frequency-domain and demonstrated to work with similar probes to those used with TDR.

2.9 IDENTIFIED KNOWLEDGE GAPS

A significant knowledge gap found in the literature, which impacts significantly on the aims of this research, is that there is no fully developed simple and robust method available for measuring signal velocities <u>and</u> dispersion magnitude that is suitable for widespread geotechnical use. However, there is significant useful literature which may provide an opportunity for development of such a system, particularly that of Heimovaara et al. (1996).

Potentially the most important knowledge gap identified in this literature search is that no examples were found to illustrate the electromagnetic properties of even a single soil over both the full water content range of interest to geotechnical engineering (i.e. all water contents), and the full frequency range of interest to most electromagnetic survey methods (e.g. ground penetrating radar up to 1GHz). Given the variations likely to occur in such properties between soils, and the limited geotechnical data provided in many papers, it is unlikely that a full overview of soil electromagnetic properties can be

constructed from the available literature. To a certain extent this gap can be attributed to a need to measure electromagnetic properties in soils with low fine-grained soil fractions that exhibit limited swelling and shrinkage, although it should be noted that the bias toward unsaturated state electromagnetic data extends even to research with high clay contents.

Also, there is a lack of literature capable of relating geotechnical index tests to soil electromagnetic properties. Given the significant amount of useful geotechnical information that can be gleaned from index tests (e.g. Atterberg Limits and shrinkage percentages) this is surprising as it could be expected that the water related phases associated with them (i.e. dry, plastic and liquid) would cause variations in electromagnetic mixing models and water content measurement methods. The reason for this knowledge gap may be associated with the bias toward measurements in unsaturated soils, and so often below the Plastic Limit, but is very significant in terms of a full understanding of fine-grained soils. Similarly, an understanding of shrink/swell soil properties is considered important in geotechnical applications, but is not fully addressed in the geophysical literature, particularly in terms of relating this to relevant field water contents associated with the related geo-hazards (e.g. subsidence of structures).

A further set of knowledge gaps particularly worthy of mention relate to the multitude of mixing models available to cross-predict electromagnetic properties and water content. Given the bias toward unsaturated state geophysical research this implies an even greater level of complexity may be associated with measurements over all water contents. However, there appears to be a greater amount of research in the geotechnical

literature, compared to the geophysical literature, which could be used to inform mixing model selection (e.g. Diffuse Double Layer theory and differences in properties between inter-particle and inter-layer water). Also, as TDR based models are known to be associated with variable measurement frequencies due to loss tangent (and hence specific surface area and dry density) variations, and Wensink (1993) illustrates that only one mixing model may be required at 1GHz for fine-grained soils, it is also apparent that selective use of measurement frequencies may be a useful means of addressing mixing model complexity. Also, if a full overview of the electromagnetic properties of selected soils can be constructed, it may also aid in understanding how TDR is affected by loss tangents in saturated soils, allowing improved water content measurement. That, and the 1GHz data of Wensink, would also address another identified gap in knowledge: how to accurately measure water contents in fine-grained soils using electromagnetic signals.

Finally, two other knowledge gaps can be identified which, although outside the scope of the current research, have important impacts on future work. Firstly, for future application of this research to field testing, it should be noted that there is little literature available on which to formulate a definitive model of how temperature will affect electromagnetic measurements in the field. Based on the work of Debye (1929) it could be expected that high frequency data will show a reduction in apparent permittivity with temperature but, due to increased ionic conductivity (which affects loss tangents and so TDR measurement frequencies), it could be expected that an opposite trend may occur at lower frequencies, although this hypothesis remains to be fully tested.

Secondly, it should be noted that there is little information in the literature concerning the relationships between electromagnetic properties and the state of hydrogen-bonding in different types of soil pore water, the most useful source used herein having to be taken from literature relating to biological research. The state of hydrogen bonding could vary from non-existent in dry soils, through strained in small pores, to fully formed in very wet slurries. Therefore, an understanding of this relationship in future would benefit attempts to extend on work such as the Diffuse Double Layer theory, as well as aiding in the development of a 'universal' mixing model to relate soil water contents to electromagnetic signal velocities.

CHAPTER 3 – GEOTECHNICAL CHARACTERISATION

3.1 ADDRESSING KNOWLEDGE GAPS

The most significant knowledge gap identified in Chapter 2 relates to the limited data available on the electromagnetic properties of fine-grained soils in the saturated state. As fine-grained soils can have water contents varying between almost dry (e.g. surface soils in summer months), through plastic (e.g. many soils under urban areas), to liquid (e.g. drilling slurries and weather affected sub-grades), further knowledge of electromagnetic properties in the plastic state is required. However, a further knowledge gap is the difficulty in relating geotechnical characterisation tests, such as the Atterberg Limits, to electromagnetic property variations with water content, as it cannot be assumed that relationships will hold between soils with different ranges of plastic state water contents. Therefore, this knowledge gap requires addressing through use of soil samples providing a wide range of Atterberg Limits.

Also, while there has been much discussion in the geophysical literature on the effects of dry density and surface area on electromagnetic properties, very little work is available on the related effects of shrinkage and swelling. This is a significant limitation, as shrink/swell properties are related to mineralogy and the differences between inter-particle and inter-sheet water. Therefore, it is apparent that inclusion of a simple shrinkage index test in this research is appropriate. This will be addressed through use of linear shrinkage testing and ensuring that the soil samples used exhibit a wide range of shrinkage values. Furthermore, by using soil samples with wide ranging

Atterberg Limits and shrinkage properties, it can be expected that work in later chapters to consider potentially universal mixing models, to consider the effect of loss-tangents on TDR measurements, and therefore to consider methods of accurately measuring soil water contents using electromagnetic methods, could all be facilitated.

Therefore, soil samples were obtained with the intention of providing a broad range of Liquid Limits and Linear Shrinkage values and, therefore, are not necessarily natural or undisturbed soils. Also, as an important aspect of the electromagnetic testing was to identify relationships to geotechnical characterisations, the samples were not intended to have any specific geographic relevance.

3.2 GENERAL CHARACTERISTICS

All geotechnical testing was, unless stated otherwise, carried out in accordance with British Standard BS1377 (BSI, 1990). Test sieves, where used, were British Standard test sieves as detailed in Part 1 of BS1377 (BSI, 1990). Gravimetric water content, for all tests including it, was determined in accordance with Part 2 of BS1377, using metal tins and a drying oven at 105ºC, the water content being determined using Equation 3.1.

$$w = 100\left(\frac{m_2 - m_3}{m_3 - m_1}\right)$$ [Eq. 3.1]

where w is the gravimetric water content (%), m_1 is the mass of the tin (g), m_2 is the mass of the tin plus wet soil (g), and m_3 is the mass of the tin plus oven dry soil (g).

Eleven different fine-grained soils (particle sizes ≤425μm) were used for electromagnetic testing, as detailed in Table 3.1. Fine-grained soil samples were chosen for use in this study in order to allow straightforward comparison of electromagnetic signal velocities to standard geotechnical tests employing this size fraction. It was originally intended that this study only cover Liquid Limits commonly found for UK soils (e.g. less than 100%). However, Sample 11 was added during the testing to determine whether relationships found between geotechnical and electromagnetic tests would hold for very high surface area soils.

Samples 9 and 10, blends of Sample 6 and 11, were then later introduced during the electromagnetic testing due to the large water content gap between Samples 8 and 11 at their Liquid Limits. Therefore, these samples were not intended to be fully characterised in the following sections. For convenience in reading this thesis, the samples have been numbered in order of their Liquid Limit, Sample 1 having the lowest Liquid Limit, and Sample 11 having the highest.

The samples included 'natural' soils obtained from excavation and processed soils intended, for example, for use in clay products manufacture and as engineering fills. With the exception of Sample 8, which included only a very small number of larger particles removed by hand, the natural samples were wet sieved to obtain only the fine-grained (<425μm) fraction. Also, with the exception of Sample 6, all of the processed soil powders were dry sieved, as they were obtained in a dry powdered state. The percentages of sand sized particles were established by washing approximately 25g of each sample through a 63μm sieve (after first soaking them in a solution of sodium

hexametaphosphate and distilled water) and weighing the fraction retained on the sieve following oven drying.

Table 3.1. Soil samples and their general description.

Sample No.	Description
1	Fines from a sandy material found beneath a Birmingham roadway.
2	A weathered Mercia Mudstone obtained from laboratory stocks of powdered soils (exact origin unknown).
3	A disturbed sample of clay from a colliery spoil heap in the Carrwood area of England.
4	An oven dried and powdered clay sampled from the Harrow area of London.
5	An Oxford Clay obtained from laboratory stocks of powdered soils (exact origin unknown).
6	A commercially processed English China Clay (Kaolinite).
7	A disturbed clay sampled from the Cricklewood area of London.
8	A disturbed clay sampled from the Haringey area of London.
9	A blend of one-third English China Clay (Sample 6, in this case oven-dried) and two-thirds Bentonite (Sample 11).
10	A blend of one-third Bentonite (Sample 11) and two-thirds English China Clay (Sample 6).
11	A commercially processed Wyoming (Sodium) Bentonite powder.

Note: Sample numbers arranged in order of Liquid Limit (lowest to highest).

These data are provided in Table 3.2 and were intended only to provide an additional guide to sample textural properties. For instance, Samples 1 and 5 can be seen to be dominated by sand sized particles, whereas the other samples are predominantly silt sized and smaller. However, they were also included to facilitate interpretation of electromagnetic testing data, should the texture be found to be a critical

aspect of relating water content and electromagnetic measurement data. The same procedure was also undertaken using a 425µm sieve for Samples 6, 8 and 11, in order to confirm that no larger particles were present. Samples 9 and 10 are not included in Table 3.2 as they were subsequently created from prepared Samples 6 and 11.

Table 3.2. General description of sample types and textures.

Sample No.	Type	Sand (% mass)	Silt/Clay (% mass)
1	NW	82	18
2	PD	29	71
3	NW	29	71
4	PD	26	74
5	PD	70	30
6	PU	0	100
7	NW	5	95
8	NU	6	94
11	PU	11	89

Key to types: N = natural from excavation, P = processed powder, W = wet sieved, D = dry sieved, U = unsieved.

Sample sieving involved passing soils through a 425µm sieve, the fine-grained fraction being taken from the receiving container below. Prior to wet sieving, Sample 1 was divided using a riffle box as illustrate in Figure 3.1(a), the other samples being used in their entirety. These soils were then hydrated with distilled water in a metal tray (Figure 3.1(b)) and mixed with a palette knife. No chemical additives were used in order to prevent later effects on the electromagnetic properties. As shown in Figure 3.1(c) the

slurry was then transferred to the sieve and washed through with distilled water from a plastic washing bottle that had previously been cleaned and rinsed with distilled water.
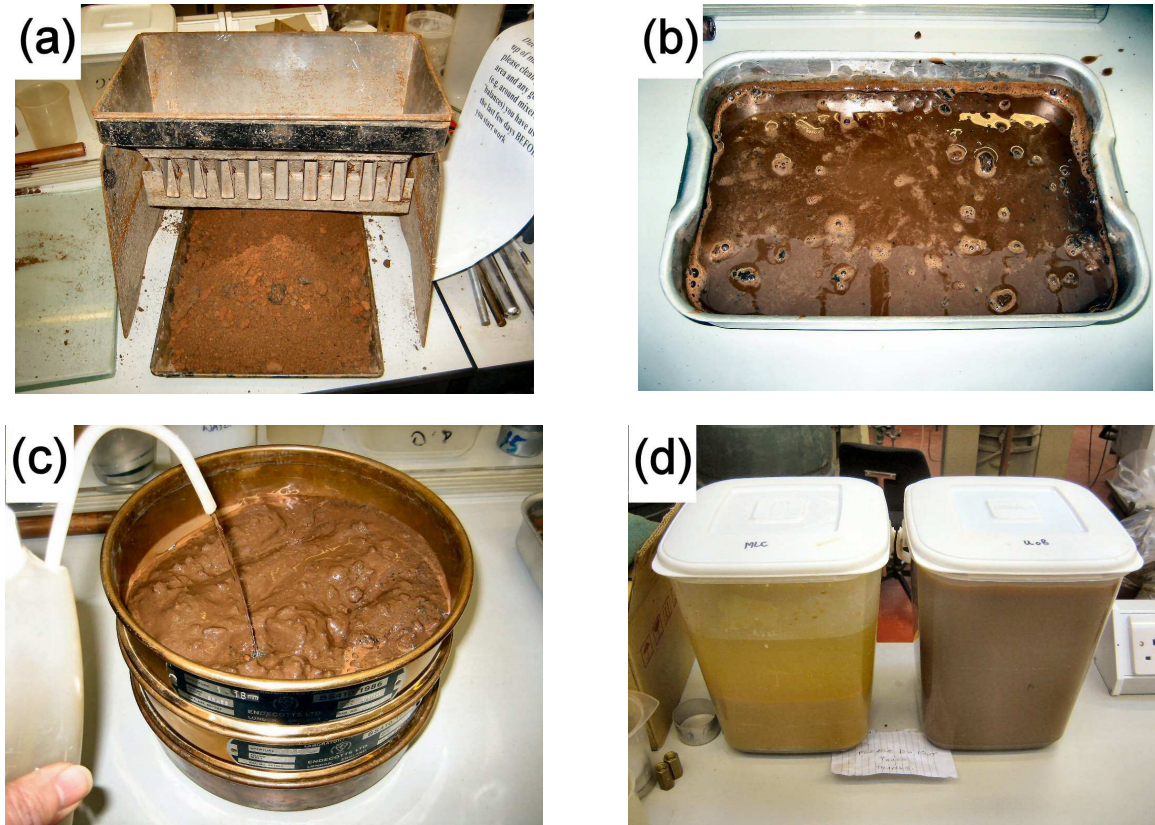
Figure 3.1. Preparation of wet sieved soil samples: (a) riffling, (b) mixing with water, (c) sieving and (d) settlement.

The wet soils passing through the sieve were then transferred to large plastic containers, cleaned and rinsed with distilled water for settlement (Figure 3.1(d)). When settlement was complete (i.e. after a number of days the supernatent water was clear) the water was syphoned out of the containers, care being taken to prevent disturbance of the settled soil mass by the syphon tube. Approximately 10mm of water was left over

the soil, to prevent disturbance, and the samples were then left to air dry before being transferred to plastic storage containers.

3.3 ATTERBERG LIMIT TESTING

Atterberg Limits provide data on changes in the properties of fine-grained soils, in terms of providing water contents at which soils pass from friable to plastic, and from plastic to liquid, states. As water content is also a significant factor in soil electromagnetic properties, and because the soil state may relate to electromagnetic-property-to-water-content relationships, the Atterberg Limits were considered an important geotechnical test to include in this study. Measurement of the Atterberg limits was undertaken as prescribed by BS1377 (BSI, 1990) Part 2. Soil samples were first hydrated using distilled water and mixed using palette knives on a glass plate until plastic, then placed in a sealed plastic container to mature for a period not less than 24 hours and, prior to testing, was further mixed. Part of the sample was then allowed to partially dry on a glass plate covered loosely with plastic film until it could be moulded into a ball and divided into two sub-samples for separate determination of the Plastic Limit. Each of these two samples was then divided into four pieces, each being moulded between the fingers and rolled on a glass plate until they were found to shear both transversely and longitudinally when rolled to a diameter of approximately 3mm. The resulting soil for each sub-sample was then placed in a metal tin (Figure 3.2(a)) and oven dried to determine the water content, the average of the two being used to determine the Plastic Limit. For the Bentonite of Sample 11 only, as illustrated in

Figure 3.2(a), the friable nature of this soil close to the Plastic Limit often led to the rolled soil having a diameter of approximately 4mm.
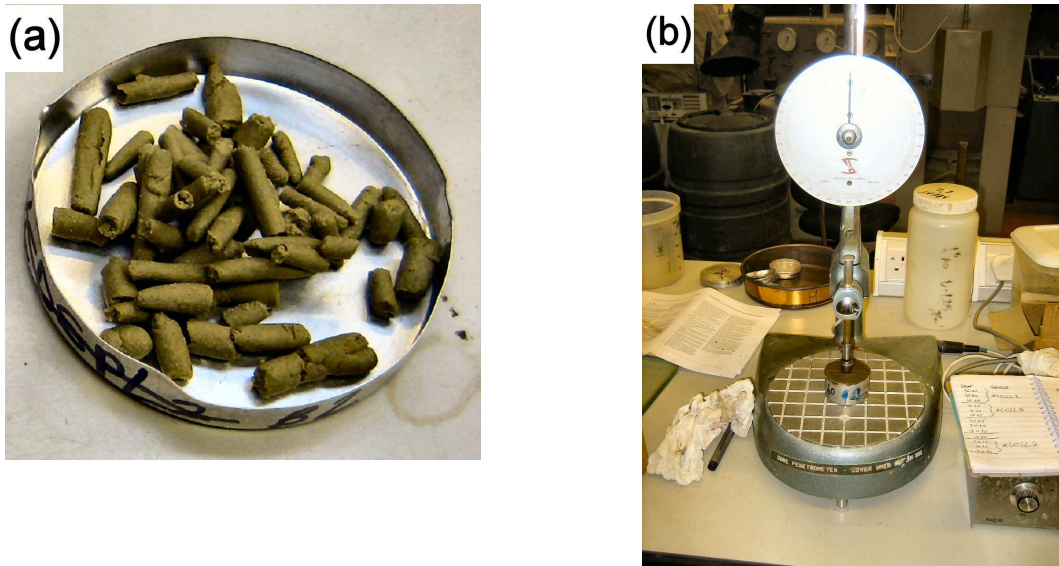
Figure 3.2. Atterberg limit testing: (a) Plastic Limit and (b) Liquid Limit.

For determination of the Liquid Limit, the cone-penetrometer method was used (Figure 3.2(b)). The pre-hydrated soil paste was first mixed for a minimum of ten minutes on the glass plate. Subsequently, water was added to the paste, with further mixing, until the penetration of the standard cone into the soil, contained in a standard metal cup, was approximately 15mm over five seconds.

The timing was controlled by an electronic timer unit, connected to the cone-penetrometer for automatic control of the fall mechanism. This process was then repeated to provide four or five water contents with penetrations between 15mm and 25mm, a small amount of soil from the centre of the cup being used in each case for oven drying to determine water content.

In accordance with BS1377 (BSI, 1990) such measurements were only undertaken where either two successive penetrations were within 0.5mm, or three within 1mm, a small amount of soil paste being used to fill the cone hole between each reading. Between each test, the soil was emptied from the cup and re-mixed with the remainder of the paste on the glass plate. The Liquid Limit was then determined by plotting the water contents against average cone penetration, and fitting a straight line to the data, from which the water content for a cone penetration of 20mm was interpolated using Equation 3.2. These graphs are illustrated in Figure 3.3.

$$W_L = 20S + c \hspace{4cm} \text{[Eq. 3.2]}$$

where W_L is the Liquid Limit (%), S is the slope of the cone penetration graph, and c is the vertical offset of the linear regression (%).
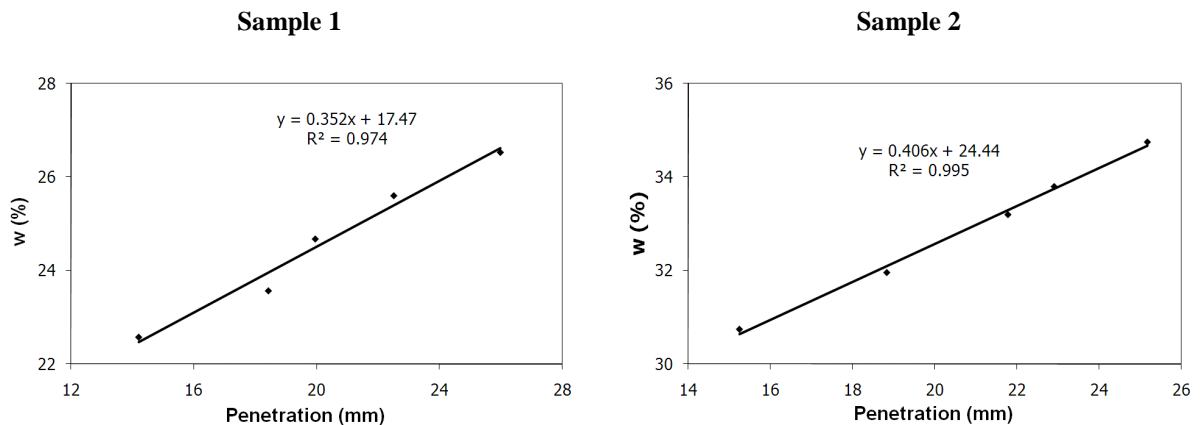
Figure 3.3. Water content versus cone penetration for the eleven samples.
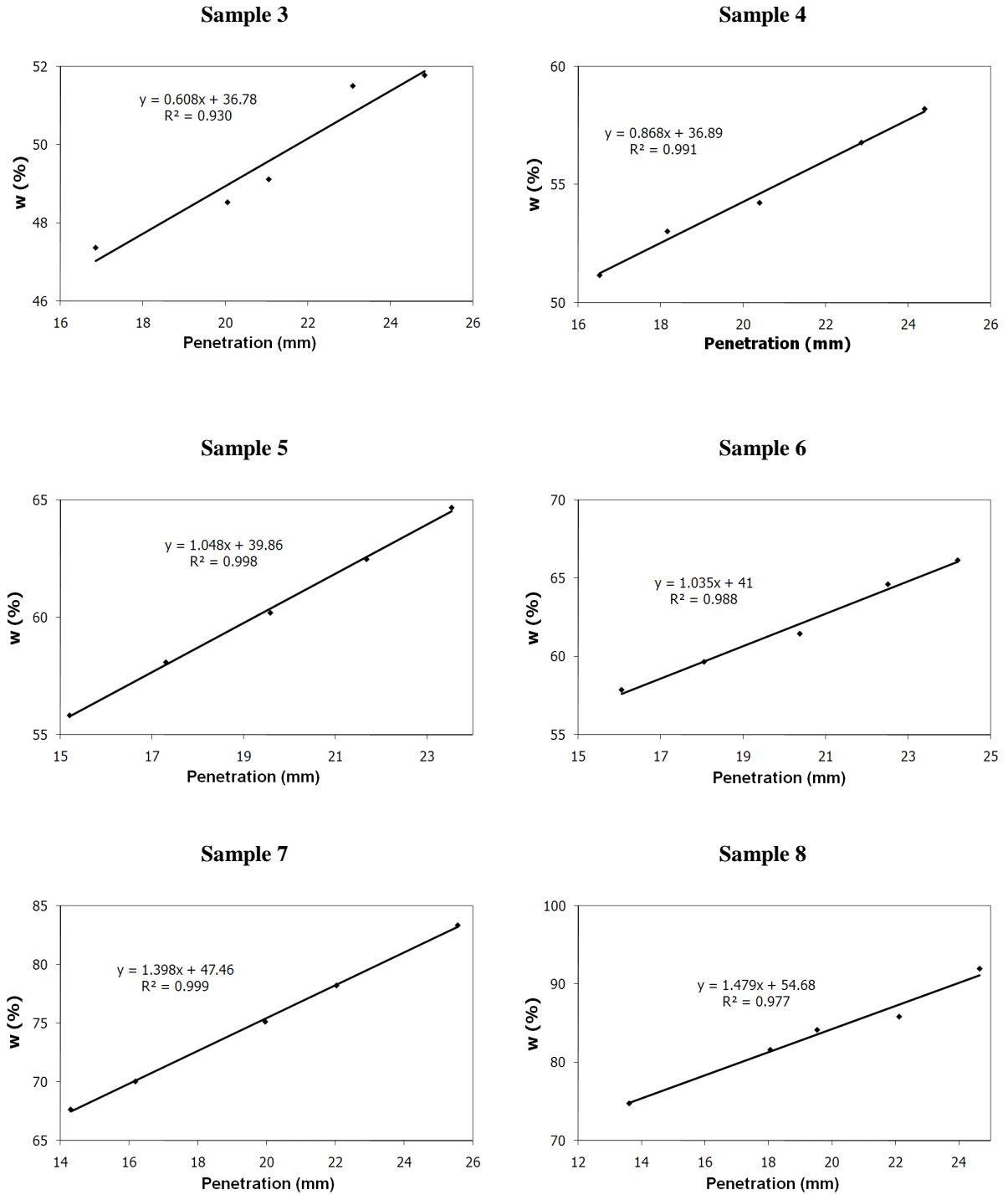
Sample 3

y = 0.608x + 36.78
R² = 0.930

Sample 4

y = 0.868x + 36.89
R² = 0.991

Sample 5

y = 1.048x + 39.86
R² = 0.998

Sample 6

y = 1.035x + 41
R² = 0.988

Sample 7

y = 1.398x + 47.46
R² = 0.999

Sample 8

y = 1.479x + 54.68
R² = 0.977

Figure 3.3. Water content versus cone penetration for the eleven samples (continued).

Sample 9
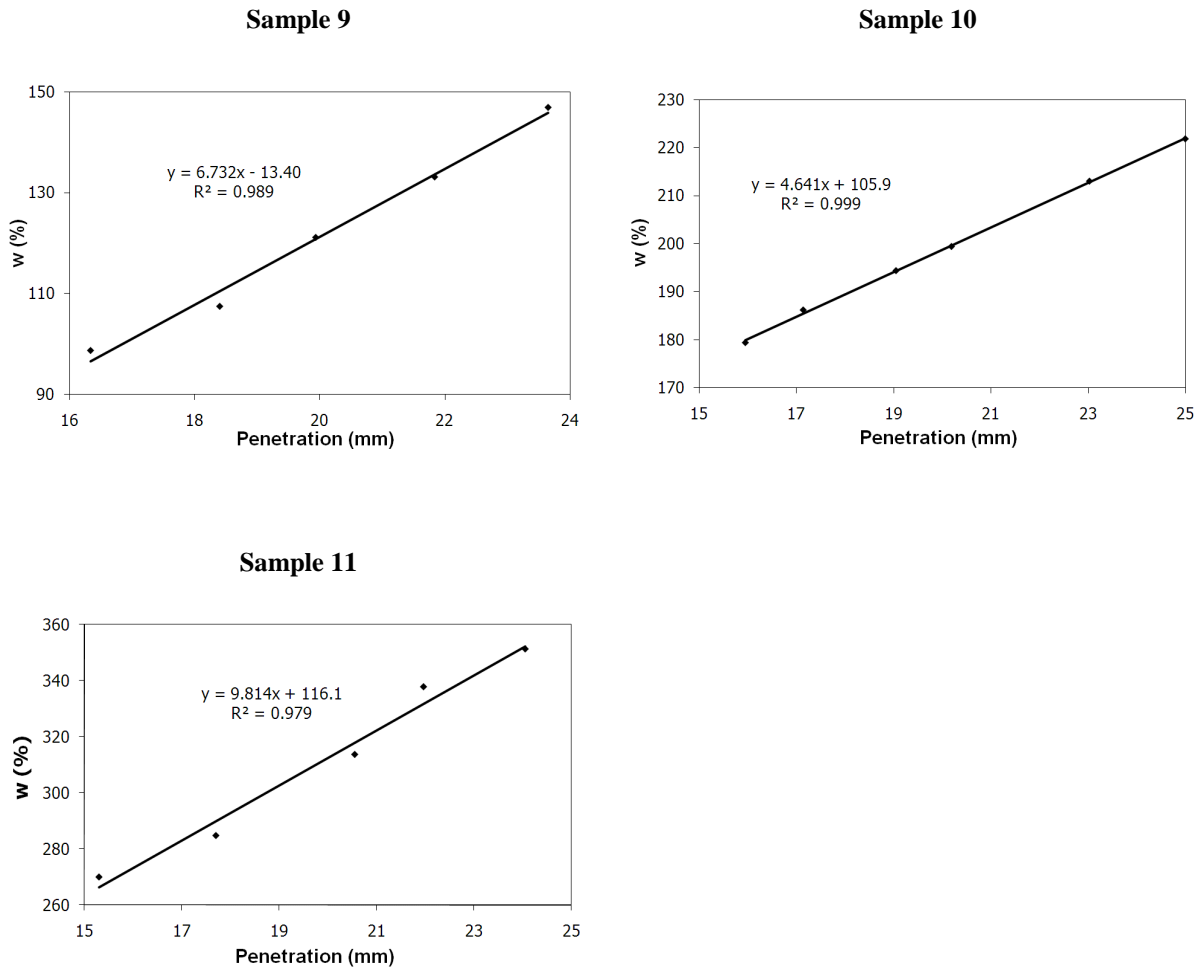
Sample 10

Sample 11

Figure 3.3. Water content versus cone penetration for the eleven samples (continued).

The index of plasticity was then determined as the difference between the Liquid and Plastic Limits. As can be seen from the test results in Table 3.3, the Atterberg limit testing indicated that the soil sample selection had been successful in achieving a very wide range of Liquid Limits. The plasticity data of Table 3.3 are also shown in relation to the A-Line in Figure 3.4: the results for all samples fell close to this line, but with an upward divergence as the Liquid Limit increases. As shown by Rogers et al. (2009)

such a divergence indicates that the samples can be considered representative of average

UK fine-grained soil plasticity values.
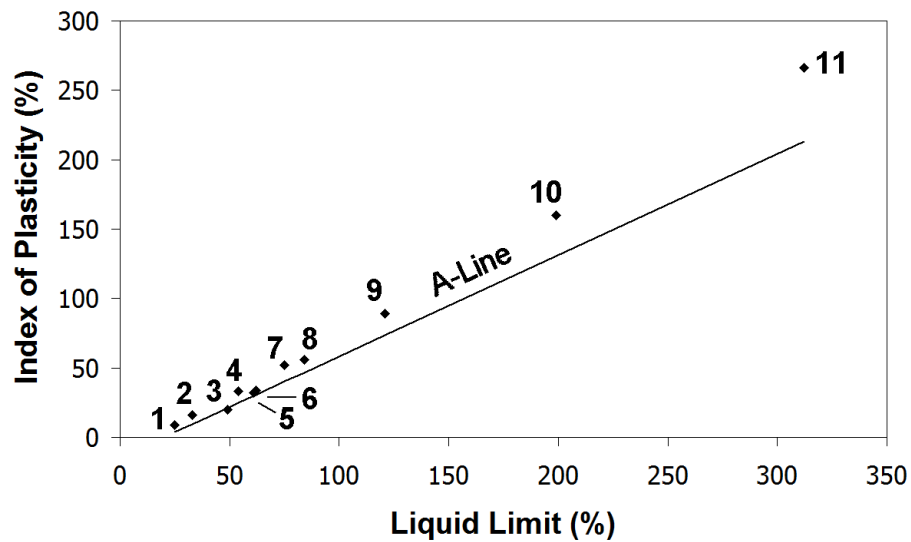
Figure 3.4. Comparison of plasticity data to the A-Line.

Table 3.3. Atterberg limits for the eleven samples.

Sample No.	Plastic Limit (%)	Liquid Limit (%)	Index of Plasticity (%)	Slope of Liquid Limit graph
1	16	25	9	0.352
2	17	33	16	0.406
3	29	49	20	0.608
4	21	54	33	0.868
5	29	61	32	1.048
6	28	62	34	1.035
7	23	75	52	1.398
8	28	84	56	1.479

Table 3.3. Atterberg limits for the eleven samples (continued).

Sample No.	Plastic Limit (%)	Liquid Limit (%)	Index of Plasticity (%)	Slope of Liquid Limit graph
9	32	121	89	6.732
10	39	199	160	4.641
11	46	312	266	9.814

3.4 LINEAR SHRINKAGE TESTING

The shrink/swell properties of fine-grained soils can be considered important to this study for a number of reasons: they represent the degree of variation in dry density that will occur with increasing water content, and potential variations in water types between silicate sheets and between soil grains. Also, as swelling soils have the ability to remain plastic above the water content where they become saturated, they illustrate the need to ensure that electromagnetic testing is carried out over a very wide water content range if it is to be of use in a geotechnical setting. Linear shrinkage was therefore undertaken as prescribed by BS1377 (BSI, 1990) Part 2. A standard mould, approximately 140mm long, was first measured for length and lightly lubricated with silicone grease. A soil sample was then hydrated and mixed as required for Atterberg testing, a cone-penetrometer being used to gauge when the sample was hydrated close to the Liquid Limit. The sample was then placed in the mould (Figure 3.5(a)), care being taken to ensure that soil was pushed into the corners to prevent voiding. Excess soil was removed using a palette knife struck flush with the top edges of the mould, including striking the mould against a solid surface. Each sample was then placed in a sealed glass dessicator with silica gel to slowly dry (Figure 3.5(b)). The dessicator was used in place

of the drying oven prescribed by BS1377 (BSI, 1990) as none were available at that time. However, no curling of samples was found using the dessicator, and so its use was considered appropriate. The samples were monitored daily until the rate in reduction of length was minimal, at which point the mould was transferred to an oven at 105ºC until shrinkage had ceased. Completed samples were then broken apart at a number of locations along the length, to ensure that no visible voiding had occurred. Linear shrinkage was calculated using Equation 3.3, and the results are presented in Table 3.4 rounded to the nearest whole number.

$$LS = 100\left(1 - \frac{L_D}{L_O}\right) \hspace{3cm} \text{[Eq. 3.3]}$$

where LS is the linear shrinkage (%), L_D is the final length (mm) and L_O is the original length (mm). As can be seen in Figure 3.5(c), the significant shrinkage of Sample 11 caused irregular cracking. Therefore, the test was repeated to provide a sample with a single transverse crack allowing the two pieces, when fully dry, to be pushed together and measured in accordance with BS1377 (BSI, 1990).

Table 3.4. Linear shrinkage values for the eleven samples.

Sample No.	Linear shrinkage (%)	Sample No.	Linear shrinkage (%)
1	2	7	17
2	10	8	18
3	9	9	16
4	16	10	27
5	13	11	45
6	10		
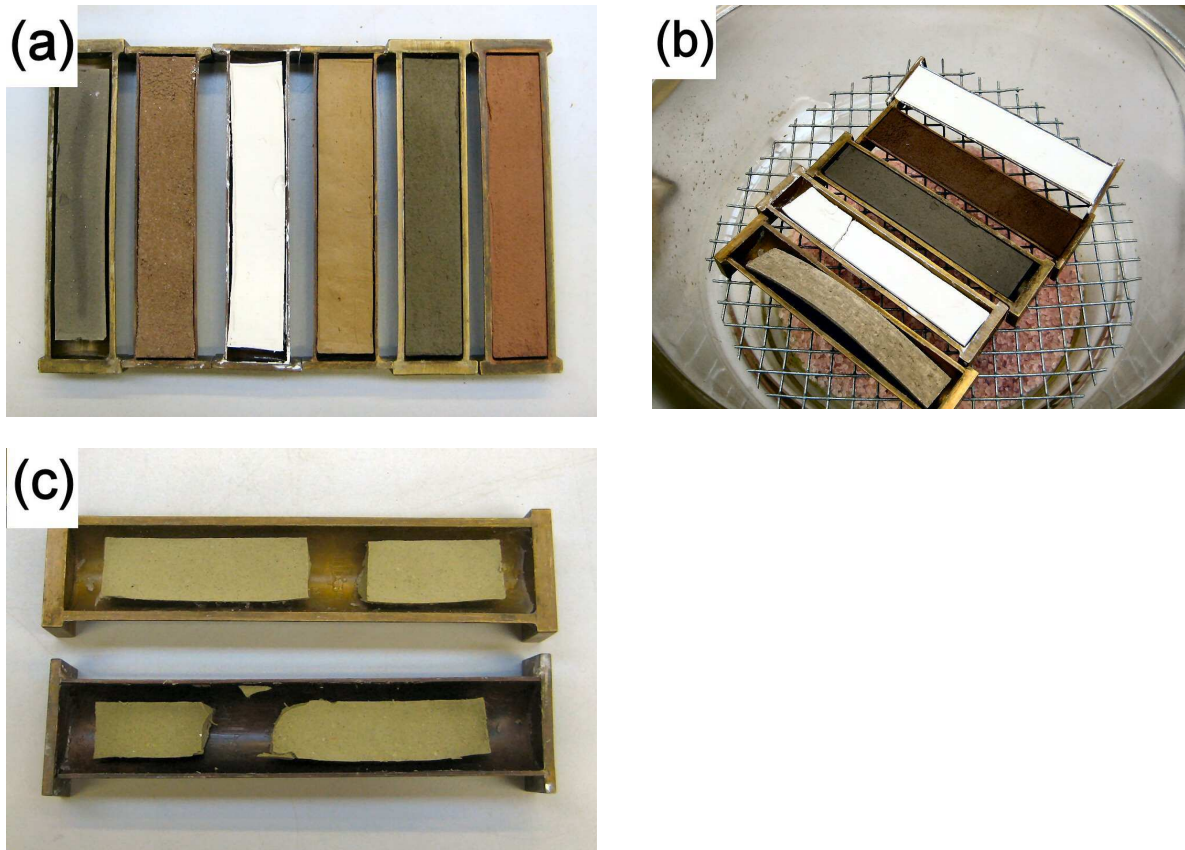
Figure 3.5. Linear shrinkage testing: (a) samples in the moulds, (b) samples in the dessicator and (c) cracked Sample 11.

3.5 PARTICLE DENSITY TESTING

Particle density data were considered appropriate to this study for a number of reasons. Most importantly, they allow estimation of bulk density for any saturated water content. Also, they provide a basis for considering any variations found in electromagnetic properties between dried soil samples, in terms of potential deviations from the most common elements associated with fine-grained soil mineralogy. Therefore, the particle density of each sample was determined as prescribed by BS1377 (BSI, 1990) Part 2, two 50ml glass density bottles being used per soil tested.

Between 5g and 10g of oven dried soil was placed in each bottle, with the exception of Sample 11 where approximately 3g had to be used due to excessive swelling that interfered with hydration of the sample. The bottles were then partially filled with de-aired distilled water, prepared in a flask under vacuum using a magnetic stirrer to remove bubbles, until the soil was covered and then placed without stoppers in a glass dessicator connected to a vacuum pump (Figure 3.6(a)). Samples were left under vacuum for a minimum of three hours, until no production of air bubbles could be observed.

At the start of, and at intervals of approximately one hour during this de-airing, the bottles were carefully stirred with a short rod to aid removal of bubbles, the rod then being rinsed with a small amount of the de-aired distilled water into the bottle to prevent loss of soil particles. The bottles were then filled to the neck with more de-aired distilled water and the stopper inserted, prior to being placed up to the neck in a water bath maintained at a temperature of 25ºC.

The bottles were kept in the water bath for a minimum of one hour until their temperature had stabilised to that of the water around them. A separate water filled bottle was used to aid in monitoring temperature (Figure 3.6(b)). Bottles were then removed from the water bath and weighed after careful drying of their outer surfaces, and were then cleaned and filled with de-aired distilled water, placed in the water bath for one hour and then weighed again. Particle densities were then calculated using Equation 3.4 and testing repeated if the difference between each of the test pairs was greater than $0.03 Mg.m^{-3}$. The test results are detailed in Table 3.5.

$$\rho_S = \frac{m_2 - m_1}{(m_4 - m_1) - (m_3 - m_2)} \qquad \text{[Eq. 3.4]}$$

where ρ_S is the particle density (Mg.m^{-3}), m_1 is the mass of the empty bottle, m_2 is as m_1 plus the mass of dry soil, m_3 is as m_2 plus the mass of distilled water, and m_4 is the mass of the bottle filled with de-aired distilled water (all masses being measured to the nearest 0.0001g).
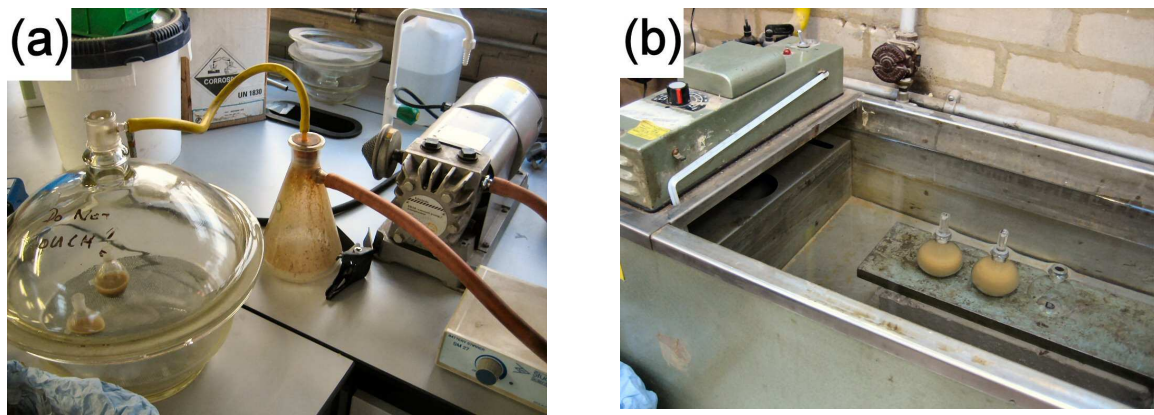
Figure 3.6. Particle density testing: (a) under vacuum and (b) in water bath.

Table 3.5. Particle densities for the eleven samples.

Sample No.	Particle density (Mg.m^{-3})	Sample No.	Particle density (Mg.m^{-3})
1	2.65	7	2.68
2	2.76	8	2.75
3	2.55	9	2.65[A]
4	2.63	10	2.71[A]
5	2.66	11	2.78
6	2.58		

Note: [A] indicates particle density was calculated based on a pro-rata of the constituent soils.

3.6 CONDUCTIVITY MEASUREMENTS

Measurement of the approximate electrical conductivity of each sample was undertaken for the purposes of additional characterisation, rather than as a feature of the electromagnetic signal measurement techniques and calculations. In principle, these tests were based on the disc electrode method of Part 3 of BS1377 (BSI, 1990). However, a suitable ohm-meter was not available and the quantities of available soil prevented use of the exact British Standard method. Therefore, an alternative apparatus was constructed for electrical conductivity measurements, as shown in Figure 3.7.
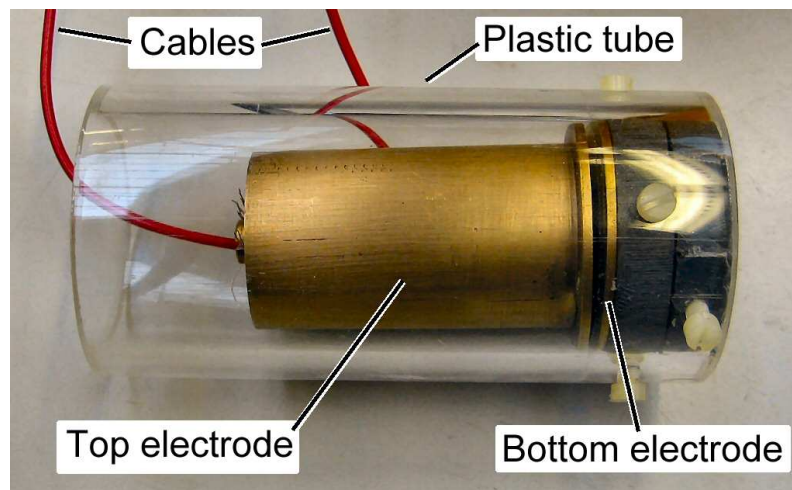
Figure 3.7. Apparatus constructed for measurement of electrical conductivity.

The apparatus consisted of two circular brass electrodes 39mm in diameter within a transparent plastic tube into which soil could be placed after hydrating to the Liquid Limit. Approximately 25mm of wet soil was placed between the electrodes, the apparatus then being connected to a Hewlett Packard HP4192A low-frequency impedance analyser set at 200Hz to minimise the effects of electrode polarisation. The

length of the soil within the cell was determined as the difference between the tube end and top of the upper plate, with and without soil, measured as the average of four equally spaced locations around the circumference. The resistance of the empty cell was checked before and after each test and, in each case, was found to be zero ohms. The conductivity was then calculated using Equation 3.5 and the results for each of the soil samples are provided in Table 3.6.

$$\sigma = \frac{1000L}{RA} \qquad\qquad \text{[Eq. 3.5]}$$

where σ is the electrical conductivity (mS.m^{-1}), L is the inter-disc spacing (c. 25mm), R is the measured electrical resistance (Ω) and A is the area of the disc (mm^2).

Table 3.6. Estimated conductivities at 200Hz for soils at their Liquid Limit.

Sample No.	Conductivity (mS.m^{-1})	Sample No.	Conductivity (mS.m^{-1})
1	96	6	53
2	58	7	127
3	94	8	99
4	120	11	621
5	231		

3.7 ELECTROMAGNETIC CHARACTERISTICS

Although the electromagnetic testing methods will not be introduced until Chapter 4, some electromagnetic test data are provided in Table 3.7 for completeness. This is considered important as a goal of this study is to facilitate incorporation of electromagnetic testing into routing geotechnical characterisation. Included in Table 3.7

is the apparent permittivity (ε_r^*) per unit of dry density for each sample, after oven drying at 105°C, measured in a coaxial cell using Quarter-Wavelength Analysis (QWA). Also included are the apparent permittivities of the samples measured at the Liquid Limit for QWA (c. 1GHz) and using Time-Domain Reflectometry (TDR).

The volumetric water content (VWC) for each of the samples, at their Liquid Limits, is also included as it is a more widely used measure of water content in geophysical research than the gravimetric values more commonly associated with geotechnics.

Table 3.7. Electromagnetic characterisation data.

Sample No.	Dry ε_r^* per unit of dry density	QWA ε_r^* at Liquid Limit	TDR ε_r^* at Liquid Limit	VWC at Liquid Limit (%)
1	1.91	23.6	29.4	38.3
2	2.13	27.7	34.3	46.9
3	2.55	30.1	36.9	53.4
4	2.25	41.4	49.8	59.3
5	2.31	32.2	39.3	58.2
6	2.48	36.9	41.9	62.8
7	2.17	40.0	46.4	66.7
8	2.03	34.3	42.7	70.4
9	2.43	47.0	59.2	78
10	2.39	51.0	63.6	85
11	2.34	51.8	62.2	86.9

3.8 EQUIPMENT CALIBRATION TESTS AND AIR TEMPERATURES

The digital scales used within the soils laboratory, stated as being accurate to 0.01g, were tested using standard calibration masses kept at the University of Birmingham engineering laboratories (Figure 3.8(a)). The results, based on ten measurements of each mass at nine different locations around the top of the scales (i.e. 90 total measurements per mass), are presented in Table 3.8. Two mass standards were used, one of 40g and one of 100g. As larger mass standards were not available, an indication of accuracy for higher masses was obtained using a 1kg counterbalance weight.

Clean gloves were used to handle all masses, with the masses also being wiped clean with a soft cloth before each test. For the two mass standards, it was found that the scales were, on average, accurate within 0.01g, but with potential for occasional measurements to be accurate only within 0.03g. While the counterbalance weight does not give exact figures for mass accuracy at 1kg, it was found that the maximum difference between the theoretical and measured masses was only 0.25g (i.e. 0.025% potential inaccuracy) out of ninety measurements.

The digital callipers, used for all length measurements included in this thesis, were tested using standard steel calibration bars maintained at the University of Birmingham engineering laboratories (Figure 3.8(b)). The results of twenty measurements of each bar are presented in Table 3.9. It can be seen from the results that the callipers measured length generally within a tolerance of 0.1mm, increasing to potentially 0.2mm for lengths above 100mm.
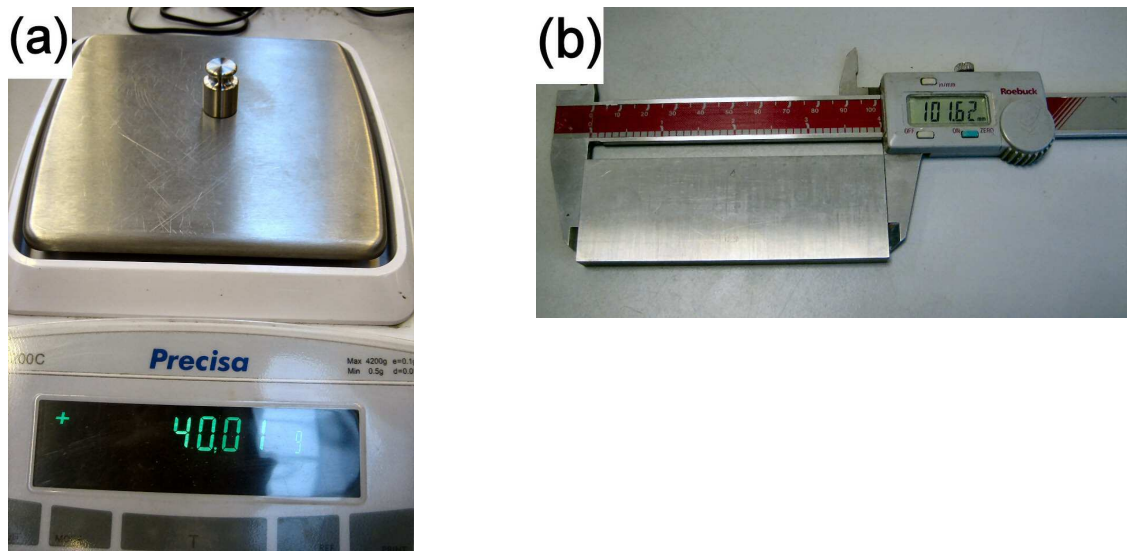
Figure 3.8. Determination of accuracy: (a) scales and (b) digital callipers.

Table 3.8. Results of tests on digital scales.

	Actual mass of calibration standard (g)		
	40	**100**	**1000**
Average measured mass:	40.01	100.01	1000.21
Minimum measured mass:	39.98	99.99	1000.16
Maximum measured mass:	40.03	100.02	1000.25
Average difference:	0.01	0.01	0.21
Maximum difference:	0.03	0.02	0.25

All laboratory testing was intended to be carried out at prevailing room temperatures within the University of Birmingham soils laboratory, i.e. under routine geotechnical testing conditions. However, it was considered useful to define the temperature variations that occur when testing under such circumstances. Therefore, a standard bulb thermometer (found to be within approximately 0.5ºC of expected

temperature when compared to a water bath at 25ºC) was used to record air temperatures.

Table 3.9. Results of tests on digital callipers.

	Actual length of standard calibration bar (mm)			
	101.60	**76.20**	**50.80**	**25.40**
Average measured length (mm):	101.61	76.21	50.77	25.37
Minimum measured length (mm):	101.52	76.14	50.70	25.29
Maximum measured length (mm):	101.74	76.29	50.85	25.46
Average difference (mm):	0.01	0.01	0.03	0.03
Maximum difference (mm):	0.14	0.09	0.05	0.06

Temperatures were recorded at both the soil preparation area and in an adjacent room used for electromagnetic testing to provide a cleaner environment for the computer and test equipment. Temperature measurements in the electromagnetic testing area greatly outnumber those for the soil preparation area, as the former was used over a much longer period, from early prototyping through to actual soil measurements. The results of this monitoring, for both locations, are provided in Table 3.10.

It was found that the average temperature for both areas varied by approximately 1ºC, with temperatures generally varying within approximately +2º and -3ºC of that average. The value of 28.5ºC in the soil preparation area occurred during the month of March and such high temperature only occurred once and is believed to have been due to heating problems.

Table 3.10. Air temperatures in soil preparation and electromagnetic testing locations.

Soil preparation area		Electromagnetic testing area	
Parameter	**Temperature**	**Parameter**	**Temperature**
Maximum (ºC):	28.5	Maximum (ºC):	21.9
95 percentile (ºC):	22.2	95 percentile (ºC):	21.6
Average (ºC):	20.0	Average (ºC):	19.3
5 percentile (ºC):	17.3	5 percentile (ºC):	17.9
Minimum (ºC):	16.7	Minimum (ºC):	17.6
Measurements (No.):	54	Measurements (No.):	146

CHAPTER 4 – DEVELOPMENT OF A TEST CELL

4.1 OVERVIEW

Based on Section 2.8.3 Quarter-Wavelength Analysis (QWA) in a transmission line has significant potential for developing an electromagnetic signal velocity testing methodology that provides the simplicity and robustness of TDR, while also extending it to provide data on dispersion. Therefore, apparent permittivity will now be introduced as a means of allowing frequency-domain data compatibility with TDR, after which the methodology for calculating apparent permittivity from quarter-wavelength frequencies will be developed. Test cells will then be described together with data used to calibrate and validate the QWA outputs. In order to more fully understand the test cell and measurements, computer modelling will then be described, and compared to measured data. This chapter will then conclude with consideration of potential measurement accuracy.
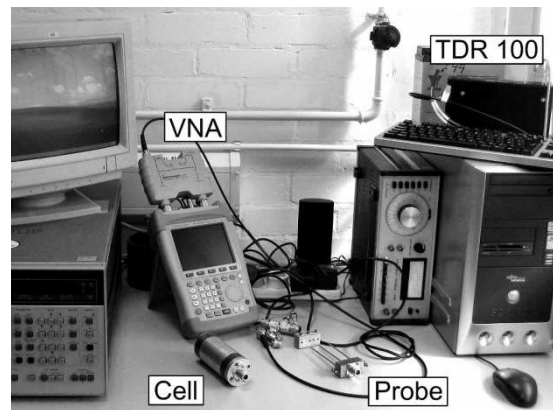
Figure 4.1. The testing arrangement utilized in this research.

The testing arrangement described in this chapter is illustrated in Figure 4.1. The computer was used for the capture of frequency-domain data from the Rohde and Schwarz

FSH6 Vector Network Analyser (VNA) as well as for capturing time-domain waveforms from a Campbell Scientific TDR100 Time-Domain Reflectometer (TDR). The cell (and probe to be described in Chapter 5) illustrated in Figure 4.1 was used with both the VNA and TDR, in order for some evidence to be available of the compatibility of the cell with both measurement methods.

4.2 APPARENT PERMITTIVITY

Compatibility between QWA and TDR data is dependent upon there being a common measurement unit. As TDR provides data in the form of apparent permittivity, which can be derived from the propagation velocity, it was adopted for this study. In a soil, the propagation velocity of an electromagnetic signal can be determined from knowledge of the permittivity and magnetic permeability, both of which can be complex parameters respectively describing charge storage and loss mechanisms (see Thomas et al., 2006). As most soils are considered to have low, and non-complex, magnetic permeability, the signal velocity can be calculated using Equation 4.1 (after Hayt and Buck, 2006).

$$V = \frac{\omega}{\beta} = \frac{1}{\sqrt{\frac{\mu\varepsilon'}{2}\left(\sqrt{1+\left(\frac{\varepsilon''}{\varepsilon'}\right)^2}+1\right)^{\frac{1}{2}}}} \qquad \text{[Eq. 4.1]}$$

where V is the velocity (m.s^{-1}), ω is the radian frequency ($\omega = 2\pi f$ where f is the frequency in Hertz), β is the phase constant (i.e. the phase change per unit distance expressed in radians.m^{-1}), μ is the magnetic permeability and ε' and ε'' are, respectively, the real and imaginary parts of the permittivity.

Loss mechanisms in soils, at high frequency, are generally considered to comprise those associated with electromagnetic dispersion - i.e. dipolar and conductivity losses. Therefore, for the purposes of Equation 4.1, losses are often included through use of Equation 4.2. These losses, when divided by the real part of the permittivity as shown in Equation 4.1, form the loss tangent associated with the soil.

$$\varepsilon'' = \varepsilon_P'' + \frac{\sigma_{DC}}{\omega} \qquad \text{[Eq. 4.2]}$$

where σ_{DC} is the static (direct current) conductivity of the material ($S.m^{-1}$) and ε''_p represents dipolar losses.

The measurement of apparent permittivity (ε_r^*) has become widespread due to the popularity of TDR and provides a single value to describe all of the electromagnetic parameters. It is based on calculation of the real relative permittivity of a lossless material (Equation 4.3) that corresponds to the velocity obtained in Equation 4.1. Therefore, the apparent permittivity is a representation of a number of parameters in one simple value and can be determined from any measurement method that can provide velocity data, rather than being limited to TDR.

$$\varepsilon_r^* = \left(\frac{c}{V}\right)^2 \qquad \text{[Eq. 4.3]}$$

where c is the velocity of light in a vacuum (2.9979×10^8 ms^{-1}).

4.3 QUARTER WAVELENGTH ANALYSIS (QWA)

When a sinusoidal signal, generated by a network analyzer, is injected into a

coaxial measurement cell, the magnitude of the reflected signal returning to the analyzer will be a function of two sinusoidal voltages: the forward travelling incident wave and the backward travelling reflected wave, as illustrated in Figure 4.2. The combined wave, also known as the voltage standing wave, therefore varies in amplitude and phase, as a function of the incident and reflected waves, and will exhibit maxima and minima spaced at multiples of a quarter-wavelength. Therefore, if the voltage is measured at the point marked 'signal in', the maxima and minima of the measured signal will occur only at frequencies where the change in phase during one way transit of the signal along the cell length is a multiple of 90º. For this reason, they are known as the quarter-wavelength frequencies.
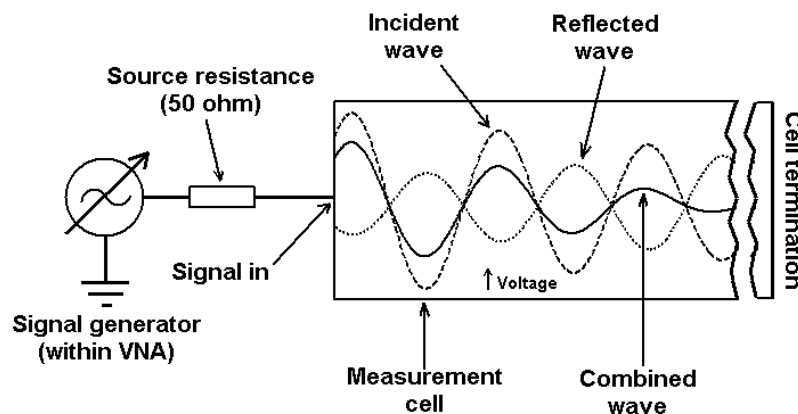
Figure 4.2. Incident and reflected signals in the measurement cell.

The fact that these quarter-wavelength points can be used to calculate the velocity, and hence apparent permittivity, of a material stems from the nature of the phase constant as a measure of radian phase change per metre. This can be used with the phase change per second (i.e. the radian frequency) to derive the velocity in metres per second. Therefore, based on Equations 4.1 and 4.3, the velocity can be described

using the progression detailed in Equation 4.4.

$$V = \frac{c}{\sqrt{\varepsilon_r^*}} = \frac{\omega 2L}{\phi - \phi_R} \qquad \text{[Eq. 4.4]}$$

where L is the cell length (m), ϕ is the total phase change in radians (i.e. over the full two way transit of the signal through the soil) and ϕ_R is the phase change that occurs on reflection at the cell end (zero for an open circuit termination and 180º - i.e. π radians - for a short-circuited termination).

As the quarter wavelength frequencies occur at total phase changes that are multiples of 180º (i.e. 90º, or 0.5 π, for each of the incident and reflected wave transits), Equation 4.4 can be simplified for the first quarter-wavelength frequency as detailed in the progression of Equation 4.5.

$$\frac{c}{\sqrt{\varepsilon_r^*}} = \frac{\omega_{qw} 2L}{\pi} = \frac{4\pi f_{qw} L}{\pi} = 4 f_{qw} L \qquad \text{[Eq. 4.5]}$$

where ω_{qw} is the first quarter-wavelength radian frequency and f_{qw} is the corresponding frequency in Hertz.

Re-arrangement of Equation 4.5 gives the apparent permittivity of the material within the cell, as detailed in Equation 4.6. The term (2n-1) is added to reflect the fact that the quarter-wavelength frequencies being used are only those associated with one-way phase changes of 90º and 270º.

$$\varepsilon_r^* = \left(\frac{(2n-1)c}{4 f_{qw} L} \right)^2 \qquad \text{[Eq. 4.6]}$$

where n is an index of the quarter-wavelength frequency (n=1,2,3...).

The voltage measured is the sum of the combined wave and variations in voltage

reflected from the interface between cable and cell/probe due to impedance mismatch, as will be more fully detailed in Section 4.7. However, QWA is based only on the frequency of the maxima and minima of voltage variations, so this can be ignored for the present. As QWA is sometimes explained in terms of the relationship between the frequency of a signal, its wavelength and its velocity, this alternative mathematical representation should also be given. As described earlier, the velocity can be determined from the apparent permittivity. These relationships are described by Equations 4.3 and 4.7.

$$f = \frac{V}{\lambda} \qquad\qquad \text{[Eq. 4.7]}$$

The actual wavelength associated with each quarter-wavelength frequency can be defined from the length of the cell or probe, and the index (N=1,2,3,4...) of all quarter-wavelength frequencies (Equation 4.8).

$$\lambda = \frac{L}{0.25N} = \frac{4L}{N} \qquad\qquad \text{[Eq. 4.8]}$$

Combining Equations 4.3, 4.7 and 4.8 leads to the definition of the quarter-wavelength frequencies detailed in Equation 4.9 (Heimovaara et al., 1996).

$$f_{qw} = \frac{(2n-1)c}{4\sqrt{\varepsilon_r^*(f_{qw})}L} \qquad\qquad \text{[Eq. 4.9]}$$

where f_{qw} is the quarter wavelength frequency (Hz), n is an index (n=1,2,3,4,...) used to reduce the quarter-wavelength frequencies to just those associated with 90º and 270º phase changes, and $\varepsilon_r^*(f_{qw})$ is the apparent permittivity at the measured quarter-wavelength frequency.

In order to determine the apparent permittivity of the material, Equation 4.9 can

then be rearranged to give Equation 4.6.

4.4 MEASUREMENT OF RESONANT FREQUENCIES

Measurement of the voltage magnitude in a transmission line is generally undertaken using S_{11} data (the scattering parameters) obtained from a Vector Network Analyzer (VNA). The S_{11} parameter is a complex number representing both the magnitude and phase of a signal based on measuring the output signal, relative to the input signal, at a single test point: hence the 'one-one' in the name representing input and output at port 1.

The VNA used was a Rohde and Schwarz portable handheld spectrum analyzer, with voltage standing wave ratio bridge and vector measurement options installed. Rohde and Schwarz produce a number of these devices, the FSH3 (3GHz) model having been used for initial prototyping and the FSH6 (6GHz) model having been used for the subsequent development and testing described in this chapter. Whilst a relatively 'low end' instrument in terms of cost, the VNA used had a significant advantage over most alternative analyzers in being highly portable and able to operate on battery power, allowing potential use for field measurements. The VNA equipment was connected to the cell by a flexible coaxial cable with N-Type connectors, and via USB to a computer for data acquisition. The FSH6 VNA provides measurements of the voltage magnitude and phase angle, whereas QWA is generally based on the measurement of the real part of S_{11} values. S_{11} values were determined using Equation 4.10 (Shang et al., 1999).

$$S_{11M} = 10^{\frac{dB}{20}} \cos\phi + j10^{\frac{dB}{20}} \sin\phi \qquad\qquad \text{[Eq. 4.10]}$$

where S_{11M} is the measured scattering parameter, dB is the return loss in decibels, ϕ is the phase angle of the returned signal relative to that of the injected signal and $j = \sqrt{-1}$.

The data used for QWA were therefore the real, left hand, part of Equation 4.10. While the quarter-wavelength frequencies could be measured directly from the phase data, the use of real S_{11} values is preferred due to the cosine function providing a representation of the voltage maxima/minima described in the literature. Calibration of the VNA was carried out by connecting successively an open, short and load termination to the end of the cable. Subsequent measurements were, therefore, automatically corrected for the effects of the cable.

However, an important aspect of the calibration to note is that it takes place at the end of the N-Type cable, rather than at the start of the soil sample, which will cause measurement errors if the change in phase angle over this additional distance is not accounted for. Therefore, the S_{11M} values require adjustment to the phase angle using Equation 4.11 (after Shang et al., 1999). It should also be noted that care was taken during the calibration and measurement to ensure that movement of the cable was minimized and the calibration was carried out immediately prior to taking the corresponding measurement, in order that the calibration data would remain valid.

$$S_{11} = \frac{S_{11M}}{\exp(-j\omega z / c)^2} \qquad \text{[Eq. 4.11]}$$

where S_{11} is the adjusted scattering parameter, S_{11M} is the measured scattering parameter, ω is the radian frequency, c is the speed of light in a vacuum and z is the difference in length between the cable end and the start of the soil sample.

The S_{11} values were calculated from VNA data files obtained using Rohde and Schwarz FSH View software, using a program written with the Light Matrix Engine (LME - Calerga, 2007), based on the above equations, ported to Matlab (Mathworks, 2007) and the quarter wavelength frequencies were obtained by inspection of the resulting graph. As the VNA used has a limited memory store, it was necessary to take a number of measurements over a fraction of the total desired frequency coverage, in order to ensure sufficient resolution and hence to identify the quarter-wavelength frequencies to an acceptable accuracy.

The data were, therefore, collected over spans of 200MHz, with the VNA re-calibrated at the end of each span. This allowed the frequency to be determined to a maximum accuracy of 333kHz, which was found to provide an acceptable balance between measurement duration and accuracy - the calibration indicating that the quarter-wavelength frequencies were being identified within 1MHz of their true frequencies.

4.5 INITIAL PROTOTYPING

Initial prototyping was carried out using a Rohde and Schwarz FSH3 VNA, which was available for only a few days. Therefore, only the return loss was used for initial testing (i.e. only scalar data) as there was not sufficient time available to formulate and implement the necessary data processing and adjustment algorithms required for analysis including phase data. However, this was not considered problematic as the tests were solely for determining the feasibility of quarter-wavelength measurements in a coaxial transmission line and the return loss, being the

magnitude of the S_{11} parameter, will include variations due to changing phase data. To enable such testing, the cell of Figure 4.3 was used, as this had already been constructed from copper and brass for use with the TDR equipment, having an internal diameter of 28mm, a length of 300mm and a central conductor of 6mm external diameter. While simple in terms of construction, having largely been built using plumbing parts from a local home improvements store, the cell offered a coaxial cross section and was considered suitable for testing whether quarter-wavelength resonances could be detected in a small cell forming a short transmission line.
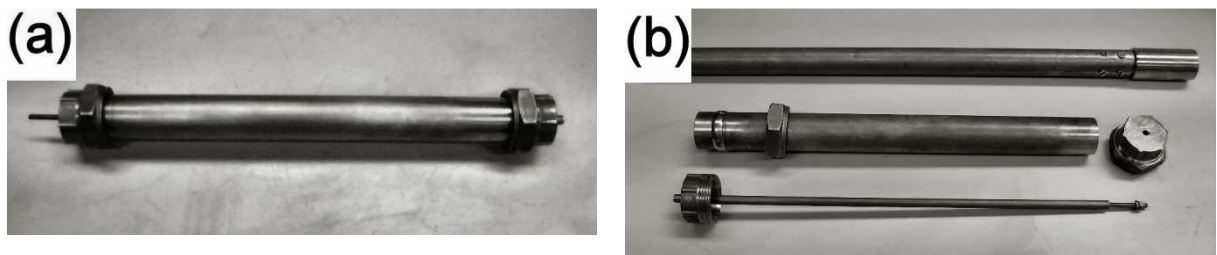
Figure 4.3. Initial prototype cell (a) assembled and (b) component parts (including a rod used with early TDR for compaction of soils).

After calibration of the VNA at its measurement port (the cable used to connect to the cell was an SMA type, precluding connection of the N-Type calibration standards to the end of the cable), return losses were measured for the cable only, with open-circuited end, the cable plus air-filled cell, and the cable plus distilled water-filled cell. The results of these tests are illustrated in Figure 4.4, using images of the VNA screen.
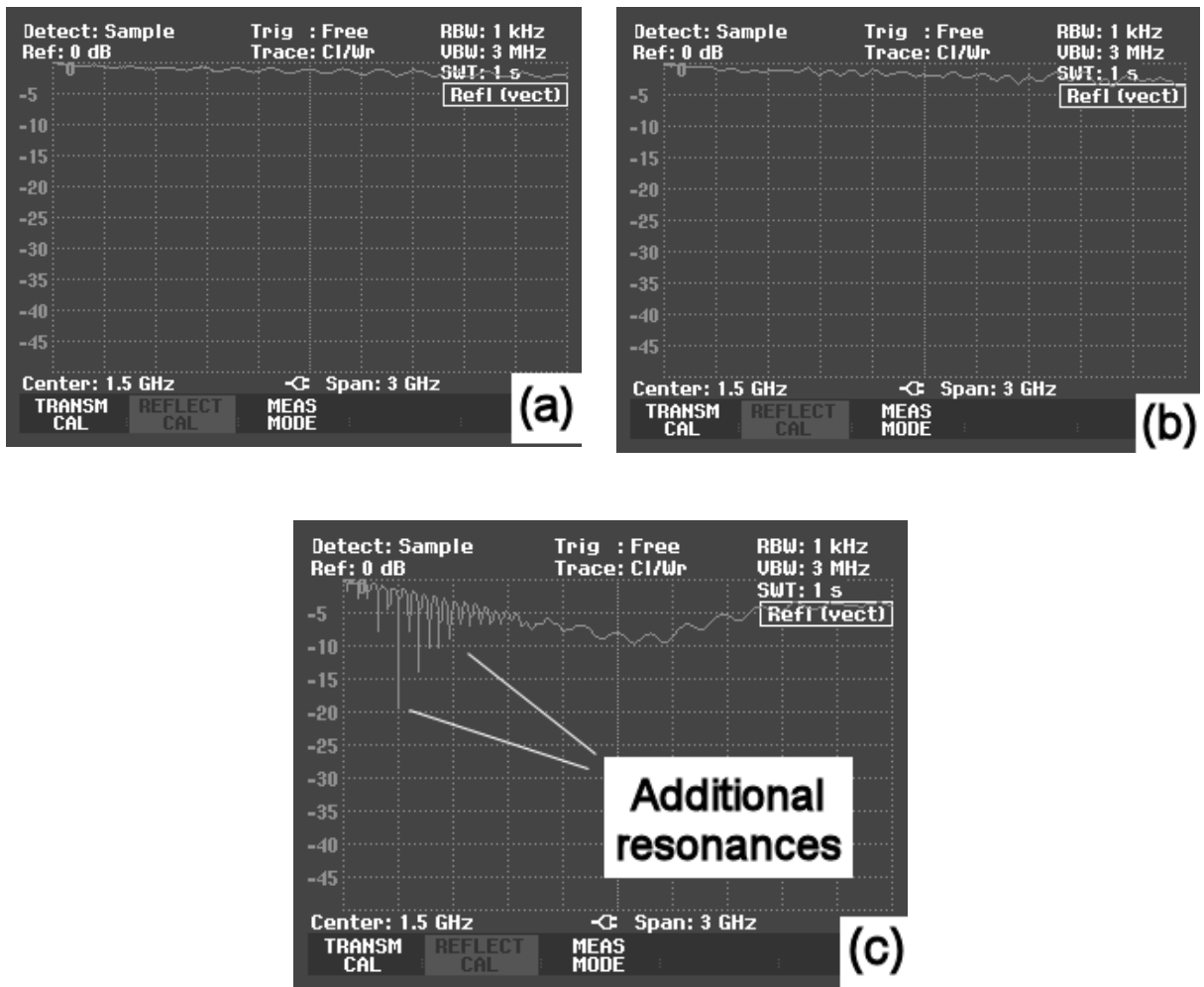
Figure 4.4. Voltage reflection measurements for prototype cell (a) just cable, (b) cable and air-filled cell, and (c) cable and distilled water-filled cell.

As can be seen from Figure 4.4(a), variations due to the cable provide maxima and minima that may mask those associated with the cell. This indicated that later development work involving a VNA would best be undertaken with a cell utilizing an N-Type connector to allow calibration at the cell end of the cable. In Figure 4.4(a) it can be seen that variations occur sinusoidally along the graph, the amplitude increasing with frequency as attenuation correspondingly increases. In Figure 4.4(b) the air-filled cell has been added to the end of the cable but, due to the low loss nature of air and the small change in phase, additional resonances due to the cell cannot be discerned.

However, in Figure 4.4(c) where the cell is now water-filled, the quarter-wavelength frequencies can be clearly seen. From these graphs the reason why real S_{11} values are generally used for QWA, in place of return losses (where a vector analyzer is available), can be seen: the former incorporates phase data that can be identified even when losses are low.

The return loss data for the water-filled cell, captured on a computer, are shown in Figure 4.5, which indicates that resonances were spaced approximately 57.2MHz apart. From Equation 4.6 it was found that this frequency interval corresponded to an apparent permittivity of 76.3 which, although less than the expected value of 80, was considered sufficiently close to illustrate that the cell could be used with a VNA to acquire apparent permittivity data. Based on Figure 4.5, it can be seen that the cell was capable of measuring the apparent permittivity of the water to at least 1GHz, variations above that frequency being dominated by resonances in the cable.
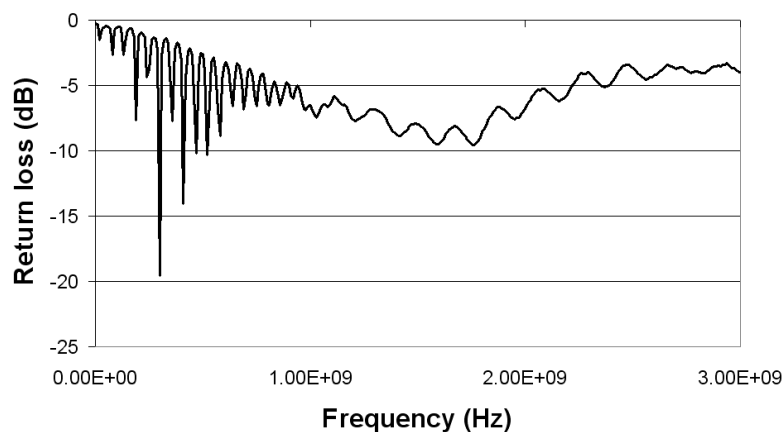
Figure 4.5. Return losses measured for the cable and water-filled cell.

Based on the preliminary tests, a number of requirements were noted for incorporation into an improved cell for full development of the QWA measurement system:

1. Use of vector data would be required (i.e. return loss and phase), as low loss, small phase change, materials (e.g. air, dry soils, etc) would make quarter-wavelength points difficult to identify in scalar data.

2. The SMA connector, which was found to be adequate for use with TDR, would need to be replaced with an N-Type connector, as this would allow resonances in the data, due to the cable, to be calibrated out in a simple manner.

3. The thin copper tubing used for the prototype cell was not sufficiently stiff to withstand accidental impact, and so a more robust design would be necessary.

4. Although the 300mm long tube provided useful data in initial tests, attenuation would be significant in lossy materials. As wet fine-grained soils are highly attenuating, this would mean that soil measurements would be limited to lower frequencies. Therefore, for the purposes of building a cell to prove the potential of QWA over a wide range of soil conditions, it was decided that the length of an improved cell would have to be significantly shorter.

4.6 DEVELOPMENT AND TESTING

A more sophisticated and robust coaxial cell was constructed, as depicted in Figure 4.6. The cell was manufactured from an aluminium tube, 23mm internal diameter and 91mm internal length, with a 3mm diameter stainless steel central conductor connected to the end plate to provide a short-circuited transmission line. It

was necessary to reduce the internal diameter of the cell by approximately 5mm over that of the prototype, in order to accommodate the largest drill bit available for use in the lathe used to construct it.

Impedance matching, to minimise reflections in the transition between cable and soil, was achieved by simply extending the coaxial geometry of the N-Type connector's inner conductor and insulation through the cell end plate. While this does not guarantee exact impedance matching, it was considered necessary only to ensure close values to minimise additional resonances. An example of such an additional resonance can be seen in Figure 4.5 as an apparently lower frequency sinusoidal variation cycling through approximately 180° up to 3GHz.
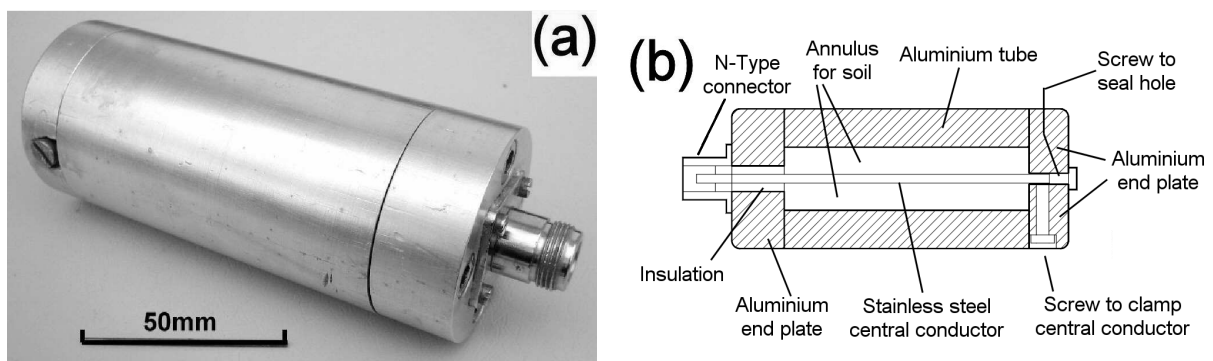
Figure 4.6. The measurement cell used in this study (a) photograph and (b) diagrammatic cross section (bolts between end plate and tube omitted for clarity).

Initial tests, using air and distilled water, yielded the real S_{11} values shown in Figure 4.7. The data contained the expected maxima at the relevant quarter-wavelength frequencies for both air and water.
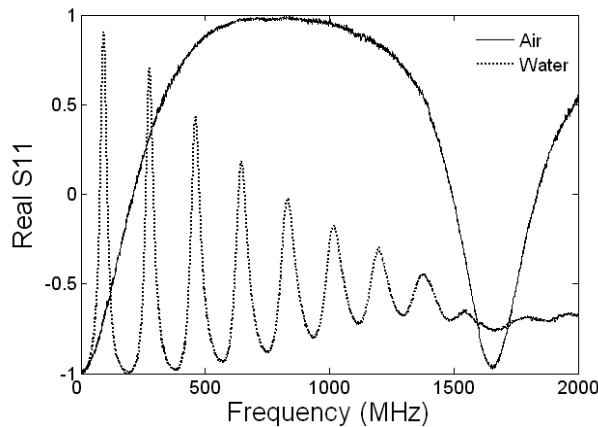
Figure 4.7. Air and water real S_{11} values measured using the cell.

The cell was tested using air and distilled water due to their well documented apparent permittivities, the electromagnetically dispersive nature of water being considered insignificant below 2GHz. The tests with water were used to calibrate the cell, i.e. by using them to calculate an apparent length (92mm) for use in Equation 4.6. The concept of apparent length is well known in TDR, and provides a simple means of removing any minor errors in the measurement set up, thus allowing the calibration data to match theory. Therefore, the simplicity of this method was adopted for QWA, in order to account for factors such as potential phase changes due to impedance mismatch between cable and cell, the accuracy of the VNA frequency generation and potential deviations of the VNA signal from a true sinusoidal voltage variation.

It was also considered appropriate to carry out an initial test with an electromagnetically dispersive material, for which Ethanol was used. The results for each of these three materials are shown in Figure 4.8 and are in close agreement with expected values (see Heimovaara, 1994) shown as dashed lines in the figure. It can be noted that the greatest variation occurs for water, which can be accounted for by the

increase in potential error associated with the measurement system at higher apparent permittivities. Tests using dry sand and penetrating oil yielded apparent permittivity values of 2.8 and 2.5 respectively, which also accorded with documented values of 2.6 for dry sand (Matzler, 1998) and 2.3 for penetrating oil (Robinson et al., 2003a).
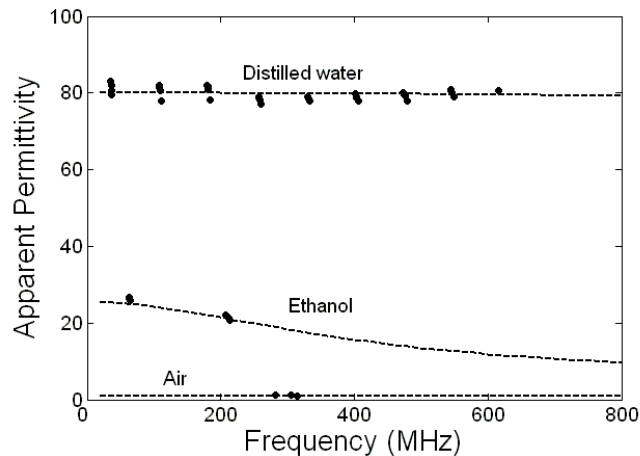
Figure 4.8. Results of three initial apparent permittivity tests, after calibration, for the measurement cell.

Since a particular need for the cell was to measure apparent permittivity in wet fine-grained soils, the cell was used to measure the electromagnetic properties of seven of the soil samples at high water contents close to their Liquid Limits. The results are illustrated in Figure 4.9, which shows each exhibiting low-frequency electromagnetic dispersion effects, and higher-frequency, more stable, values as expected from theory (Saarenketo, 1998; Wensink, 1993). The importance of measuring the apparent permittivity at the Liquid Limit is illustrated by Figure 4.10. This shows the apparent permittivity of soil Sample 8 over a wide range of frequencies and volumetric water

contents. From Figure 4.9 it should be noted that even at the Liquid Limit apparent permittivity data are available above the upper goal of 1GHz, and for the higher apparent permittivity samples the lower frequency is below the lower goal of 100MHz.
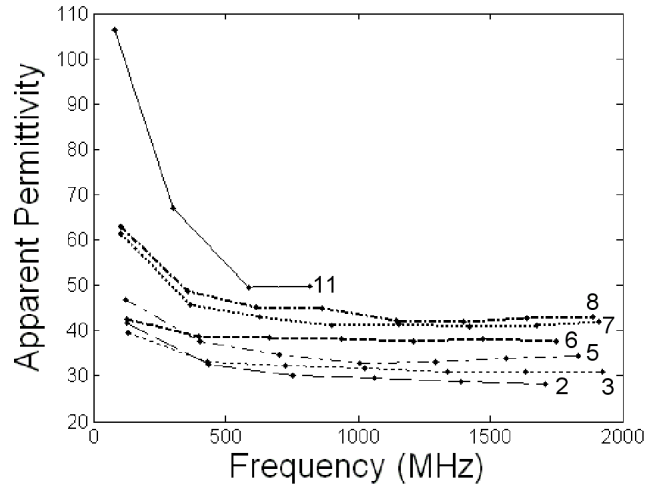
Figure 4.9. Frequency-domain effects of dispersion in a range of wet clays, measured at their Liquid Limits.
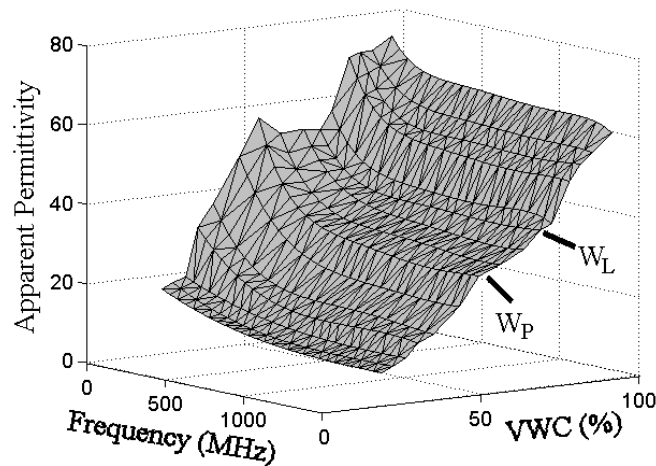
Figure 4.10. The apparent permittivity of Sample 8 measured over a wide range of volumetric water contents (VWC) and frequencies.

The range of water contents between the points marked W_P (the Plastic Limit) and W_L (the Liquid Limit) are the saturated water contents expected to be found under normal field conditions (Craig, 1997), and so of greatest interest in this study. The cell was also tested using TDR equipment (TDR100 - manufactured by Campbell Scientific Inc.), in order to allow comparison between QWA and TDR data. The end reflection distances for air and distilled water were used to calibrate the cell TDR measurements and Equation 4.12 was used to relate apparent permittivity to end reflection distances.

$$\varepsilon_r^* = \left(\frac{L_{TDR}}{L_{PROBE}} \right)^2 \qquad\qquad \text{[Eq. 4.12]}$$

where L_{TDR} is the probe length calculated from the distance to the end reflection measured using the TDR equipment, and L_{PROBE} is the apparent probe length derived from the TDR calibration process.

In order to allow comparison between QWA and TDR, QWA data were reduced to a single interpolated value for the data points either side of 1GHz to provide a reference apparent permittivity for the higher frequencies (after Logsdon 2006a). 1GHz was chosen for this purpose as it was above the effects of electromagnetic dispersion in Figure 4.9 and allows comparison with other literature, such as that of Wensink (1993). In this thesis, such high-frequency data are referred to as HF QWA. These data, together with the TDR data, are plotted against volumetric water contents in Figure 4.11. Also presented in the figure is the Topp model (Topp et al., 1980), a widely used method for relating TDR data to water content. It is apparent that QWA values vary significantly from both the TDR values and the Topp model.

However, this variation between the QWA and TDR data is not unexpected, as the power level of the frequency band generated by the electrical pulse in TDR

equipment has been shown to be significantly biased to frequencies below 500MHz (Friel and Or, 1999). This leaves higher frequencies to be attenuated in conductive soils to the extent that they have limited influence on time-domain measurements. Therefore, the TDR data were compared to the frequency-domain data of Figure 4.6 and it was found that the TDR values intersected with the corresponding data lines within a frequency range of approximately 200 to 400MHz.
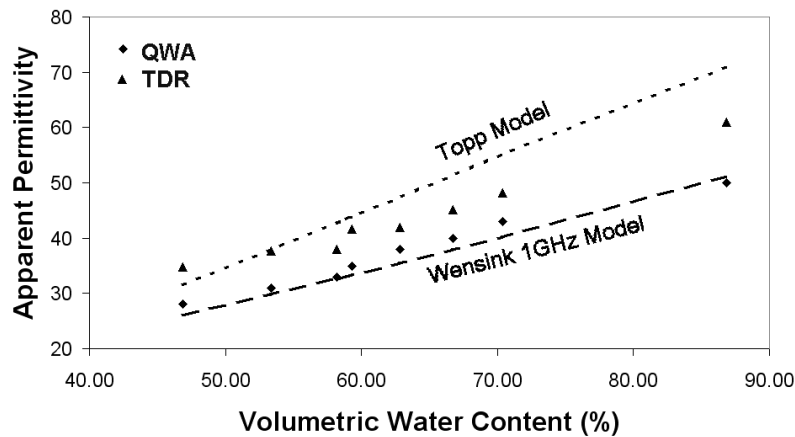
Figure 4.11. Apparent permittivity values for the studied soils, at their

Liquid Limits, using QWA (c. 1GHz) and TDR.

To investigate these differences between HF QWA and TDR data, the HF QWA apparent permittivity values were compared to other research relating to the permittivity of soils at high water contents. One such study (Wensink, 1993) showed good correlation between the permittivity of wet dispersive soils at 1GHz and the volumetric water content. The Wensink model has therefore been included in Figure 4.11, and it can be seen that the HF QWA data show good correlation with this model. Therefore, HF QWA data are potentially more appropriate than TDR data for analysis

of soil electromagnetic properties, and water content, at frequencies where dispersion has minimal effect.

4.7 COMPUTER MODELLING

Computer models allow a greater understanding of the operational mechanisms of QWA, and allow measured data to be critically analysed to aid in the validation and interpretation of results. In order to model the cell as an electromagnetic circuit element, it was first necessary to determine the elements involved. These can be summarised as the cable connecting to the VNA, the measurement cell, the connection between cable and cell, the cell end termination and the material within the cell, as illustrated in Figure 4.12.

Of these elements, the cable and connection were considered to be simple entities with an impedance of $50+j0\Omega$ (the connection being considered simply an extension of the cable). Similarly, the termination, a short circuit being decided upon for this research, can be modelled as an impedance of $0+j0\Omega$. However, the measurement cell cannot be considered a simple entity, because the electromagnetic properties of the cell contents are not constant: changing with the electromagnetic properties of the contents and, for electromagnetically dispersive materials, with the measurement frequency.

To determine the magnitude of reflections at a change in impedance, it is first necessary to know the impedance either side of a mismatch in materials (e.g. cell/cable and cell/end termination). The reflection strength can then be determined using Equation 4.13 (Hayt and Buck, 2006).
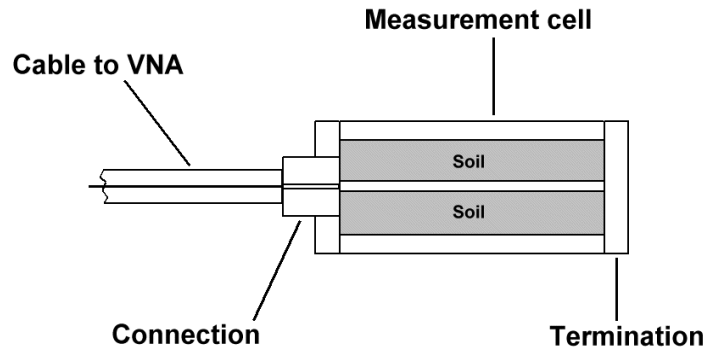
Figure 4.12. Elements Required for Measurement Cell Modelling.

$$\Gamma = \frac{Z_1 - Z_0}{Z_1 + Z_0} \qquad \text{[Eq. 4.13]}$$

where Γ is the reflection coefficient, Z_0 is the impedance of the material through which the signal passes toward the interface and Z_1 is the material through which any transmitted signal travels after the interface.

To determine the reflection magnitude at the cable/cell interface, due to the mismatch between the two, it is necessary to know the cell characteristic impedance, which can be determined using Equation 4.14 (after Wadell, 1991).

$$Z_{cell} = \frac{138}{\sqrt{\varepsilon_r}} \log_{10}\left(\frac{r_{outer}}{r_{inner}}\right) \qquad \text{[Eq. 4.14]}$$

where ε_r is the permittivity of the cell contents, r_{outer} is the inner diameter of the cell annulus (m), and r_{inner} is the outer diameter of the inner conductor (m).

However, from Equation 4.14 only the reflection magnitude at the cable/cell interface can be determined, the electromagnetic energy not reflected being transmitted into the cell. This transmitted energy will resonate within the cell, and pass back

149

through the cell/cable interface to combine, constructively or destructively, with the original reflected signal within the cable. In order to determine the combined reflection coefficient caused by the cable/cell interface and the cell itself, it is necessary to determine the cell input impedance. This can be more easily visualised through Figure 4.13, which shows modelled real S_{11} values for salty water in the cell (i.e. a conductive fluid). The reflections due to the characteristic impedance vary with frequency because of the dispersive nature of conductive fluids, but no resonances are seen because the characteristic impedance is the impedance of the coaxial transmission line at infinite length (or when signals are fully attenuated). The input impedance, on the other hand, combines the characteristic impedance with variations due to resonance within the cell.

The cell input impedance was determined using Equation 4.15 (after Wadell, 1991) and may be used with Equation 4.14 to predict the reflection magnitude detected by the VNA and, hence, the real S_{11} values.

$$Z_{in} = Z_{cell} \left(\frac{Z_{term} \cosh \gamma L + Z_{cell} \sinh \gamma L}{Z_{cell} \cosh \gamma L + Z_{term} \sinh \gamma L} \right) \qquad \text{[Eq. 4.15]}$$

where Z_{in} is the cell input impedance (Ω), Z_{cell} is the cell characteristic impedance (Ω), Z_{term} is the termination impedance (Ω), γ is the complex wave number and L is the cell length (m).

The complex wave number can be determined from Equations 4.16 to 4.18 (Hayt and Buck, 2006). For the fine-grained soils used in this study, the magnetic permeability was taken as that for free space for the purposes of modelling, the soil samples described in Chapter 3 having been checked with a strong rare-earth magnet to ensure that no magnetically susceptible particles were present.
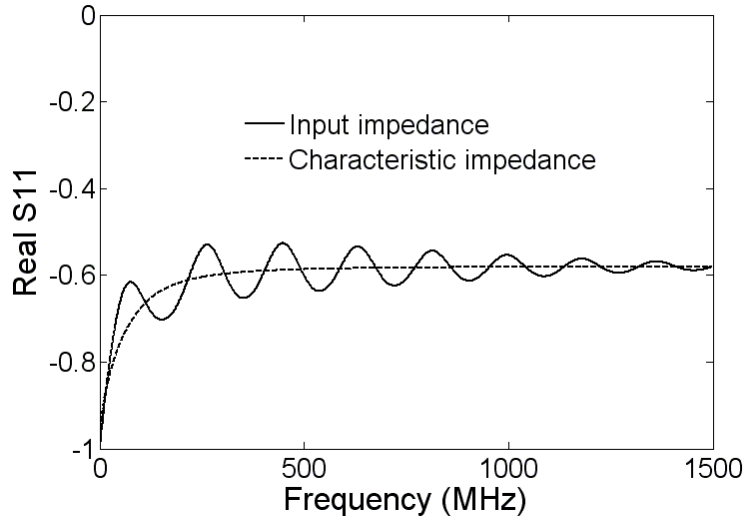
Figure 4.13. Real S_{11} values for salty water showing those associated with the characteristic and input impedances.

$$\gamma = \alpha + j\beta \qquad\qquad\qquad\qquad\qquad \text{[Eq. 4.16]}$$

$$\alpha = \omega \sqrt{\frac{\mu \varepsilon'}{2} \left(\sqrt{1 + \left(\frac{\varepsilon''}{\varepsilon'} \right)^2} - 1 \right)^{\frac{1}{2}}} \qquad\qquad \text{[Eq. 4.17]}$$

$$\beta = \omega \sqrt{\frac{\mu \varepsilon'}{2} \left(\sqrt{1 + \left(\frac{\varepsilon''}{\varepsilon'} \right)^2} + 1 \right)^{\frac{1}{2}}} \qquad\qquad \text{[Eq. 4.18]}$$

where α is the attenuation constant (nepers.m^{-1}) and ß is the phase constant (rad.s^{-1}).

Determination of the frequency-dependent complex permittivity parameters was derived using the Debye model of Equation 4.19. Based on the literature review, the permittivity of water was taken as varying between 80 at low frequencies and 3 at high frequencies, with a relaxation frequency of 17GHz. For air, the apparent permittivity

was assumed to be 1 at both high and low frequencies. For all other modelled

materials, values from the literature were used as described earlier in this chapter.

$$\varepsilon_r = \varepsilon_{r\infty} + \frac{\varepsilon_{rs} - \varepsilon_{r\infty}}{1 + (j\omega\tau)} \qquad \text{[Eq. 4.19]}$$

where ε_r is the frequency dependent complex relative permittivity, $\varepsilon_{r\infty}$ is the high

frequency relative permittivity (i.e. at frequencies significantly above relaxation), ε_{rs} is

the low frequency relative permittivity (i.e. significantly below relaxation), and τ_D is the

relaxation time of the water molecule.

The above equations were incorporated into a MatLab program in order to

calculate modelled real S_{11} values and then plot them against measured values for the

materials used for calibration and testing of the cell. Modelling results for air and water

are illustrated in Figure 4.14 and good correlation can be seen between modelled and

measured data.
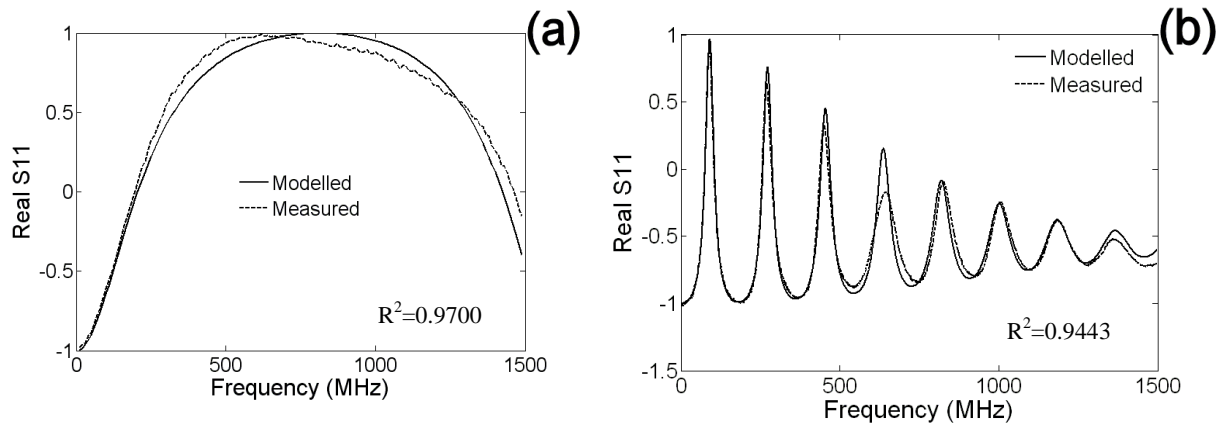
Figure 4.14. Comparison of modelled and measured real S_{11} values for (a) air and (b) distilled water used for calibrations.

The three other materials used to validate the cell measurement methodology

(ethanol, penetrating oil and dry sand) were also modelled. For the ethanol (Figure

4.15(a)) and dry sand (Figure 4.15(c)), good correlation was found between modelled and measured data. However, the degree of correlation between modelling and measurement for the penetrating oil (Figure 4.15(b)) was not as good, although the difference was only that between a measured apparent permittivity of 2.5 and modelled of 2.3, the latter being based on a single report in the literature by Robinson et al. (2003b). Also, the lack of correlation is largely associated with the second quarter-wavelength, which is not used for QWA calculations, and so may indicate greater than expected attenuation due to undocumented electrical conductivity.
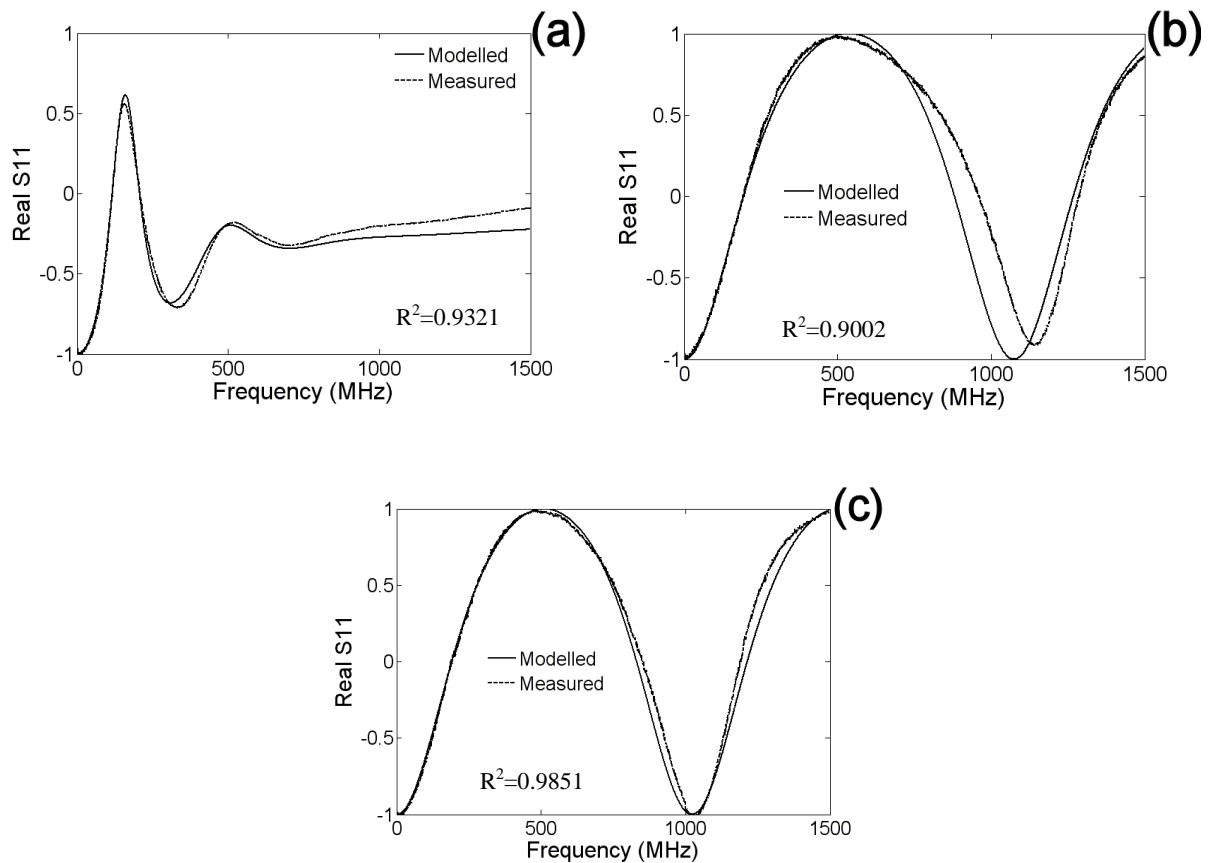
Figure 4.15. Comparison of modelled and measured real S_{11} values for (a) ethanol, (b) penetrating oil and (c) dry sand.

Dispersive properties due to electrical conductivity were also modelled, using distilled water to which was added table salt to produce conductivities of $0.58S.m^{-1}$, $1.22S.m^{-1}$ and $2.28S.m^{-1}$. Conductivity was measured using a Hannah Instruments HI9033 meter and liquid conductivity probe, and the results of modelling and measurement in the cell are presented in Figure 4.16.
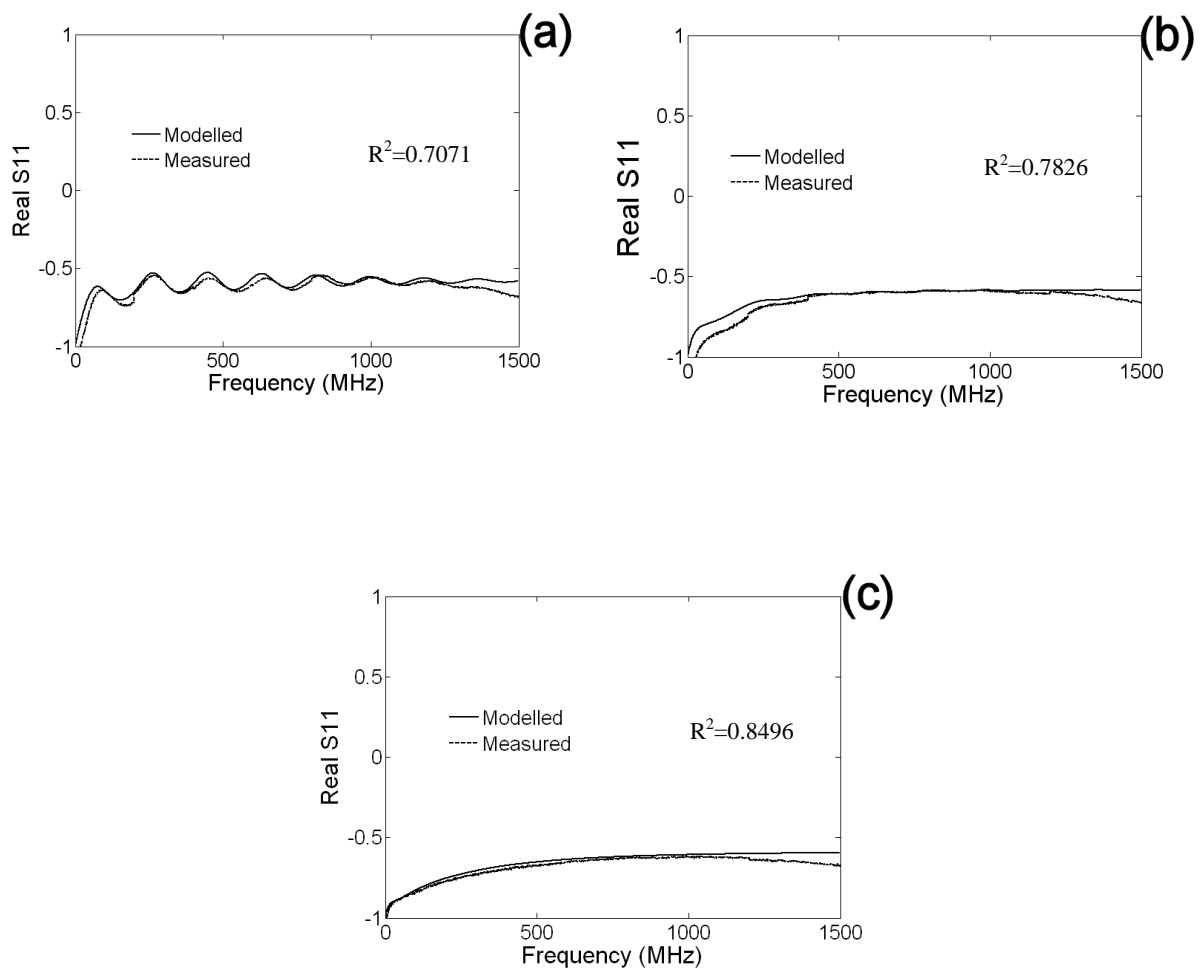
Figure 4.16. Comparison of modelled and measured real S_{11} values for distilled water with electrical conductivities of (a) $0.58S.m^{-1}$, (b) $1.22S.m^{-1}$ and (c) $2.28S.m^{-1}$.

These results were considered to show acceptable correlation, although some discrepancies are apparent at lower frequencies which, due to the reflection coefficients at higher frequencies being generally consistent (as the apparent permittivity of the distilled water will be relatively constant between tests) may be due to slight inaccuracies in the conductivity measurement system available. Also, it can be seen that the modelled and measured data start to diverge above approximately 1.2GHz and it is possible that this is due to the propagation of additional electromagnetic modes and variations due to small mismatches between the cable and cell head. Furthermore, QWA is unaffected by these higher frequency variations as the resonances have been almost fully attenuated. However, despite any minor discrepancies between the measured and modelled data, the purpose of the modelling was to validate and better understand QWA in a cell, rather than to provide exact data. The above results can be seen to accomplish this, but for future parameter matching work, further research and modelling will be required.

4.8 ACCURACY CONSIDERATIONS

Understanding potential accuracy is central to any measurement system and the importance of fully understanding the effects of frequency resolution, which includes the measurement equipment frequency accuracy and quarter-wavelength frequency measurement indeterminacy due to noise, is apparent from Equation 4.6. This illustrates that inability to determine accurately the quarter wavelength frequency results in variation of the calculated apparent permittivity. Also, it should be noted that the apparent permittivity of the tested material affects the spacing between quarter wavelength frequencies, and so measurement errors rise with an increase in the

apparent permittivity. This is illustrated in Figure 4.17 for a range of frequency resolutions, for the cell and probe described below, calculated as the difference between the true apparent permittivity and that calculated for a frequency different by the value of the measurement resolution.
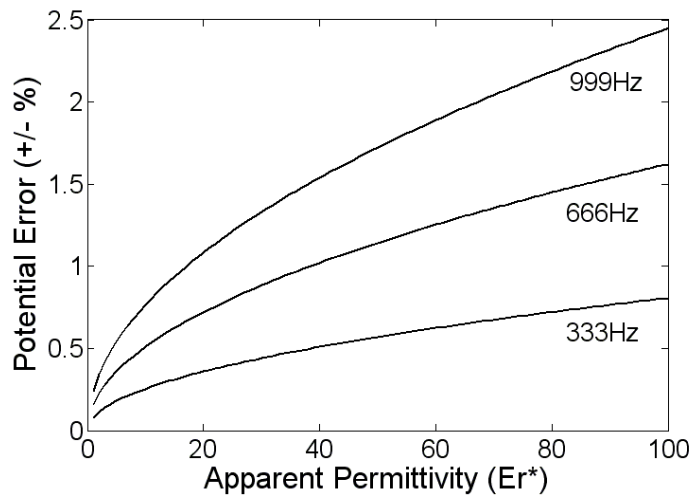
Figure 4.17. Potential QWA cell apparent permittivity errors for three different frequency measurement resolutions.

Furthermore, because loss tangents will cause reductions in the amplitude of quarter-wavelength frequencies, higher frequency maxima/minima may become difficult to identify clearly and the accuracy associated with them will diminish. Also, some noise is unavoidable and it was found that the effects of noise became more pronounced as the amplitude of the maxima/minima became small - i.e. the signal-to-noise ratio decreases with increasing attenuation. Therefore, in such attenuating soils it may be advisable to ignore the higher frequency value, or adjust the cell/probe dimensions to reduce attenuation. An example of noise in real S_{11} data is provided in

Figure 4.18, which shows that it can be difficult to exactly determine the apex of the sinusoidal signal waveform. However, with the aid of a moving average filter, and with experience, it was found from the calibration results that the resonant frequencies could be manually identified within the potential accuracies of Figure 4.17.
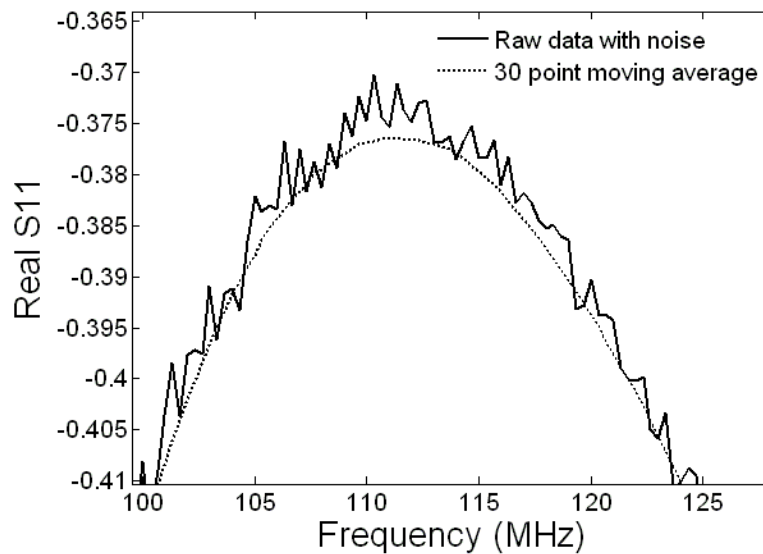
Figure 4.18. Noise in a signal compared to a moving average filtered version.

Electromagnetic tests in coaxial transmission lines are based on the transverse electromagnetic mode (TEM) of propagation and, as frequencies increase past a particular cut-off frequency (determined by the coaxial geometry) other unwanted modes may exist and degrade the data. While this does not mean that TEM modes will not propagate above this frequency, it is advisable to take care in measuring quarter-wavelength resonances to recognise variations that may occur in the data due to additional propagation modes, particularly above the cut-off frequency. For the coaxial geometry of the cell, Equation 4.20 (Winder and Carr, 2002) provides an

estimate of the cut-off frequency. This equation has been used to draw the graph of Figure 4.19 which indicates that the transverse electromagnetic mode should dominate in cell measurements for frequencies up to 1.5GHz for most materials intended to be measured in it.

$$f_{cutoff} = \frac{1}{3.76(D_{inner} + D_{outer})\sqrt{\varepsilon_r^*}}$$ [Eq. 4.20]

where f_{cutoff} is the cut-off frequency (GHz), D_{inner} is the diameter of the cell annulus (mm) and D_{outer} is the diameter of the inner conductor.
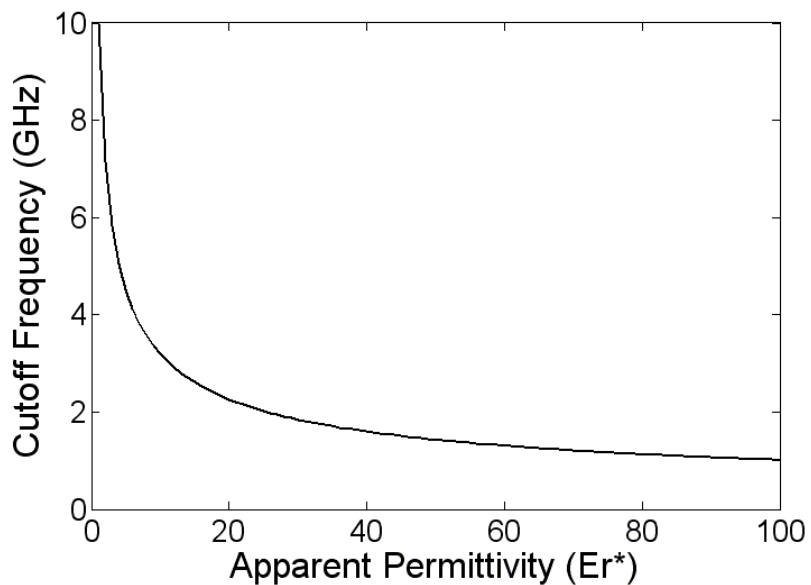
Figure 4.19. Approximate cut-off frequencies for the cell.

CHAPTER 5 – MEASUREMENTS USING THE DEVELOPED METHODOLOGY

5.1 OVERVIEW

QWA shows significant promise as an extension to TDR that can facilitate consideration of electromagnetic dispersion. As well as for calibration materials such as air and water, data can be obtained even for very wet fine-grained soils at their Liquid Limits. Therefore, in order to explore the potential use of the developed test apparatus, and to consider the potential for future research into the use of TDR-style probes with QWA, four series of tests were undertaken:

1. Measurement of apparent permittivity in two soils, over a wide range of signal frequencies and water contents, the results being related to Atterberg limits.

2. Measurement of apparent permittivity in eleven soils, over a wide frequency range at their respective Liquid Limits.

3. Measurement of apparent permittivity using a TDR-style probe suitable for large-samples and to facilitate future field testing of fine-grained soils.

4. Measurement of the apparent permittivity of an anthropogenic soil having significant iron content, as a cautionary illustration of variations that may occur due to magnetic susceptibility.

5.2 ELECTROMAGNETIC VELOCITIES IN TWO SELECTED CLAY SOILS

5.2.1 Background

Apparent permittivity of soils is not commonly measured as three-dimensional data covering wide frequency and water content ranges. Such three-dimensional data have significant advantages for soil electromagnetic research in a geotechnical context, most notably the potential to relate the magnitude of electromagnetic dispersion to variations in water content and soil states. Also, in combination with TDR, it provides the potential for obtaining soil calibration data which allow consideration, in the field, of dispersive properties based on the single value provided by the TDR data. Furthermore, such data allow investigation of the relationships between geotechnical and geophysical data, which would otherwise be difficult to investigate, as the relationships may be associated with both frequency and water content domains.

Therefore, the objectives of this study were to obtain apparent permittivity data in both the frequency and water content domains, for two fine-grained clay soils in a saturated state; to include in the test data illustrative apparent permittivity values at low, unsaturated water contents in order to consider how trends may vary from those in the saturated state; and to investigate whether relationships exist between apparent permittivity and such parameters as dry density, Plastic Limit and Liquid Limit. The two soils used for this study were Samples 6 and 8 in order to provide significant contrast in dispersive properties.

5.2.2 Methodology

As it was considered necessary to ensure that significant variations in water content

did not occur within each sample (i.e. it should be homogenous), the soil for each test was prepared outside of the cell following initial hydration to a water content close to the Plastic Limit. This included significant mixing with palette knives on a glass plate, and maturation for a minimum of 24 hours in a sealed plastic container. Samples with lower water contents were then prepared by kneading and rolling (except for zero water contents where oven dried samples were used) and, for higher water contents, by mixing with distilled water for a minimum of twenty minutes on a glass plate or, for slurries, in a porcelain dish.

Stiff samples of soil were then placed in the cell, in small pieces torn from the main sample by hand, using a 22mm diameter brass rod suited to the internal geometry to compact them. At the higher water contents the soil slurry was poured into the cell and a thin stainless steel rod used to carefully remove any trapped air. However, samples falling into neither of these categories (i.e. plastic samples at high water contents) posed a greater challenge as they were generally sticky and so more difficult to place in the cell. Therefore, these samples were placed in the annulus using a 10ml plastic syringe, cut at the end to have an open diameter of 15mm, and tamped using the rubber ended syringe plunger in order to prevent air voids occurring (Figure 5.1(a)). The cell end plate with N-Type cable connection was then attached to the body by carefully inserting the central conductor through the soil (Figure 5.1(b)). Although the sticky soil would be expected to adhere to the central conductor during insertion, it was considered wise to also place the cell on a vibrating table, running at approximately 50Hz, for thirty seconds in order to help ensure the soil would be in close contact with the conductor (Figure 5.1(c)).
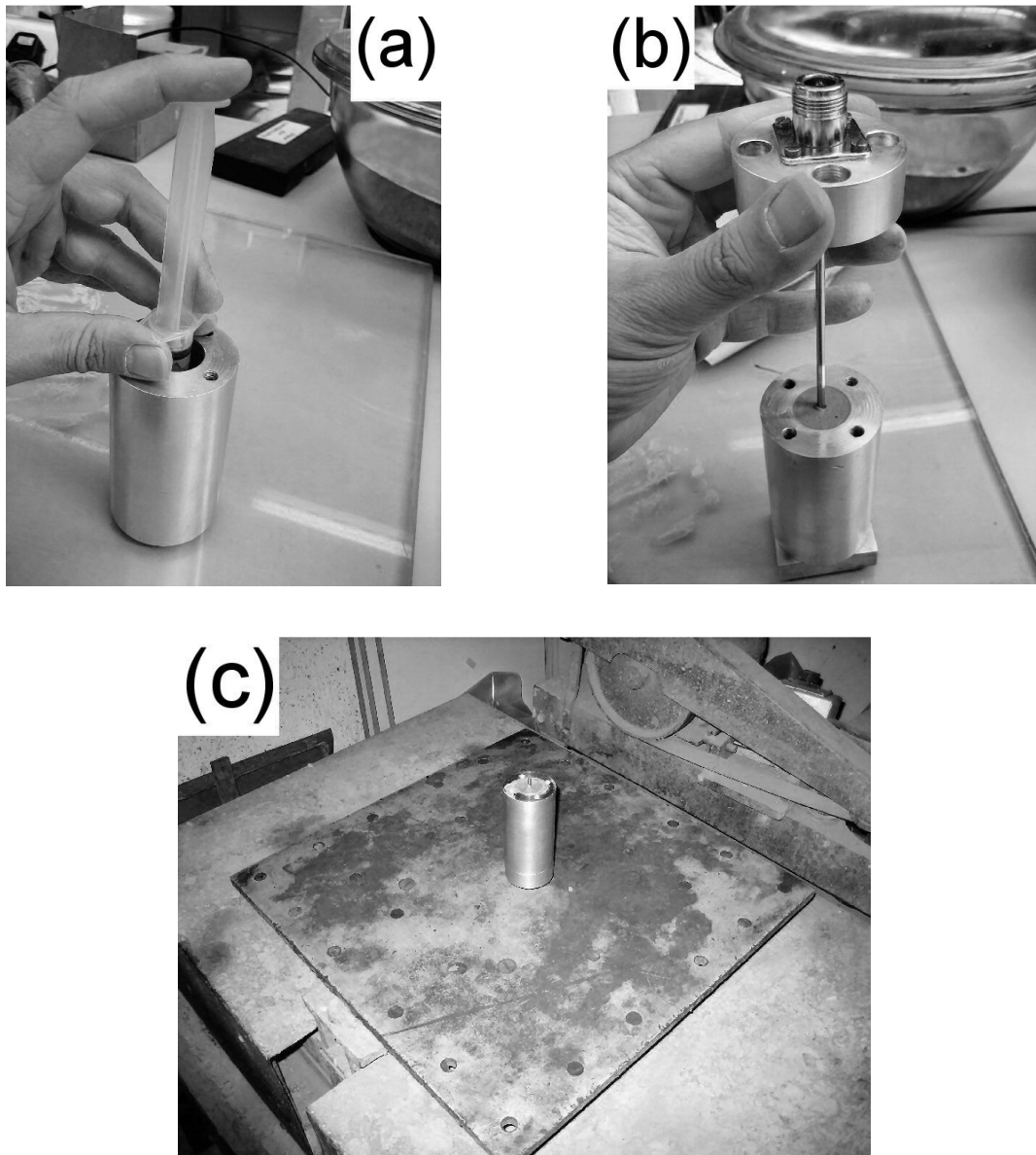
Figure 5.1. Filling the cell with wet soil: (a) placing soil into the cell, (b) inserting the centre conductor and (c) vibration.

Where it was considered possible that soil could be lost into the bolt holes during filling (e.g. at low water contents, when trimming the ends of wetter samples, and when pouring in slurries) the holes were covered with small pieces of plastic insulation tape.

The end of the aluminium body was carefully cleaned with slightly-dampened and dry tissue paper prior to connection of the end plates, in order to ensure electrical contact. The re-assembled cell was carefully cleaned on the outside, to remove any attached soil, and any water or soil in the N-Type connector carefully removed, prior to it being weighed. As the cell was also weighed immediately prior to being filled, this allowed determination of the soil mass.

QWA and TDR tests were then carried out as detailed in Chapter 4 and, following testing, the samples were removed and re-mixed with the remainder of the sample for further testing. This was carried out carefully in order to allow visual inspection to determine whether any voids were present. A small amount of the soil from the cell was oven dried at 105°C to determine gravimetric water content in accordance with British Standard BS1377 (BSI, 1990). Wet slurry samples were gently shaken prior to each measurement (i.e. each 200MHz span on the VNA) and prior to removal of the slurry for water content testing (for slurries the entire contents were used to determine water content), the cell masses were then used with the cell volume and gravimetric water content to determine the dry density and volumetric water content.

Data from the testing are presented in three formats, these being full QWA data in the frequency and water content domains, HF QWA data close to 1GHz, and TDR data, all as described in Chapter 4. The HF QWA data are provided as they are largely unaffected by electromagnetic dispersion and so can be expected to have values close to the real permittivity due to reduced loss tangents. Three-dimensional full QWA graphs were prepared by fitting fifth-order polynomials to frequency-domain data for each water content and surface plotting this data over all water contents using MatLab, for a frequency range of 100MHz to 1.5GHz. This was considered acceptable, as a substitute

for use of discrete quarter-wavelength frequencies, as the three-dimensional graphs are used solely for illustrating trends.

5.2.3 Relationships Between Water Content and Dry Density

The dry densities of the samples are plotted against volumetric water content in Figures 5.2 and 5.3, together with the theoretical saturated volumetric water content to dry density relationships derived using Equation 5.1.

$$\rho_{dry} = \rho_{min} - \frac{\rho_{min}}{100}\theta \qquad\qquad \text{[Eq. 5.1]}$$

where ρ_{dry} is the dry density, ρ_{min} is the particle density and θ is the volumetric water content (%).
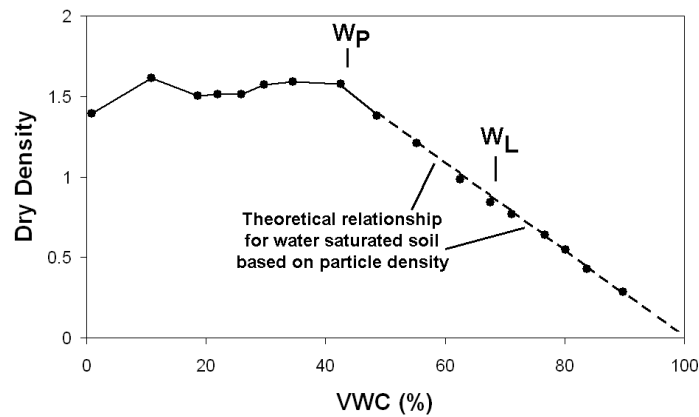
Figure 5.2. London Clay dry density results in the volumetric water content (VWC) domain.

Above the Plastic Limit the measured data fell close to the theoretical saturation line as shown in Figures 5.2 and 5.3. The dry density provided a useful method of quality

control, as only using samples with dry densities falling close to the predicted values aids in improving data quality. Therefore, above the Plastic Limit any sample data not falling close to the predicted relationship of Equation 5.1 were discarded. Often this occurred due to a void in the sample, which was often identified prior to electromagnetic measurement during weighing of the sample filled cell, and subsequently confirmed during visual examination.
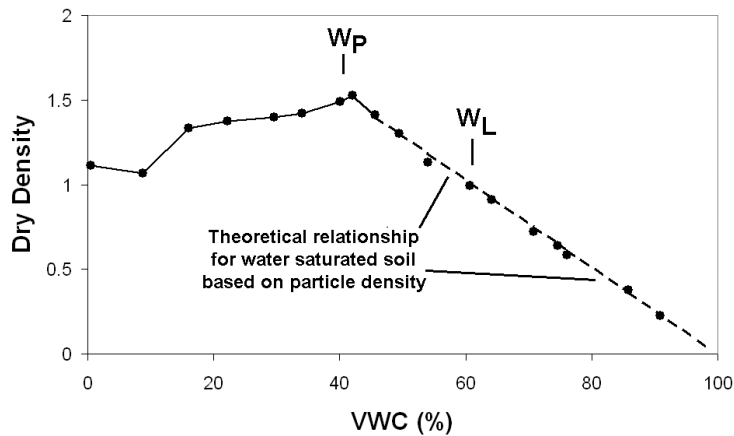
Figure 5.3. English China Clay dry density results in the volumetric water content (VWC) domain.

5.2.4 Apparent Permittivity Spectra

The apparent permittivity spectra for both soils are presented in Figures 5.4 and 5.5. It was found that the soils exhibited increasing apparent permittivity approximately to the point where they were close to saturation near the Plastic Limit. Above this point, both soils showed HF QWA apparent permittivities that generally followed the Wensink 1GHz model (Wensink, 1993) until the water content was a short distance

above the Liquid Limit, at which point a step change (marked A in Figures 5.4 and 5.5)

occurred and the apparent permittivity started to approach the 'free water' value above

the Liquid Limit.
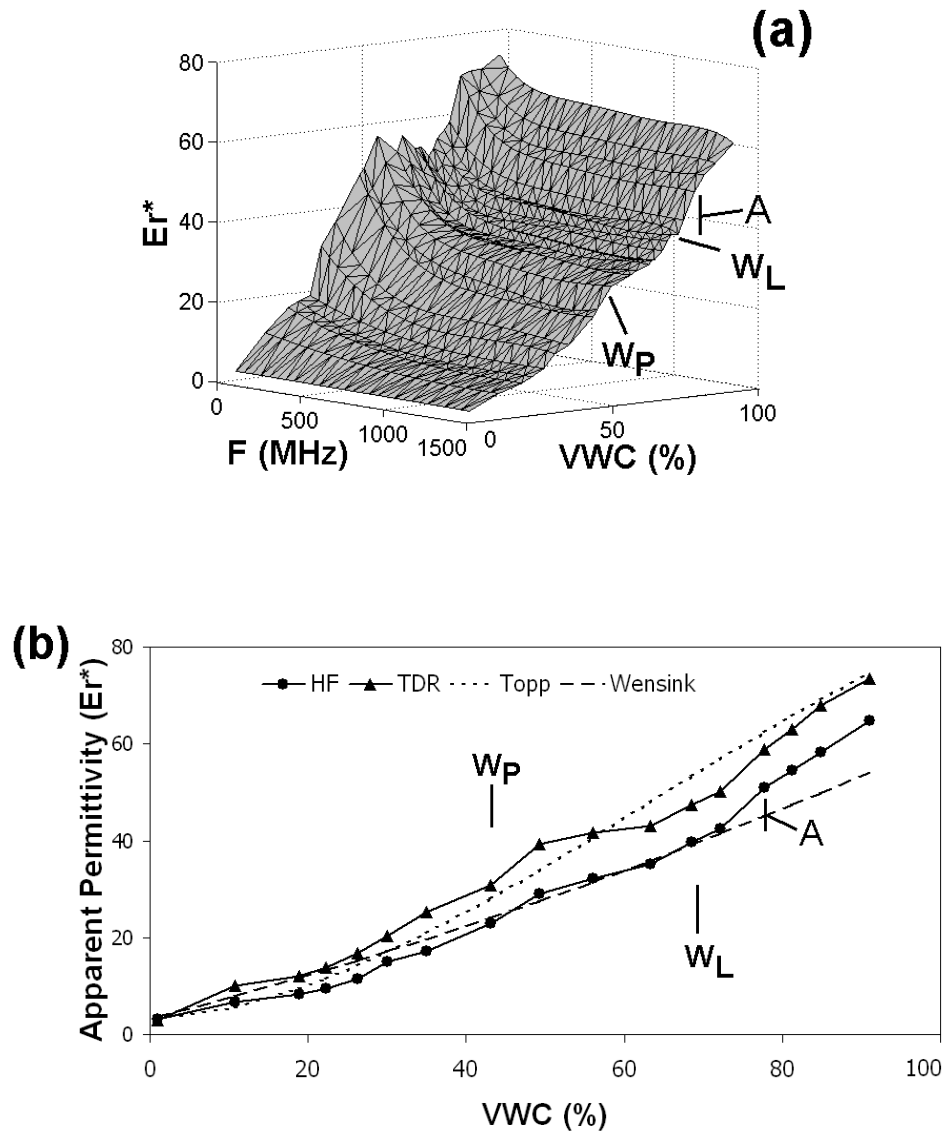
Figure 5.4. London Clay apparent permittivity data in the volumetric water content

(VWC) domain (a: full QWA data and b: TDR and high frequency (HF) QWA data).
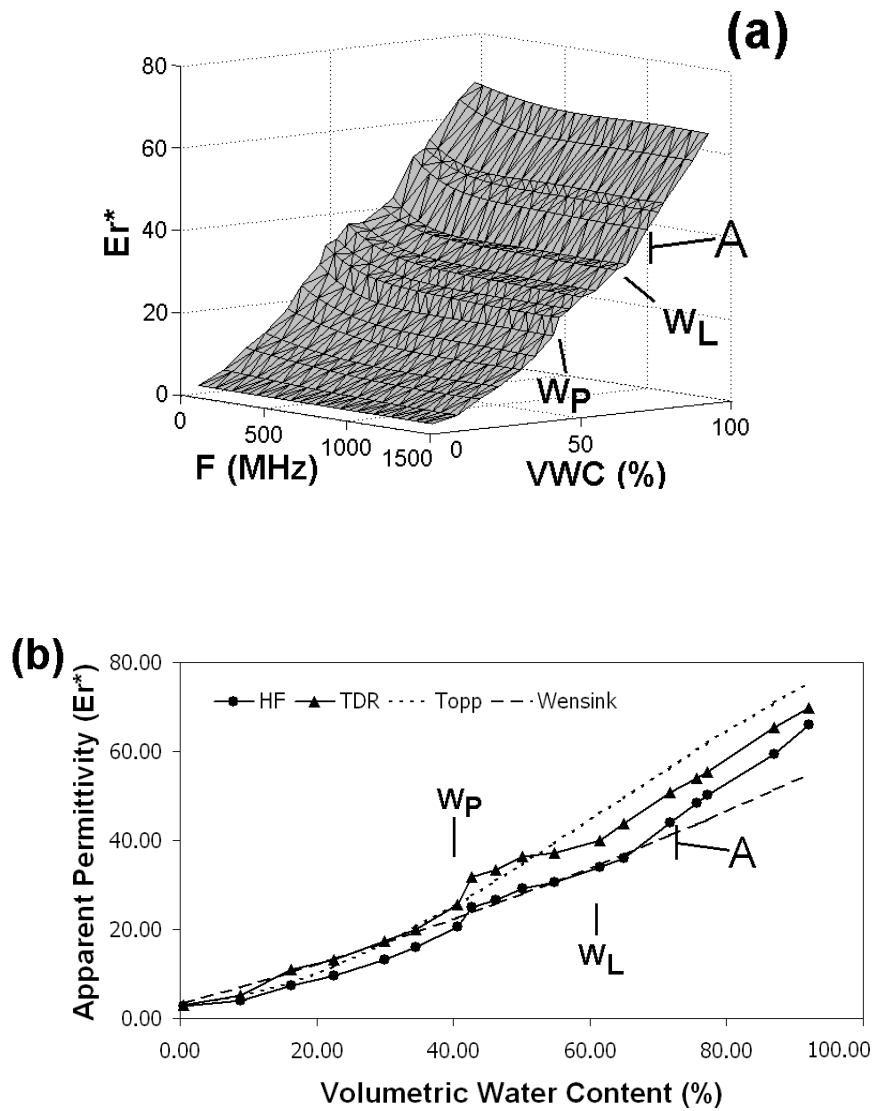
Figure 5.5. **English China Clay apparent permittivity data in the volumetric water content (VWC) domain (a: full QWA data and b: TDR and high frequency (HF) QWA data).**

It is also apparent from the figures that the English China Clay electromagnetic dispersion magnitude was less than the London Clay. Also included in Figures 5.4(b) and 5.5(b) are the TDR data and the commonly used relationship described by the Topp

model (Topp et al, 1980). It can be seen that, while the Topp model is close to the TDR data below the Plastic Limit, it does not provide a useful relationship between the Plastic and Liquid Limits. This can potentially explain why this model has been reported as not being representative of electromagnetically dispersive soils. Therefore, HF QWA with the Wensink model appears to provide a more reliable method of measuring water content in fine-grained dispersive soils, compared to use of TDR with the Topp model.

The TDR derived apparent permittivity values were found to be higher than the high frequency QWA data. This was expected as TDR data are considered to be associated with low frequencies where the effects of conductivity can be expected to raise the measured apparent permittivity (Friel and Or, 1999).

5.2.5 Signal Velocity Spectra

As apparent permittivity is simply an inverse property of signal velocity, it was considered appropriate to consider the variations in this latter parameter with water content and frequency. Therefore, velocity spectra calculated as a percentage of the velocity of light in a vacuum, from the apparent permittivity spectra using Equation 4.3, are shown in Figures 5.6 and 5.7.

It is evident from these figures that frequency domain variations are smaller than for electromagnetic dispersion of the apparent permittivity, and that variations per unit of water content change are significantly greater at water contents below the Plastic Limit than for the saturated state. Between the Plastic and Liquid Limits, the velocities for HF QWA data varied between 21% and 16% of the vacuum speed of light for the London

Clay, and between 20% and 17% for the English China Clay. The velocity associated with TDR measurements was slightly lower than the high frequency QWA data, which can be attributed to the associated lower frequencies. However, as water contents increased the velocities for TDR and HF QWA data were found to converge.
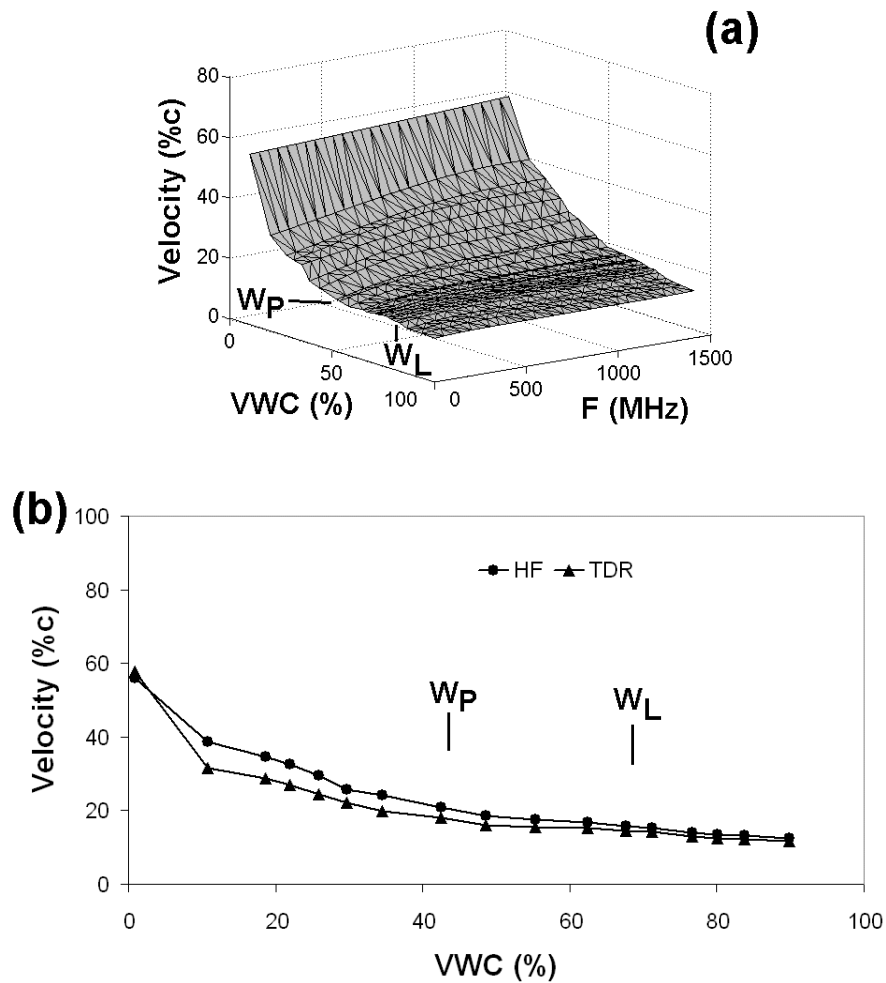
Figure 5.6. London Clay velocity data in the volumetric water content (VWC) domain as a percentage of the speed of light in a vacuum (a: full QWA data and b: TDR and high frequency (HF) QWA data).
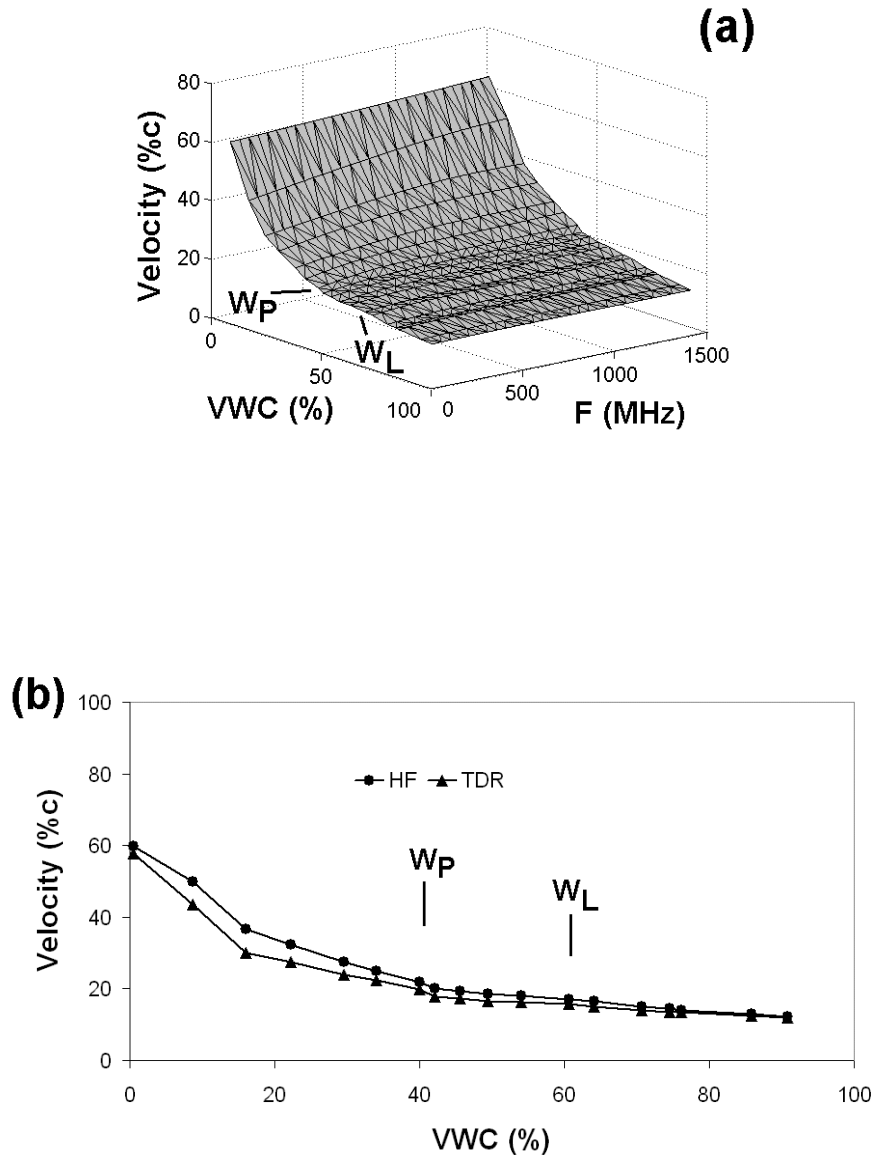
Figure 5.7. English China Clay velocity data in the volumetric water content (VWC) domain as a percentage of the speed of light in a vacuum (a: full QWA data and b: TDR and high frequency (HF) QWA data).

5.2.6 Effects of Dry Density

The electromagnetic properties of soils are dependent upon the prevailing dry density (e.g. Saarenketo, 1998). Therefore, the apparent permittivity spectra were corrected by dividing the volumetric water content and apparent permittivity by the dry density (Figures 5.8 and 5.9). It is important to note that dividing the volumetric water content by dry density naturally results in the gravimetric water content, illustrating the importance of using both types of water content in analysing the electromagnetic properties of soils. From the three-dimensional data of Figures 5.8(a) and 5.9(a), it can be seen that the magnitude of the dispersion becomes approximately constant when corrected for dry density. From this it can be concluded that the dispersive properties of the soils are largely a function of surface area, as dry density accounts for the majority of apparent permittivity variation.

Also, from the TDR and higher frequency QWA data of Figures 5.8(b) and 5.9(b) it can be seen that there is a gradual build-up of the apparent permittivity below the Plastic Limit but, once saturated, an approximately linear relationship is observed between the Atterberg Limits. Above the Liquid Limit the step change noted for the raw apparent permittivity data is still visible and an approximately linear relationship is also found above this point.

Such a potential change in phase of 'bound' water to 'free' water, at a critical water content, has been suggested for instance by Boyarskii et al. (2002), although it does not figure prominently in the majority of soil electromagnetic literature.
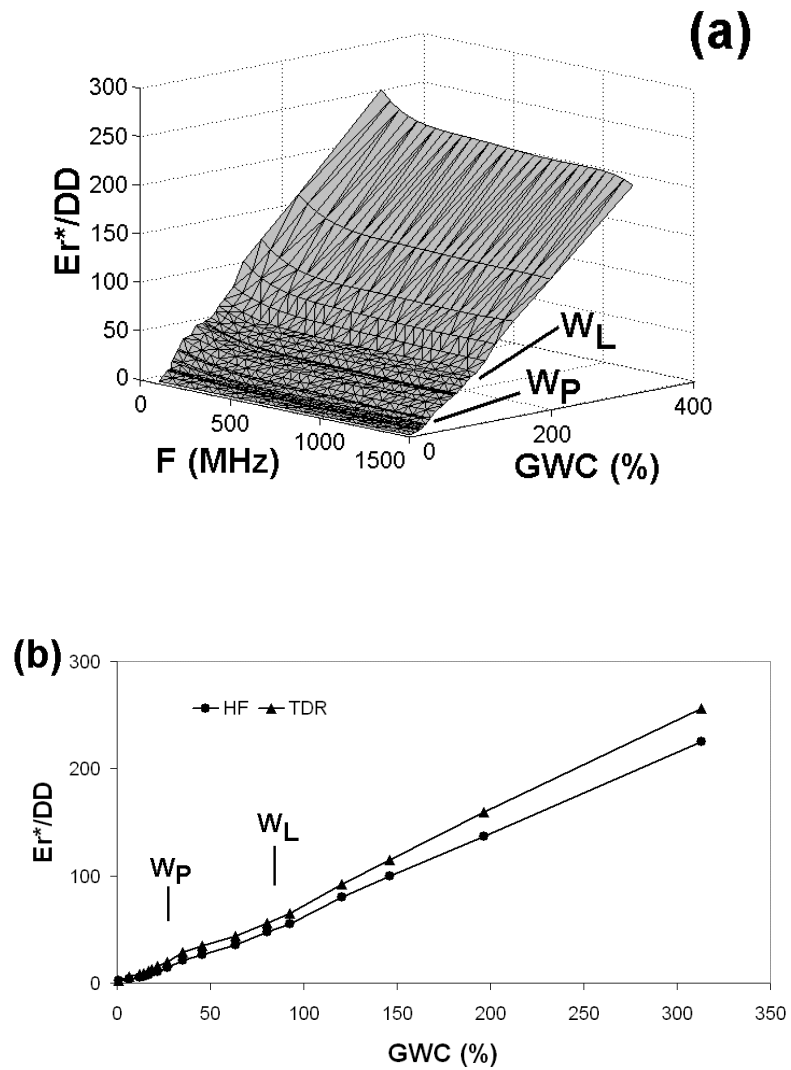
Figure 5.8. London Clay apparent permittivity corrected for dry density, in the gravimetric water content (GWC) domain (a: full QWA data and b: TDR and high frequency (HF) QWA data).
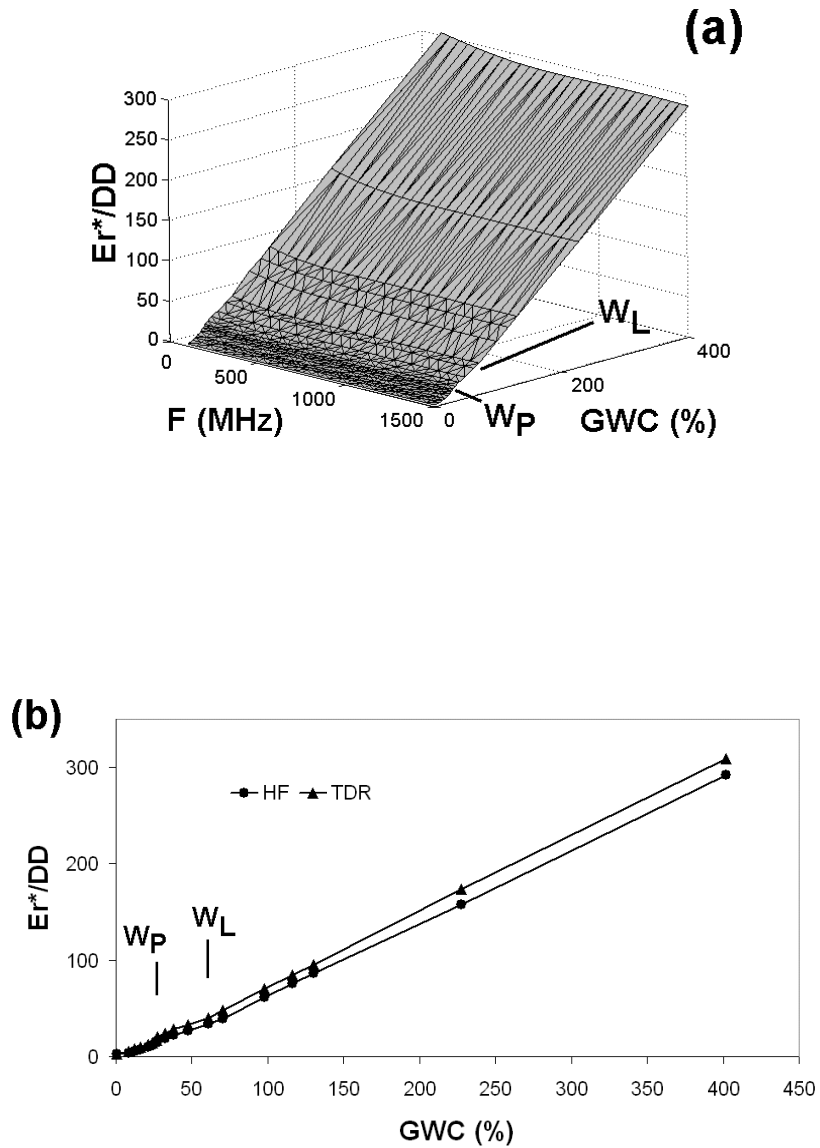
Figure 5.9. **English China Clay apparent permittivity corrected for dry density, in the gravimetric water content (GWC) domain (a: full QWA data and b: TDR and high frequency (HF) QWA data).**

5.3 ELECTROMAGNETIC VELOCITIES IN SOILS AT THE LIQUID LIMIT

5.3.1 Background

As the Liquid Limit can be considered representative of the specific surface area of a soil, and relates to a similarity in properties for a wide range of soils (Mitchell and Soga, 2005), it was instructive to compare the Liquid Limit of the soil samples to the apparent permittivity they would exhibit. It was considered important that these tests be carried out in a manner consistent with normal laboratory Liquid Limit testing, even though it may have meant that variations in dry density could mask relationships between signal velocity and the Liquid Limit. Therefore, this case study was conducted with the objectives of measuring the apparent permittivity of a wide range of soils close to their Liquid Limits, as measured using a cone penetrometer, and investigating whether there are links between the apparent permittivities and Liquid Limits of fine-grained soils.

5.3.2 Methodology

Testing was undertaken in the same manner as for the two soils described in Section 5.2, using the syringe method to place soils in the measurement cell. However, much of the Liquid Limit testing was carried out prior to a VNA being available for electromagnetic testing. Therefore, matured samples were slowly hydrated during mixing on a glass plate (Figure 5.10(a)) until a cone drop of 20mm was achieved, using the same cone-penetrometer as for Liquid Limit testing (Figure 5.12(b)), the resulting soil paste then being placed in the cell and the water content determined by oven drying the contents once apparent permittivity had been measured.
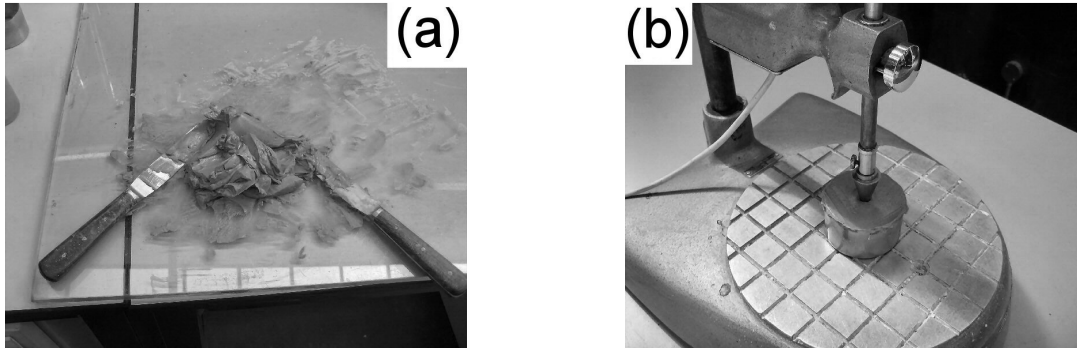
Figure 5.10. Hydration of Liquid Limit samples: (a) mixing and (b) determination of cone drop.

As shown in Figure 5.11, there was a high degree of correlation between these water contents and the Liquid Limit. Due to the significant differences between the gravimetric Liquid Limit water contents of Samples 8 and 11, Samples 9 and 10 were added specifically to fill that gap for this case study. These samples were blends of English China Clay (Sample 6) and Sodium Bentonite (Sample 11) and were intended to be used only for illustrative purposes to show whether a linear trend would exist over the full Liquid Limit range.
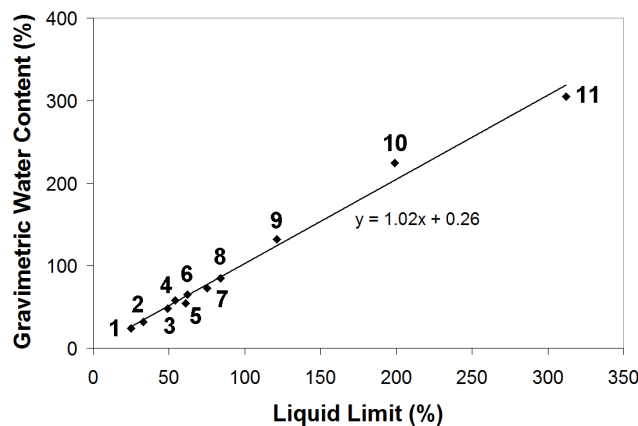
Figure 5.11. Comparison between the Liquid Limit of each sample and the gravimetric water content at which apparent permittivity was measured.

The dry densities of each sample, at the Liquid Limit, were calculated from the wet soil mass and water content, the results being presented in Figure 5.12 together with their predicted values based on Equation 5.1. Samples were not discarded due to them not falling exactly at predicted values. This is because, while the data of Section 5.2 were intended to illustrate variations in apparent permittivity in saturated soils, this study concentrated on how electromagnetic signal velocity testing could be incorporated into geotechnical testing regimes.
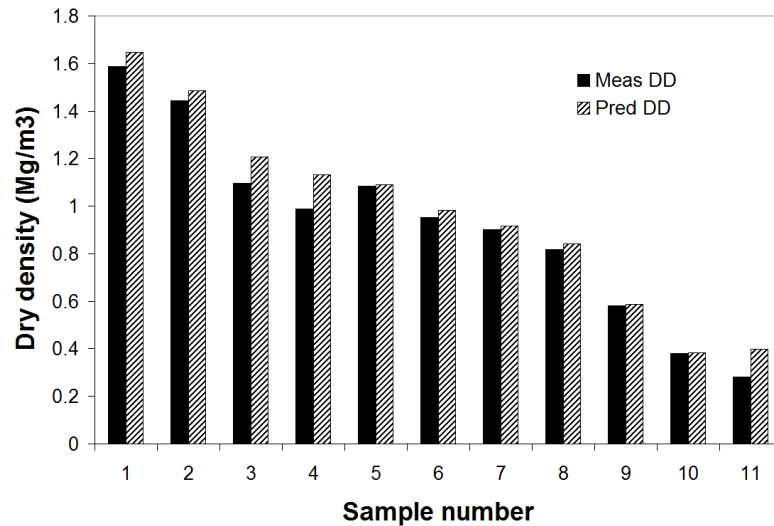
Figure 5.12. Calculated and predicted dry densities of the Liquid Limit samples.

While the Liquid Limit is an important geotechnical test, it includes limited safeguards against small voids and variations in dry density from the saturated state. It was, therefore, considered important to undertake this study with such limited safeguards, any relationships then found being known to be possible within tolerances achievable under routine geotechnical conditions.

5.3.3 Apparent Permittivity Spectra

The apparent permittivity spectra for all eleven samples are presented in Figure 5.13.
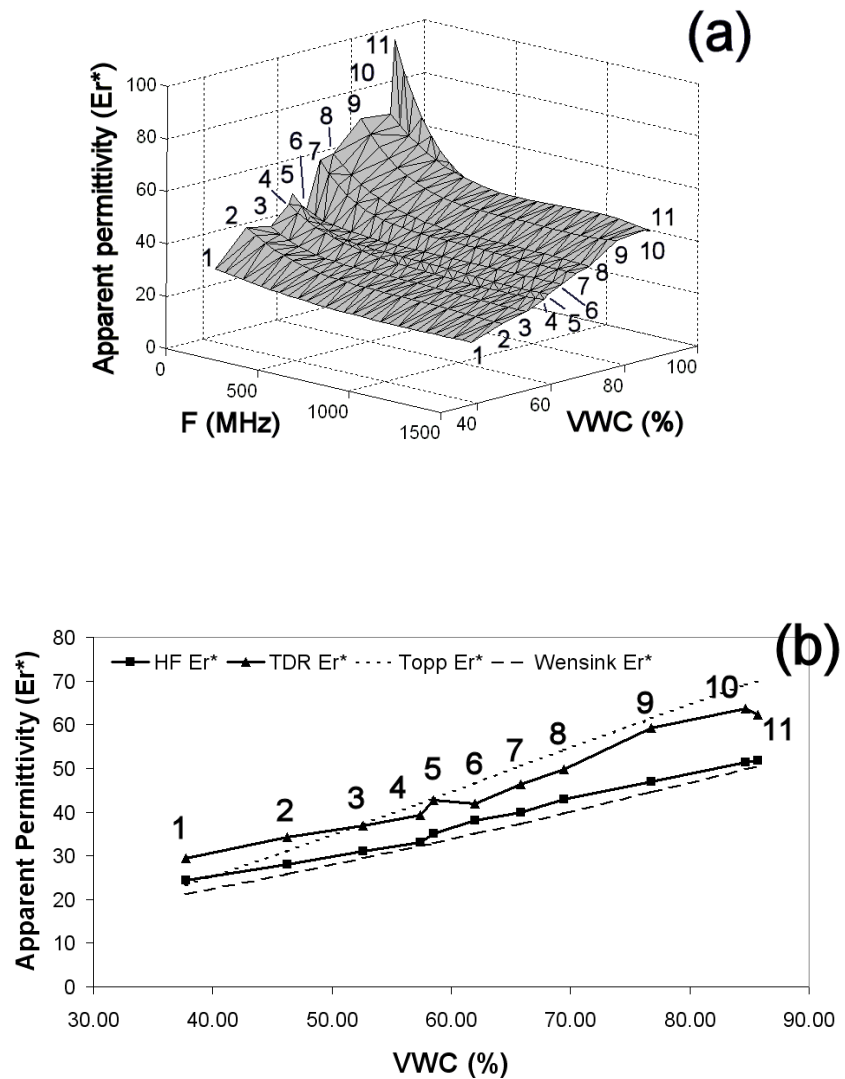
Figure 5.13. Liquid Limit apparent permittivity data in the volumetric water content (VWC) domain (a: full QWA data and b: TDR and high frequency (HF) QWA data).

In general, the soils exhibited increasing apparent permittivity approximately in proportion to the water content at the Liquid Limit. All samples showed HF QWA apparent permittivities generally following the Wensink 1GHz model (Wensink, 1993), while the TDR data were generally closer to the Topp model (Topp et al., 1980). The TDR data exhibited greater variability and, as seen in Figure 5.13(a), while the higher frequency apparent permittivities appear to follow an almost linear relationship, the dispersion magnitude showed considerable variability. Furthermore, the TDR data show a general trend toward an apparent permittivity of 80 at 100% volumetric water content, while the HF QWA data do not. Based on the data in Section 5.2, it is therefore apparent that saturated soils at the Liquid Limit do not exhibit higher frequency apparent permittivities following a mixing model utilising 80 as the apparent permittivity of the water phase.

5.3.4 Signal Velocity Spectra

The apparent permittivity data were used to calculate signal velocity (Figure 5.14). As highlighted in Section 5.2, the nature of the apparent permittivity amplifies the effects of dispersion. For both HF QWA and TDR, the variations in signal velocities over all samples were of the order of 5% of the velocity of light *in-vacuo* (and significantly less if the very high Liquid Limit samples containing Sodium Bentonite are ignored). TDR velocities were expectedly lower than HF QWA due to the lower frequencies. The TDR data also show less variability when expressed as a velocity, as expected from Equation 4.3. Of further interest is that both datasets in Figure 5.14(b) show almost linear trends which appear to be parallel rather than converging.
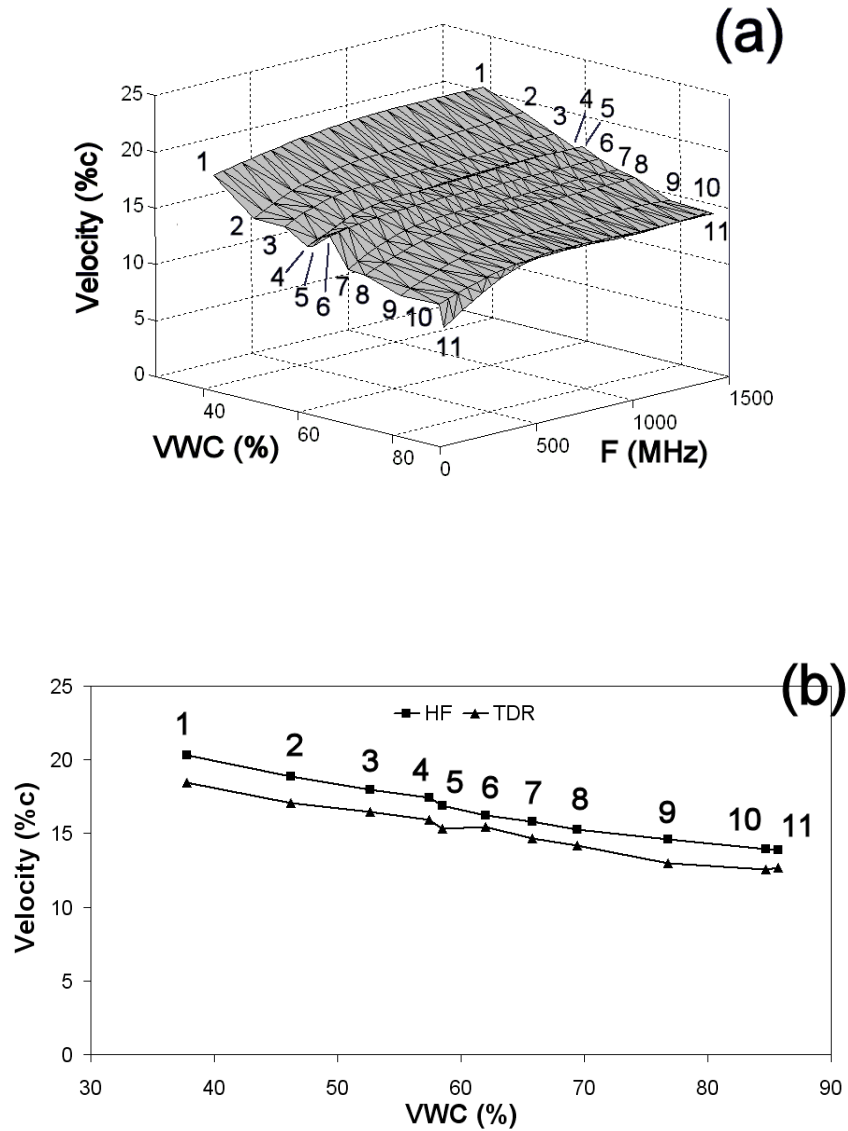
Figure 5.14. **Liquid Limit velocity data in the volumetric water content (VWC) domain as a percentage of the speed of light in a vacuum (a: full QWA data and b: TDR and high frequency (HF) QWA data).**

5.3.5 Effects of Dry Density

As for Section 5.2, the apparent permittivity data for the samples at their Liquid Limits were corrected by dividing by the dry density and plotting against gravimetric water content (Figure 5.15).
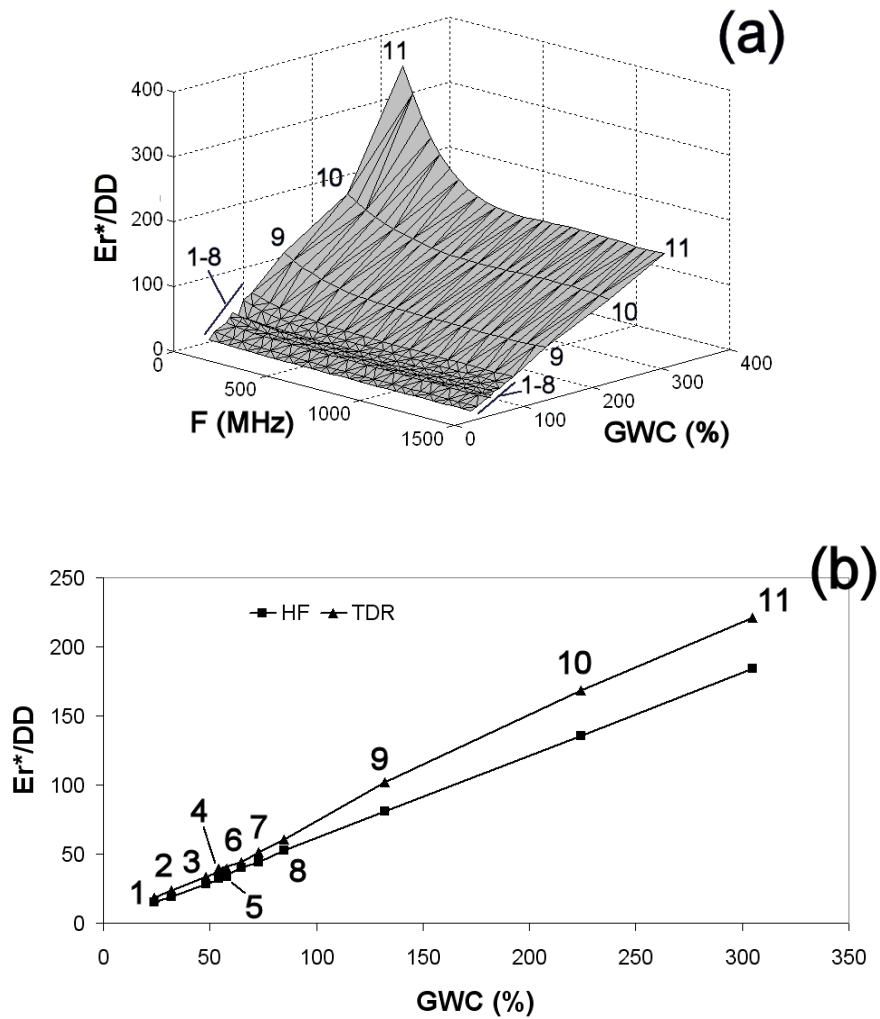
Figure 5.15. Liquid Limit apparent permittivity corrected for dry density, in the gravimetric water content (GWC) domain (a: full QWA data and b: TDR and high frequency (HF) QWA data).

Again it can be seen that the corrected apparent permittivity follows an almost linear relationship for both HF QWA and TDR data, and that the degree of dispersion appears much less variable between samples than in raw apparent permittivity data.

However, the TDR data appear to exhibit two linear relationships generally divided by a point between Samples 8 and 9, the higher water content relationship in Samples 9 to 11 appearing elevated in comparison to lower water contents. As can be seen in Figure 5.15(a), the degree of dispersion in samples 9 to 11 also appears greater than for other samples and it could be speculated that this is because they all contained Sodium Bentonite.

5.4 ELECTROMAGNETIC VELOCITY MEASUREMENT USING PROBES

5.4.1 Background

While this thesis predominantly focuses on use of a coaxial cell, there are circumstances where it could be advantageous to use probes: for instance, where large geotechnical samples are being tested, or where the signal velocity must be measured in combination with other tests. The options for use of probes, particularly ones that can be inserted into the bulk soil mass, are limited.

For this reason, QWA use with TDR probes has been investigated, as TDR probes are simple, quasi-coaxial, transmission lines (see e.g. Robinson et al., 2003a). The objective of this case-study was therefore to investigate whether TDR probes can be used with QWA and whether they can be modelled as simple coaxial transmission lines.

5.4.2 Probe Construction

A three pin TDR probe design was chosen as a basis for this case study as it is easily inserted into soil with minimal disturbance. The length and diameter of the stainless steel rods was 100mm and 3mm respectively, with a separation of 19mm between rod centres (Figure 5.16).
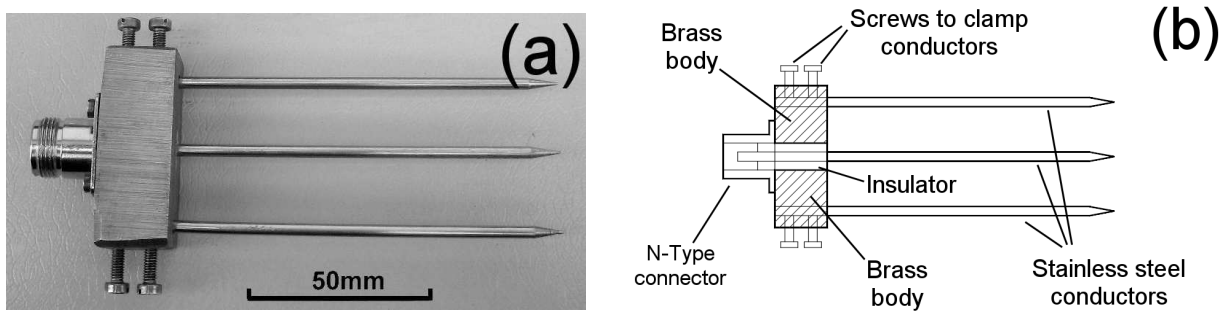
Figure 5.16. The three-pin probe used in this study (a) photograph and (b) diagrammatic cross section.

Other probe configurations were considered, including ones with four and eight outer conductors around a single centre conductor. However, for the purposes of this case study the three pin probe (i.e. two outer conductors placed either side of a single centre conductor) provides greater compatibility with the literature (see Chapter 2), as it is a very widely employed TDR probe geometry. For connection to a VNA, the head of the TDR probe was constructed using the same N-Type connector and impedance matching method employed for the cell. However, in all other respects there is very little difference between it and most alternative TDR probes.

5.4.3 Calibration and Initial Testing

Initial tests were carried out in air and distilled water, the real S_{11} values being presented in Figure 5.17.
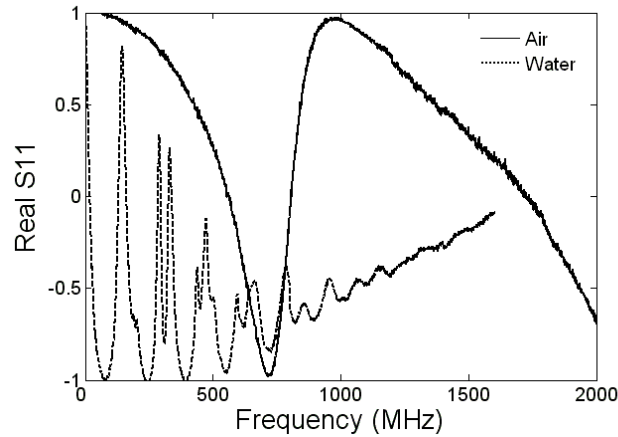
Figure 5.17. Air and water S_{11} values for the three-pin probe.

Several features are evident when comparing this figure to the S_{11} coaxial cell values of Figure 4.7, the most evident being that the resonant frequencies exhibit themselves as minima, due to the absence of the 180º phase change at the short-circuited end of the cell. Also, multiple reflections are obvious in the water data, associated with radiation losses past the end of the probe reflecting back from the base of the calibration vessel. As the vessel used allowed 300mm of water to be contained beyond the end of the probe, it was evident that multiple reflections could affect calibration data quality for similar probes using relatively lossless dielectrics, within practical limitations. Multiple reflections were not found in the air data, as it was not necessary to contain it within a vessel, nor in soil tests due to the higher attenuation associated with them. The problem of multiple reflections was, therefore, only associated with the need for use of water for calibration. In order to calibrate the probe in water, the effects of multiple reflections

were reduced by taking the average of four measurements and calculating an apparent

probe length - 105mm, which correlated with the TDR apparent length - that allowed

the apparent permittivity variations to be centred on a value of 80. The calibration

results are detailed in Figure 5.18.
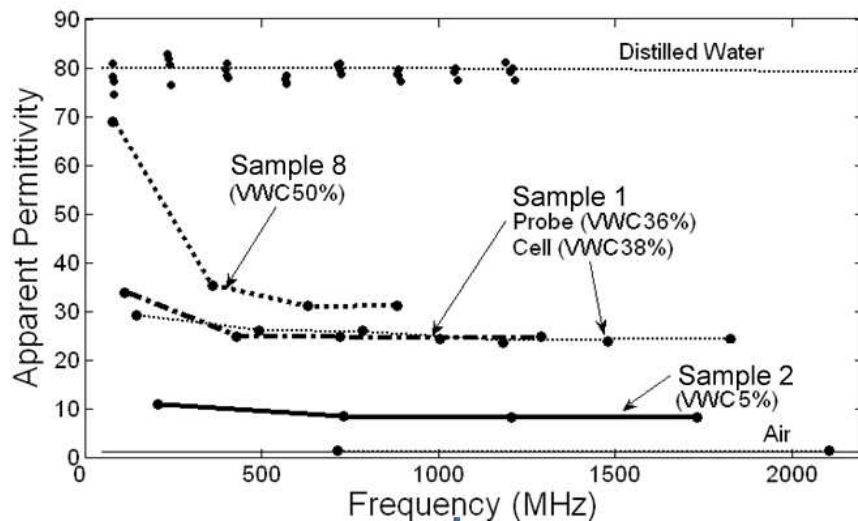
Figure 5.18. Apparent permittivity versus frequency, after calibration, for

the modified TDR probe.

It can be seen from this figure that variations in the values for water reduce with

frequency, due to multiple reflections suffering increased attenuation in comparison to

lower frequencies. However, it was found that once a suitably large vessel was used to

contain the water the variations were generally within two units of apparent permittivity

of theoretical values. The probe was also tested on Samples 1, 2 and 8 (in a plastic tube

100mm diameter and 300mm long), providing a range of dispersive properties, the

results being included in Figure 5.18. The higher frequency apparent permittivity values

of these tests were found to correlate with the Topp and Wensink models, which are

similar at low water contents. Also, as can be seen from the inclusion of Sample 1 measured at a similar water content in the cell, the results of the cell and probe tests are comparable. Also, while increased water content resulted in reduction in the highest frequency at which the quarter-wavelengths could be identified, data were obtained with the probe, even in wet clay, over a useful range approaching 1GHz.

5.4.4 Comparison of QWA and TDR Data

As it was intended that QWA data be compatible with TDR data when testing with the probe, it was considered necessary to take measurements in soils exhibiting low dispersion, in which case HF QWA and TDR values should correlate. This was accomplished using Samples 1 and 2: in this case the fraction up to 2mm was used, to reduce dispersion (Figure 5.19).
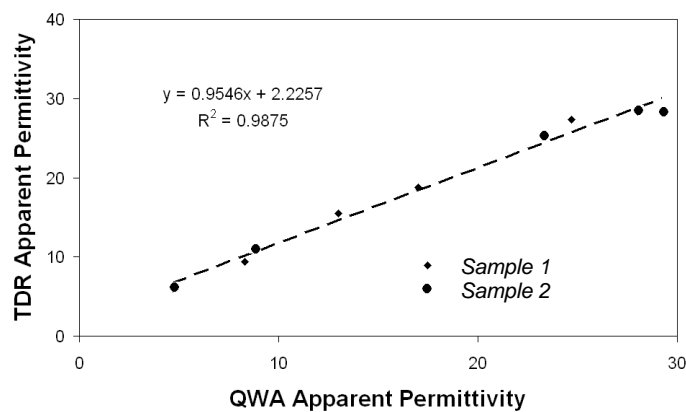
Figure 5.19. Comparison between apparent permittivity measured by QWA and TDR techniques for two soils exhibiting low dispersion.

The linear regression slope is almost unity, indicating that the two techniques provided comparable data. Some divergence was found at the highest values of apparent permittivity for the Weathered Mercia Mudstone, although this is considered to be within measurement tolerances and does not detract from consideration of the data to show significant compatibility of the QWA and TDR techniques.

5.4.5 Computer Modelling

In order to consider whether the probe could be modelled using the same methods used for the coaxial cell, the equations detailed in Section 4.7 were employed, the only difference being that the end termination was set to $1e99\Omega$ to approximate an open-circuited end. Results for air and distilled water are shown in Figure 5.20 and the measured data show quarter-wavelength resonances very similar to the model. The effects of multiple reflections in water can be seen to degrade the quarter-wavelength frequencies, and the rate at which the real S_{11} values decrease with frequency is significantly greater for measured, than for modelled, data which may indicate that electromagnetic signals are 'leaking' from the poorly contained transmission line.

However, as with the cell modelling, the probe modelling is intended only to illustrate that probe QWA works in the manner predicted by theory, rather than to obtain exact measurement values. Therefore, some further research on probe modelling is considered necessary before use of QWA probes with parameter matching models.
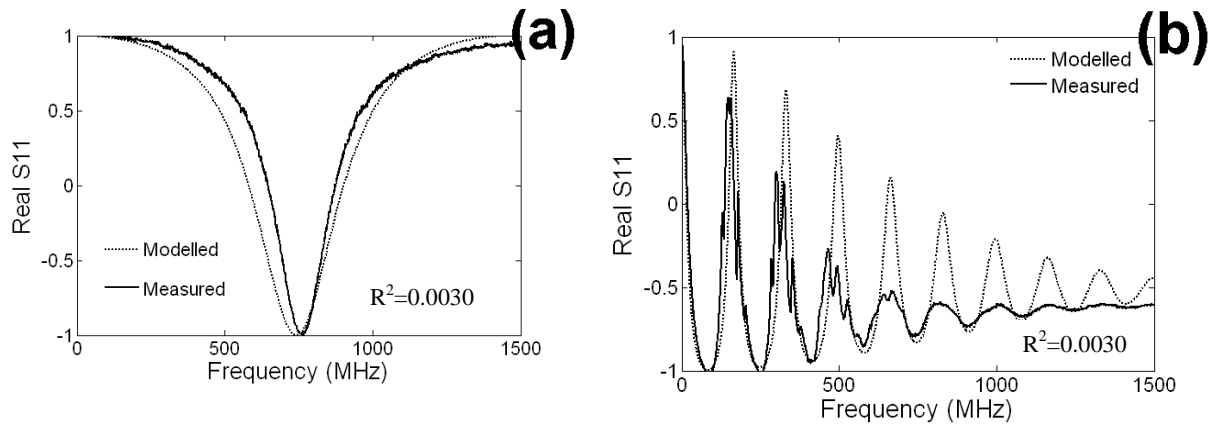
Figure 5.20. Comparison of modelled and measured probe real S_{11} values for (a) air and (b) distilled water used for calibrations.

5.4.6 Accuracy Considerations

Due to the similarities in lengths, the cell and probe potential inaccuracies are similar (Figure 5.21).
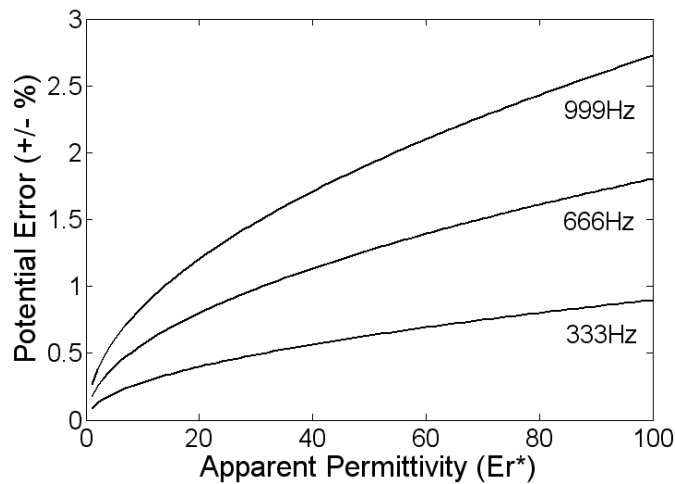
Figure 5.21. Potential QWA probe apparent permittivity errors for three different frequency measurement resolutions.

Calibrations with water (Figure 5.18) exhibited variations greater than expected from Figure 5.21, particularly at lower frequencies. It is apparent from 5.21 that this is due to the difficulty in discriminating between true quarter-wavelengths and the effects of multiple reflections, from which it can be implied that further research should focus either on improving the calibration methods or reducing energy loss from the probe.

Finally, the potential cut-off frequencies for the probe were estimated (Figure 5.22), although it should be noted that these are valid for a coaxial transmission line and so may not be fully representative of the probe. The cut-off frequencies are lower than for the cell, due to the spacing between outer conductors being larger than the inside diameter of the cell. For higher apparent permittivities, the cut-off frequency may be close to 1GHz, although this is not considered problematic as higher frequencies were not required of the QWA methodology.
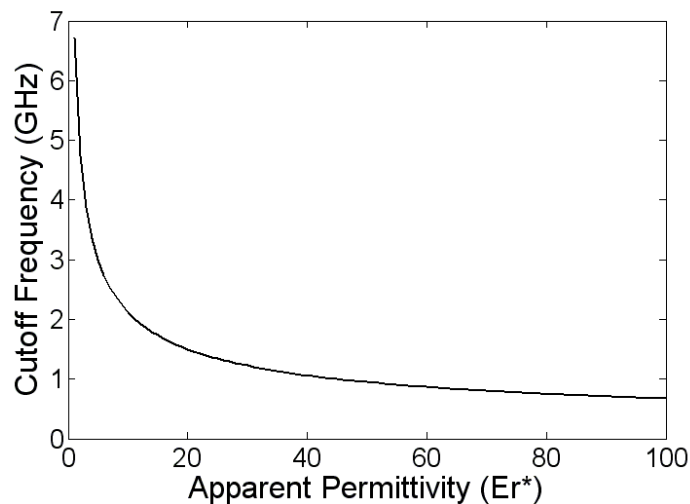
Figure 5.22. Approximate cut-off frequencies for the probe.

5.5 EFFECTS OF MAGNETICALLY SUSCEPTIBLE MATERIALS

5.5.1 Background

A study of a Victorian railway embankment at East Leake, in the British Midlands (for full details see Nelder et al., 2006), provided an opportunity to consider the potential effects of anthropogenic iron-bearing soils on apparent permittivity to water content relationships. The East Leake site (Figure 5.23), has been operated as a private railway line since the Great Central Railway was decommissioned in the 1960s and is being studied by the British Geological Survey, together with its partners, due to the possibility that it will be restored to full rail transport use in the future.
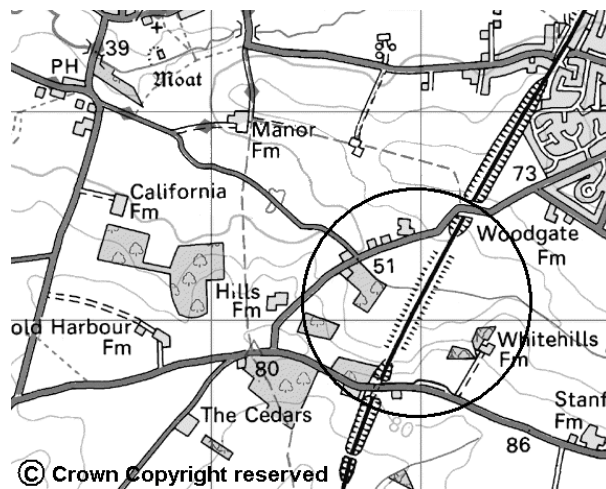
Figure 5.23. East Leake site location and surroundings (north up).

During laboratory testing it was found that surface soils included furnace ash and slag relatively rich in iron. During initial TDR tests it was found that these anthropogenic 'soils' have electromagnetic properties significantly different to the soils tested in Sections 5.2 and 5.3. Therefore, this study has the objective of considering the

potential effects of iron bearing soils on apparent permittivity, and to provide caution in considering the relationships found in other section of this chapter to be 'universal' under all circumstances.

5.5.2 Initial Tests

Soil samples from the site were first sieved to remove ballast and to leave only the sand, silt and clay fractions (i.e. ≤2mm in size). This was considered appropriate as no geotechnical tests were intended for this case study. These particles were found to form between 24% and 38% of the overall samples, by mass, for the locations tested, and so their electromagnetic properties were considered important. The soil was placed in the coaxial measurement cell in order to carry out simple TDR tests to show whether it conformed to a water content to apparent permittivity relationship described by the Topp et al. (1980) model. The resulting data (Figure 5.24) show a significant departure from the predicted data. On closer examination it was found that 75% of the soil particles, by dry mass, were attracted to a permanent magnet.
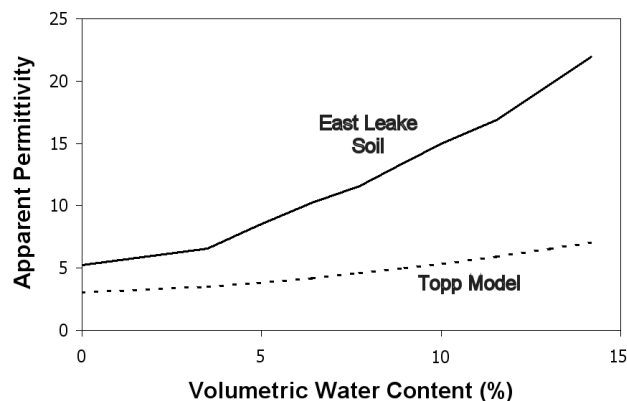
Figure 5.24. Initial TDR test results for the East Leake soil.

As magnetic susceptibility impacts on electromagnetic signal velocities, this was considered to be a potential source of the anomalous apparent permittivities. The relative magnetic permeability of the sample was therefore measured, by the British Geological Survey, at three densities using a Bartington Instruments (Oxford, UK) MS2 magnetic susceptibility meter with MS2B dual frequency sensor set to 4.65 kHz.

For dry densities of 1.10, 1.22 and 1.33 gcm^{-3}, the relative magnetic permeabilities were respectively 18, 51 and 82. This indicated that, even though the relative magnetic permeabilities would be expected to reduce with frequency, the magnetic properties could be significant enough to have an impact on TDR measurements.

5.5.3 Microscopy and Chemical Analysis

Due to the unusual nature of the soil, it was studied using a scanning electron microscope (SEM) and an example image is presented in Figure 5.25.
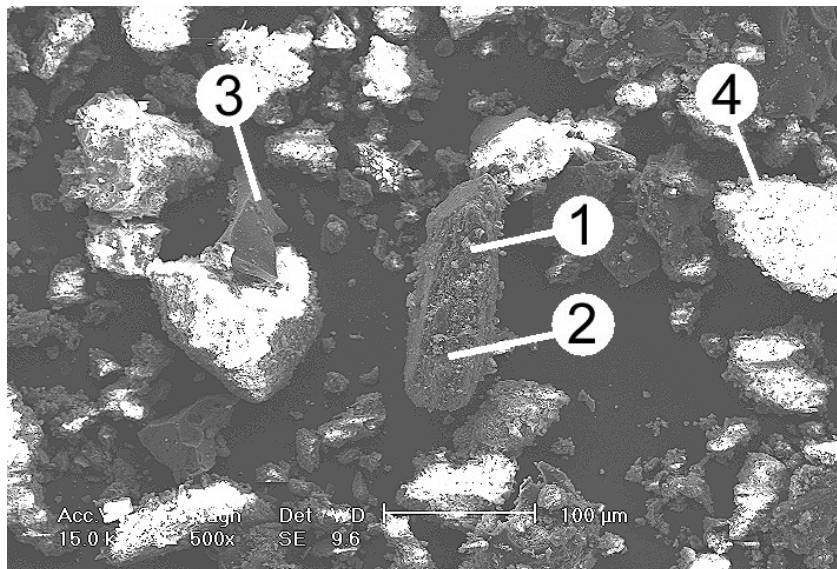
Figure 5.25. SEM image of East Leake soil particles.

The SEM image shows areas of high reflectivity, due to the presence of iron, and was used to provide an approximate chemical analysis (Figure 5.26: locations as shown on Figure 5.25). This provided some insight into the nature of the material and confirmed that it has a small, but significant, iron content. The soil particles largely comprise carbon, oxygen, silicon, aluminium and iron. It is known that furnace ash was used in the construction of the Great Central Railway and, therefore, it is assumed that the high carbon content is due to the presence of burnt fuel coal, contaminated with iron from the foundry from which the ash originated. It is not clear whether the silicon and oxygen represent foundry sand from the same origin as the ash, or whether the material was contaminated with other sands known to have been used in the upper surfaces of the embankment construction.
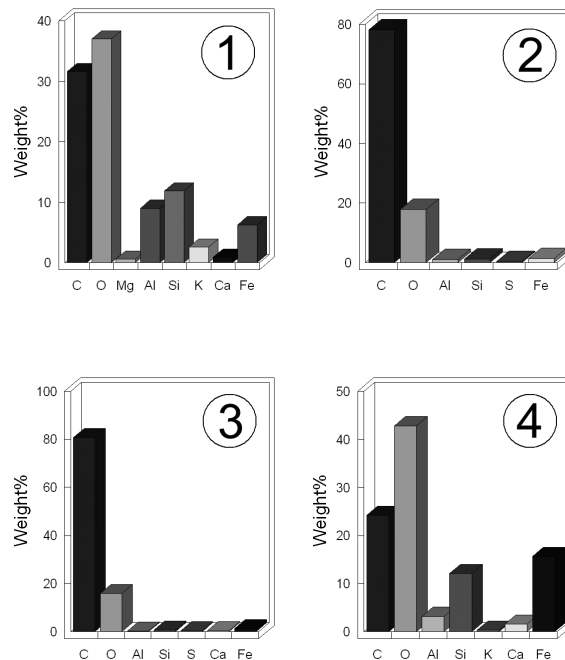
Figure 5.26. Surface analysis of East Leake soil particles.

5.5.4 Dry Mineral Permittivity

In order to understand the soil particle properties the apparent permittivity was measured in the cell using QWA with oven-dried samples. Small amounts of soil were weighed and, after placing them in the cell, were compacted using the brass rod marked with engraved rings at 5mm intervals. This allowed consistent masses of soil to be placed in the same length of cell, thus ensuring relatively uniform density. By using different masses of soil per 5mm length, and trial and error to determine the maximum density achievable, a number of different dry densities were achieved.

By taking measurements over a wide frequency range at each density Figure 5.27 was produced. This indicates that significant electromagnetic dispersion occurs at lower frequencies due to relaxation mechanisms associated with the magnetic properties (tests having indicated that the dry material exhibited negligible electrical conductivity).
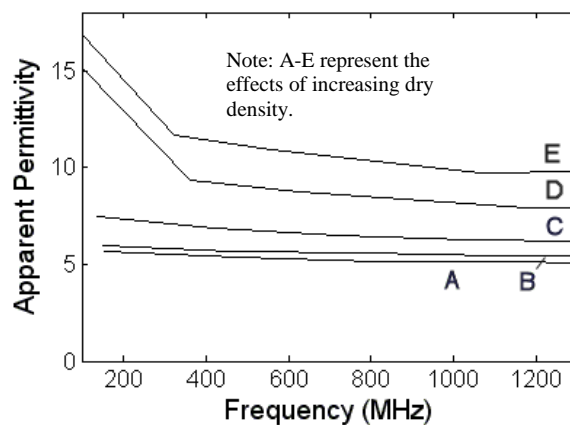
Figure 5.27. Apparent permittivity variations with density and frequency in the East Leake soil.

A further outcome was variation in the apparent permittivity with increasing dry density out of proportion to the change in mass of dry minerals present. This is a known property of materials exhibiting magnetic effects, (Thompson, 1986). The data of Figure 5.27 have not had curve fits applied, so electromagnetic dispersion between the data points should not be considered to be linear. The variations with dry density are illustrated in Figure 5.28 for the more stable apparent permittivities above 600MHz, corresponding to lines A to E in Figure 5.28, together with an example of the more usual linear relationship for a sample of dry clay solids. Two factors may cause this effect, alone or in combination: firstly the increase in density may allow iron bearing particles to come into more intimate contact. Secondly, the particles may be able to realign during compaction to create an increased magnetic susceptibility, the higher dry densities requiring greater compactive effort. However, while the exact nature of variations in apparent permittivity at different dry densities has not been determined, both mechanisms could be considered possible under field conditions at the East Leake site, and so provide an insight into potential geophysical property variations there.
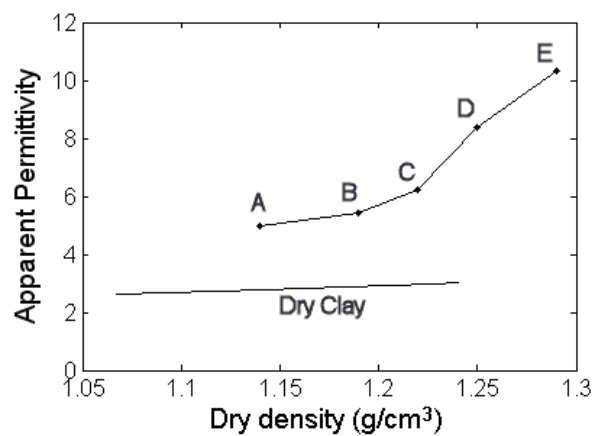
Figure 5.28. Variations due to dry density for the East Leake soil.

5.5.5 Effect of Water Content

Laboratory QWA testing was undertaken on the soil compacted to a dry density of 1.3g/cm^3, at a number of water contents achieved by adding water to the end of the cell (Figure 5.29) and, after fitting the end plate, allowing it to permeate through the sample for at least 24 hours. As illustrated in Figure 5.30, at high water contents the soil showed significantly elevated apparent permittivity values. This is exemplified by the values for saturated Sample 8 which, despite having almost double the volumetric water content (VMC) of the wettest East Leake sample (70.4%, compared to 37.1% by volume), exhibits a much lower apparent permittivity.

The conductivity of the material, in dry and saturated states, was estimated by placing the soil between two parallel metal plates and measuring the resistance using a Hewlett Packard low frequency impedance analyser as described in Chapter 3.
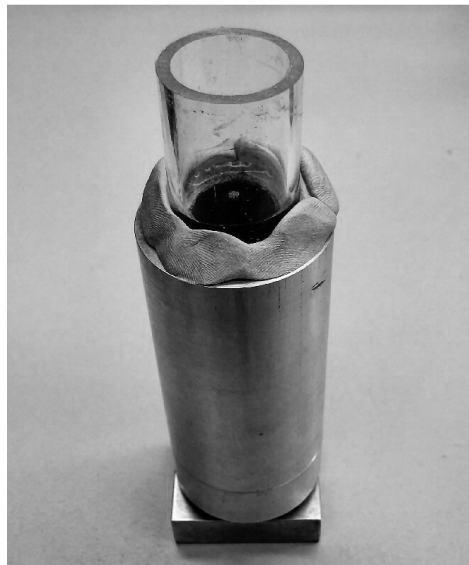
Figure 5.29. Adding water to the East Leake soil samples.

The conductivity of the dry soil was negligible (i.e. so low that the analyser was only able to report 0 S/m). When saturated, the conductivity increased to approximately 49 mS/m, which would contribute to the low frequency variations in apparent permittivity found in Figure 5.30. It was therefore deduced that the soil could exhibit lower than expected signal velocities in geophysical surveys and that this effect could be highly variable with water content and compacted densities. In terms of TDR, these effects could be expected to cause the unusual apparent permittivity to water content relationships originally found for this material.
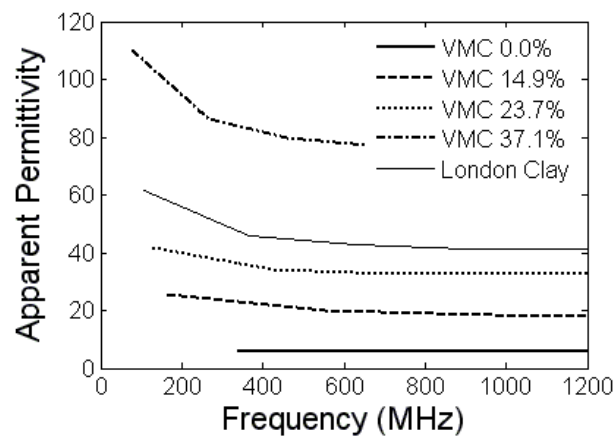
Figure 5.30. Apparent permittivity variations with water content for the East Leake soil.

CHAPTER 6 – DISCUSSION

6.1 OVERVIEW

It was seen in previous chapters that undertaking signal velocity measurements using the apparent permittivity can potentially be applied to use in a geotechnical testing environment, and utilise relationships found between geotechnical and electromagnetic soil properties. Therefore, this discussion is formed of the following sections:

6.2 Extending TDR data into the frequency domain: This section will discuss QWA and TDR as means of measuring electromagnetic signal velocities in fine-grained soils, and the extent to which they provide complementary information. The compatibility of coaxial cell and probe measurements, using QWA, will also be considered.

6.3 Accuracy considerations: Having briefly considered the accuracy of QWA in Chapter 4, this section will further discuss that accuracy together with the potential accuracy of TDR measurements.

6.4 Linking geotechnical and electromagnetic properties: This section will briefly discuss the links found between soil geotechnical and geophysical properties. Discussion of the cause of electromagnetic dispersion, based on swell/shrink properties, will also be advanced in this section.

6.5 The role of the pore water: This section will extend on the studies presented in Chapter 5, and the discussions of Section 6.4, to discuss whether

relationships between soil geotechnical and geophysical properties are due to the properties of the pore water phases.

6.6 Water content measurement using TDR and QWA: This section will discuss TDR measurement of soil water content and how complementary use of QWA could improve TDR water content measurements in fine-grained soils.

6.7 Relevance to Engineering: Potential engineering uses of the research will be discussed.

6.2 EXTENDING TDR DATA INTO THE FREQUENCY DOMAIN

An important aspect in understanding the value of any research lies in the reason for its conception. In the case of the work described herein, it evolved from tests undertaken very early in the research using a Tektronix 1503C TDR cable tester, with simple probes and a coaxial cell manufactured largely using copper and brass plumbing parts (Figure 6.1).
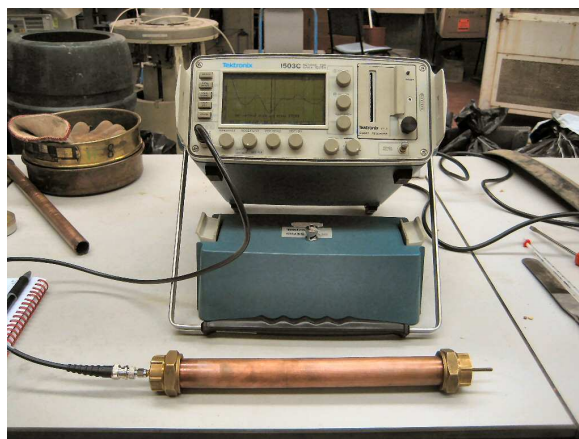
Figure 6.1. Early testing using a Tektronix 1503C TDR cable tester.

The 1503C is identical in functionality to the Tektronix 1502 cable testers, cited as the most widely used TDR soil research tool (Robinson et al., 2003a). Unfortunately, as it has been a discontinued model for many years, it was not possible to obtain a computer interface for the 1503C, and so it was not subsequently used in this thesis (being replaced by a Campbell Scientific TDR100). However, it provided a very useful introduction to measuring soil electromagnetic properties and brought forward a number of important questions. Most notably, what are the frequencies of the single values of apparent permittivity obtained, and to what extent will the apparent permittivity vary for other electromagnetic signal frequencies in electromagnetically dispersive soils?

For instance, in non-dispersive soils TDR probes and cells can be simply modelled using their characteristic impedance, which is easily calculated from a single value of permittivity (Todoroff and Lan-Sun-Luk, 2001). However, for a dispersive soil, the characteristic impedance will vary in proportion to the permittivity and hence frequency. Furthermore, the measurement frequency of TDR may vary with permittivity and water content (Robinson et al., 2005; Friel and Or, 1999). Therefore, a greater understanding of electromagnetic dispersion effects can be considered essential to adequate modelling and interpretation of TDR data (which could potentially be obtained using QWA). Additionally, TDR provides an integration of real and imaginary permittivities, including the associated loss tangent and the effects of electromagnetic dispersion (Cosenza and Tabbagh, 2004). Therefore, for higher frequencies where the extended Debye model (Debye, 1929; Hasted, 1973) would predict small loss tangents, is there a less complex relationship between water content

and apparent permittivity that is masked by the additional complexities inherent in the TDR data integration?

The research described in previous chapters can therefore be summarised as attempting to extend, rather than replace, the data outputs from TDR to include frequency domain variations typical of dispersive soils. This was not a decision taken arbitrarily, but rather because a very significant portion of the literature on soil electromagnetic measurements has been undertaken using TDR. It is apparent that this popularity is due, at least in part, to the simplicity of using only start- and end-reflection points, which masks the cross-disciplinary complexities that would otherwise occur when attempting to combine more sophisticated electromagnetic measurements with geotechnical research.

A further factor of note is that the work of Topp et al. (1980) allowed use of commercial cable testers for soil TDR measurements, allowing time-domain electromagnetic measurements without the complexity, and cost, associated with previous use of separate pulse generators and high-speed oscilloscopes. From a geotechnical perspective this is important, as it allows for widespread use of TDR for quality control, such as in measuring soil compaction (Runkles et al., 2006). From a more general soil monitoring perspective, it is also important as the work of Topp et al. (1980) showed that a general, and initially controversial (Topp et al., 2003), relationship exists between volumetric water content and TDR apparent permittivity for a wide range of soils (the Topp Model: Topp et al., 1980). Therefore, for scenarios where soils exhibit only very limited electromagnetic dispersion, a single value of apparent permittivity, and unknown frequency, obviously poses little difficulty.

However, for dispersive soils, if their properties are to be compared on a like-for-like basis it is obviously equally important that variations due to frequency must be accounted for. Determining this frequency is difficult, as it requires a full understanding of the frequency-spectrum of the TDR pulse (including the relative amplitudes of each frequency component), knowledge of the characteristic impedance of the probe or cell (which can be expected to vary with frequency in an electromagnetically dispersive soil), and the frequency-dependent attenuation coefficient of the soil. Robinson et al. (2005) considered that for a Tektronix 1502 TDR system, with well constructed probes, signal frequency components up to 1.75GHz could exist, but that for poorly constructed probes the maximum frequency may reduce to below 1GHz. In a lossy, electromagnetically dispersive, material each individual frequency associated with the TDR pulse will be associated with different signal velocities (Robinson et al., 2003a).

As for such soils the higher frequencies will be expected to have higher velocities, it is to be expected that the end reflection point will be biased toward those frequencies, as lower frequency reflections will arrive at slightly later times. However, a bias toward higher frequency components at the end reflection point means that the measurement frequency can be expected to reduce as attenuation increases. In addition, the spreading out of the signal frequencies in time causes a deformation of the shape of the TDR pulse (Robinson et al., 2005), which then influences the shape of the TDR trace at the end reflection point. Under such circumstances, the measurement frequency has been found to reduce to below 500MHz (Friel and Or, 1999), due to the loss of higher frequency signal components due to attenuation. This was found also to be the

case in this study, through comparing the measured TDR values for all saturated samples to the fitted curves for QWA data (Figure 6.2).
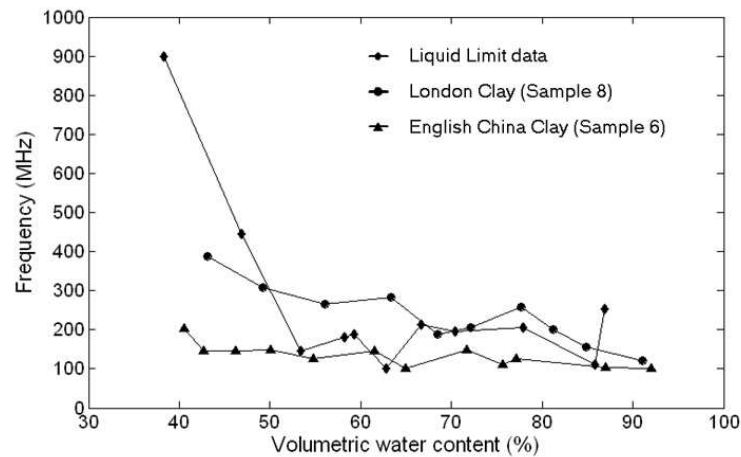
Figure 6.2. Approximate frequencies where TDR data coincide with QWA curves.

While even for the saturated state the QWA data measurement tolerance will not allow certain determination of the TDR measurement frequency (especially for the low-dispersion samples associated with low Liquid Limits), it is apparent from Figure 6.2 that the TDR data are generally associated with frequencies below 500MHz in saturated fine-grained soils. These low frequencies can be associated with significant electromagnetic dispersion (Wensink, 1993) and so it is apparent that the TDR data integration described by Cosenza and Tabbagh (2004) will cause additional complexity in interpreting TDR data due to the effects of the loss tangent as well as that of the real permittivity. For the two very low Liquid Limit samples the intersection frequency was found to be higher. However, these soils exhibit limited electromagnetic dispersion and

so, in combination with the measurement tolerances of both the TDR and QWA measurements, it is not possible to conclude their exact frequencies with any significant degree of certainty.

However, while TDR measurements will generally relate to a sub-500MHz frequency band, they do not provide frequency-domain data. Inversions of time-domain TDR traces to the frequency-domain have been undertaken, but are complicated. Additionally, they are dependent on the underlying electromagnetic modelling of the probe, cables and TDR equipment used, which may often change. Verification of such inverted data, and other novel attempts to gain measurement-frequency data from the time-domain (e.g. Robinson et al., 2005), is difficult if comparison cannot be made to VNA data directly measured in the frequency domain, utilising the same cell or probe used for the time-domain measurements. QWA could allow such verification and could, therefore, be used to calibrate inverted data and thus provide increased confidence in the inversion methodology. Furthermore, it offers a means of validating attempts to gain continuous data (i.e. data at all measured frequencies) from TDR probes using VNAs, as well as providing a basis to obtain such data through parameter matching with dispersion models (e.g. Jones and Or, 2004; Logsdon, 2005a). However, use of TDR traces to provide frequency-domain data for use with QWA is considered outside of the scope of this study due to it being counter to the goal of a simple and robust system, but an opportunity for future exploration.

Even without determining the TDR measurement frequency, it is possible to make some comparison between its data and that of QWA because attenuation can be expected to increase with water content (Doolittle and Collins, 1995). Therefore the higher frequency components will be gradually eroded as the attenuation increases

(Robinson et al., 2003a), from which it could be expected that the TDR derived data will correspond to those of higher frequency QWA for low apparent permittivities, with increasing divergence as the apparent permittivity increases. To investigate this, these two data sets have been compared as shown in Figure 6.3. It was found that the TDR and QWA data did start close to the line of equality, and diverged as expected with rising apparent permittivity. For the higher apparent permittivities there is also suggestion in Figure 6.3 that the TDR and QWA data may begin to approach equality. As was shown in Section 5.2, above a point close to the Plastic Limit, where the dry density is at a maximum, the magnitude of dispersion (and hence potentially of the loss tangent) reduces. As the amount of 'bound' water is related to the surface area (Cosenza and Tabbagh, 2004), which is decreasing with increasing higher apparent permittivity, it could be expected that the loss tangent contribution to the TDR measurement will reduce. Therefore, for very high or low apparent permittivities (and hence water contents) it could be expected that QWA and TDR data will correlate, but at intermediate values the two data sets would diverge due to elevated loss tangents, with maximum divergence expected close to the Plastic Limit.

This relationship between the HF QWA and TDR data can also be seen in the volumetric water content domain in Figure 6.4. For the HF QWA (Figure 6.4(a)) data it can be seen that there is only minor variation between Samples 6 and 8 over all water contents. This could be expected due to their Plastic and Liquid Limits being close in value, from which it could be deduced that their specific surface areas are similar. For the plastic range, between approximately 40% and 70% water by volume, it is apparent that there are close similarities in trends for the two soils tested over wide water contents, and for the other soil samples tested at the Liquid Limit. However, for the

TDR data (Figure 6.4(b)) there is much less correlation between the three data sets and, for use in geotechnical testing, it is of particular note that the apparent permittivity values for the plastic state were found to vary between samples by up to five units.
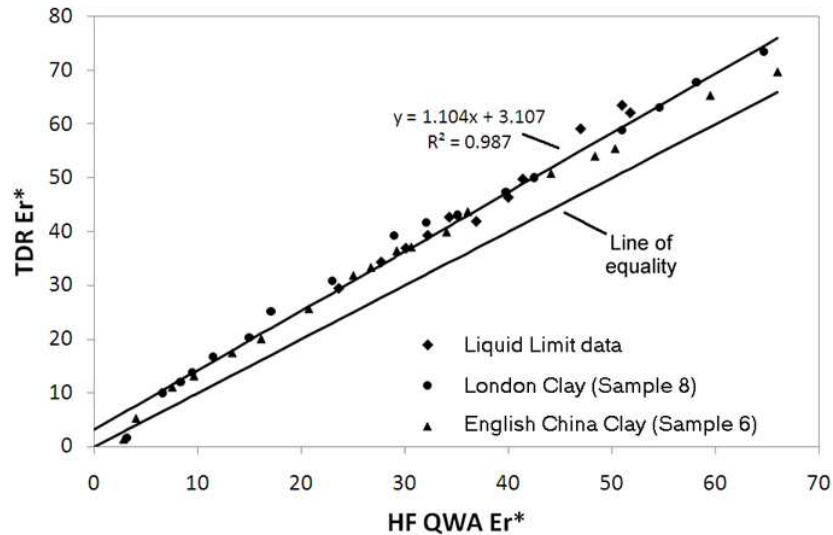
Figure 6.3. Comparison of QWA and TDR apparent permittivity.

Therefore, as the TDR measurement frequency is expected to be low in wet soils, as previously described the resulting apparent permittivity can be expected to be associated with greater loss tangents than the HF QWA data. As both the real part of the permittivity and the loss tangent impact on signal velocity, the loss tangent forms an additional variable that must be contended with in relating water content to apparent permittivity. For the HF QWA data dispersion is much reduced and so, according to the Debye model, loss tangents can be expected to provide much smaller contributions to the signal velocity. In this respect, the HF QWA data could be expected to be much closer to the values of real permittivity due to those reduced loss tangents.

205
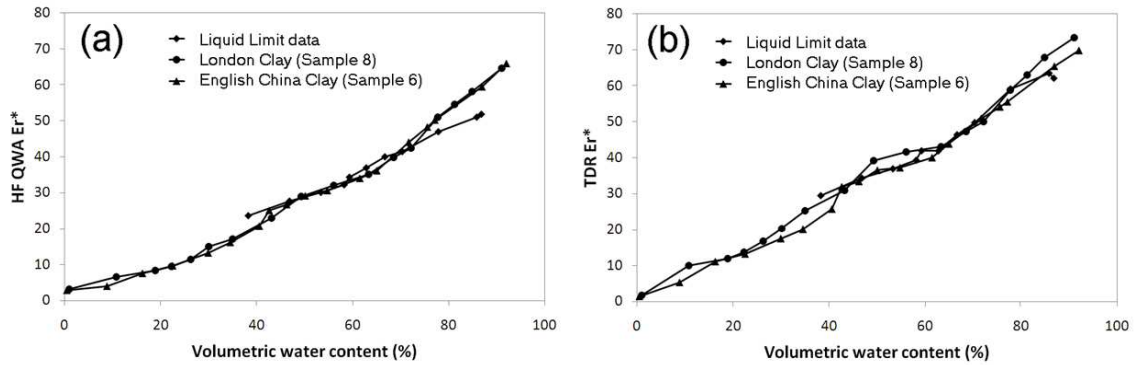
Figure 6.4. Relationships between volumetric water content and (a) HF QWA, and (b) TDR data.

As the loss tangent is closely related to the magnitude of dispersion, it would therefore be expected that more dispersive soils will fall further from the 1:1 line than less dispersive soils. On this basis, it could be argued that it would not be possible to provide a TDR mixing model, based solely on start and end reflection distances, that provide accurate water content estimation for all dispersive soils. However, for the HF QWA data, which are much less affected by variations due to loss tangents, it could be argued that the closer relationships between soils in Figure 6.4 provides an opportunity for improved water content monitoring in fine-grained soils.

It should additionally be noted that Chapter 5 showed that it is possible for QWA apparent permittivity to reduce at single frequencies with increasing water content, between the Plastic and Liquid Limits. This was considered due to the interplay between the magnitude of the dispersion, the increasing high-frequency permittivity, and reduction in soil surface area. Such a reduction was not noted in the TDR data, although this was not necessarily expected as the TDR data cannot be considered to be at a fixed frequency (Friel and Or, 1999) as shown in Figure 6.2 (slight reductions in

frequency causing increases in apparent permittivity). However, the TDR data of Figure 6.4(b) do show a significant levelling of the apparent permittivity to water content relationship for the two soils tested, within the plastic state. For the London Clay in particular, that relationship becomes almost level and, for a more dispersive soil, it may be possible that a reducing relationship will occur, which is considered a useful subject for future research. However, given that TDR will suffer significant increases in apparent permittivity with small reductions in frequency, for such a highly dispersive soil, it is perhaps more likely that another single frequency measurement system would be required to confirm the existence of this effect.

Finally, in terms of direct application of QWA for soils research, it should be noted that use of a coaxial cell limits potential measurement scenarios. For this reason, one objective was to investigate potential for developing QWA for use with TDR probes and, in Chapter 5, it was shown to be possible. In order to fully exploit this potential it will be necessary to consider how well data from undisturbed samples relate to those disturbed during testing with the coaxial cell, which is largely outside the scope of this research. However, for sample 8 (a London Clay), this can be illustrated as the soil was obtained in a fresh state from excavation and so a relatively undisturbed block of soil was available (approximately 230 x 130 x 90mm). Density and gravimetric water content measurements undertaken on this sample, together with QWA measurements using the three pin probe, allow comparison to the nearest water content QWA measurement undertaken in the coaxial cell. For these three pin probe and cell measurements respectively, the volumetric water contents were 49.6% and 48.6%, and the dry densities were $1.31g.cm^{-3}$ and $1.38g.cm^{-3}$. As shown in Figure 6.5, the undisturbed and disturbed samples show close correlation.
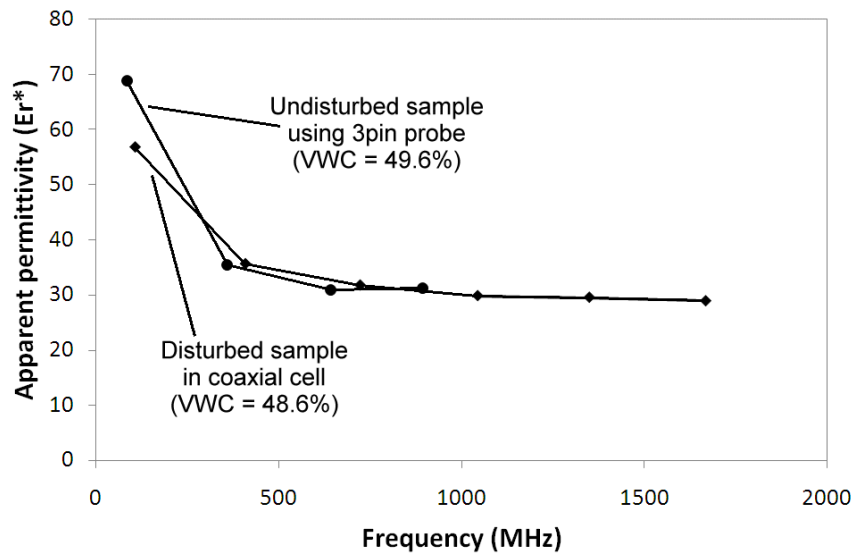
Figure 6.5. Comparison between QWA measurements on Sample 8 for the soil in an undisturbed state, using the 3pin probe, and disturbed in the coaxial cell.

At lower frequencies the difference between the probe and cell data is greater, which can largely be explained by the difference of 22MHz in quarter-wavelength frequency between the first points of each measurement, caused by the difference in length between the probe and cell. These data can be taken to indicate that probe and cell measurements can correlate well and that measurements in the coaxial cell can be considered representative of plastic field states, subject to further research. It also validates the hypothesis that probes and cells should be equally applicable for frequency-domain measurements, as is the case for time-domain measurements in Figure 6.6.

As Figure 6.6 shows, there is little significant difference between the two TDR traces, the vertical offsets within the cell and probe being a function of coaxial geometry and the slight difference in end reflection distances being due to the

differences in sample length. After the end reflections, the two traces diverge due to differences in reflection phase between open and short circuit terminations.
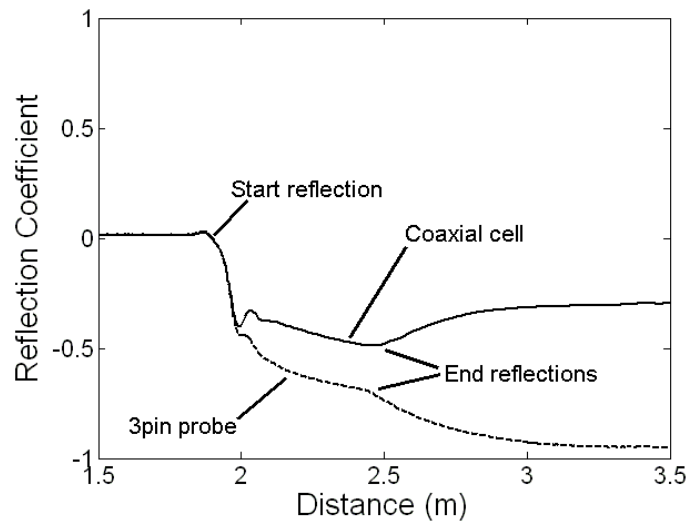
Figure 6.6. Comparison of TDR waveforms for the undisturbed (3pin probe) and disturbed (coaxial cell) measurements on Sample 8.

The most significant difference between the two TDR traces is that the probe exhibits greater attenuation due to its longer length, which also makes the end reflection less distinct (Robinson et al., 2003a) in comparison to the coaxial cell. Similarly (Figure 6.7), there is significant similarity between the real S11 values for the corresponding QWA measurements. The most distinct difference is the inverted nature of the graph for the coaxial cell in Figure 6.7(b), which has a short circuited termination, compared to the probe in Figure 6.7(a). The low frequency impedance measured by QWA can additionally be seen to have some correlation to that of the TDR traces of Figure 6.6 (in TDR exhibited by the steady reflection coefficient

following the end reflection). For QWA the relevant reflection coefficients were -0.25 and -1.00 for the probe and cell respectively, with corresponding values for TDR of - 0.30 and -0.95. The low frequency impedance can be used to estimate soil conductivity in TDR (Topp et al., 1988), and so a similar possibility should also exist for QWA. However, this potential was not progressed as the measurement bridge for the VNA was only stated to provide accurate reflection measurement above 10MHz.
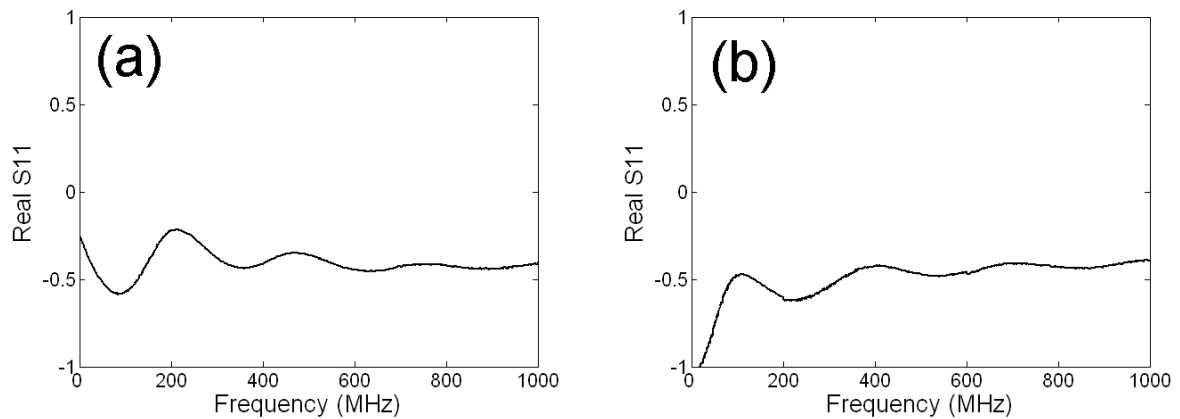
Figure 6.7. Comparison of real S_{11} values for the (a) undisturbed (3pin probe) and (b) disturbed (coaxial cell) QWA measurements on Sample 8.

6.3 ACCURACY CONSIDERATIONS

The accuracy of QWA measurement can be expected to be variable as discussed in Section 4.8 although, for the apparent permittivity values associated with even wet clays, usable levels of accuracy were achieved. Cell and probe accuracies during development were considered to be approximately two units of apparent permittivity for water, with reduced error for lower apparent permittivity. However, this level of

accuracy is a baseline: where quarter-wavelength frequencies are obtained within signals of low signal to noise ratio larger errors could result. Therefore, it is considered appropriate to compare the measurement of TDR data to QWA, including how the accuracies associated with them compare. The start reflection associated with TDR (Figure 6.8(a)) is usually signified by a 'bump' in the data due to impedance mismatch between the cable and probe/cell head: in this case the very small change in reflection coefficient indicates a similarly small impedance mismatch. The impedance mismatch at the end of the cell/probe is then determined by constructing tangent lines at the end reflection point (Figure 6.8(b)). However, determining time-zero for calculation of signal travel times is not simple in electromagnetic measurements, including GPR data (Yelf, 2004).
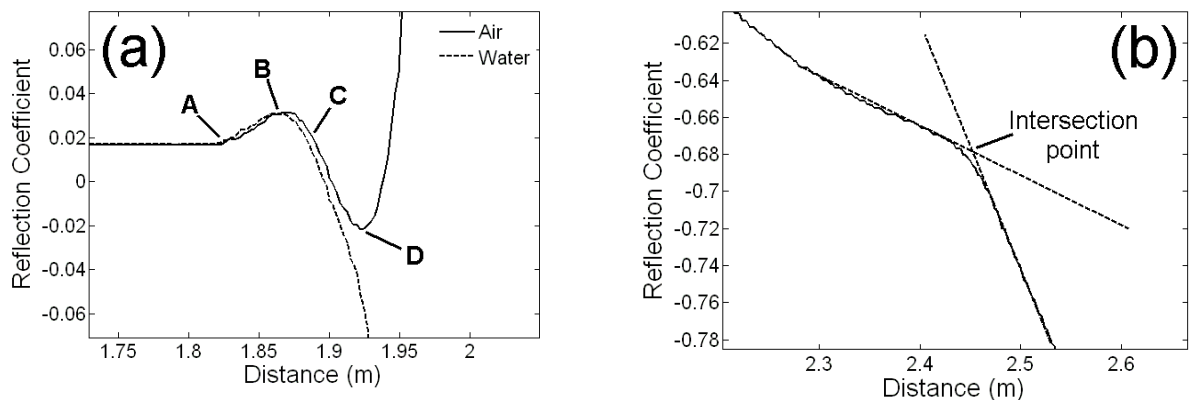
Figure 6.8. TDR (a) start and (b) end reflection points (Sample 5 at Liquid Limit in coaxial cell).

In general TDR use, point B in Figure 6.8(a) is often used for measurement of the start reflection distance (Topp et al., 1980). However, as described by Robinson et

al. (2003a), even though a readily identifiable feature the centre of the bump is not necessarily the distance to the start of the interface between the probe/cell head and the soil. Therefore, other potential locations must be considered and their accuracy evaluated. The start points considered by Robinson et al. (2005) included points A and C (Figure 6.8(a)), and for this study point D was added as there is an obvious change in the reflection coefficient. If the wrong start point is used then there will obviously be an impact on the accuracy of the TDR measurement. Therefore, each of the four start points can be used with the physical length of the measurement cell to determine the apparent permittivity of air, water and Samples 1 to 11 at the Liquid Limit (to provide a wide range of end reflection distances), as shown in Figure 6.9(a). It is apparent that the choice of start point could cause significant variations in the resulting TDR measurements, up to at least ten units of apparent permittivity for water, due to the measurement distance encompassing either part of the probe head, or less than the total length of the sample.
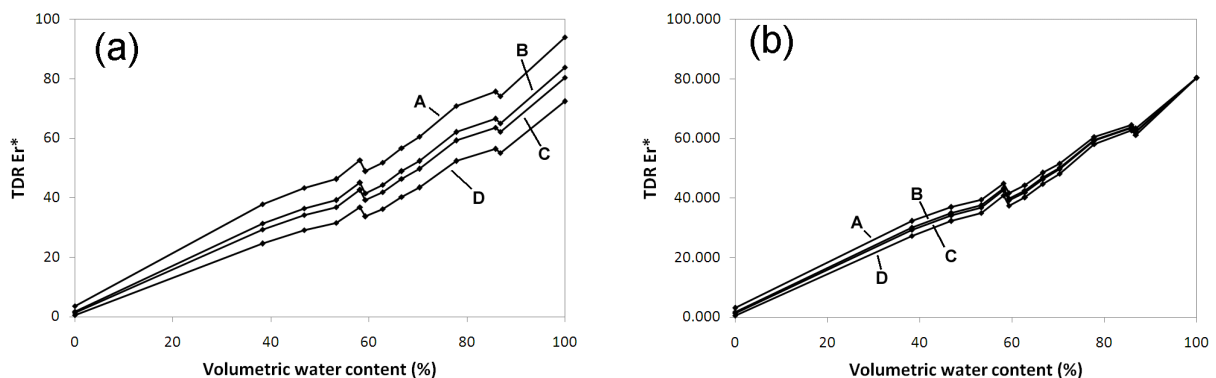
Figure 6.9. Variations in TDR apparent permittivity with volumetric water content due to start reflection position (a) using physical cell length and (b) after adjustment of probe lengths based on water end reflection position (air, water and Liquid Limit samples).

212

However, an important feature of TDR is that it allows for use of an apparent probe/cell length. Therefore, the data were adjusted such that they used an apparent probe length giving an apparent permittivity for distilled water of 80. The results of this exercise (Figure 6.9(b)) show variations much reduced from those of Figure 6.9(a). So, while there are still variations between apparent permittivities for each start point, the similarities illustrate the robustness of TDR with an apparent length within a few percent of the true physical length. Robinson et al. (2003a) considered that the true start point was slightly to the right of the impedance mismatch 'bump', close to point C (see Figure 6.8(a)): the location chosen for this study. As shown in Figure 6.10(a) the range of apparent probe lengths varied considerably in this exercise, between approximately 8% longer, and 5% shorter, than the true physical length. In addition (Figure 6.10(b)), each of the start points gave different values for air, the closest to the true value being point C.
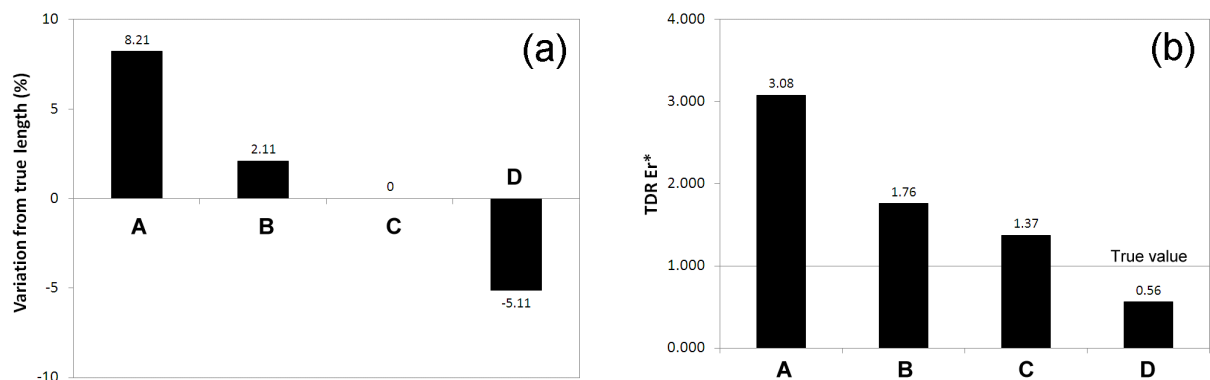
Figure 6.10. Cell (a) apparent length variations from the true physical length, and (b) calculated air apparent permittivity, for each start reflection point.

For QWA there is no need to determine the start reflection point, but it is necessary to determine the phase change between the calibration plane and the start of the sample, which is comparable. In its simplest sense, this involves physically measuring the difference in length with a digital calliper. In practice it is necessary to make very small adjustments to the length to compensate for measurement errors, and make use of an apparent length in order to provide acceptable values of apparent permittivity for air and water calibrations. Therefore, for both QWA and TDR there are similar difficulties involved in the setting up and calibration.

A further important aspect of TDR, in comparison to QWA, is that the effects of the cable are not generally removed during calibration. For both TDR and QWA, as long as the physical dimensions of the cell or probe do not vary, the calibration associated with them should remain valid. However, this is not necessarily so for the cable, which may be influenced by changes in length (e.g. if stretched), changes in the permittivity of the annulus material due to temperature, and kinking of the cable. For QWA, these effects are removed during calibration for each measurement. For TDR they are not and so it is possible that the start point may vary. For this reason, measurements were undertaken in a room with a relatively stable temperature and the same cable was used for all TDR testing. There was very little variation in the position of the start point over approximately a year of testing (Figure 6.11): approximately ±2.5mm deviation from the average correlating to a potential apparent permittivity tolerance of ±0.05 for air and ±0.5 for distilled water.

Therefore, cable effects were small for TDR measurements under controlled conditions, although under field conditions more significant variations should be expected (Robinson et al., 2003b).
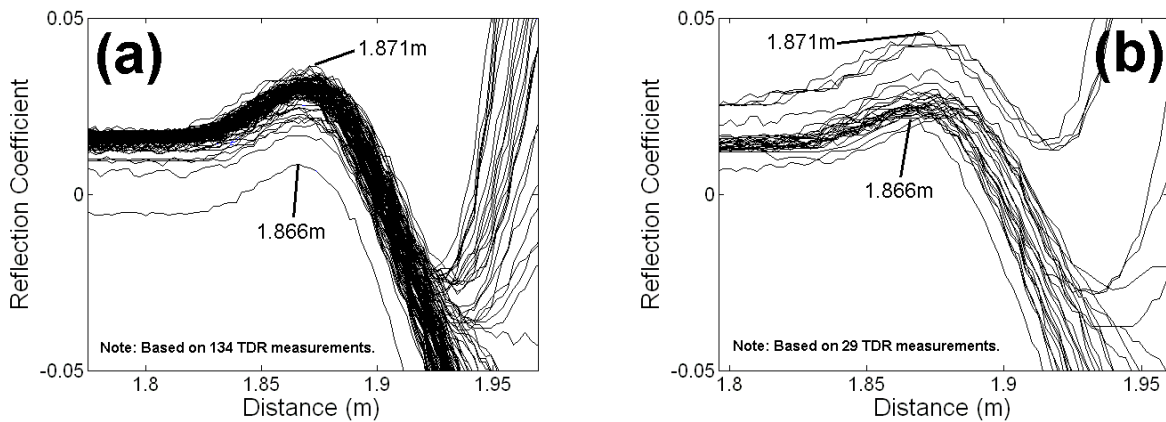
Figure 6.11. Variations in the start reflection distance over one year for (a) the coaxial measurement cell and (b) the three pin probe.

Having a constant start point, and with no change to the physical length of a TDR cell or probe, the end reflection distance should also be invariant for a constant apparent permittivity. However, this neglects the difficulties inherent in constructing tangents (Figure 6.12): there is no true curve or line after the end reflection so the construction of a tangent is somewhat subjective. Furthermore, noise in the data gives rise to difficulties in determining the vertical offset of tangent lines that leads to potential variability in the determination of the tangent line intersection points.

In order to investigate the effects of this 'fuzziness' in the end reflection, a number of measurements were undertaken for air and water in the coaxial cell, each having individually constructed tangent lines. This allowed the measurement differences from the true end point to be determined as a percentage, as shown in Figure 6.13. For air (Figure 6.13(a)), it was found that the trace was relatively free of

noise and that confidence in the apparent permittivity being within ±0.2 was approximately 100%.
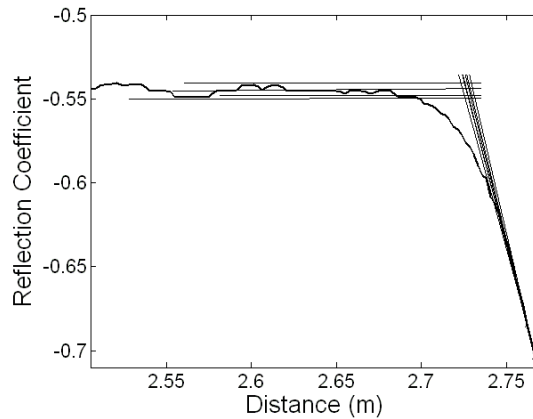
Figure 6.12. Potential variations in TDR end reflection tangent construction for water due to noise and human error.

However, for water (Figure 6.13(b)) it was found that for a confidence level of 90% the apparent permittivity tolerance would be ±1.2. It has been said that it should be possible for TDR to be used to obtain measurements within 0.1 units of apparent permittivity under controlled conditions (Robinson et al., 2003a). However, for this study, it was considered that a tolerance within ±2 units of apparent permittivity would potentially be more appropriate.

In order to fully consider the tolerances associated with QWA measurements air and water tests were used to determine the percentage that fell into a range of tolerances from the true values. From Figure 6.14(a) air measurement tolerances of ±0.6 for 90% of measurements are expected, and the maximum tolerance was found to be ±0.7. For water (Figure 6.14(b)), where quarter-wavelengths are more closely spaced, it was found that 90% of measurements should fall within ±2.5 units of

apparent permittivity, but with a confidence level of approximately 95% that the tolerance would be ±3.5. For intermediate apparent permittivities, measurement tolerances can be expected to be between the values for air and water.
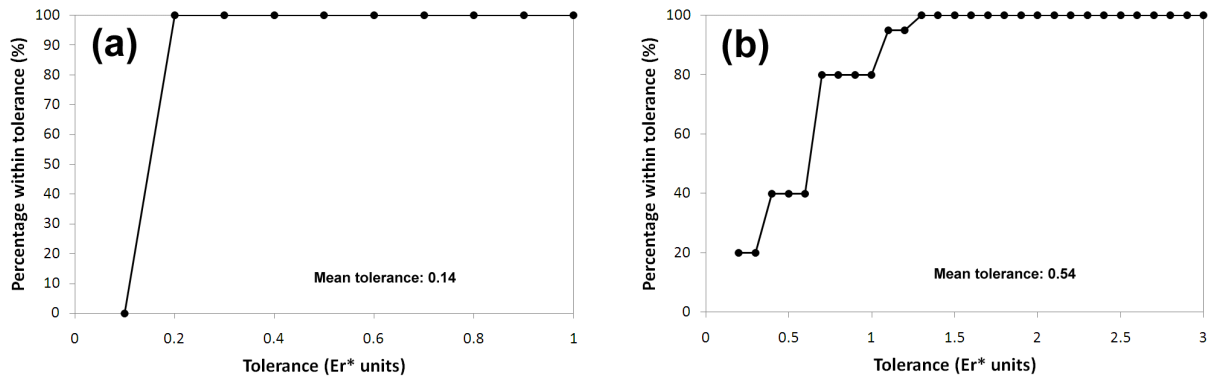
Figure 6.13. TDR end reflection distance tolerances for the coaxial cell: (a) air for 20 measurements and (b) water for 20 measurements.
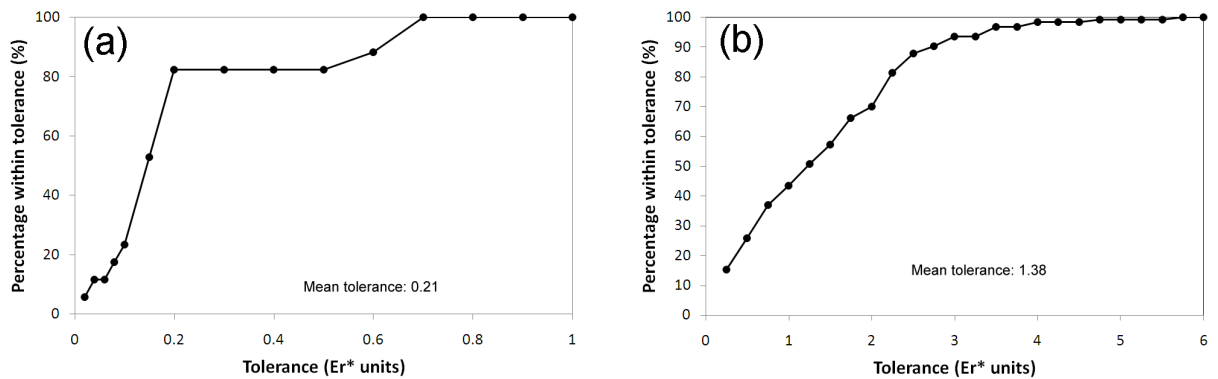
Figure 6.14. Measurement tolerances for the coaxial cell: (a) air for 17 measurements and (b) water for 124 measurements.

A potential factor that must be considered is whether the VNA causes any errors in apparent permittivity measurement due to temperature, as this can be introduced by signals (Reynolds, 1997; Knott, 2005). Testing over a 2GHz range required less than twenty minutes to undertake. However, of that time only approximately five minutes (in ten 30 second periods) required connection of the cell to the VNA, the remainder of the time being required for calibration. Therefore, it was considered that heating would not be significant. To test this, the coaxial cell was filled with distilled water and connected to the VNA for a period of fifty minutes, the temperature being recorded at two minute intervals (Figure 6.15(a)).
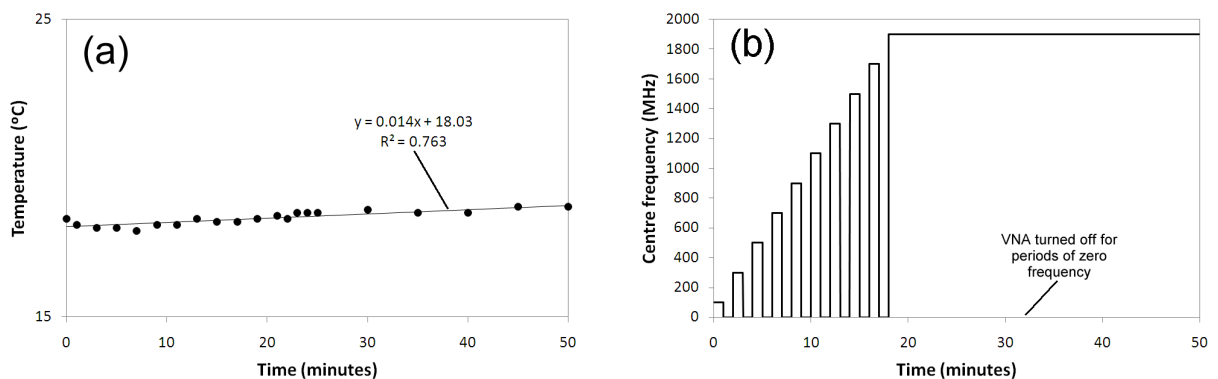
Figure 6.15. **Distilled water in the coaxial cell: (a) temperatures over fifty minutes and (b) the centre frequency set on the VNA (span 200MHz).**

In order to replicate testing conditions, signals were only introduced into the cell for one minute periods (approximately twice that for actual testing) before each temperature measurement, the VNA being switched off during each intervening minute. This is illustrated in Figure 6.15(b), together with the VNA centre frequency setting, which was increased after each temperature measurement to cover the whole

range employed in QWA. After the nineteenth minute, the centre frequency was maintained at 1900MHz, and after 25 minutes temperature measurements were reduced to once every five minutes to reduce the need to open the cell end plate momentarily to insert the bulb thermometer. Small changes in temperature (less than 2°C) were found, with a linearly increasing trend over time (Figure 6.15). For a sample of distilled water with table salt added to an electrical conductivity of 2.3S.m^{-1}, much higher than expected for soils, a rise of 4.2°C was found over a QWA testing period of twenty minutes, and this is considered the maximum temperature variation that would occur in normal use.

While small changes in soil temperature will affect apparent permittivity, Drnevich et al. (2001b) considered that no significant change to water content estimation by TDR would be necessary within a temperature range of 15°C to 25°C: much greater than variations found in this study. This agrees with the findings of Topp et al. (1980) that there is little variation in apparent permittivity with temperature between 10°C and 40°C. Furthermore, the work of Drnevich et al. (2001b) usefully indicated that apparent permittivity to temperature variations are greater for more cohesive soils, but still indicated that the variation is likely to be no more than ±5% for a corresponding ±10°C variation in temperature. In contrast, a 40ml sample of distilled water placed in a 650W microwave oven was found to rise by 20°C in only ten seconds, illustrating the relatively low heating potential of the VNA and cell.

From the above, it can be seen that QWA outside tolerances were greater, and potentially more prone to sporadic variation, in comparison to TDR. However, this can be balanced against the potential for QWA to provide measurement frequencies and data on electromagnetic dispersion. In addition, future development of QWA could be

based around use of more sophisticated portable VNA models that should bring greater accuracy and less variability. Overall, therefore, it can be concluded that QWA provides a relatively simple and acceptably accurate method for broadband velocity measurements in soils. As with TDR, when combined with use of relatively inexpensive and portable VNA equipment, these measurements become accessible to a wide sector of the geophysical community, rather than being limited to those practitioners with extensive knowledge of electromagnetic measurements and access to more expensive and sophisticated frequency domain measurement equipment.

6.4 LINKING GEOTECHNICAL AND ELECTROMAGNETIC PROPERTIES

Considering the complex responses of the soils in Chapter 5 to variations in water content and signal frequency, it is interesting to note that the dry soils all had similar apparent permittivities when adjusted for variations in dry density (Figure 6.16).
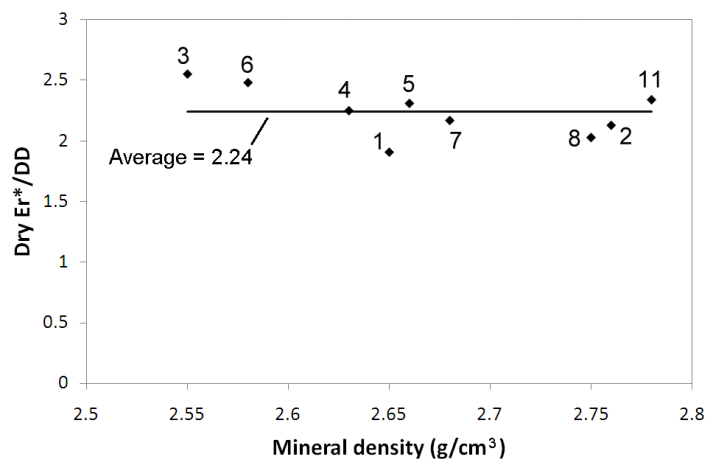
Figure 6.16. Dry apparent permittivity values for the soil samples used, corrected for dry density.

However, as soils can generally be considered to incorporate the same elements (e.g. silicon and oxygen - Craig, 1997) this fact is not surprising. Based on a dry density of 2.7g.cm^{-3}, the data of Figure 6.16 would give an average apparent permittivity of the mineral phase of between 5 and 7, which is compatible with values quoted in the literature (Robinson, 2004; Lebron et al., 2004). Although the electrical conductivity, at the Liquid Limit, was only intended as an initial indicator of the properties of the wet soil samples, it is instructive to compare those values with the magnitude of the electromagnetic dispersion, as both could be expected to involve the soil surface area (Cosenza and Tabbagh, 2004).
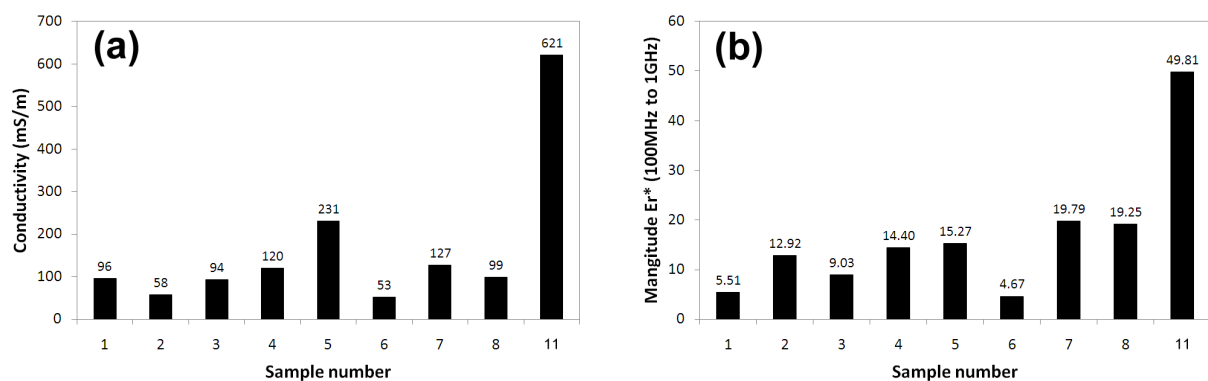
Figure 6.17. The (a) conductivity and (b) dispersion magnitude of the soil samples at their Liquid Limits.

The conductivity (Figure 6.17(a)) and dispersion magnitude (Figure 6.17(b)) showed no exact relationship, as would be expected due to the conductivity not including the effects of polarization of water molecules, which have been indicated as potentially being a 50% greater contribution to the loss tangent than those associated with conductivity (Topp et al., 2000). However, it can be seen from Figure 6.17 that

there are similarities and, overall, the electrical conductivities generally fell within the common range for soils of up to 100 mS.m^{-1} (Giao et al., 2003).

Properties of soils associated with water content are of significant interest in linking geotechnical and electromagnetic properties (Carreón-Freyre et al., 2003), as they control both signal velocity and attenuation (Doolittle and Collins, 1994), and so contribute strongly to soils being complex systems in geophysical terms (Ben-Dor et al., 2002). Two such geotechnical parameters are the Liquid Limit and Linear Shrinkage, both of which can be expected to relate to the soil specific surface area (Mitchell and Soga, 2005). On this basis, it could be expected that these two parameters would show some correlation, and a comparison between them is therefore shown in Figure 6.18.
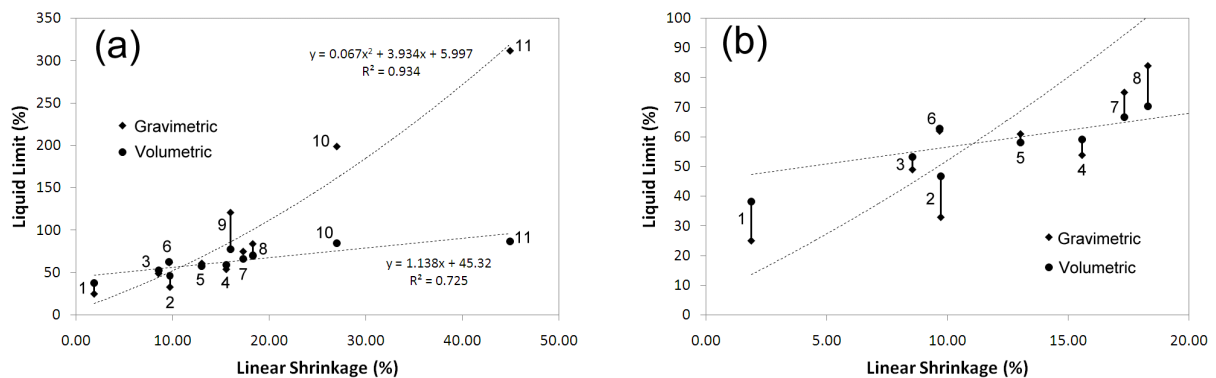
Figure 6.18. Relationships between Linear Shrinkage and Liquid Limit (a) for all samples and (b) zoomed to illustrate variations in Samples 1 through 8.

From Figure 6.18(a) it can be seen that all of the soil samples at their Liquid Limits followed a general relationship of increasing shrinkage with increasing specific

surface area. However, as shown in Figure 6.18(b), the correlation appears to be a loose trend, and potential reasons for this will be elaborated on in the next section. However, even as a general trend, this is a useful relationship as geophysical methods are increasingly being utilised to image the subsurface for engineering purposes (Anderson et al., 2008) and shrink/swell properties of soils, and the potential for ground movement associated with them, are of particular interest (Waltham, 1994).

However, it should be noted from Chapter 5 that the magnitude of dispersion is greatest close to the Plastic Limit and varies between soils, and many field soils may have a low Liquidity Index. On this basis, measuring the magnitude of electromagnetic dispersion in the field could provide clues as to both the Liquid Limit and shrinkage properties of a soil. Therefore, the Liquid Limit of each sample can be compared to the magnitude of electromagnetic dispersion (between 100MHz and 1GHz): see Figure 6.19. As with Figure 6.18, a general trend was found, but it is apparent that the match is poorly correlated.

An important factor in improving on that trend is the study of relationships between the specific surface area and Liquid Limit by Dolinar and Trauner (2005). These researchers considered that the inter-grain water content at the Liquid Limit is proportional to the specific surface-area, other water being confined to inter-sheet locations. As the higher-frequency apparent permittivity data appear to show a linear relationship to the Liquid Limit, it is possible that these data are related to inter-grain water, with the lower-frequency dispersion being related to the more confined inter-sheet water.

If this is the case, low-frequency dispersion in the water phase may be a function of mineralogy, the associated degree of inter-sheet water therefore determining the

magnitude of the dispersion. This fits with the hypothesis that relationships between silicate layers and water are associated with variations in permittivity, electrical conductivity and shrink/swell behaviour (Cosenza and Tabbagh, 2004), as well as the suggested relationship between electromagnetic dispersion magnitude and cation exchange capacity found, for frequencies below 100MHz, by Fernando et al. (1977).
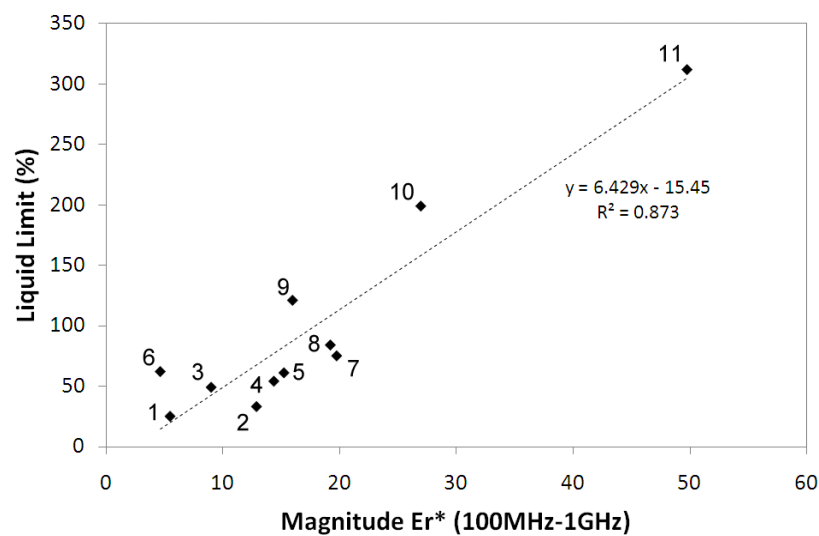
Figure 6.19. The relationship between Liquid Limit and the magnitude of the apparent permittivity (100MHz to 1GHz).

In order to investigate this possibility, the magnitude of the dispersion for each soil can be compared to the linear shrinkage (Figure 6.20). As shrinkage properties are largely dictated by the potential for water to build up between mineral sheets (Grim, 1962), it would be expected that any differences in electromagnetic properties of the inter-sheet water may show some relationship to the amount of shrinkage exhibited by each soil.

224
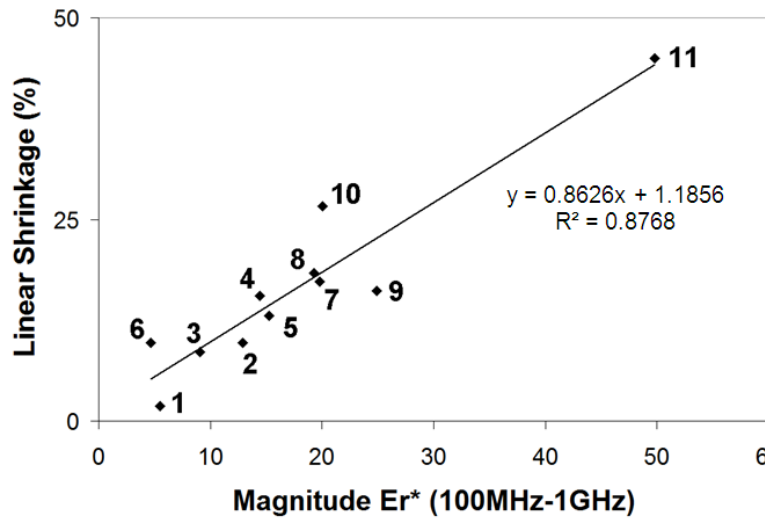
Figure 6.20. The relationship between linear shrinkage and the magnitude of the apparent permittivity (100MHz to 1GHz).

It can be seen that Sample 6, and the two mixtures of it with Sample 11 (Samples 9 and 10), are the only samples to show significant departure from a linear relationship, and the correlation appears much better than that for the Liquid Limit in Figure 6.19. However, when the effects of dry density are accounted for the variations from a linear fit are much reduced (Figure 6.21). Under normal field circumstances the Liquid Limit can be expected to be below 100% (Rogers et al., 2009), where the linear relationship is most evident, although it should be noted that further research will be required to ascertain the properties of less common soils departing significantly from the A-Line. In terms of Samples 9 and 10, it has been noted previously in the literature that the shrinkage limit of artificial mixtures of fine-grained soils can depart from a strict pro-rata of the component shrinkage limits (Sridharan and Prakash, 2000a). This may account for the greater variations Samples 9 and 10 exhibit from the relationship

225

shown for the other, non-composite, soils studied and illustrates that further research is required to characterise signal velocities in such soils.
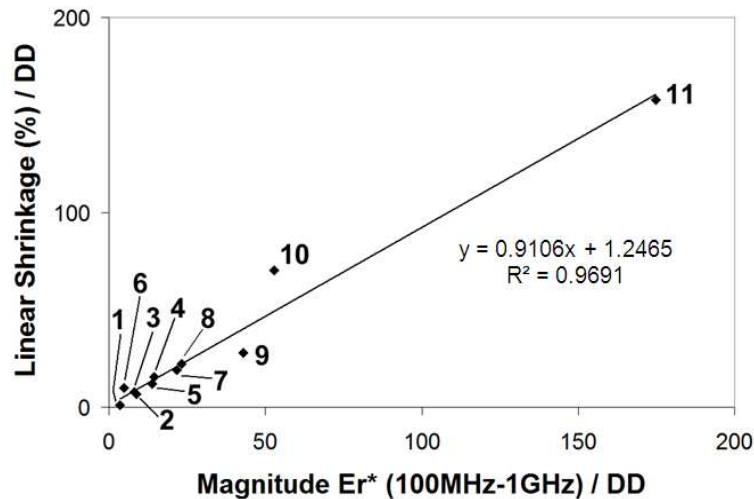
Figure 6.21. The relationship found between linear shrinkage and the magnitude of the apparent permittivity (100MHz to 1GHz), when adjusted for the effects of dry density.

6.5 THE ROLE OF THE PORE WATER

The literature often describes the electromagnetic properties of fine-grained soils as incorporating adjacent 'bound' and 'free' water phases with markedly different apparent permittivities (e.g. Serbin et al., 2001). Given that the higher-frequency QWA data show a relationship to the Liquid Limit, and the dispersion magnitude appears more related to the shrinkage properties, it could be speculated that these two geotechnical properties are related, respectively, to the 'free' and 'bound' water phases. Therefore, it is possible that electromagnetic signal velocity data could be used in engineering estimates of the potential for shrinkage, or swelling, of soils, and at higher frequencies

for measurement of soil volumetric water content. Identifying soils with high shrink/swell properties is of great importance (Gray and Frost, 2003), as is measurement of soil water content (Topp et al., 1988), and so the ability to identify these properties without intrusive excavation has obvious benefits.

An indication of the complexity of the soil pore water phases can be taken from the number of mixing models available in the literature (see Section 2.6). According to van Dam et al. (2005) there are at least twenty two such models available for calculating composite electromagnetic properties. However, as this study chose to cover the full saturated water content range, and due to the consistency of apparent permittivity data in the plastic range, it is instructive to consider variations in the pore water apparent permittivity at water contents above the Plastic Limit.

This was achieved by calculating the water phase apparent permittivity as a simple volumetric fraction (Equation 6.1). As air has an apparent permittivity of unity, its effect at small fractions was assumed negligible. The apparent mineral permittivity was determined by testing the soils, immediately following oven drying, in the coaxial cell.

$$\varepsilon_{rW}^* = \frac{100}{\theta}\left(\varepsilon_r^* - \frac{\varepsilon_{rOD}^* \rho_{LL}}{\rho_{OD}}\right) \qquad\qquad \text{[Eq. 6.1]}$$

where ε_{rW}^* and ε_{rOD}^* are the apparent permittivities of the water phase and oven dried soil respectively and θ is the volumetric water content (%). ρ_{LL} and ρ_{OD} are the dry densities of the soil during tests at the Liquid Limit and after oven drying.

The range of mixing models available indicate that there should be a complex relationship between the water content and water phase electromagnetic properties, although the work of Saarenketo (1998), and others as far back as Cownie and Palmer

(1951), provide some indication that the water phase permittivity may level off above the Plastic Limit. However, it was found that the apparent permittivity of the water phase at high frequencies appears largely constant, at least within the plastic range (Figure 6.22). Above the Liquid Limit there is a change in the apparent permittivity and a general increase toward a value close to 80 - the approximate apparent permittivity of 'free water'. For the TDR data there is much greater variability, potentially due to variations in the loss tangent. In the lower frequency QWA data it can be seen that significant variations occur, but that these need not preclude use of an average water phase apparent permittivity in mixing models, depending on accuracy requirements.

The average water phase apparent permittivities, together with details of the amount of variation occurring for both higher frequency QWA and TDR, are detailed in Table 6.1. The HF QWA data were found to vary within a range of ±3 units of apparent permittivity from the mean. Based on Section 6.3, these variations may be largely due to the expected measurement tolerance of ±2 units of apparent permittivity. The TDR water phase data provided consistently higher values of apparent permittivity compared to QWA, which can be attributed to the lower dominant measurement frequency.

Furthermore, in Table 6.1 there is greater variability in the TDR data (c. -5 to +6 from the mean) and this may be attributed to the varying effects of the loss tangent on signal velocities. This is not an inherent aspect of the HF QWA data due to the weaker dependence of the permittivity on pore water salinity (Wensink, 1993).
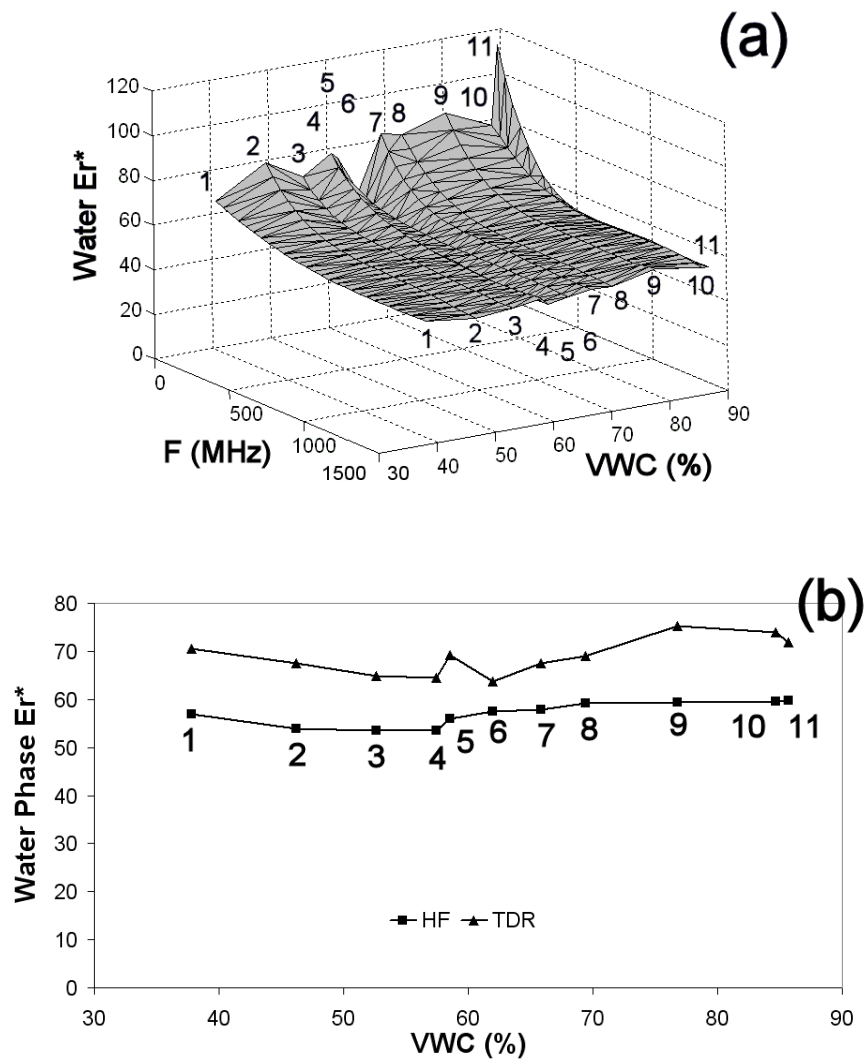
Figure 6.22. Liquid Limit apparent permittivity of the pore water phase, in the volumetric water content (VWC) domain (a: full QWA data and b: HF QWA and TDR data).

Table 6.1. Variations in water phase apparent permittivity.

	Water phase apparent permittivity	
	HF QWA	**TDR**
Minimum	53.5	63.8
Mean	57.0	68.9
Maximum	59.7	75.2

Having determined that the water phase apparent permittivity shows a degree of consistency between soils at the Liquid Limit, it is important to investigate whether the relationships found were applicable to other water contents. The analyses of Samples 6 and 8 allowed such investigation. As can be seen in Figures 6.23 and 6.24 the water phase data are very similar to the previously described Liquid Limit data in that the HF QWA data show a consistent apparent permittivity within the plastic range. This could be considered remarkable as the calculated water phase apparent permittivity is based on a single water phase: i.e. without consideration of separate 'bound' and 'free' water. Of course, a second water phase does exist in the lower frequency data exhibiting itself as electromagnetic dispersion, but is fully relaxed in this HF QWA data. This appears to rule out the possibility that bound water becomes free water at a critical water content, as posited by Boyarskii et al. (2002). However, based on Chapter 5 it is apparent that a successful mixing model for fine-grained soils, to relate apparent permittivity to volumetric water content, could be based on an underlying linearity in the water phase at high frequencies (c. 1GHz), with lower frequency variations being based on a dispersion magnitude that respects the shrink/swell properties. This may not be unrealistic as simple volumetric fraction mixing is used in the literature (e.g. Nedeltchev, 1999). Additionally, of particular note is that the magnitude of the dispersion can be seen to be reducing in proportion to water content for these two soils, whereas for the Liquid Limit data there is an increase. As higher Liquid Limits relate to higher mineral specific surface areas (Farrar and Colemanm, 1967), and higher water contents in saturated fine-grained soils relate to lower mineral surface areas, this is to be expected if the surface area of a soils mineral phase is considered linked to its shrinkage and electromagnetic dispersion properties.
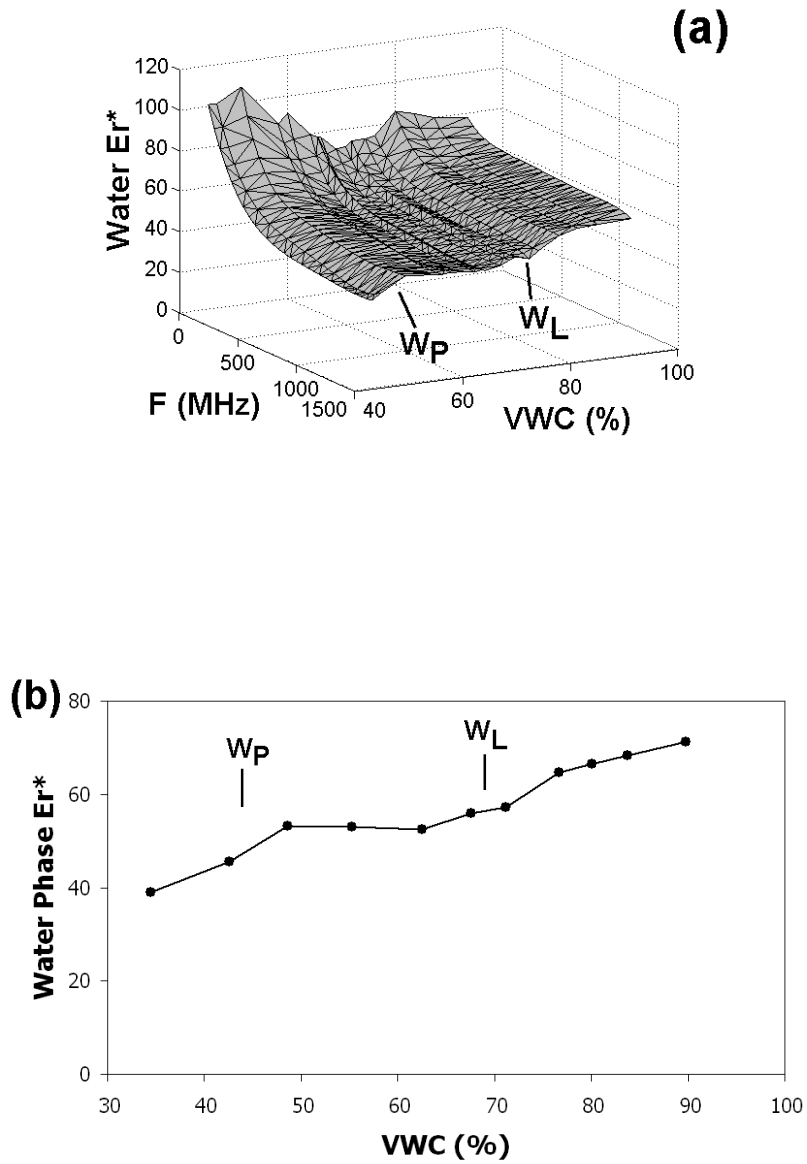
Figure 6.23. London Clay apparent permittivity of the pore water phase, in the volumetric water content (VWC) domain (a: full QWA data and b: HF QWA data).
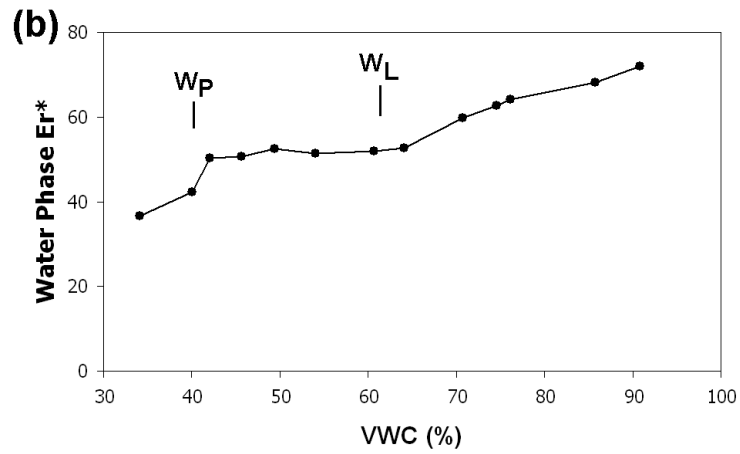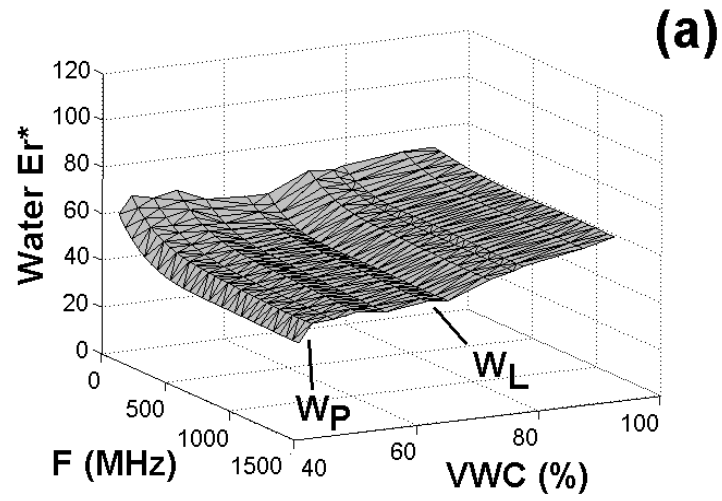
Figure 6.24. English China Clay apparent permittivity of the pore water phase, in the volumetric water content (VWC) domain (a: full QWA data and b: HF QWA data).

The data of Figures 6.23 and 6.24 also indicate that the marked differences in electromagnetic dispersion magnitude between the English China Clay and London clay, at their Liquid Limits, is representative of the whole plastic state. It was found that the English China Clay exhibited much less dispersion between the Plastic and Liquid Limits than the London Clay, the former also exhibiting a much lower linear shrinkage.

Therefore, it appears that the geotechnical parameters of Liquid Limit and linear shrinkage could provide very useful indicators of the degree of dispersion that will occur in individual fine-grained soils, potentially helping inform field electromagnetic surveys in future. In addition, it is apparent that development of methods to measure electromagnetic dispersion, and water content, in the field would allow the potential estimation of the shrink/swell properties of soils *in situ*. As soil swelling is considered a significant problem, and even highly ranked among natural hazards (Kariuki et al., 2003; Chabrillat et al., 2002), such methods could prove very useful in engineering and construction. Furthermore, the greater understanding of the electromagnetic properties of plastic fine-grained soils found in this study should be of potential use in extending other methods for geophysical determination of subsurface properties, such as the work of Lambot et al. (2004) and Serbin and Or (2004), which both utilised GPR for such purposes. It may even be of use in informing seismic methods to induce measurable electrokinetic effects, such as by Pride and Morgan (1991), which may be of interest given potential relationships between electromagnetic and acoustic data for porous media (Pride, 1994).

Also, for both samples there was a noticeable change in the water phase apparent permittivity above the Liquid Limit: as well as a step increase there is also a rising

trend in the HF QWA data toward the 'free' water value of apparent permittivity at 100% volumetric water content. This indicates that, for the saturated state, different water content to apparent permittivity relationships exist above and below the Liquid Limit. While no example has been found in the literature of this effect occurring (electromagnetic literature for these water contents being very limited), the differences are known geotechnically as the plastic and liquid states (Craig, 1997) so the need for two separate relationships could be expected.

Further evidence for this could be taken from Laird (2006) who described the swelling of smectites as being based on different processes depending on the state of the soil, with increasing water content giving rise to an initial breakup of quasi-crystals into smaller sub-units, followed later by complete de-lamination of silicate sheets, with correspondingly decreasing interactions between them. Therefore, it could be speculated that as de-lamination occurs, the reducing inter-sheet ('bound') water would give rise to increasing inter-grain ('free') water that could cause the apparent permittivity of the water phase to approach that of unconfined water, as 100% volumetric water content is approached. As well as being of interest from the perspective of studying such potential de-lamination processes at high water contents, the close to linear relationship between apparent permittivity and volumetric water content above the Liquid Limit may also be of use for such applications as monitoring drilling slurries (Abichou et al., 2004), or even for location of water pipe leakage (Millard et al., 2004) where soil water contents may be locally elevated.

While the exact mechanisms determining this almost constant nature of the water phase EM properties between the Atterberg Limits is not yet known, it is interesting to consider these data in terms of double-layer theory. In this theory, it is considered that

the water phase will comprise a thin bound layer of ion-rich water (Gouy layer) around mineral particles which are themselves surrounded by a diffuse layer (Chapman layer) that is influenced by the surface charge of the minerals in a manner reducing with distance (Mitchel and Soga, 2005). Beyond the diffuse double layer, any remaining pore water must therefore be presumed 'free water'. However, there are many limitations to this theory (Mitchell and Soga, 2005), including that the permittivity of the water phase is often considered the same as free water, which is not found to be the case in soil electromagnetics research (e.g. Saarenketo, 1998). In addition, the theory considers the impact of charged surfaces on adjacent ions and water molecules, but does not include the effects of the water structure itself (Low, 1979; Mitchell and Soga, 2005), which includes three-dimensional hydrogen-bonding that may affect the attraction of charged surfaces (Ball, 1999). Furthermore, bound water has been described as firmly attached to mineral surfaces and rotationally hindered, yet those water molecules will be surrounded by ions associated with the diffuse double layer, which Debye (1929) would argue should neutralize surrounding hydrogen bonds. Of significant interest, therefore, is that for biological systems Despa et al. (2004) were able to illustrate changes in water dielectric properties in terms of a permittivity decreasing with increasing proximity to interfaces, due only to reduced potential for formation of hydrogen bonds between water molecules. If it is also true that confined water dipoles experience a reduced translation energy barrier (Choi et al., 2005), and fine-grained soils can have pores as small as 3nm (Sills et al, 2006), then again the theory that 'bound' water is firmly adsorbed and rotationally hindered appears to be to some extent incomplete.

In soil EM research there is considered to be a marked difference in apparent permittivity of bound and diffuse water (e.g. Serbin et al, 2001; Serbin and Or, 2005).

Furthermore, it can be expected that large changes in dry density should reduce the proportion of bound water in favour of increases in the proportion of diffuse water, as fine-grained soils should have water absorption characteristics (Prakash and Sridharan, 2004), electromagnetic dispersion characteristics (Raythatha and Sen, 1986; Arcone et al., 2008), and bound water contents (Cosenza and Tabbagh, 2004), linked to their surface areas. However, it can be seen from Figures 5.2 and 5.3 that the dry density, and hence theoretically the available soil surface area, of Samples 6 and 8 approximately halves between the Plastic and Liquid Limits. Also, Dolinar and Trauner (2005) discussed the potential for two types of water to exist in fine-grained soil: that between silicate sheets and that between soil grains. Therefore, for the saturated plastic state, such a reduction in surface area, with no significant change in water phase apparent permittivity, could be considered an indication that the inter-grain pore water is homogenous within the plastic range. This would agree with the single water layer speculated by Boyarskii et al. (2002), if not applied to the inter-sheet water, and does not disagree with the concept of Or and Wraith (1999) that the proportions of bound and free water may vary with temperature. It is, therefore, interesting to note that Low (1979) found substantial changes in the properties of pore water between mineral layers in montmorillonite with increasing layer separation. Low (1979), and Pickett and Lemcoe (1959), found that the first few molecular layers of water around mineral sheets have significantly different properties (e.g. viscosity) to unconfined water. Based on the work of Despa et al. (2004) this may be due to reduced hydrogen bonding potential, and so the changes in those properties toward those of unconfined water, as water content increases, could then be due to increased bonding potential.

Therefore, it can be argued that, when saturated and plastic, the two soils studied show evidence against a double layer existing in the pore water, or at least against there being differing adjacent layers with markedly different electromagnetic properties. From this it can be speculated that the inter-sheet and inter-grain waters discussed by Dolinar and Trauner (2005) offer a more lucid illustration of the nature of 'bound' and 'free' water for geotechnical purposes. Additionally, the apparent permittivity data indicate that assuming free water values for fine-grained soil pore water may be inappropriate as, for Samples 6 and 8, there was an increase in apparent permittivity above the Liquid Limit. This indicates that the pore water apparent permittivity is likely to be lower than that of 'free water' within the plastic range, implying a difference in water hydrogen bonding.

6.6 WATER CONTENT MEASUREMENT USING TDR AND QWA

The motivation behind TDR development was the desire to provide data for use with GPR particularly in terms of water content profiling (Topp et al., 2003) and both methods have been found to give complementary soil water content data (Huisman et al., 2003a). However, models such as that of Topp et al. (1980) have been shown to be very variable in applicability (Kelleners et al., 2005a). In particular, TDR has been found to provide poor accuracy for highly plastic clays and soils of high and low density (Siddiqui et al., 2000). Therefore, the demonstration of compatible data between TDR and GPR does not necessarily indicate that water contents calculated from those data will be correct if a mixing model is used indiscriminately.

It has been shown that so called 'universal' (Shuai et al., 2009; Nadler et al., 2006) mixing models, such as that of Topp et al. (1980), can be biased toward water contents below approximately 40% by volume, or not fully representative of the dispersive nature of fine-grained soils. This is important not just in terms of TDR and QWA, but also in wider electromagnetic surveying applications where common mixing models are used, such as for GPR water content determination (Huisman et al., 2003b). As illustration, Figure 6.25(a) shows the volumetric water contents for all of the TDR data against the Topp et al. (1980) model values and illustrates an agreeing general trend for volumetric water contents below 40% for Samples 6 and 8 (approximately the Plastic Limit). But, calculated water contents form a different relationship in the plastic state and start to converge on an apparent permittivity of 80 at a volumetric water content of 100%.

While little literature exists for high water contents, this departure from the Topp et al. (1980) model above 40% volumetric water content, and closer agreement at very high water contents, agrees with the findings of Curtis (2001) at 100MHz. For frequencies below 50MHz, Campbell (1990) found significant similarities between his data and the Topp et al. (1980) model up to 40% volumetric water content, but with equally significant departures from it at higher water contents up to his maximum value at c.50%.

It is therefore interesting to note that there was significant opposition in the 1970s to the assertion that a single empirical TDR model could relate to all soil types, particularly those including significant amounts of silt or clay (Topp et al., 2003). From Figure 6.25 it is apparent that both camps may have been correct: the Topp et al.

(1980) model appears to loosely describe the unsaturated state, but for the saturated state there is no real correlation to measured data.
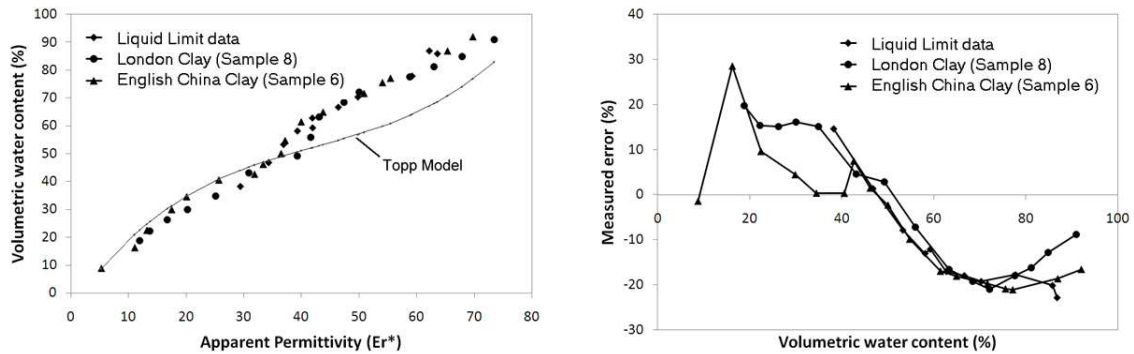
Figure 6.25. TDR and the Topp et al. model: (a) comparison of apparent permittivity to volumetric water content relationships and (b) errors found using the model with all fine-grained soil samples tested.

It should, however, be noted that the Topp et al. (1980) model has not been singled out for criticism in this thesis: it is very commonly used and so provides a good basis for illustrating that the apparent permittivity of fine-grained soils does not follow the same water content relationship above and below the Plastic Limit. It was also chosen to illustrate (Figure 6.25(b)) the degree of error that can occur in water content measurements due to use of mixing models, for the fine-grained soils studied, over the full water content range applicable to geotechnical engineering. For the plastic state, Figure 6.25 shows that volumetric water content errors can be as large as 20%, but other studies have shown errors between TDR water contents, and those determined through oven drying, of up to 100% where soil specific apparent permittivity models are not established (e.g. Zupanc et al., 2005).

The Topp et al. (1980) model was considered by its authors to have an inherent standard volumetric water content error of 1.3% for 93% of their measured data and the differences they found for a range of materials between glass beads and organic soil showed potential volumetric water content variations greater than 10% for the same value of apparent permittivity. Furthermore, the data used to form the polynomial curve fit was from materials whose apparent permittivity was only weakly dependent on frequency (Topp et al., 1980). These variables illustrate the difficulty associated with attempting to devise a truly 'universal' mixing model. Therefore, the potential for creating a new model for water content estimation, for saturated fine-grained soils, requires discussion. This can be achieved through determining a linear relationship for all HF QWA and TDR data points close to and above 40% volumetric water content (Figure 6.26).
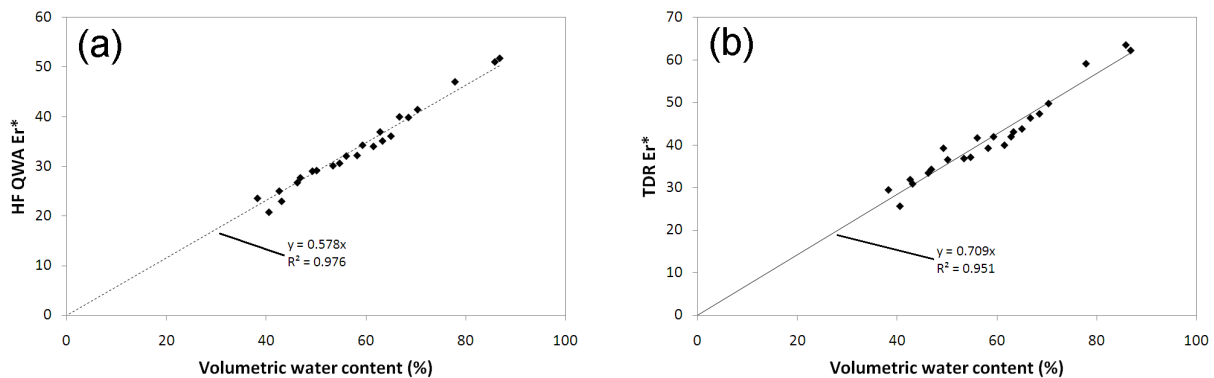
Figure 6.26. Predictive water content relationships for all samples above the Plastic Limit: (a) HF QWA and (b) TDR.

These two relationships allow comparison of the results to the measured water contents, allowing determination of the associated error (Figure 6.27). The TDR

prediction model of Figure 6.26(b) provides significant improvement over simply assuming that the Topp et al. (1980) model is applicable, the error being generally within 10%.

Obtaining exact water content estimation in soils with variable loss tangent contributions can be expected to be difficult, but potentially less so for HF QWA. This was found to be the case for the HF QWA prediction model (Figure 6.27(a)): volumetric water content estimation was generally achievable within a tolerance of 5%. The greatest errors (up to 8%) were found for the lowest water content samples close to the Plastic Limit.
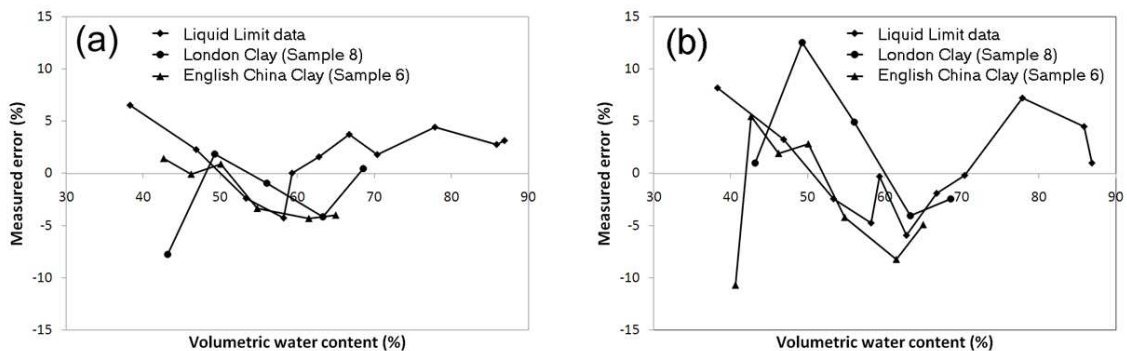
Figure 6.27. Errors in water content estimation associated with the predictive models for

(a) HF QWA and (b) TDR.

The predictive models for TDR and HF QWA data could be improved further by splitting them into the plastic and liquid phases. Furthermore, even greater improvements may be possible if the effects of dry density are corrected for: such as through combined seismic and electromagnetic measurements (Fratta et al., 2005) which can be considered coupled (Pride, 1994). However, these two potential

improvements were not included because under normal field use water contents could be expected to vary widely with location and it may not be possible to directly measure the dry density.

However, based on these initial results, measurements of the apparent permittivity of fine-grained soils in the plastic state could provide a useful model for volumetric water content estimation. But, use of signal frequencies associated with reduced dispersion, as with HF QWA, could provide a more accurate method than TDR, although for field use temperature corrections would need to be devised.

However, for large area soil monitoring the use of multiplexers would be required which have some effect on TDR measurements (Castiglioni et al., 2006; Logsdon, 2006b). While the effects of these devices can be calibrated out of TDR measurements, further research would be required to determine their effects on frequency-domain signals before they could be considered for use with QWA. Additionally, in terms of the measurement data obtained in this study, it should be noted that effort has been made to ensure that the samples were homogenous in terms of water content distribution, in order to reduce the potential for convoluted waveforms due to water content gradients. For TDR, reconstruction of water content profiles along probes has been documented (Heimovaara et al., 2004), and for field use such reconstruction methods could also be required for QWA. However, it should be noted that the TDR literature largely describes average permittivities without correction for gradients. Furthermore, techniques such as those of Heimovaara et al. (2004) are based on modelling of TDR signal propagation and reflection, and so could be incorporated into the modelling described in Chapter 4. However, under many circumstances, use of short probes in fine-grained soils could involve a significant degree of homogeneity in

tested soils, and under such circumstances the use of QWA described in this thesis has been found adequate.

6.7 RELEVANCE TO ENGINEERING

This research provides a number of opportunities in civil engineering, most notably the potential for accurately measuring fine-grained soil water contents. This is significant as common use of TDR in fine-grained soils suffers due to elevated loss tangents and so use of HF QWA data may provide an opportunity to overcome that difficulty and reduce the need for soil-specific calibrations. In the field this may allow improvements such as simple monitoring of weather sensitive sub-grades during construction, and advance warning in geo-hazard monitoring (e.g. landslide warning systems and monitoring of potential shrinkage and swelling close to sensitive structures). Also, links found between linear shrinkage and dispersion magnitudes provide a potentially simple means of assessing and geospatially mapping shrink/swell potentials, as knowing both the dispersion magnitude and its associated water content provides useful clues as to the potential for volume changes to occur.

In the laboratory, potentially calibration free measurements of water contents in fine-grained soil fractions may also allow for improved monitoring of water related changes within geotechnical experiments (e.g. measurements on collapsible soils such as Loess), as well as potentially expediting the delivery of index test results which may currently be delayed for up to 24 hours while water contents are determined. Furthermore, measurements of electromagnetic dispersion during laboratory Liquid Limit testing should provide the opportunity to very rapidly estimate linear shrinkage without having to wait a

number of days for controlled shrinkage to occur (as quick drying is associated with undesired curling and cracking). If QWA is utilised to determine volumetric water content over all cone-drops included in the Liquid Limit test, this also facilitates rapid estimation of particle densities (as this would only require a known cup size and simple mass measurements). Given that there appears to be a linear variation in electromagnetic dispersion magnitude between the Plastic and Liquid limits in a soil, it is also possible that future work may identify means of estimating the Plastic Limit using QWA data.

Further research opportunities can also be found in the differences between electromagnetic properties at low and high frequencies: the former including the effects of loss tangents and ionic conductivity associated with 'bound' water phases, and the latter largely being dependent on the Debye (1929) relaxation process for 'free' water. Therefore, it is possible that the properties of both of these forms of water, and their variation with time and temperature, could be monitored through use of QWA measurements, which is not currently practicably achieved through simple use of TDR. Example applications could include monitoring diffusion of ions into and out of soils, monitoring of contaminant diffusion in contaminated land and landfills, and as a means of illuminating the nature of pore water in experiments relating to Diffuse Double Layer theory. It is also possible that simultaneously monitoring both water content and electromagnetic dispersion could provide a useful means of monitoring contaminant containment systems using clays (e.g. Bentonite in landfill leachate barriers), where simply measuring water content may give little clue as to whether chemical changes have occurred that may cause failure.

In the future, once further work has established the full correlations between plastic fine-grained soil dispersion magnitudes and water content, and temperature corrections

have been devised, it may be possible to rapidly estimate geotechnical index test values in the field, and even map variations spatially for earthworks planning. Also, where geophysical surveys are planned in engineering, it is now possible to estimate potential signal velocities from geotechnical index tests, and even to use geotechnical databases as a basis for development of soil suitability maps as a desk study aid for such surveys. This may also help in reducing the complexity of current mixing model literature, through categorising their usability in terms of soil geotechnical phases.

It should also be noted that QWA has potential for providing a field-applicable geophysical survey method that can be used, with adequate VNA equipment, to provide conductivity, water content, and shrinkage information from a single measurement. This significantly improves over TDR survey methods and even allows for construction of more useful computer-generated survey plans utilising different frequencies. For instance, low frequency data can be used to provide an indication of geospatial variations in loss tangents (i.e. conductivity and dipolar polarisation variations), high frequency data can provide water content, and the dispersion magnitude between the two could provide clues to mineralogy and variations in soils type. This could provide significantly enhanced data for engineering and archaeological geophysical surveys, including allowing post-processing variation of measurement frequency to optimise contrast in plotted survey data.

CHAPTER 7 - CONCLUSIONS AND RECOMMENDATIONS FOR FUTURE WORK

7.1 OVERVIEW

This chapter provides conclusions and details potential future research work through the following two sections:

7.2. Research outcomes: Discussion of the most relevant research outcomes.

7.3. Recommendations for future work: Discussion of potential future research.

7.2 RESEARCH OUTCOMES

Current knowledge of electromagnetic signal velocity measurement in soils was investigated through a comprehensive literature search and review, including consideration of geotechnical factors that may be relevant to soil electromagnetic properties. In this regard, it was found that there is significant literature on soil electromagnetic properties but often limited either to single frequencies or small water content ranges and, in the majority of cases, do not cover the full range of fine-grained soil water contents likely to prevail in the field. Also, literature is available on the forms of water that may exist within soils, and so which may affect the electromagnetic properties, although it should be noted that connections between water electromagnetic and geotechnical properties, and associated hydrogen-bonding structures in soil pores, are not well covered. For this study, recourse had to be made to other disciplines for relevant data (e.g. biological sciences literature).

However, very little research has been found that can be used to directly relate the different forms of water to electromagnetic and geotechnical properties. In particular, it can be noted that there is relatively little agreement in the electromagnetics literature on an exact form of 'bound' and 'free' water in fine-grained soils that adequately represents geotechnical states. However, it was found that the soil electromagnetics research community is an active one with many examples of novel research that can be made use of for geotechnical applications. Furthermore, many examples of potentially useful electromagnetic measurement systems were found in the literature, from which it was possible to develop QWA as a useful extension to TDR.

A range of fine-grained soils were obtained suitable for use in both geotechnical and electromagnetic testing, including characterisation of their geotechnical and electromagnetic properties. A significant aspect of this work was that geotechnical characterisation of the selected soils required use only of the soil fines (i.e. less than, or equal to, 425μm in size). This is significant, as it was recognised that full comparison of the geotechnical and electromagnetic properties should also require use of the same soil fraction. Therefore, through removing variability associated with inclusion of coarser soil particles in the electromagnetic measurements, the ability to determine relationships was facilitated. Also, Atterberg Limit testing was shown to relate acceptably to the A-Line, the particle densities related well to later dry density measurements and the linear shrinkages related well to later measurements of the magnitude of electromagnetic dispersion. Furthermore, through undertaking characterisation of a wide range of soils, a similarly wide range of Liquid Limits and shrinkage values became inherent in the samples used, which enhances the quality of relationships found in subsequent apparent permittivity tests.

An electromagnetic measurement cell was devised, tested and modelled, including formulating a methodology for its use suitable for extending TDR to include data on electromagnetic dispersion directly measured in the frequency domain, and with similar simplicity to use of TDR. In terms of extending TDR, QWA provides a useful improvement in that not only does it provide a number of data points, but also their frequencies are known within acceptable tolerances. More importantly, QWA not only provides enhanced data in comparison with TDR, but the measurement cell allows use of both technologies to provide comparisons between the two techniques. In terms of potentially validating inversions of time- and frequency-domain data, this is invaluable. In terms of ease of use, QWA could be considered more difficult to use as it requires time consuming collection of data and multiple re-calibrations. Also, the degree of noise inherent in measurements causes a need for significant practice before the user is able to obtain useful data. However, it is possible that use of a more sophisticated VNA, also with significantly improved memory, connected to automatic data retrieval and processing software, could much improve ease-of-use.

Use of the cell in a geotechnical testing environment was developed, with similar levels of quality safeguards to those appropriate to routine geotechnical testing, including consideration of whether relationships exist between geotechnical and electromagnetic data. Of particular significance is that the decision to undertake measurements in an environment that was not closely regulated, in terms of such factors as temperature, introduced some risk of masking relationships between soil electromagnetic and geotechnical properties. However, even though there is some variability apparent in the data, the relationships found were nonetheless considered well defined and variations appeared mostly attributable to differences in dry density between samples at different water contents. In the early stages,

the most important 'discovery' was that the high-frequency apparent permittivity related linearly to the Liquid Limit. However, of equal significance was that this related to the Wensink (1993) model, which therefore provides a potential high-frequency water content measuring relationship akin to the Topp (1980) model used often with TDR. This resulted in further measurements in two soils over a wide range of water contents, and it was found that the high-frequency apparent permittivity values also linearly relate to water content and, in addition, followed the Wensink (1993) model. Linear trends imply that pore water apparent permittivity will be constant over wide ranging pore sizes. It was also found that signal velocities in fine-grained soils also relate to the geotechnical states divided by the Plastic and Liquid Limits (i.e. friable, plastic and liquid). The further discovery that a step change in apparent permittivity occurs above the Liquid Limit also provided insight into the possible occurrence of a phase transition in water structure, although this was not investigated in depth as to do so would have worked against the desire to provide a full overview of properties rather than focussing on 'small parts of the jigsaw'.

In addition, through measurements of the apparent permittivity of the East Leake soils, it was found that magnetically susceptible, anthropogenic, soils derived from industrial processes can show significantly different trends than 'natural' soils. Furthermore, the data gave cause to speculate that the magnitude of electromagnetic dispersion may be associated with water between mineral sheets, as indicated by the relationship to linear shrinkage. This also highlights the possibility that inter-sheet and inter-grain water may provide some insights into the nature of 'bound' and 'free' water often referred to in geophysical and geotechnical research.

The potential for improvements to geophysical water content measurement in fine-grained soils was also considered, as determination of their water content can be considered problematic due to a bias in the literature toward data for water contents below the Plastic Limit. It was found that for saturated fine-grained soils the apparent permittivity to volumetric water content relationship is approximately linear for both HF QWA and TDR, which facilitated a preliminary model that provided useful water content estimation. Of particular significance is that the HF QWA data were found to provide better accuracy in comparison to TDR, due to the reduced impact of the loss tangent on the apparent permittivity. This outcome can also be considered significant as only a single, very simple, mixing model was shown to be required, rather than the multitude of models implied necessary in the literature review.

Finally, it should be noted that a number of potential uses for this research, within the engineering and geophysical communities, have been found, as detailed in Section 6.7.

7.3 RECOMMENDATIONS FOR FUTURE WORK

The research detailed in this thesis can only be considered a starting point on a voyage of discovery through soil electromagnetic properties and their relationships to geotechnical parameters. Therefore, a number of potential ideas for extending this work into future research are detailed below:

1) The measurement methodology does not fully reach its potential level of simplicity of use, so further work should be undertaken to develop it to utilise more sophisticated current VNAs and extend the software to allow automatic data retrieval and processing.

This would remove the need for human interpretation of the quarter-wavelength frequencies and would facilitate averaging of a number of measurements to reduce the effects of noise.

2) Using a VNA with significantly more memory would allow a wide range of frequencies to be covered with just one calibration. It would then be possible to undertake measurements in dynamic systems, such as during consolidation of soils. This would also allow for reduced impact of QWA on the samples being tested, such as in removing small variations due to small temperature changes.

3) The tests described in this research were undertaken within a relatively narrow range of temperatures. Therefore, it would be instructive to measure the apparent permittivity of selected soils over a wide temperature range to allow consideration of how the low- and high-frequency relationships vary. This could also provide valuable insights into the properties of different types of water present in the soil matrix, and illuminate the potential phase transition close to the Liquid Limit.

4) A wide range of soils have been covered in this thesis. All fall close to the A-Line which implies that the results should be representative of the majority of fine-grained soils. However, for completeness it is considered appropriate that future research include electromagnetic and geotechnical testing on a range of soils not falling close to the A-Line. Also, it may be considered appropriate to extend the QWA methodology to include simple methods of ensuring that samples do not have significant magnetic susceptibility before QWA is used in routine geotechnical testing (e.g. through simple use of a magnet to locate iron-containing inclusions, as undertaken on soils in this study).

5) For field use, including longer periods of monitoring, the relatively high cost of commercial VNAs could be overcome by development of a dedicated return loss and phase

angle measurement system based on commercial semiconductor devices. While providing a lower accuracy than more sophisticated commercial systems, this could potentially be achieved at much reduced cost. This could also facilitate development of QWA for use in progressing the engineering opportunities detailed in Section 6.7.

6) It is possible that much more data can be obtained from a VNA than just the apparent permittivity at quarter-wavelength frequencies. For instance, parameter matching, using a Debye (1929) model of soil water properties, to the S_{11} or return loss data could provide much closer spaced discrete apparent (and potentially real and imaginary) permittivity data over the full measured frequency range. Also, using probes and open-circuited cells, conductivity estimates may also be achievable.

7) This thesis has given only a brief account of the potential use of TDR-style probes in place of coaxial cells. In many instances, such as for field use and during consolidation of large samples, probes have obvious advantages. Therefore, it is considered important that further research be undertaken on the use of probes with QWA, including with commercial TDR probes where cable effects cannot be calibrated out prior to measurements with a VNA (i.e. de-convolution of resonances from the cable and probe).

8) Finally, it should be noted that some researchers have attempted to obtain frequency-domain data through inversion of TDR data, but this could be considered limited by lack of validation through comparison with data measured using frequency-domain equipment. If such inversion methods were validated using the raw data from the VNA measurements detailed herein, a greater degree of confidence could be held in the inverted TDR data.

REFERENCES

Abichou, T., Tawfiq, K. and Abdelraziq, Y. "Using Electrical Conductivity to Estimate Properties of Mineral Slurries Used in Drilled Shaft Construction" *Geotechnical Testing Journal*, 2004, Vol. 27 No. 6, 1-7.

Agmon, N. "Tetrahedral Displacement: The Molecular Mechanism behind the Debye Relaxation in Water" *Journal of Physical Chemistry*, 1996, Vol. 100, 1072-1080.

Alex, Z.C. and Behari, J. "Laboratory Evaluation of Emissivity of Soils" *International Journal of Remote Sensing*, 1998, Vol. 19 No 7, 1335-1340.

Al-Qadi, I.L., Lahouar, S. and Loulizi, A. "In Situ Measurements of Hot-Mix Asphalt dielectric properties" *NDT&E International*, 2001, Vol. 34, 427-434.

Anderson, N., Croxton, N., Hoover, R. and Sirles, P. "Geophysical Methods Commonly Employed for Geotechnical Site Characterization", Transportation Research Circular No. E-C130, Transportation Research Board, Washington DC, 2008.

Arcone, S., Grant, S., Boitnott, G., and Bostick, B. "Complex Permittivity and Clay Mineralogy of Grain-Size Fractions in a Wet Silt Soil", *Geophysics*, 2008, Vol. 73, No. 3, 1-13.

Arulanandan, K. and Smith, S.S. "Electrical Dispersion in Relation to Soil Structure", *Journal of the Soil Mechanics and Foundations Division*, 1973, 1113-1133.

Backhtiari, S., Ganchev, S.I. and Zoughi, R. "Analysis of Radiation From an Open-Ended Coaxial Line into Stratified Dielectrics", *IEEE Transactions on Microwave Theory and Techniques*, 1994, Vol. 42 No. 7, 1261-1267.

Ball, P. 'H$_2$O A Biography of Water', Phoenix, London, 1999.

Bandara, N. and Briggs, R.C. "Nondestructive Testing of Pavement Structures" *Materials Evaluation* [abstract], 2004, Vol. 62 No. 7, 733-740.

Ben-Dor, E., Patkin, K., Banin, A., Karnieli, A. "Mapping of Several Soil Properties Using DAIS-7915 Hyperspectral Scanner Data – A Case Study Over Clayey Soils in Israel" *International Journal of Remote Sensing*, 2002, Vol. 23 No. 6, 1043-1062.

Beroual, A., Brosseau, C. and Boudida, A. "Permittivity of Lossy Heterostructures: Effect of Shape Anisotropy" *Journal of Physics D: Applied Physics*, 2000, Vol. 33, 1969-1974.

Birchak, J.R., Gardner, C.G., Hipp, J.E. and Victor, J.M. "High Dielectric Constant Microwave Probe for Sensing Soil Moisture", *Proceedings of the IEEE*, 1974, Vol. 62, No. 1, 93-98.

References

Boyarskii, D.A., Tikhonov, V.V. and Komarova, N.Y. "Model of Dielectric Constant of Bound Water in Soil for Applications of Microwave Remote Sensing", *Progress in Electromagnetics Research*, 2002, Vol. 35, 251-269.

Brownlow, A.H. 'Geochemistry' Prentice-Hall Inc., New Jersey, 1996.

BSI. 1999, "Magnetic Materials - Methods for the Determination of the Relative Magnetic Permeability of Feebly Magnetic Materials", BS5884, British Standards Institution, London, UK.

BSI. 1990, "Methods of Test for Soils for Civil Engineering Purposes: Part 2: Classification Tests", BS1377-2, British Standards Institution, London, UK.

Buettner, M., Ramirez, A. and Daily, W. "Electrical Resistance Tomography for Imaging the Spatial Distribution of Moisture in Pavement Sections" *Structural Materials Technology: An NDT Conference, San Diego, Feb. 20-23 1996* [abstract], 1996, 342-347.

Buchner, R., Barthel, J. and Stauber, J. "The Dielectric Relaxation of Water Between 0ºC and 35 ºC" *Chemical Physics Letters*, 1999, Vol. 306, 57-63.

Cajori, F. "A History of Physics in its Elementary Branches", The Macmillan Company, New York, 1935.

Calerga. Light Matrix Engine - LME. www.calerga.com. Accessed 5th August 2007.

Calvert, J.R. and Farrar, R.A. "An Engineering Data Book", Palgrave Publishers Ltd., Basingstoke, 1999.

Campbell, J.E. "Dielectric Properties and Influence of Conductivity in Soils at One to Fifty Megahertz" *Soil Science Society of America Journal*, 1990, Vol. 54, 332-341.

Carreon-Freyre, D., Cerca, M. and Hernández-Marín, M. "Correlation of Near-Surface Stratigraphy and Physical Properties of Clayey Sediments from Chalco Basin, Mexico, using Ground Penetrating Radar" *Journal of Applied Geophysics*, 2003, Vol. 53, 121-136.

Cassidy, N.J. "Frequency-Dependent Attenuation and Velocity Characteristics of Nano-to-Micro Scale, Lossy, Magnetite-Rich Materials", *Near Surface Geophysics*, 2008, Vol. 6, 341-354.

Cassidy, N.J. "Frequency-Dependent Attenuation and Velocity Characteristics of Magnetically Lossy Materials", 4th International Workshop on Advanced Ground Penetrating Radar, June 27-29, 2007, Naples, Italy, 142-146.

References

Castiglione, P., Shouse, P.J. and Wraith, J.M. "Multiplexer-Induced Interference on TDR Measurements of Electrical Conductivity" *Soil Science Society of America Journal*, 2006, Vol. 70, 1453-1458.

Cataldo, A., Catarinucci, L., Tarricone, L., Attivissimo, F. and Trotta, A. "A Frequency-Domain Method for Extending TDR Performance in Quality Determination of Fluids". *Measurement Science and Technology*, 2007, Vol. 18, 675-688.

Chabrillat, S., Goetz, A.F.H., Krosley, L., Olsen, H.W. "Use of Hyperspectral Images in the Identification and Mapping of Expansive Clay Soils and the Role of Spatial Resolution" *Remote Sensing of Environment*, 2002, Vol. 82, 431-445.

Chazelas, A.J.L., Derobert, B.X., Adous, C.M., Villain, D.G., Baltazart, E.V., Laguerre, F.L. and Queffelec, G.P. "EM Characterization of Bituminous Concretes Using a Quadratic Experimental Design", 4th International Workshop on Advanced Ground Penetrating Radar, June 27-29, 2007, Naples, Italy, 278-283.

Choi, E.M., Yoon, Y.H., Lee, S. and Hang, H. "Freezing Transition of Interfacial Water at Room Temperature under Electric Fields" *Physical Review Letters*, 2005, Vol. 95, 085701, 1-4.

Cole, K.S. and Cole, R.H. "Dispersion and Absorption in Dielectrics I. Alternating Current Characteristics" *Journal of Chemical Physics*, 1941, Vol. 9, 341-351.

Cosenza, P. and Tabbagh, A. "Electromagnetic Determination of Clay Water Content: Role of the Microporosity" *Applied Clay Science*, 2004, Vol. 26, 21-36.

Cownie, A. and Palmer, L.S. "The Effect of Moisture on the Electrical Properties of Soil" *Proceedings of the Physical Society*, 1951, 295-301.

Craig, R.F. 'Soil Mechanics - Sixth Edition' E & FN Spon, London, 1997.

Crease, R.P. "The Great Equations: The Hunt for Cosmic Beauty in Numbers", Constable and Robinson Ltd., London, 2009.

Curtis, J.O. "Moisture Effects on the Dielectric Properties of Soils" *IEEE Transactions on Geoscience and Remote Sensing*, 2001, Vol. 39 No. 1, 125-128.

Dashevsky, Y.A., Dashevsky, O.Y., Filkovsky, M.I. and Synakh, V.S. "Capacitative Sounding: A New Geophysical Method for Asphalt Pavement Quality Evaluation" *Journal of Applied Geophysics*, 2004, Vol. 57, 95-106.

Debye, P. 'Polar Molecules', The Chemical Catalog Company Inc, New York, 1929.

References

Dérobert, X., Fauchard, C., Côte, Le Brusq, E., Guillanton, E., Dauvignac, J.Y. and Pichot "Step-Frequency Radar Applied to Thin Road Layers" *Journal of Applied Geophysics*, 2001, Vol. 47, 317-325.

Despa, F., Fernández, A. and Berry, R.S. "Dielectric Modulation of Biological Water" *Physical Review Letters*, 2004, Vol. 93, 228104-1-4.

Dirksen, C., 'Soil Physics Measurements', Catena Verlag GMBH, Reiskirchen, Germany, 1999.

Dobbs, E.R. 'Electricity and Magnetism' Routledge and Kegan Paul plc, London, 1984.

Dobson, M.C., Ulaby, F.T., Hallikainen, M.T. and El-Rayes, M.A. "Microwave Dielectric Behaviour of Wet Soil. Part II: Dielectric Mixing Models", *IEEE Transactions on Geoscience and Remote Sensing*, 1985, Vol. 23, 35-46.

Dolinar, B. and Trauner, L. "Liquid Limit and Specific Surface of Clay Particles" *Geotechnical Testing Journal [pre-publication version as at 10th October 2005]*, 2005, Vol. 27 No. 6, 1-5.

Doolittle, J.A., Minzenmayer, F.E., Waltman, S.W., Benham, E.C., Tuttle J.W. and Peaslee, S. "State Ground-Penetrating Radar Soil Suitability Maps", Proc. of 11th International Conference on GPR, Ohio State University, Columbia, Ohio, USA 19 – 22 June 2006 (CD ROM).

Doolittle, J.A. and Collins, M.E. "Use of Soil Information to Determine Application of Ground Penetrating Radar" *Journal of Applied Geophysics*, 1995, Vol. 33, 101-108.

Dorsey, D.J., Hebner, R. and Charlton, W.S. "Application of Prompt Gamma Activation Analysis for the Determination of Water Content in Composite Materials" *Journal of Radioanalytical and Nuclear Chemistry*, 2005, Vol. 265 No. 2, 315-319.

Dowding, C.H., Summers, J.A., Taflove, A. and Kath, W.L. "Electromagnetic Wave Propagation Model for Differentiation of Geotechnical Disturbances Along Buried Cables", *Geotechnical Testing Journal*, 2002, Vol. 25, No. 4, 1-10.

Drnevich, V.P., Yu, X., Lovell, J. and Tishmack, J. "Temperature Effects on Dielectric Constant Determined by Time Domain Reflectometry" TDR 2001 - Second International Symposium and Workshop on Time Domain Reflectometry for Innovative Geotechnical Applications, 2001a, Infrastructure Technology Institute, Northwestern University, Evanston, IL, September.

Drnevich, V.P., Siddiqui, S.I., Lovell, J., and Yi, Q. "Water Content and Density of Soil Insitu by the Purdue TDR Method," TDR 2001: Innovative Applications of TDR Technology, 2001b, Infrastructure Technology Institute, Northwestern University, Evanston, IL, September.

References

Drude, P. 'The Theory of Optics', Longmans, Green and Co., New York, 1902.

Duncan, T. 'Success in Electronics 2nd Edition', John Murray (Publishers) Ltd, London, 1997.

Eisenberg, D. and Kauzmann, W. 'The Structure and Properties of Water', Clarendon Press, Oxford, 1969.

Everitt, C.W.F. 'James Clerk Maxwell: Physicist and Natural Philosopher', Charles Scribner's Sons, New York, 1975.

Evitt, S.R. and Parkin, G.W. "Advances in Soil Water Content Sensing: The Continuing Maturation of Technology and Theory", *Vadose Zone Journal*, 2005, Vol. 4, 986-991.

Evitt, S.R., Tolk, J.A. and Howell, T.A. "Time Domain Reflectometry Laboratory Calibration in Travel Time, Bulk Electrical Conductivity, and Effective Frequency", *Vadose Zone Journal*, 2005, Vol. 4, 1020-1029.

Faraday, M. "A Course of Six Lectures on the Various Forces of Matter and Their Relations to Each Other", Richard Griffin and Company, London, 1861.

Farrar, D. M. and Coleman, J. D., "The Correlation of Surface Area with Other Properties of Nineteen British Clay Soils", *Journal of Soil Science*, 1967, Vol. 18, No. 1, 118–124.

Fernando, M.J., Burau, R.G. and Arulanandan, K. "A New Approach to Determination of Cation Exchange Capacity", 1977, *Soil Science Society of America Journal*, Vol. 41, 818-820.

Feynman, R.P. "QED: The Strange Theory of Light and Matter", Princeton University Press, Guildford, 1985.

Fleisch, D. "A Student's Guide to Maxwell's Equations", Cambridge University Press, Cambridge, UK, 2008.

Fratta, D.F., Alshibli, K.A., Tanner, W.M. and Roussel, L. "Combined TDR and P-Wave Velocity Measurements for the Determination of In Situ Soil Density" *Geotechnical Testing Journal [pre-publication version as at 10th October 2005]*, 2005, Vol. 28 No. 6, 1-11.

Friel, R. and Or, D. "Frequency Analysis of Time-Domain Reflectometry (TDR) with Application to Dielectric Spectroscopy of Soil Constituents". Geophysics. 1999, Vol. 64, 1-12.

References

Gamba, P. and Belotti, V. "Two Fast Buried Pipe Detection Schemes in Ground Penetrating Radar Images" *International Journal of Remote Sensing*, 2003, Vol. 24 No. 12, 2467-2484.

Giao, P.H., Chung, S.G., Kim, D.Y. and Tanaka, H. "Electric Imaging and Laboratory Resistivity Testing for Geotechnical Investigation of Pusan Clay Deposits" *Journal of Applied Geophysics*, 2003, 52, 157-175.

Good, R.H. 'Classical Electromagnetism' Saunders College Publishing, Orlando, 1999.

Gorritti, A.G. and Slob, E.C. "A New Tool for Accurate S-Parameters Measurements and Permittivity Reconstruction", *IEEE Transactions on Geoscience and Remote Sensing*, 2005, Vol. 43, No. 8, 1727-1735.

Gray, C.A. and Frost, M.W. "An Investigation Into Atterberg Limits and Their Suitability for Assessing the Shrinkage and Swelling Characteristics of Clay Soils for Foundation Design", International Conference on Problematic Soils, 2003, Nottingham, UK, 29-30 July.

Gray, G.W., Sowerby, B.D. and Youdale, G.P. "In-situ Determination of Moisture in Road Pavement by Nuclear Methods" *Energy Res. Abstr* [abstract], 1982, Vol. 7 No. 4.

Grim, R.E. 'Applied Clay Mineralogy', McGraw-Hill Book Company Inc., New York, 1962.

Hasted, J.B. 'Aqueous Dielectrics', Chapman and Hall, London, 1973.

Hayt, W.H. Jr. and Buck, J.A. 'Engineering Electromagnetics – Seventh Edition', McGraw-Hill, New York, 2006.

Heimovaara, T.J., Huisman, J.A., Vrugt, J.A. and Bouten, W. "Obtaining the Spatial Distribution of Water Content Along a TDR Probe Using the SCEM-UA Bayesian Inverse Modeling Scheme, *Vadose Zone Journal*, 2004, Vol. 3, 1128-1145.

Heimovaara, T.J. "Frequency Domain Modelling of TDR Waveforms in Order to Obtain Frequency Dependent Dielectric Properties of Soil Samples: A Theoretical Approach" TDR 2001 - Second International Symposium and Workshop on Time Domain Reflectometry for Innovative Geotechnical Applications, 2001.

Heimovaara, T.J., de Winter, E.J.G., van Loon, W.K.P. and Esveld, D.C. "Frequency-Dependent Dielectric Permittivity from 0 to 1 GHz: Time Domain Reflectometry Measurements Compared with Frequency Domain Network Analyzer Measurements" *Water Resources Research*, 1996, Vol. 32 No. 12, 3603-3610.

References

Heimovaara, T.J. "Frequency Domain Analysis of Time Domain Reflectometry Waveforms 1. Measurement of the Complex Permittivity of Soils" *Water Resources Research*, 1994, Vol. 30 No. 2, 189-199.

Hilhorst, M.A., Dirksen, C., Kampers, F.W.H. and Feddes, R.A. "New Dielectric Mixture Equation for Porous Materials Based on Depolarization Factors" *Soil Science Society of America Journal*, 2000, Vol. 64, 1581-1587.

Hoekstra, P. and Delaney, A. "Dielectric Properties of Soils at UHF and Microwave Frequencies", *Journal of Geotechnical Research*, 1974, Vol. 79, No. 11, 1699-1708.

Hoekstra, P. and Doyle, W.T. "Dielectric Relaxation of Surface Adsorbed Water", *Journal of Colloid and Interface Science*, 1970, Vol. 36, No. 4, 513-521.

Holden, j., Burt, T.P. and Vilas, M. "Application of Ground-Penetrating Radar to the Identification of Subsurface Piping in Blanket Peat" *Earth Surface Processes and Landforms*, 2002, Vol. 27, 235-249.

Hook, W.R., Ferré, T.P.A. and Livingston, N.J. "The Effects of Salinity on the Accuracy and Uncertainty of Water Content Measurement" *Soil Science Society of America Journal*, 2004, Vol. 68, 47-56.

Huang, H., SanFilipo, B. and Won, I.J. "Planetary Exploration Using a Small Electromagnetic Sensor" *IEEE Transactions on Geoscience and Remote Sensing*, 2005, Vol. 43 No. 7, 1499-1506.

Huang, Y. "Design, Calibration and Data Interpretation for a One-Port Large Coaxial Dielectric Measurement Cell", *Measurement Science and Technology*, 2001, Vol. 12, 111-115.

Huisman, J.A., Hubbard, S.S., Redman, J.D. and Annan, A.P. "Measuring Soil Water Content with Ground Penetrating Radar: A Review" *Vadose Zone Journal*, 2003a, Vol. 2, 476-491.

Huisman, J.A., Snepvangers, J.J.J.C., Bouten, W. and Heuvelink, G.B.M. "Monitoring Temporal Development of Spatial Soil Water Content Variation: Comparison of Ground Penetrating Radar and Time Domain Reflectometry", *Vadose Zone Journal*, 2003b, Vol. 2, 519-529.

Institute of Electrical and Electronics Engineers (IEEE), "IEEE Standard Definitions of Terms for Radio Wave Propagation", IEEE Standard 211-1990, The Institute of Electrical and Electronics Engineers Inc., New York, 1990.

Ishida, T., Makino, T. and Wang, C. "Dielectric-Relaxation Spectroscopy of Kaolinite, Montmorillonite, Allophane, and Imogolite Under Moist Conditions", *Clays and Clay Minerals*, 2000, Vol. 48 No. 1, 75-84.

References

Janezic, M.D. and Jargon, J.A. "Complex Permittivity Determination from Propagation Constant Measurements", *IEEE Microwave and Guided Wave Letters*, 1999, Vol. 9, No. 2, 76-78.

Jansson, H. and Swenson, J. "Dynamics of Water in Molecular Sieves by Dielectric Spectroscopy" *Journal of European Physics E*, 2003, Vol. 12, 51-54.

Jaselskis, E.J., Grigas, J. and Brilingas, A. "Dielectric Properties of Asphalt Pavement" *Journal of Materials in Civil Engineering* [abstract], 2003, Vol. 15 No. 5, 427-434.

Jones, S.B., Mace, R.W. and Or, D. "A Time Domain Reflectometry Coaxial Cell for Manipulation and Monitoring of Water Content and Electrical Conductivity in Variably Saturated Porous Media", *Vadose Zone Journal*, 2005, Vol. 4, 977-982.

Jones, S.B. and Or, D. "Frequency Domain Analysis for Extending Time Domain Reflectometry Water Content Measurement in Highly Saline Soils" *Soil Science Society of America Journal*, 2004, Vol. 68, 1568-1577.

Jones, S.B. and Or, D. "Surface Area, Geometrical and Configurational Effects on Permittivity of Porous Media" *Journal of Non-Crystalline Solids*, 2002, Vol. 305, 247-254.

Jones, S.B., Wraith, J.M. and Or, D. "Time Domain Reflectometry Measurement Principles and Applications", *Hydrological Processes*, 2002, Vol. 16, 141-153.

Jones, S.B. and Friedman, S.P. "Particle Shape Effects on the Effective Permittivity of Anisotropic or Isotropic Media Consisting of Aligned or Randomly Oriented Ellipsoidal Particles" *Water Resources Research*, 2000, Vol. 36 No. 10, 2821-2833.

Kaatze, U. "Complex Permittivity of Water as a Function of Frequency and Temperature", *Journal of Chemical and Engineering Data*, 1989, Vol. 34, No. 4, 371-374.

Kao, K.C. 'Dielectric Phenomena in Solids' Elsevier Academic Press, San Diego, 2004.

Kariuki, P.C., van der Meer, F., Siderius, W. "Classification of Soils Based on Engineering Indices and Spectral Data" *International Journal of Remote Sensing*, 2003, Vol. 24 No. 12, 2567-2574.

Kärkkäinen, K., Sihvola, A., Nikoskinen, K. "Analysis of a Three-Dimensional Dielectric Mixture with Finite Difference Method" *IEEE Transactions on Geoscience and Remote Sensing*, 2001, Vol. 39 No. 5, 1013-1018.

Kelleners, T.J., Robinson, D.A., Shouse, P.J., Ayars, J.E. and Skaggs, T.H. "Frequency Dependence of the Complex Permittivity and Its Impact on Dielectric Sensor Calibration in Soils" *Soil Science Society of America Journal*, 2005a, Vol. 69, 67-76.

References

Kelleners, T.J.. Seyfried, M.S.. Blonquist, J.M., Bilskie, J. and Chandler D.G. "Improved Interpretation of Water Content Reflectometer Measurements in Soils", *Soil Science Society of America Journal*, 2005b, Vol. 69, 1684-1690.

Kirby, R.S., Withington, S., Darling, A.B. and Kilgour, F.G. "Engineering in History", Dover Publications Inc., New York, 1990.

Klein, K. and Wang, Y.H. "Towards a Better Understanding of the Electro-Magnetic Properties of Soils", in Huyghe et al. (eds) "IUTAM Proceedings on Physiochemical and Electromechanical Interactions in Porous Media", Springer, Netherlands, 2005.

Klein, K. and Santamarina, J.C. "Methods for Broad-Band Dielectric Permittivity Measurements (Soil-Water Mixtures, 5 Hz to 1.3 GHz)" *Geotechnical Testing Journal*, 1997, Vol. 20 No. 2, 168-178.

Knight, J.H. "Sensitivity of Time Domain Reflectometry Measurements to Lateral Variations in Soil Water Content", *Water Resources Research*, 1992, Vol. 28, No. 9, 2345-2352.

Knott, M. "Crunch Time" *New Scientist*, 7th May 2005, 38-39.

Kropman, M.F. and Bakker, H.J. "Effects of Ions on the Vibrational Relaxation of Liquid Water" *Journal of the American Chemical Society*, 2004, Vol. 126, 9135-9141.

Laird, D.A. "Influence of Layer Charge on Swelling of Smectites", *Applied Clay Science*, 2006, Vol. 34, 74-87.

Lal, R. and Shukla, M.K., "Principles of Soil Physics", Marcel Dekker Inc., New York, 2004.

Lambot, S., Slob, E.C., van den Bosch, I., Stockbroeckx, B., Vanclooster, M. "Modeling of Ground-Penetrating Radar for Accurate Characterization of Subsurface Electric Properties" *IEEE Transactions on Geoscience and Remote Sensing*, 2004, Vol. 42 No. 11, 2555-2564.

Lebron, I., Robinson, D.A., Goldberg, S. and Lesch, S.M. "The Dielectric Permittivity of Calcite and Arid Zone Soils with Carbonate Minerals", *Soil Science Society of America Journal*, 2004, Vol. 68, 1549-1559.

Leckerbusch, J. and Peikert, R. "Investigating the True Resolution and Three-dimensional Capabilities of Ground-penetrating Radar Data in Archaeological Surveys: Measurements in a Sand Box" *Archaeological Prospection*, 2001, 8, 29-40.

Lin, C.P., Chung, C.C., Huisman, J.A. and Tang, S.H. "Clarification and Calibration of Reflection Coefficient for Electrical Conductivity Measurement by Time Domain Reflectometry", *Soil Science Society of America Journal*, 2007, Vol. 72, No. 4, 1033-1040.

References

Lin, C.P. and Tang, S.H. "Development and Calibration of a TDR Extensometer for Geotechnical Monitoring" *Geotechnical Testing Journal*, 2005, Vol. 28 No. 5, 1-7.

Lin, C., Greenwald, D. and Banin, A. "Temperature Dependence of Infiltration Rate During Large Scale Water Recharge into Soils", *Soil Science Society of America Journal*, 2003, Vol. 67, 487-493.

Lin, C.P. "Frequency Domain Versus Travel Time Analysis of TDR Waveforms for Soil Moisture Measurements", *Soil Science Society of America Journal*, 2003, Vol. 67, 720-729.

Lin, C.P. "Full Waveform Analysis of a Non-Uniform and Dispersive TDR Measurement System" TDR 2001 - Second International Symposium and Workshop on Time Domain Reflectometry for Innovative Geotechnical Applications, 2001.

Logsdon, S.D. "Uncertainty Effects on Soil Electrical Conductivity and Permittivity Spectra", *Soil Science*, 2006a, Vol. 171, No. 10, 737-746.

Logsdon, S.D. "Experimental Limitations of Time Domain Reflectometry Hardware for Dispersive Soils" *Soil Science Society of America Journal*, 2006b, Vol. 70, 537-540.

Logsdon, S.D. "Soil Dielectric Spectra from Vector Network Analyser Data" *Soil Science Society of America Journal*, 2005a, 983-989.

Logsdon, S.D. "Time Domain Reflectometry Range of Accuracy for High Surface Area Soils", *Vadose Zone Journal*, 2005b, Vol. 4, 1011-1019.

Logsdon, S. and Laird, D. "Cation and Water Content Effects on Dipole Rotation Activation Energy of Smectites" *Soil Science Society of America Journal*, 2004, Vol. 68, 1586-1591.

Logsdon, S.D. and Hornbuckle, B.K. "Soil Moisture Probes for a Dispersive Soil". TDR2006, Purdue University, West Lafayette, USA, September 2006, Paper ID 13.

Lorenzo, H., Cuéllar, V. and Hernández, M.C. "Close Range Radar Remote Sensing of Concrete Degradation in a Textile Factory Floor" *Journal of Applied Geophysics*, 2001, Vol. 47, 327-336.

Low, P.F. "Nature and Properties of Water in Montmorrilonite-Water Systems", *Soil Science Society of America Journal*, 1979, Vol. 43, 651-658.

Mathworks. 2007. Matrix Laboratory - Matlab. www.mathworks.com. Accessed 5th August 2007.

Mätzler, C, "Microwave Permittivity of Dry Sand" *IEEE Transactions on Geoscience and Remote Sensing*, 1998, Vol. 36 No. 1, 317-319.

References

Mcmahon W., Burtwell M.H. and Evans M., "Minimising Street Works Disruption: The Real Costs of Street Works to the Utility Industry and Society", UKWIR Report 05/WM/12/8, UK Water Industry Research, London, 2005.

Metje N., Rogers C.D.F., Chapman D.N., Thomas A.M. and Parker J.M., "Minimizing Streetworks Disruption by Mapping the Underworld", Proceedings of Pipelines 2008, American Society of Civil Engineers, 2008, Atlanta, 22nd – 25th July (CDROM).

Metje, N., Atkins, P.R., Brennan, M.J., Chapman, D.N., Lim, H.M., Machell, J, Muggleton, J.M., Pennock, S., Ratcliffe, J., Redfern, M.,. Rogers, C.D.F, Saul,A.J., Shan, Q., Swingler, S., and Thomas, A.M., "Mapping the Underworld – State-of-the-Art Review", Tunnelling and Underground Space Technology, 2007, Vol. 22, 568-586.

Millard, S.G., Shaw, M. and Bungey, J.H. "The Use of Ground-Penetrating Radar for Investigating Leakage from Water Pipes Beneath Highway Pavements, in Clay Sub-Strata" *Structural Materials Technology VI, An NDT Conference, Buffalo, New York,* September 14-17, 2004, 157-165.

Millard, D.J. "The Electrical Measurement of Moisture in Granular Materials", *British Journal of Applied Physics*, 1953, Vol. 4, 84-87.

Milsom, J. 'Field Geophysics Second Edition', John Wiley and Sons Ltd, Chichester, 1996.

Mitchell, J.K. and Soga, K. 'Fundamentals of Soil Behaviour: Third Edition', John Wiley and Sons Inc., Hoboken, New Jersey, 2005.

Morus, I.R. 'Michael Faraday and the Electrical Century', Icon Books UK, 2004.

Muhunthan, B., Masad, E. and Assaad, A. "Measurement of Uniformity and Anisotropy in Granular Materials" *Geotechnical Testing Journal*, 2000, Vol. 23 No. 4, 423-431.

Nabighian, M.N. (ed) 'Electromagnetic Methods in Applied Geophysics Volume 1 – Theory' Society of Exploration Geophysicists, Tulsa, 1987.

Nadler, A., Raveh, E., Yermiyahu, U. and Green, S. "Stress Induced Water Content Variations in Mango Stem by Time Domain Reflectometry" *Soil Science Society of America Journal*, 2006, Vol. 70, 510-520.

Nedeltchev, N.M. "Thermal Microwave Emission Depth and Soil Moisture Remote Sensing" *International Journal of Remote Sensing*, 1999, Vol. 20 No. 11, 2183-2194.

Negi, J.G. and Saraf, P.D. 'Anisotropy in Geoelectromagnetism', Elsevier Science Publishers B.V., Amsterdam, 1989.

References

Nelder, L.M., Gunn, D.A. and Reeves, H.J. "Investigation of the Geotechnical Properties of a Victorian Embankment", RailFound 06, 1st International Conference on Railway Foundations, Birmingham, UK, 11th-13th September, 2006, 34-47.

Nussberger, M., Benedickter, H., Bächtold, W., Flühler, H. and Wunderli, H. "Single-Rod Probes for Time Domain Reflectometry: Sensitivity and Calibration", *Vadose Zone Journal*, 2005, Vol. 4, 551-557.

Olhoeft, G.R. "Electrical, Magnetic, and Geometric Properties That Determine Ground Pentrating Radar Performance" Proceedings of GPR'98, Seventh International Conference on Ground Penetrating Radar, May 27-30, 1998, The University of Kansas, Lawrence, KS, 177-182.

Or, D. and Wraith, J.M. "Temperature Effects on Soil Bulk Dielectric Permittivity Measured by Time Domain Reflectometry: A Physical Model" *Water Resources Research*, 1999, Vol. 35 No. 2, 371-383.

ORFEUS Project, www.orfeus-project.eu, accessed 7th March 2009.

Ovchinkin, O.A. and Sugak, V.G. "The Influence of Soil Electric Properties upon the Ground-Penetrating Radar (GPR) Signal Characteristics" *Telecommunications and Radio Engineering*, 2002, Vol. 57 No. 10, 101-109.

Peplinski, N.R., Ulaby, F.T., Dobson, M.C. "Dielectric Properties of Soils in the 0.3-1.3-GHz Range" *IEEE Transactions on Geoscience and Remote Sensing*, 1995, Vol. 33 No. 3, 803-807.

Persson, M., Wraith, J.M. and Dahlin, T. "A Small-Scale Matric Potential Sensor Based on Time Domain Reflectometry", *Soil Science Society of America Journal*, 2006, Vol. 70, 533-536.

Pettinelli, E., Vannaroni, G., Di Pasquo, B., Mattei, E., Di Matteo, A., De Santis, A., and Annan, P.A. "Correlation Between Near-Surface Electromagnetic Soil Parameters and Early-Time GPR Signals: An Experimental Study", *Geophysics*, 2007, Vol. 72, No. 2, 25-28.

Pettinelli, E., Cereti, A., Galli, A. and Bella, F. "Time Domain Reflectometry: Calibration Techniques for Accurate Measurement of the Dielectric Properties of Various Materials", *Review of Scientific Instruments*, 2002, Vol. 73 No. 10, 3553-3562.

Pickett, A.G. and Lemcoe, M.M. "An Investigation of Shear Strength of the Clay-Water System by Radio-Frequency Spectroscopy", *Journal of Geophysical Research*, 1959, Vol. 64, No. 10, 1579-1586.

Pitchford, A. "Civil Engineering Applications of Geophysical Investigation Techniques" *CIRIA News*, 1996, Issue 3, 6.

References

Poole, I. "Basic Radio Principles and Applications", Newnes, Oxford, 1998.

Prakash, K. and Sridharan, A. "Free Swell Ratio and Clay Mineralogy of Fine-Grained Soils", *Geotechnical Testing Journal*, 2004, Vol. 27, No. 2, 1-6.

Pride, S. "Governing Equations for the Coupled Electromagnetics and Acoustics of Porous Media" *Physical Review B*, 1994, Vol. 50 No. 21, 15678-15696.

Pride, S.R., Morgan, F.D. "Electrokinetic Dissipation Induced by Seismic Waves" *Geophysics*, 1991, Vol. 56 No. 7, 914-925.

Raythatha, R. and Sen, P.N. "Dielectric Properties of Clay Suspensions in MHz to GHz Range" *Journal of Colloid and Interface science*, 1986, Vol. 109 No.2, 301-309.

Reppert, P.M., Morgan, F.D. and Toksöz, N.M. "Dielectric Constant Determination Using Ground-Penetrating Radar Reflection Coefficients" *Journal of Applied Geophysics*, 2000, Vol. 43, 189-197.

Reynolds, J.M. 'An Introduction to Applied and Environmental Geophysics', John Wiley and Sons Ltd, Chichester, 1997.

Robert, A. "Dielectric Permittivity of Concrete Between 50 Mhz and 1 Ghz and GPR Measurements for Building Materials Evaluation" *Journal of Applied Geophysics*, 1998, Vol. 40, 89-94.

Robinson, D.A., Schaap, M.G., Or, D. and Jones, S.B. "On the Effective Measurement Frequency of Time Domain Reflectometry in Dispersive and Nonconductive Dielectric Materials" *Water Resources Research*, 2005, Vol. 41, WO2007 1-9.

Robinson, D.A. "Measurement of the Solid Dielectric Permittivity of Clay Minerals and Granular Samples using a Time Domain Reflectometry Immersion Method", *Soil Science Society of America Journal*, 2004, Vol. 3, 705-713.

Robinson, D.A., Jones, S.B., Wraith, J.M. and Friedman, S.P. "A Review of Advances in Dielectric and Electrical Conductivity Measurement in Soils Using Time Domain Reflectometry" *Vadose Zone Journal*, 2003a, Vol. 2, 444-475.

Robinson, D.A., Schaap, M.G., Jones, S.B., Friedman, S.P. and Gardner, C.M.K. "Considerations for Improving the Accuracy of Permittivity Measurement Using Time Domain Reflectometry - Air-Water Calibration and Effects of Cable Length". *Soil Science Society of America Journal*, 2003b, Vol. 67, 62-70.

References

Rogers, C.D.F., Chapman, D.N., Entwisle, D., Jones, L., Kessler, H., Metje, N., Mica, L., Morey, M., Pospíšil, P., Price, S., Raclavsky, J., Raines, M., Scott, H., and Thomas, A.M., "Predictive Mapping of Soil Geophysical Properties for GPR Utility Location Surveys", 5th International Workshop on Advanced Ground Penetrating Radar (IWAGPR), 2009, Granada, Spain, 27-29 May.

Runkles, B., White, N. and Ashmawy, A. "Calibration and Accuracy Assessment of the TDR One-Step Method for Quality Control of Compacted Soils", Florida Department of Transportation, 2006.

Saarenketo, T. and Scullion, T. "Road Evaluation with Ground Penetrating Radar" *Journal of Applied Geophysics*, 2000, Vol. 43, 119-138.

Saarenketo, T. "Electrical Properties of Water in Clay and Silty Soils" *Journal of Applied Geophysics*, 1998, 40, 73-88.

Schaap, M.G., Robinson, D.A., Friedman, S.P. and Lazar, A. "Measurement and Modelling of the TDR Signal Propagation Through Layered Dielectric Media" *Soil Science Society of America Journal*, 2003, 1113-1121.

Scholte, J.W., Shang, J.Q. and Rowe, R.K. "Improved Complex Permittivity Measurement and Data Processing Technique for Soil-Water Systems" *Geotechnical Testing Journal*, 2002, 187-198.

Serbin, G., Or, D., Blumberg, D.G. "Thermodielectric Effects on Radar Backscattering from Wet Soils' *IEEE Transactions on Geoscience and Remote Sensing*, 2001, Vol. 39 No. 4, 897-901.

Serbin, G. and Or, D. "Ground-Penetrating Radar Measurement of Soil Water Content Dynamics Using a Suspended Horn Antenna" *IEEE Transactions on Geoscience and Remote Sensing*, 2004, Vol. 42 No. 8, 1695-1705.

Serbin, G. and Or, D. "Ground-Penetrating Radar Measurement of Crop and Surface Water Content Dynamics" *Remote Sensing of Environment*, 2005, Vol. 96, 119-134.

Shadowitz, A. 'The Electromagnetic Field', Dover Publications Inc., New York, 1988.

Shang, J.Q., Rowe, R.K., Umana, J.A. and Scholte, J.W. "A Complex Permittivity Measurement System for Undisturbed/Compacted Soils" *Geotechnical Testing Journal*, 1999, Vol. 22 No. 2, 165-174.

Shuai, X., Wendroth, O., Lu, C. and Ray, C. "Reducing the Complexity of Inverse Analysis of Time Domain Reflectometry Waveforms", *Soil Science Society of America Journal*, 2009, Vol. 73, 28-36.

References

Siddiqui, S. I., Drnevich, V. P., and Deschamps, R. J., "Time Domain Reflectometry Development for Use in Geotechnical Engineering," *Geotechnical Testing Journal*, 2000, Vol. 23 No. 1, 9–20.

Sihvola, A.H. "How Strict are Theoretical Bounds for Dielectric Properties of Mixtures?" *IEEE Transactions on Geoscience and Remote Sensing*, 2002, Vol. 40 No. 4, 880-886.

Sihvola, A.H. "Studies of Mixing Formulae in the Complex Plane" *IEEE Transactions on Geoscience and Remote Sensing*, 1991, Vol. 29 No. 4, 679-687.

Sills, I.D., Aylmore, L.A.G. and Quirk, J.P. "Relationships Between Pore Size Distributions and Physical Properties of Clay Soils" *Australian Journal of Soil Research*, 2006, Vol. 12 No. 2, 107-117.

Smith-Rose, R.L. "The Electrical Properties of Soil at Frequencies up to 100 Megacycles Per Second; With a Note on the Resistivity of Ground in the United Kingdom" *Proceedings of the Physical Society*, 1935, Vol. 47 923-931.

Souza, C.F., Or, D. and Matsura, E.E. "A Variable-Volume TDR Probe for Measuring Water Content in Large Soil Volumes" *Soil Science Society of America Journal*, 2004, Vol. 68, 25-31.

Sridharan, A. and Prakash, K. "Shrinkage Limit of Soil Mixtures," *Geotechnical Testing Journal*, 2000a, Vol. 23, No. 1, 3–8.

Sridharan, A., and Prakash, K. "Percussion and Cone Methods of Determining the Liquid Limit of Soils" *Geotechnical Testing Journal*, 2000b, Vol. 23, No. 2, 242–250.

Sridharan, A., Nagaraj, H. B., and Prakash, K. "Determination of the Plasticity Index from Flow Index," *Geotechnical Testing Journal*, 1999, Vol. 22, No. 2, 169–175.

Sridharan, A. and Nagaraj, H.B. "Absorption Water Content and Liquid Limit of Soils" *Geotechnical Testing Journal*, 1999, Vol. 22 No. 2, 121-127.

Staubach, S. "Clay: The History and Evolution of Humankind's Relationship with Earth's Most Primal Element", The Berkley Publishing Group, New York, 2005.

Sugak, V.G. "Reconstruction of Electrical Constants of Soil and Depth of Subsurface Objects Using Data of Subsurface Sounding" *Telecommunications and Radio Engineering*, 2003, Vol. 59 No. 1, 54-63.

Tareev, B. 'Physics of Dielectric Materials' Mir Publishers, Moscow, 1975.

Telford, W.M., Geldart, L.P., Sheriff, R.E. 'Applied Geophysics Second Edition', Cambridge University Press, Cambridge, 1990.

References

Thomas A.M., Rogers C.D.F., Chapman D.N., Metje N. and Castle, J., "Stakeholder Needs for Ground Penetrating Radar Utility Location", *Journal of Applied Geophysics*, 2008a, Vol. 67, 345–351.

Thomas, A.M., Chapman, D.N., Rogers, C.D.F., Metje, N., Atkins, P.R. and Lim, H.M. "Broadband Apparent Permittivity Measurement in Dispersive Soils Using Quarter-Wavelength Analysis", *Soil Science Society of America Journal*, 2008b, Vol. 72, No. 5, 1401-1409.

Thomas A.M., Rogers C.D.F. Metje N., and Chapman D.N., "Soil Electromagnetic Mapping for Enhanced GPR Utility Location". Proceedings of 25th International No-Dig Conference and Exhibition, 2007, Rome, Italy, 9th to 12th September. (CD ROM).

Thomas A.M., Metje N., Rogers C.D.F. and Chapman D.N. "Ground Penetrating Radar Interpretation as a Function of Soil Response Complexity in Utility Mapping". Proc. of 11th International Conference on Ground Penetrating Radar, Columbus, Ohio, USA, June 19-22, 2006. (CD ROM).

Thomas, A.M. "In Situ Measurement of Moisture in Soil and Similar Substances by 'Fringe' Capacitance" *Journal of Scientific Instruments*, 1966, Vol. 43, 21-27.

Thompson, R. 'Environmental Magnetism', Allen & Unwin (Publishers) Ltd., London, 1986.

Todoroff, P. and Lan Sun Luk, J.D. "Calculation of In Situ Soil Water Content Profiles from TDR Signal Traces", *Measurement Science and Technology*, 2001, Vol. 12, 27-36.

Topp, G.C., Davis, J.L. and Annan, A.P. "The Early Development of TDR for Soil Measurements" *Vadose Zone Journal*, 2003, Vol. 2, 492-499.

Topp, G.C., Zegelin, S. and White, I. "Impacts of the Real and Imaginary Components of Relative Permittivity on Time Domain Reflectometry Measurements", *Soil Science Society of America Journal*, 2000, Vol. 64, 1244-1252.

Topp, G.C., Yanuka, M., Zebchuk, W.D. and Zegelin, S. "Determination of Electrical Conductivity Using Time Domain Reflectometry: Soil and Water Experiments in Coaxial Lines" *Water Resources Research*, 1988, Vol. 24 No. 7, 945-952.

Topp, G.C., Davis, J.L. and Annan, A.P. "Electromagnetic Determination of Soil Water Content: Measurements in Coaxial Transmission Lines" *Water Resources Research*, 1980, Vol. 16 No. 3, 574-582.

Van Blaricom, R. 'Practical Geophysics for the Exploration Geologist' Northwest Mining Association, Spokane, 1980.

References

van Dam, R.L., Borchers, B. and Hendrickx, J.M.H. "Methods for Prediction of Soil Dielectric Properties: A review". Detection and remediation technologies for mines and minelike targets X. 2005. Vol. 5794, Orlando, FL, SPIE, 188-197.

Van Dam, R.L. and Schlager, W. "Identifying Causes of Ground-Penetrating Radar Reflections Using Time-Domain Reflectometry and Sedimentological Analyses" *Sedimentology*, 2000, 47, 435-449.

Venkatesh, M.S. and Raghavan, G.S.V. "An Overview of Dielectric Properties Measuring Techniques" *Canadian Biosystems Engineering*, 2005, Vol. 47, 7.15-7.30.

Waddel, B.C. "Transmission Line Design Handbook", Artech House Inc., Norwood, M.A., 1991.

Waltham, T., 'Foundations of Engineering Geology', Spon Press, London, UK, 1994.

Weir, W.B., "Automatic Measurement of Complex Dielectric Constant and Permeability at Microwave Frequencies", *Proceedings of the IEEE*, 1974, Vol. 62, No. 1, 33-36.

Wensink WA. "Dielectric-Properties of Wet Soils in the Frequency-Range 1-3000 MHz", *Geophysical Prospecting*, 1993, Vol. 41, No. 6, 671-696.

Whalley, W.R. "Considerations on the Use of Time-Domain Reflectometry (TDR) for Measuring Soil Water Content", *Journal of Soil Science*, 1993, Vol. 44, 1-9.

Whites, K. W. and Wu, F. "Effects of Particle Shape on the Effective Permittivity of Composite Materials With Measurements for Lattices of Cubes" *IEEE Transactions on Microwave Theory and Techniques*, 2002, Vol. 50 No. 7, 1723-1729.

Wilson, F.A. 'An Introduction to the Electromagnetic Wave' Bernard Babani (publishing) Ltd, London, 1993.

Winder, S. and Carr, J. 'Radio and RF Engineering' Newnes, Oxford, 2002.

Wraith, J.M., Or, D. and Jones, S.B. "Dielectric Properties of Bound Water: Application to Porous Media Surface Area and Grain Moisture Determination" TDR 2001 - Second International Symposium and Workshop on Time Domain Reflectometry for Innovative Geotechnical Applications, 2001.

Wu, T.H. "A Nuclear Magnetic Resonance Study of Water in Clay" *Journal of Geophysical Research*, 1964, Vol. 69 No. 6, 1083-1091.

Xu, Y., Shang, J.Q. and Yanful, E.K. "A Short-Circuit Electromagnetic Sensor for Measurement of Soil Complex Permittivity", *Geotechnical Testing Journal*, 2007, Vol. 30, No. 4, 1-11.

References

Yanuka, M., Topp, G.C., Zegelin, S. and Zebchuk, W.D. "Multiple Reflection and Attenuation of Time Domain Reflectometry Pulses: Theoretical Considerations for Applications to Soil and Water" *Water Resources Research*, 1988, Vol. 24 No. 7, 939-944.

Yelf, R. 'Where is True Time Zero?', Tenth International Conference on Ground Penetrating Radar, 21-24 June, Delft, The Netherlands, 2004.

Zahn, D "How Does Water Boil?" *Physical Review Letters*, 2004, 93, 227801-1-4.

Zegelin, S.J., White, I. and Jenkins, D.R. "Improved Field Probes for Soil Water Content and Electrical Conductivity Measurement Using Time Domain Reflectometry" *Water Resources Research*, 1989, Vol. 25 No. 11, 2367-2376.

Zheng, H. and Smith, C.E. "Permittivity Measurements Using a Short Open-Ended Coaxial Line Probe" *IEEE Microwave and Guided Wave Letters*, 1991, Vol. 1 No.11, 337-339.

Zupanc, V., Adam, G. and Pintar, M. "Comparison of Laboratory TDR soil water measurements", *Acta Agriculturae Slovenica*, 2005, Vol. 85 No. 2, 359-374.

LIST OF ASSOCIATED PUBLICATIONS

The following publications are those in which significant portions of the research in this thesis have been previously disseminated:

Thomas, A.M., Curioni, G., Foo, K.Y., Atkins, P.R., Rogers, C.D.F. and Chapman, D.N. (2010) "Improving TDR for use with Fine-grained Soils", Proceedings of the First International Conference on Frontiers in Shallow Subsurface Technology, Delft, The Netherlands, 169-172.

Rogers, C.D.F., Chapman, D.N., Entwisle, D., Jones, L., Kessler, H., Metje, N., Mica, L., Morey, M., Pospíšil, P., Price, S., Raclavsky , J., Raines, M., Scott, H., Thomas, A.M. (2009) "Predictive Mapping of Soil Geophysical Properties for GPR Utility Location Surveys" Proceedings of the 5th International Workshop on Advanced Ground Penetrating Radar, Granada, Spain, May 27-29, p. 60-67.

Thomas, A.M., Chapman, D.N., Rogers, C.D.F., and Metje, N. (2010) "Electromagnetic Properties of the Ground: Part I - Fine-Grained Soils at the Liquid Limit", *Tunnelling and Underground Space Technology*, doi:10.1016/ j.tust.2009.12.002.

Thomas, A.M., Chapman, D.N., Rogers, C.D.F., and Metje, N. (2010) "Electromagnetic Properties of the Ground: Part II - The Properties of Two Selected Fine-Grained Soils", *Tunnelling and Underground Space Technology*, doi:10.1016/ j.tust.2009.12.003.

Thomas, A.M., Chapman, D.N., Rogers, C.D.F., Metje, N., Atkins, P.R. and Lim, H.M. (2008) "Broadband apparent permittivity measurement in dispersive soils using quarter-wavelength analysis", *Soil Science Society of America Journal*, Vol. 72, No. 5, 1401-1409.

Thomas, A.M., Yelf, R., Gunn, D.A., Self, S., Chapman, D.N., Rogers, C.D.F. and Metje, N. (2008) "The Role of Geotechnical Engineering for Informed GPR Planning and Interpretation in Fine Soils", 12th International Conference on Ground Penetrating Radar, Birmingham, UK, June 16-19 (CDROM).

Thomas, A.M., Gunn, D.A., Nelder, L.M., Burrows, M.P.N., Metje, N., Rogers, C.D.F. and Chapman, D.N. (2008). "Electromagnetic Characterisation of a Victorian Railway Embankment Fill Material", 3rd International Conference on Site Characterization, Taipee, Taiwan, April 1-4.

Thomas A.M., Rogers C.D.F. Metje N., and Chapman D.N. (2007). "Soil Electromagnetic Mapping for Enhanced GPR Utility Location". Proc. of 25th International No-Dig Conference and Exhibition, Rome, Italy, 9th to 12th September. (CD ROM).

Metje, N.,. Atkins, P.R,. Brennan, M.J, Chapman, D.N., Lim, H.M., Machell, J, Muggleton, J.M., Pennock, S., Ratcliffe, J., Redfern, M.,. Rogers, C.D.F, Saul,A.J.,

Shan, Q., Swingler, S., Thomas, A.M. (2007) "Mapping the Underworld – State-of-the-Art Review", *Tunnelling and Underground Space Technology*, Vol. 22, 568-586.

Thomas AM, Lim HM, Metje N, Rogers CDF, Chapman DN and Atkins PR (2006). "The Complexity of GPR Data Interpretation in Railway Foundation Surveys". Proc. of RailFound 06, 1st International Conference on Railway Foundations, Birmingham, UK, 11th -13th September, p. 48-61.

Thomas AM, Metje N, Rogers CDF and Chapman DN (2006). "Ground Penetrating Radar Interpretation as a Function of Soil Response Complexity in Utility Mapping". Proc. of 11th International Conference on Ground Penetrating Radar, Columbus, Ohio, USA, June 19-22. (CD ROM).